

Posh  
Posh  
ONE

Date: November 19, 1974

use DP250

Project Director: Mr. J. D. Adams

Effective Nov. 15, 1974 Estimated to run until Nov. 14, 1975 (R&D Work Period)

Type Agreement: Contr. F30602-75-C-0065 Amount: \$ 95,888

Reports Required: Monthly Status Reports; Final Technical Report

Sponsor Contact Person ( s ):

## Contractual Matters

(Thru GTRIO

David J. Powell

Contract Specialist

Hq., Rome Air Dev. Center

Attn: PMRZ

Griffiss AFB, New York 13441  
(315) 330-4731

\*Partially funded at \$68,000 thru 6/30/75.

DEFENSE PRIORITY RATING: DO-A7 under DMS Reg. 1

signed to TRADAR Division

☐ **Project Director**☐ Director☐ Assistant Director

☐ **GTRI**

☐ Division Chief ( s )

### ❑ Branch Heads

☐ **Service Groups**

☐ Patent Coordinator☐ Photographic Laboratory

**1 Security, Property, Reports Coordinator**

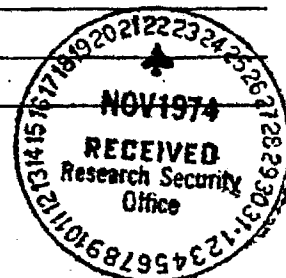
☐ **EES Accounting**

☐ **EES Supply Services**

☐ Library☐ Office of Computing Services☐ **Project File**

☐ Other Sue Corbin

Bonnee Wettlaufer



GEORGIA INSTITUTE OF TECHNOLOGY  
OFFICE OF CONTRACT ADMINISTRATION  
SPONSORED PROJECT TERMINATION

Date: July 1, 1976

Project Title: Broadband Antenna Measurement Techniques - Phase II

Project No: A-1694

Project Director: J. D. Adams

Sponsor: Rome Air Development Center; Griffiss AFB, New York 13441

Effective Termination Date: 4/15/76 (Final Report due date)

Clearance of Accounting Charges: 4/30/76

Grant/Contract Closeout Actions Remaining:

☒ Final Invoice and Closing Documents

☐ Final Fiscal Report

☒ Final Report of Inventions

☒ Govt. Property Inventory & Related Certificate

☐ Classified Material Certificate

☐ Other \_\_\_\_\_

Assigned to: Applied Engineering Laboratory (School/Laboratory)

COPIES TO:

Project Director  
Division Chief (EES)  
School/Laboratory Director  
Dean/Director-EES  
Accounting Office  
Procurement Office  
Security Coordinator (OCA)  
Reports Coordinator (OCA)

Library, Technical Reports Section  
Office of Computing Services  
Director, Physical Plant  
EES Information Office  
Project File (OCA)  
Project Code (GTRI)  
Other \_\_\_\_\_

# ENGINEERING EXPERIMENT STATION

GEORGIA INSTITUTE OF TECHNOLOGY • ATLANTA, GEORGIA 30332

12 December 1974

Rome Air Development Center  
Griffiss Air Force Base  
New York 13441

Attention: Mr. Martin Jaeger, OCTS

Reference: Contract No. F30602-75-C-0065

Title: Broadband Antenna Measurement Techniques - Phase II

Subject: Monthly Status Report No. 1

A summary of progress on the referenced contract for the period 15 November through 30 November 1974 is contained herein. The effective starting date of the contract was 15 November 1974. This program has been designated at Georgia Tech as Engineering Experiment Station Project A-1694. The project is under the overall supervision of Dr. H. A. Ecker, Chief of the Radar Division. The project has been assigned to the Electromagnetic Effectiveness Technical Area, under Mr. F. L. Cain, with Mr. J. D. Adams as the Project Director. To facilitate the reporting of manpower expenditures, future status reports will be made on a calendar month basis, beginning with the December 1974 period. Thus, the present status report covers a period of only fifteen days. To keep the RADC project engineer fully informed and up-to-date on project activities, status reports will be reasonably detailed and complete.

The technical efforts to be included in this research program may be divided into three major tasks. Task 1 involves the design completion, breadboarding, and checkout of an amplitude only (Hybrid System) S-band (2-4 GHz) broadband measurement system. This system will be based upon preliminary design information contained in the Final Report on Contract F30602-73-C-0194. The system will be capable of providing either CW or broadband antenna gain and pattern information over any preselected frequency range within the 2-4 GHz band. The breadboard system will utilize a linearly polarization transmit antenna. However, analysis will be conducted to define the measurement error associated with various degrees of departure from a perfectly circularly polarized test signal. This analysis will be conducted so that specifications can be developed for future circularly polarized transmit antennas.

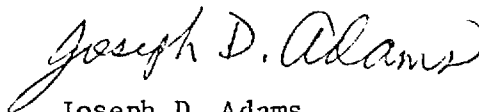
Task 2 will involve expanded design and analysis of a computer-controlled broadband phase-plus-amplitude antenna measurement system. These efforts will include tradeoff analysis between direct phase reference measurement techniques and group velocity phase measurement techniques, accuracy versus cost and complexity tradeoffs, and completion of a recommended preliminary system design. Task 3, pulse distortion analysis, will develop tools to use measured phase and amplitude data to predict antenna response to broadband pulses.

During this reporting period, review of the Hybrid system design, component requirements, and hardware availability has been initiated. Overall project planning and milestone schedules have been prepared. The Task 1 (Hybrid System) milestone chart illuminates the relatively "tight" schedule which must be maintained to insure completion of the Hybrid system within the contract period. However, the situation is not critical unless unusually severe delays in hardware deliveries are experienced. It is planned that purchase orders will be placed beginning in early January so that any potential problem areas can be identified at an early date.

Next month, efforts on Task 1 will include continued design review and completion and the updating of component tradeoffs and selection. Contacting of potential suppliers will begin so that current delivery and price data can be obtained. On 4 December, Mr. J. D. Adams will visit RADC to discuss project planning and scheduling and technical tasks requirements with the RADC project engineer.

During this reporting period, it is estimated that 27 professional man-hours were expended and that approximately 1% of the technical effort has been completed. These estimates also are cumulative because this is the first reporting period.

Respectfully submitted,



Joseph D. Adams  
Project Director

Approved:



Fred L. Cain  
Technical Area Manager  
Electromagnetic Effectiveness





# ENGINEERING EXPERIMENT STATION

GEORGIA INSTITUTE OF TECHNOLOGY • ATLANTA, GEORGIA 30332

13 January 1975

Rome Air Development Center  
Griffiss Air Force Base,  
New York 13441

Attention: Mr. Martin Jaeger, OCTS

Reference: Contract No. F30602-75-C-0065

Title: "Broadband Antenna Measurement Techniques-Phase II"

Subject: Monthly Status Report No. 2

Dear Sir:

A summary of progress on the referenced contract for the period 1 December through 31 December is contained herein. During the month, a trip was made to RADC to discuss detailed research plans for the project. Technical efforts were concentrated on design review and hardware tradeoffs for the Hybrid system.

On 4 December, Mr. J.D. Adams visited the RADC Project Engineer to discuss project planning, scheduling, and technical task requirements. Organization of the project into three major tasks with milestone schedules for each was discussed. Initially, efforts will be concentrated on Task 1, Hybrid system design and breadboarding. This concentration of effort is necessary so that the Hybrid system design can be completed, hardware specifications can be defined, and hardware availability can be determined at an early date. As these efforts proceed, purchase orders will be placed. It is hoped that in this way, delays due to purchase leadtimes can be either reduced or avoided. Efforts on Task 2, phase/amplitude system design and analysis, will be spread throughout the contract period at a relatively constant rate. It is currently planned that efforts on Task 3, pulse distortion analysis, will begin in February, and then be completed within three or four months.

During December, efforts on the Hybrid system task involved further definition of hardware requirements for the transmitter and the RF portion of the receiver, along with a review of commercially available components. As part of this review, vendors were contacted to obtain updated price and delivery information. As expected, substantial price increases either have been put into effect or have been planned for 1975. Purchase requests are currently being prepared for the transmitter sweep oscillator, the TWT amplifier, and the receiver low noise amplifier. These requests will be released to Georgia Tech purchasing early in January. Two of these items (the sweep oscillator and the TWT amplifier) will cost over \$1000,

and, hence, Air Force approval must be obtained before their purchase is completed. However, this approval cannot be requested until negotiations have been completed and the particular manufacturer's model and price are known.

During December, Mr. W.P. (Bill) Cooke was added to the project staff as a full-time member. Mr. Cooke is an experienced electrical engineer, having been a full-time research engineer at Georgia Tech since 1972. Prior to that time, he was a graduate research assistant for two years. Initially, Mr. Cooke will be primarily responsible for completing the design and breadboarding of the data processor and controller portions of the Hybrid system. Effort in these areas was begun in December.

Next month, efforts on Task 1 will include continued component reviews and tradeoffs, release of some purchase requests, and continued detailed design in the data processor and controller areas. On Task 2, optimum phase measurement tradeoffs and accuracy studies will be initiated.

During this reporting period, it is estimated that 169 professional manhours were expended. It is estimated that the cumulative professional manhours expended since contract initiation is 196 and that approximately 6% of the technical effort has been completed.

Respectfully submitted,



Joseph D. Adams  
Project Director

Approved:



Fred L. Cain  
Technical Area Manager  
Electromagnetic Effectiveness

A-1694



# ENGINEERING EXPERIMENT STATION

GEORGIA INSTITUTE OF TECHNOLOGY • ATLANTA, GEORGIA 30332

12 February 1975

Rome Air Development Center  
Griffis Air Force Base,  
New York 13441

Attention: Mr. Martin Jaeger, OCTS

Reference: Contract No. F30602-75-C-0065

Title: "Broadband Antenna Measurement Techniques-Phase II"

Subject: Monthly Status Report No. 3

Dear Sir:

A summary of progress on the referenced contract for the period 1 January through 31 January is contained herein. During this reporting period, efforts have focused on further design and hardware definition of the Hybrid system. In addition, efforts were initiated on the pulse distortion analysis task.

As indicated in Monthly Status Report No. 2, contract efforts are initially being concentrated on Task 1, Hybrid system design and breadboarding. This concentration of effort is necessary so that the Hybrid system design can be completed, hardware specifications can be defined, hardware availability can be determined, and purchase orders can be placed at the earliest practical date. It is hoped that in this way, delays due to purchase leadtimes can be either reduced or avoided. During January, final selection was made of several microwave components for the Hybrid system transmitter and receiver. Since the sweep oscillator and the traveling wave tube amplifier (TWTA) will cost over \$1,000 each, competitive bids are required for their purchase. Request for bids have been issued for both of these items. Bids for the TWTA have been received and reviewed by project personnel. Of the bids meeting required specifications, the best offer was made under an existing General Services Administration (GSA) contract. RADC approval to purchase under the GSA contract will be required, and it has been requested. Bids for the sweep oscillator have not yet been received.

Except for the sweep oscillator and the TWTA, sole-source procurement will be used. Source selection for these other components is by project technical personnel, based on surveys of known manufacturers and a cost effectiveness tradeoff between candidate components. Components in this category which have been selected and for which purchase requests

have been issued include (1) a directional detector for transmitter power leveling, (2) a low-noise receiver amplifier, (3) a broadband coupler and detector for power monitoring at the receiver, (4) a wide dynamic range detector which provides the video output for processing, and (5) a bandpass filter to reject possible interfering signals at the receiver input. These components and their general requirements have been previously discussed in the Final Report on Contract F30602-73-C-0194. Required microwave components for which a final selection has not yet been made include the transmit antenna and a single-pole/double-throw (SPDT) switch for switching the receiver between the test and the reference antennas. Switch candidates are currently being evaluated. It is expected that transmit antenna design will be finalized early in March.

Previously, the Hybrid system has been considered to consist of transmitter, receiver, and data processor subsystems. However, for further clarity in discussion, the data processor and the logic controller are now considered as individual subsystems. The data processor subsystem acts on the detected receiver output, from both the reference antenna and the test antenna, to produce an "average" antenna response over the desired frequency range. Recall that the Hybrid system "time shares" inputs from the test antenna and the reference antenna. The logic control subsystem is responsible for controlling the time sharing of the receiver and the data processor subsystems, and for synchronization of these subsystems with transmitter sweep cycles.

The circuit design for the data processor subsystem has been finalized. However, it is anticipated that as the development of this subsystem moves into the construction phase, minor hardware changes may be required. Components required to construct this unit have been selected, and it is planned that a purchase request for most of these components will be released next month. The costs for purchasing some of these components have increased significantly over that originally anticipated by Georgia Tech. In one case, current cost and performance data were requested on a particular sample-and-hold module previously considered appropriate for use in the data processor. Not only has the unit cost of the module increased, but the manufacturer revealed that certain previously published critical specifications could not be met. Current data indicate that an appropriate sample-and-hold module will cost approximately twice that originally anticipated.

Various approaches to a circuit design for the logic control subsystem have been identified and reviewed. Currently, selected circuit designs are being further examined to determine what tradeoffs may exist when considering performance, interface requirements, and overall system costs. Final selection of a logic control subsystem circuit design requires some specific

Monthly Status Report  
Contract No. F30602-75-C-0065  
12 February 1975

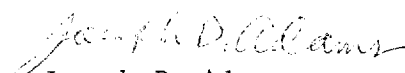
Page 3

information about the sweep oscillator's sweep accuracy; this information will be obtained from the manufacturer of the selected sweep oscillator.

Next month, efforts on Task 1 will be devoted to the final design of the transmit antenna, the selection of the SPDT switch, the release of purchase requests for data processor components, and the continued analysis of logic control circuit designs. It is anticipated that a tentative list of the components required to construct this unit will be selected, and information on their availability will be obtained from appropriate manufacturers. Efforts on Task 3, pulse distortion analysis, involve the development of a computer program for calculating pulse distortion for broadband antennas whose complex (phase plus amplitude) transfer function has been empirically determined. An existing Fast Fourier Transform algorithm will be adapted for the program in order to efficiently perform the necessary computations, and computer graphics techniques will be used to display the distorted pulse shapes. Next month, it is anticipated that the computer algorithms will be coded and de-bugged and that preliminary test calculations will be performed to check for proper execution of the program.

During this reporting period, it is estimated that 279 professional manhours were expended. It is estimated that the cumulative professional manhours expended since contract initiation is 475 and that approximately 14% of the technical effort has been completed.

Respectfully submitted,



Joseph D. Adams  
Project Director

Approved:



Fred L. Cain  
Technical Area Manager  
Electromagnetic Effectiveness



A-1694

# ENGINEERING EXPERIMENT STATION

GEORGIA INSTITUTE OF TECHNOLOGY • ATLANTA, GEORGIA 30332

13 March 1975

Rome Air Development Center  
Griffis Air Force Base,  
New York 13341

Attention: Mr. Martin Jaeger, OCTS

Reference: Contract No. F30602-75-C-0065

Title: "Broadband Antenna Measurement Techniques - Phase II"

Subject: Monthly Status Report No. 4

Dear Sir:

A summary of progress on the referenced contract for the period 1 February through 28 February is contained herein. During this reporting period, efforts have continued on further design and hardware definition of the Hybrid system, computer software for calculating pulse distortion has been modified and debugged, and further tradeoff studies for the phase/amplitude system were begun.

During February, microwave hardware tradeoffs for the transmitter and the receiver were completed, and all remaining purchase orders were placed. As indicated in Monthly Status Report No. 3, RADC approval to purchase the traveling wave tube amplifier (TWTA) under General Services Administration (GSA) contract was requested. This approval was obtained from the administrative contracting officer, and as a result of competitive bidding, a purchase order for the TWTA was placed under an existing GSA contract with Hughes Aircraft. Delivery of the TWTA is expected near the end of April.

For the sweep oscillator, the Weinschel Engineering Company bid was accepted as being the lowest priced unit providing the required performance and quality. Delivery of this unit is expected during the latter part of March. All other transmitter and receiver components have been ordered, and expected delivery times vary from early March to late April. Of course, component checkout and subsystem assembly will begin before all components are received.

The design of the data processor subsystem, after thorough review and hardware tradeoffs, has reached the breadboard construction state of development. The circuit design for this subsystem is basically the same as the preliminary design discussed in the Final Technical Report on Contract No. F30602-73-C-0194. However, some refinements have been made. These re-

finements include a more accurate integrator circuit and the addition of amplifiers to maintain voltage levels within the proper range at all points in the circuit. Component requirements for the data processor include five operational amplifiers (Op Amps), three sample-and-hold amplifiers (SHAs), and one logarithmic amplifier (Log Amp). Performance and cost data on candidate devices in each of these categories have been thoroughly reviewed. One Op Amp which can be used in all of the data processor functional modules requiring Op Amps (integrate, log, and subtract) has been identified and ordered. Also, a suitable Log Amp has been identified and ordered.

With regard to the sample-and-hold amplifiers, it was reported in Status Report No. 3 that the device originally intended for use here had been found to be unsatisfactory due to the manufacturer's change in certain specifications. For the current application, two SHA device parameters are of critical importance. These two parameters are (1) the time required to acquire the input signal upon command, and (2) how accurately the sampled voltage is maintained during the "hold" interval. These two parameters can generally be traded one for the other. However, simultaneously meeting the current requirements on both parameters dictate a high performance SHA. Three units which have potential for meeting design requirements at a reasonable price have been identified. Arrangements have been made to obtain no obligation samples of each of these three units for laboratory evaluation. Upon completion of these evaluations, the selected unit will be retained (i.e., purchased), and the others will be returned.

Investigations to determine a cost-effective transmit antenna design that will satisfy the necessary Hybrid system requirements were continued this month. Conceptually, a paraboloidal dish with an appropriate feed is an attractive antenna design for the Hybrid system. In order to insure that an adequate power density is incident on the receiving antenna under test, the gain of the antenna must be approximately 30 dB at the upper end of the 2.0 to 4.0 GHz band. Because the space attenuation is 6 dB less at the low end of the frequency band of interest (2.0 GHz), a constant gain antenna is not required. Under ideal conditions, the transmit antenna gain at 2.0 GHz would be exactly 6 dB less than it is at 4.0 GHz. Consequently, the reduced transmit antenna gain would be offset by the reduced space loss, resulting in the same power density incident on the test antenna across the 2.0 to 4.0 GHz band. These ideal results, however, require that the phase and amplitude illumination function across the aperture of the paraboloidal dish be identical at all frequencies across the 2.0 to 4.0 GHz frequency band. These illumination functions cannot be ideally achieved with simple practical feed systems because both the phase center and the amplitude illumination pattern generally change with frequency. Fortunately, however, it is not critical that the incident power density at the test antenna remain constant because any variation in incident power density will be accounted for by

the Hybrid system data processor in conjunction with a known reference antenna.

In the antenna investigations this month, several commercial antenna feed systems and paraboloidal dishes were reviewed for possible applicability. In addition, several designs previously developed at Georgia Tech have been considered. The results of the investigations indicate that a concept involving a waveguide feed slightly loaded with low-loss dielectric material to increase the bandwidth of the feed itself should be experimentally studied in conjunction with an existing paraboloidal dish.

Work is continuing on the development of the computer program for pulse distortion analysis. This month, the FFT (Fast Fourier Transform) subroutine was de-bugged and successfully tested for proper execution, and a computer graphics subroutine was developed to visually display the distorted output time domain pulse. For these program execution tests, several different incident time domain pulses and relatively simple frequency domain antenna response data were assumed. The resulting time domain pulse output was studied and checked for proper characteristics. The assumed incident pulse shapes included "cosine bell" pulses with 3 dB pulse widths of 1, 2, and 3 nanoseconds. The rise and fall time of the 1 nanosecond pulse was 0.5 nanosecond, and the rise and fall time of both the 2 and 3 nanosecond pulses was 1 nanosecond. The assumed antenna response consisted of linear amplitude and phase variations over the bandwidth of the incident pulses. For these initial tests, the incident pulse amplitude and the antenna response data were assumed for the same frequency increments. However, in practical applications, the actual discrete frequencies for which the antenna response is measured and for which the incident pulse amplitude is known may not exactly coincide. Consequently, work was also initiated this month to develop a subroutine to perform frequency interpolations on a measured data set.

To assist in the phase/amplitude system tradeoff analysis, a sub-contract for Scientific-Atlanta (S-A) support services was issued. Currently, S-A is addressing the advisability of modifying an existing Government owned Series 1750 Receiver to provide a swept frequency phase/amplitude measurement capability. Initial indications are that this approach would not be significantly less costly than purchasing one of the new swept frequency phase/amplitude receivers currently under development at S-A. This conclusion is based on an assumption that S-A will have the new receiver series essentially developed to production status by the time it is required for the application under consideration now.

Next month, breadboard testing of the data processor will begin. Design of the logic control subsystem will be completed and parts will be ordered. De-bugging of the various elements of the pulse distortion analysis



Monthly Status Report No. 4  
Contract No. 30602-75-C-0065  
13 March 1975

page 4

program will continue, and more realistic trial data will be run. Experimental studies of a possible Hybrid system transmit antenna will be performed.

During this reporting period, it is estimated that 391 professional manhours were expended. It is estimated that the cumulative professional manhours expended since contract initiation is 866 and that approximately 25% of the technical effort has been completed.

Respectfully submitted,



Joseph D. Adams  
Project Director

JDA:jm

Approved:



Fred L. Cain  
Technical Area Manager  
Electromagnetic Effectiveness

A-1694



## ENGINEERING EXPERIMENT STATION

GEORGIA INSTITUTE OF TECHNOLOGY • ATLANTA, GEORGIA 30332

14 April 1975

Rome Air Development Center  
Griffiss Air Force Base,  
New York 13341

Attention: Mr. Martin Jaeger, OCTS

Reference: Contract No. F30602-75-C-0065

Title: "Broadband Antenna Measurement Techniques - Phase II"

Subject: Monthly Status Report No. 5

Dear Sir:

A summary of progress on the referenced contract for the period 1 March through 31 March is contained herein. During this reporting period, efforts have continued on evaluation of sample-and-hold amplifiers for the Hybrid system, refinement of computer software for the pulse distortion analysis has continued, a possible transmit antenna feed design was evaluated, and phase/amplitude system studies were begun.

As reported in Monthly Status Report No. 4, three sample-and-hold amplifier (SHA) modules are being evaluated for possible use in the data processor subsystem of the Hybrid system. Two different modules were obtained from Optical Electronics, Inc. (OEI), and the third module was obtained from Analog Devices. A summary of manufacturer's specifications for these units is given in Table I. In selecting samples for evaluation, a fourth unit, the Analog Devices SHA-4, was also considered. However, the SHA-4 differs from the SHA-3 in only one parameter which is not considered critical in the present application. Hence, laboratory tests of the SHA-3 for the Hybrid system data processor will also be applicable to the SHA-4. Costs of the three units shown in Table I are not significantly different.

Critical parameters for this application include: (1) droop rate--reflects how accurately the "sampled" voltage is maintained during the "hold" interval, (2) acquisition time--reflects the time required to switch from the "sample" to the "hold" mode, and (3) settling time--refers to the time required for the SHA output to "settle" after a step perturbation at the SHA input. Analyses have established acceptable performance guidelines for these three parameters as 10 $\mu$ V/msec, 300 msec, and 150 msec, respectively. Based on the manufacturer's specifications given in Table I both the Analog Devices SHA-3 and the OEI 5022 should meet these requirements. With the OEI 5021, values of these parameters depend on the size of an external capacitor which the user provides.

TABLE I

Manufacturer's Specifications for Selected  
Sample-and-Hold Amplifiers

MODEL SPECIFICATIONS	ANALOG DEVICES SHA-3	OEI 5022	OEI 5021
Settling time (sample-to-hold)	10 $\mu$ s to within 1 mV of final value	3 $\mu$ s to within 0.1%	(1)
Acquisition time	75 $\mu$ s to 0.01% of value	6 $\mu$ s	(1)
Droop rate	10 $\mu$ V/ms max	typ. 5 mV/ms	(1)
Aperture Delay	50 ns	1 $\mu$ sec max	(1)
Ext. Capacitor Capability	yes	yes	yes
Cost (1-9 units)	\$105	(1-2) \$108 (3-9) \$97	(1-2) \$112 (3-9) \$102
(1) The OEI 5021 does not have an internal capacitor. The user must provide one.			

Acceptable performance was not obtained during tests on the OEI 5021; depending on the size of the external capacitor which is used, either the droop rate or the acquisition time is unacceptable. Tests on the Analog Devices SHA-3 indicate that acceptable performance is being obtained in terms of the three parameters previously discussed. However, in these tests, this unit has exhibited undesirable noise on the output signal. This performance is contrary to expectations, and further investigation to locate the source of this difficulty is in progress.

With regard to the OEI 5022, the manufacturer has recommended use of a special circuit, designed by OEI, to obtain optimum performance from this unit. Initial results with this circuit and the OEI 5022 were unsatisfactory. In discussing these results with OEI, the difficulty was attributed to Georgia Tech's substitution of an equivalent transistor and diode. These substitutions were originally made because of their ready availability. The recommended transistor and diode (Texas Instruments products) have been ordered, and further evaluation will be conducted when they are received.

Efforts this month on the computer program for pulse distortion analysis primarily involved development of the frequency interpolation subroutine and test executions of the entire program for an assumed set of dispersive antenna response data. As mentioned in Monthly Status Report No. 4, frequency interpolation is required since the actual discrete frequencies for which the antenna response is measured may not correspond to those frequencies for which the incident pulse amplitude is known. The interpolation subroutine, which has been designated "CRVFIT," has been developed and partially debugged. The subroutine presently executes properly except for interpolation between data points which are very near the ends of the measured data set. Various techniques are being investigated for eliminating this problem, and the most suitable technique will subsequently be incorporated in the subroutine. The pulse distortion program was used this month to compute the distorted time domain pulses for an incident "cosine bell" pulse (2 nanosecond pulsewidth) propagated down various lengths of waveguide. Preliminary analysis of the distorted pulses indicate that the overall distortion effects are in agreement with theory. Additional computations and analyses will subsequently be performed after the interpolation subroutine is modified for proper execution near the endpoint data.

As a first cut effort to obtain a broadband transmit antenna, pattern tests were performed to characterize a dielectrically loaded C-band waveguide feed with a paraboloidal dish for operation at S-band. These pattern tests

Monthly Status Report No. 5  
Contract No. F30602-75-C-0065  
14 April 1975

page 4

indicate that because of the octave bandwidth requirement (2-4 GHz) with the attendant possibility of propagating higher-order modes in the feed, the dielectrically loaded waveguide approach may not be satisfactory. Currently, use of a rather simple double-ridged rectangular waveguide feed is being evaluated. Design information on ridged waveguide feeds covering various frequency ranges has been reported, and it is being evaluated.

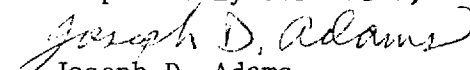
Scientific-Atlanta (S-A) has addressed the advisability of modifying a Series 1750 phase/amplitude receiver to provide a swept-frequency phase/amplitude measurement capability. Scientific-Atlanta judges this approach to be economically unsound. This judgement is based on the high probability that S-A will have swept-frequency phase/amplitude receivers by the time such a capability is required for this application. The possibility of obtaining one of these new receivers for feasibility demonstrations of a complete computer controlled phase/amplitude antenna measurement system will be explored with S-A management.

Several components for various subsystems were received during the month. They include the receiver low noise amplifier, the transmitter TWTA, and several components for the data processor. Delivery of components should now accelerate, with several expected during April.

Next month work will continue on SHA evaluations, transmit antenna design, pulse distortion analyses, and further definition of the phase/amplitude system. In addition, the RADC Project Engineer is expected to visit Georgia Tech to review program efforts to date.


During this reporting period, it is estimated that 404 professional manhours were expended. It is estimated that the cumulative professional manhours expended since contract initiation is 1270 and that approximately 37% of the technical effort has been completed.

Respectfully submitted,

  
Joseph D. Adams  
Project Director

JDA:jm

Approved:

  
Fred L. Cain  
Technical Area Manager  
Electromagnetic Effectiveness

A-1694



# ENGINEERING EXPERIMENT STATION

GEORGIA INSTITUTE OF TECHNOLOGY • ATLANTA, GEORGIA 30332

13 May 1975

Rome Air Development Center  
Griffiss Air Force Base,  
New York 13441

Attention: Mr. Martin Jaeger, OCTS

Reference: Contract No. F30602-75-C-0065

Title: "Broadband Antenna Measurement Techniques-Phase II"

Subject: Monthly Status Report No. 6

Dear Sir:

A summary of progress on the referenced contract for the period 1 April through 30 April is contained herein. During this reporting period, evaluation of sample-and-hold amplifiers for the Hybrid system data processor was completed and a purchase order was placed for the selected unit, further definition of the direct phase measurement phase-and-amplitude system continued, the frequency interpolation subroutine of the pulse distortion analysis program was refined and properly executed, and a double-ridged rectangular waveguide feed for the transmit antenna was designed. In addition, the RADC project engineer visited Georgia Tech on 2 and 3 April to review project accomplishments and plans.

As reported in Monthly Status Report No. 5, the pulse distortion analysis program requires a frequency interpolation subroutine since the actual discrete frequencies for which antenna response is measured may not correspond to those frequencies for which incident pulse amplitude is known. Consequently, interpolation would be required to produce both antenna and pulse data at corresponding frequencies. During this reporting period, the frequency interpolation subroutine, called "CRVFIT", has been modified to correct for a previously reported improper execution near the end points of a data set. The pulse distortion analysis program has been executed with the modified subroutine for both 1 and 2 nanosecond incident "cosine bell" pulses propagated down various lengths of waveguide. Analysis of the calculated distorted pulses indicate that the results are in agreement with theory, and that the program is executing properly. Currently, efforts are under way to expand the main program so that it will accept discrete arbitrary time domain data points in lieu of analytically generated data points.

Recall that for phase and amplitude measurements, both a direct phase measurement and group velocity concepts are being evaluated. Recent efforts on the phase/amplitude system have concentrated on determining the projected

hardware availability and the system configuration for a direct phase measurement system. It has been previously reported that Scientific-Atlanta (S-A) has addressed the advisability of modifying a Series 1750 Phase/Amplitude receiver to provide a swept frequency phase/amplitude measurement capability. This approach was judged to be economically unsound, based on S-A's projected availability of a new receiver series. Scientific-Atlanta personnel have indicated that this new receiver series will be ready for pilot production by January 1976. Several engineering models of this receiver have been built; three models are now being assembled for delivery to customers. Indications are, then, that S-A has overcome the technical problems which are involved in developing a tracking swept frequency phase/amplitude receiver. Advance product information on this new instrument is being used to refine the preliminary direct phase/amplitude measurement system design which was presented in the Final Technical Report on Contract F30602-73-C-0194. Indications are that under computer control and with the proper interfaces, this instrument will be suitable for the receiver of a direct phase measurement swept frequency system. Efforts are currently under way to define a compatible hardware system with a consistent and practical set of operating parameters (sweep rate, sweep time, sample rates, storage requirements, etc.). As the direct phase measurement system becomes more defined, efforts to expand and up-date preliminary design of the group velocity system will be accelerated so that a direct comparison of the two approaches can be made.

Investigations to determine a cost-effective transmit antenna design were continued this month. As reported in Monthly Status Report No. 5, use of a double-ridged rectangular waveguide feed appears to be an attractive approach. Adding the double ridges to standard S-band waveguide will lower the cutoff frequency below 2 GHz without leading to the possibility of higher order modes at 4 GHz (as would occur with dielectrically loaded S-band guide). A feed horn design which incorporates the double-ridges is ready for fabrication. This double-ridged feed will be fabricated so that, if required, minor modifications can be relatively easily accomplished during pattern test on the transmit antenna.

During this reporting period, evaluation of the sample-and-hold amplifier (SHA) modules described in Monthly Status Report No. 5 was completed. Acceptable performance guidelines for these modules were described in that Status Report. Three modules, the Analog Devices SHA-3 and Optical Electronics, Inc. (OEI) Models 5022 and 5021, were evaluated. These three modules were selected because their published specifications indicated that they had potential for meeting performance guidelines at relatively low unit cost. It was claimed by OEI that with proper choice of an external capacitor the 5021 would meet our performance guidelines; it was further claimed that use of a special zero droop rate circuit designed by OEI would lead to optimum results

with the 5022. It should be noted that the manufacturer's performance specifications given in Table I of Status Report No. 5 for the OEI 5022 do not reflect use of this special circuit.

The performance of these three SHA modules was determined with respect to droop rate, settling time, and acquisition time. Measurements of these SHA module capabilities in these areas were considered to provide a good indication of their performance for this application. Data were recorded for a variety of input voltage levels, hold times, etc.

The OEI model 5022 failed before it was completely evaluated and before its performance using the zero droop rate circuit could be determined. However, based on the performance of the OEI model 5021 with the zero droop rate circuit, it is reasonable to assume that use of this circuit would not have improved the performance of the model 5022 sufficiently to make it suitable for use in the data processor subsystem. Measured data for the OEI model 5022 with an external capacitor shows it does not have the needed capabilities to meet design requirements even under these conditions.

The droop rate performance of the OEI modules was never satisfactory, using either external capacitors or the zero droop rate circuit. Another area of marginal performance was the magnitude of input signal feedthrough to the output. It must be noted, however, that use of the zero droop rate circuit did affect droop performance without degrading acquisition or settling time.

The performance of the Analog Devices SHA-3 was superior with respect to droop rate, settling time, acquisition time, and input signal feedthrough. The only area in which the SHA-3 did not excel was in the noise level, and this is not considered to be a problem here. Also, due to the excellent performance of the SHA-3, it has the capability to accept some additional capacitance for droop rate reduction (currently, it does not appear that this will be necessary) without increasing acquisition time beyond performance guidelines.

Based on these results, the SHA-3 is seen to be the better of the SHA modules tested for use in the data processor subsystem. However, a potential problem with the SHA-3 (as well as the OEI modules) is that when switched from hold to sample, switching transients up to several volts were observed depending on the type of input applied. Specifications on this parameter were not included in initial catalog data, and therefore, switching transients were not considered to be a problem. As discussed in Monthly Status Report No. 5, the performance of the Analog Devices modules SHA-3 and SHA-4 only differ in one area. Fortunately, according to the latest detailed information, the SHA-4 has improved switching performance with the



Monthly Status Report No. 6  
Contract No. F30602-75-C-0065  
13 May 1975


page 4

maximum switching transient for the SHA-4 being only 200 mV while for the SHA-3 it is 7V. As a result, the SHA-4 has been ordered for use throughout the data processor.

Next month, work will continue on the breadboarding and test of circuits for the logic control subsystem, transmit antenna fabrication and test, pulse distortion analysis program development, and further definition of the direct measurement phase/amplitude system.

During this reporting period, it is estimated that 425 professional manhours were expended. It is estimated that the cumulative professional manhours expended since contract initiation is 1695 and that approximately 45% of the technical effort has been completed.

Respectfully submitted,



Joseph D. Adams  
Project Director

JDA:jm

Approved:



Fred L. Cain  
Technical Area Manager  
Electromagnetic Effectiveness



# ENGINEERING EXPERIMENT STATION

GEORGIA INSTITUTE OF TECHNOLOGY • ATLANTA, GEORGIA 30332

17 June 1975

Rome Air Development Center  
Griffiss Air Force Base,  
New York 13441

Attention: Mr. Martin Jaeger, OCTS

Reference: Contract No. F30602-75-C-0065

Title: "Broadband Antenna Measurement Techniques - Phase II"

Subject: Monthly Status Report No. 7

Dear Sir:

A summary of progress on the referenced contract for the period 1 May through 31 May is contained herein. During this reporting period, on-site storage requirements for the direct phase measurement amplitude-plus-phase system were addressed, detailed design of the logic control subsystem of the Hybrid system was finalized, breadboard construction of the data processor subsystem was begun, and the remainder of the major equipment items of the Hybrid system were received.

As indicated in Monthly Status Report No. 6, efforts are underway to design a direct phase measurement swept frequency system which employs a new Scientific-Atlanta (S/A) tracking phase measurement receiver. During the past month, the data rate and the total data quantity, data conditioning and recording, and data analyses have been addressed for this system. The data rates which can be achieved with the new S/A swept frequency receivers (Series 1700) will be essentially the same as those which are achievable with the current S/A Series 1750 receivers. The maximum data rate will be limited by the bandwidth of the receiver's output circuits, which is approximately 100 Hz. In addition, a maximum receiver frequency tracking rate of 10 MHz/msec must be observed. Assuming a 1 GHz frequency sweep range (the 1-2 GHz octave, for example), compatible spatial and frequency sampling rates have been identified, and the corresponding total data requirements for various antenna pattern cuts have been defined.

The RADC owned Raytheon 703 minicomputer can accommodate the above identified maximum data rate while storing frequency, amplitude, and phase data words at each spatial sample point. Recall that with this broadband phase/amplitude system, the antenna under test would normally be continuously rotated, and at the prescribed spatial sample points the test frequency

would be stepped across the measurement interval (1-2 GHz in this example). With a maximum frequency track rate of 10 MHz/msec, an appropriate spatial scan rate is on the order of 0.15 deg/sec. At this spatial scan rate, forty minutes are required to scan a full 360 degrees.

While the Raytheon 703 minicomputer has an adequate memory cycle rate, its storage capacity is insufficient for the intended application. For example, a typical data set might consist of frequency, amplitude, and phase data at each of 10 frequencies for each of the spatial sample points of an antenna pattern cut (30 data words at each spatial point). Spatial sampling each 0.1 degree for a 180 degree pattern therefore requires 54,000 data words. The basic Raytheon 703 has only a 4096 word storage capacity. Fortunately, additional storage can be provided, either through addition of memory blocks to the Raytheon 703 or through the use of auxiliary devices such as a cassette recorder. The above and other questions are currently being addressed in detail in the overall phase/amplitude system design.

Regarding development of the computer program for pulse distortion analysis, efforts this month were primarily directed toward (1) developing the capability to input discrete time domain pulse data, (2) inserting appropriate explanatory comments to aid the user in executing the program, and (3) modification of previously-existing plotting subroutines in order to graphically display the distorted pulses. Items (1) and (2) are essentially completed, and only minor modifications are needed on Item (3).

Development of the Hybrid system data processor subsystem and logic controller subsystem continued during the month of May. The logic controller subsystem is responsible for providing five sets of digital commands to segments of the Hybrid system. These commands are an integrate or dump command to the integrator, commands to three sample and hold amplifiers, and a command to control the antenna selection switch. This switch allows the Hybrid system to process data from either the reference antenna or the test antenna. The logic controller subsystem monitors the response of the sweep generator through the reference antenna and uses this information to synchronize its operations with the sweep generator.

The logic controller must provide not only digitally compatible commands to each stage, but these commands must be precisely timed in order for the system to function properly. Built into the logic controller are circuits designed to preset the system and to reset it after each sweep of the sweep generator. The reset capability reduces the probability of errors causing the subsystem to generate false commands.

Monthly Status Report No. 7  
Contract No. F30602-75-C-0065  
17 June 1975

page 3

After thorough review, the circuit design for the logic controller subsystem has been finalized. Performance and cost data for the necessary digital hardware were obtained from a variety of potential vendors. In a manner similar to that previously used for selecting hardware for the data processor subsystem, cost and performance data were examined to determine what hardware tradeoffs could be made to minimize overall construction cost while maintaining or improving system performance. As a result of these efforts, the necessary digital hardware have been identified and purchase orders for these items have been submitted. The majority of these items have been received, and it is anticipated that the remaining digital hardware will arrive next month.

Construction of the data processor subsystem was initiated during this month. Beginning with the integrator (first stage), and continuing with subsequent stages, each stage is being individually constructed and tested before going on to the next section. This approach allows the ability to evaluate the performance of each stage and to determine any deviation from expected operational characteristics.

Construction of the double-ridged rectangular waveguide feed, which was described in Monthly Status Report No. 6, was completed during May. In addition, the remaining two microwave hardware components were received from their vendors. Consequently, assembly and checkout of the transmitter, receiver, and transmit antenna can be completed.

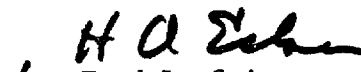
Next month, efforts will include breadboard construction, assembly, and testing of various subsystems of the Hybrid system, completion of the pulse distortion analysis program, and further design definition of the group velocity type of phase measurement system.

During this reporting period, it is estimated that 330 professional manhours were expended. It is estimated that the cumulative professional manhours expended since contract initiation is 2025 and that approximately 55% of the technical effort has been completed.

Respectfully submitted,

  
Joseph D. Adams  
Project Director

Approved:

  
Fred L. Cain  
Manager,  
Electromagnetic Effectiveness



# ENGINEERING EXPERIMENT STATION

GEORGIA INSTITUTE OF TECHNOLOGY • ATLANTA, GEORGIA 30332

16 July 1975

Rome Air Development Center  
Griffiss Air Force Base,  
New York 13441

Attention: Mr. Martin Jaeger, OCTS

Reference: Contract No. F30602-75-C-0065

Title: "Broadband Antenna Measurement Techniques - Phase II"

Subject: Monthly Status Report No. 8

Dear Sir:

A summary of progress on the referenced contract for the period 1 June through 30 June is contained herein. During this reporting period, the pulse distortion analysis task was essentially completed, checkout of the Hybrid system subsystems was begun, and design definition of phase plus amplitude measurement systems was continued.

The pulse distortion analysis computer program employs Fast Fourier Transform (FFT) techniques to predict the distortion effects of a bandlimited component on a broadband pulse. Use of the FFT allows rapid and efficient digital computer computation of these effects. Input data requirements to the computer program include the pulse amplitude versus time and the complex (amplitude and phase) transfer function of the component (e.g., antenna) whose distortion effects are to be calculated. The computer program has been developed so that these input data sets may be in the form of either an analytical expression or discrete measured data points. In the case of discrete input data, subroutines perform any interpolation which may be required to obtain compatible sets of data at the required time and frequency intervals. For demonstration and validation, the program has been used to compute the distortion effects on three different broadband pulses (1, 3, and 5 nanosecond 3-dB pulsewidths) due to propagation of each pulse down three different lengths of X-band waveguide. For these computations, the amplitude of the complex transfer function was set equal to the frequency-dependent transmission coefficients at the interface between free space and the waveguide. The phase of the complex transfer coefficients was calculated from standard waveguide equations as a function of both frequency and waveguide length. For illustration, the incident 1 nanosecond

pulse and the resulting distortions are shown in Figures 1 through 4. From the complete family of curves, useful insights into pulse distortion effects have been obtained. To aid in utility of the program to other users, a complete flow diagram has been prepared and descriptive comments are currently being incorporated. Upon completion, a copy of the program can be supplied to RADC either in the form of a card deck or a magnetic tape.

During checkout of various Hybrid system subsystems, some severe equipment difficulties were experienced. Recall that the transmitter subsystem consists of a sweep oscillator, a travelling wave tube (TWT) power amplifier, and associated power leveling and band controlling components. During transmitter checkout, the sweep oscillator was found to be defective. When operating properly, RF output from this sweeper can either be set to any fixed frequency within the 2-4 GHz band or it can be swept across the entire 2-4 GHz range. However, the RF output from the subject sweeper was clamped at the 4 GHz point; the output could not be tuned to another frequency, nor would it sweep. This problem was discussed with the manufacturer's repair personnel who believed the fault to be in the RF plug-in module. Consequently, this plug-in was returned to the manufacturer for repair. The temporary loss of availability of this unit has a potential serious impact on project scheduling since this unit is needed in tests for proper operation of the other subsystems.

Reliability of the TWT has been partially verified through operating over several days by using sources available at Georgia Tech as drivers. In the receiver subsystem, it was found that the diode switch which selects either the test or the reference antenna positions was inoperative. One port of the switch had only a 3-dB off/on ratio (typical value is 60 dB), and the other port had an unacceptable loss in the on position. This switch was returned to the manufacturer for repair. In the data processor, two sample-and-hold amplifiers (SHAs) are used to hold the reference and the test antenna response voltages on alternate RF sweep cycles, and a third SHA is used to sample the integrator output at the end of each RF sweep cycle. In order to have a spare SHA module, four identical SHAs were purchased. Upon tests of these SHA units, it was found that three out of the four were defective in some way. These three units have been returned to the manufacturer for repair or replacement.

As stated earlier, these various equipment failures have a potential for deleterious impact on project schedules. The extent of this impact depends primarily on how quickly the various equipments are returned to Georgia Tech. Upon their return, extra effort will be devoted to regaining overall project schedule. Assessment for any un-recoverable schedule slippage is being made on a continuous basis.

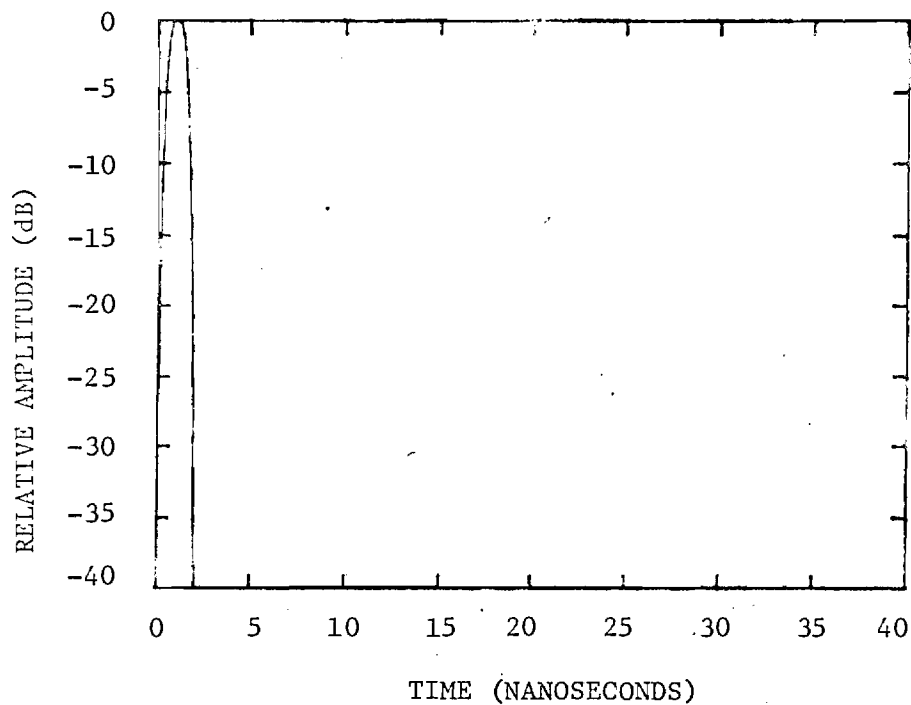


Figure 1. Incident 1-nanosecond pulse

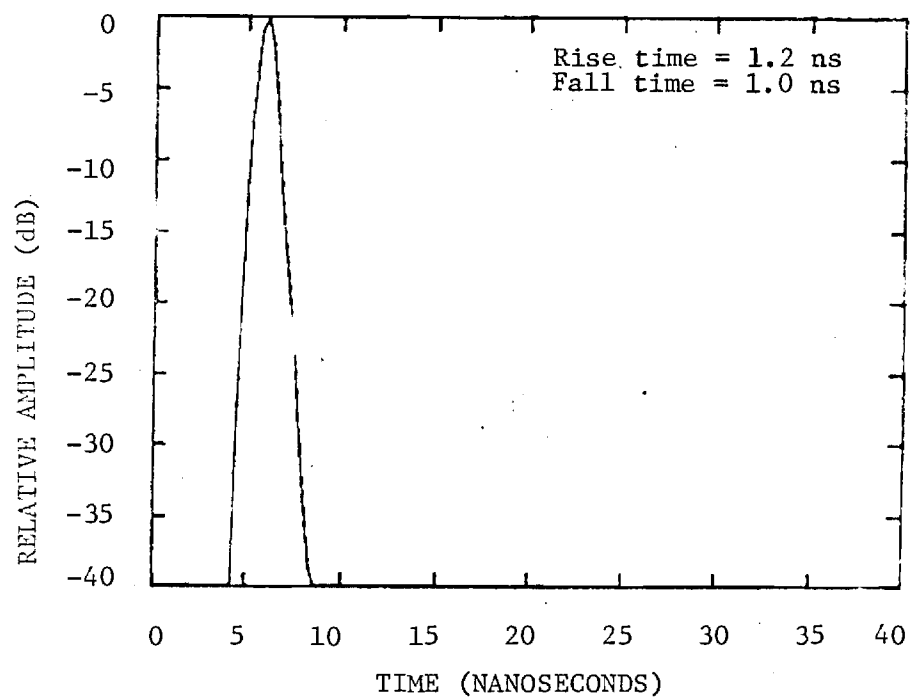


Figure 2. Degraded 1-nanosecond pulse after propagation along a 100-cm length of X-band waveguide.

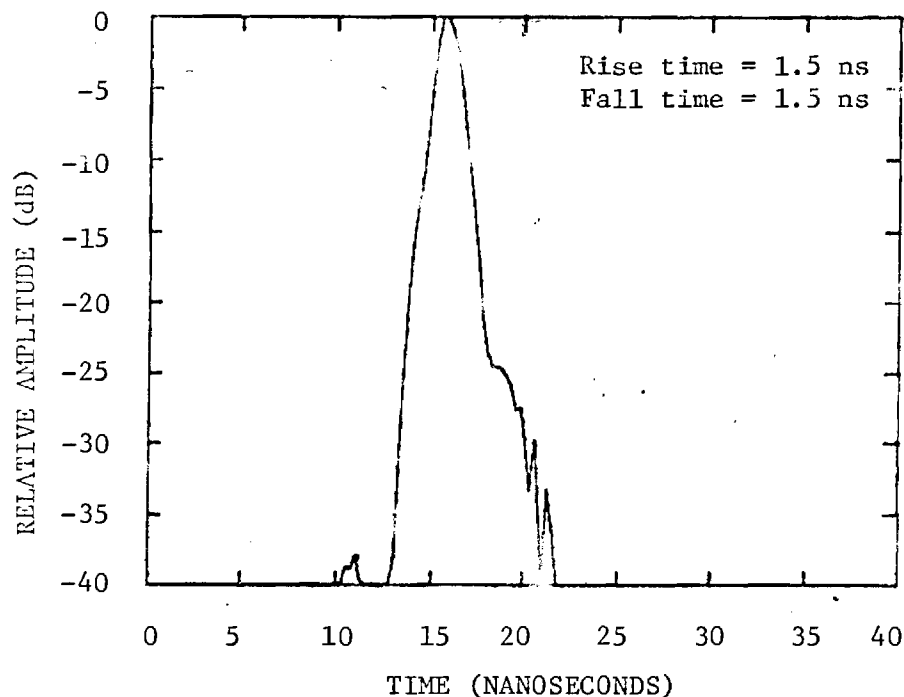


Figure 3.. Degraded 1-nanosecond pulse after propagation along a 300-cm length of X-band waveguide.

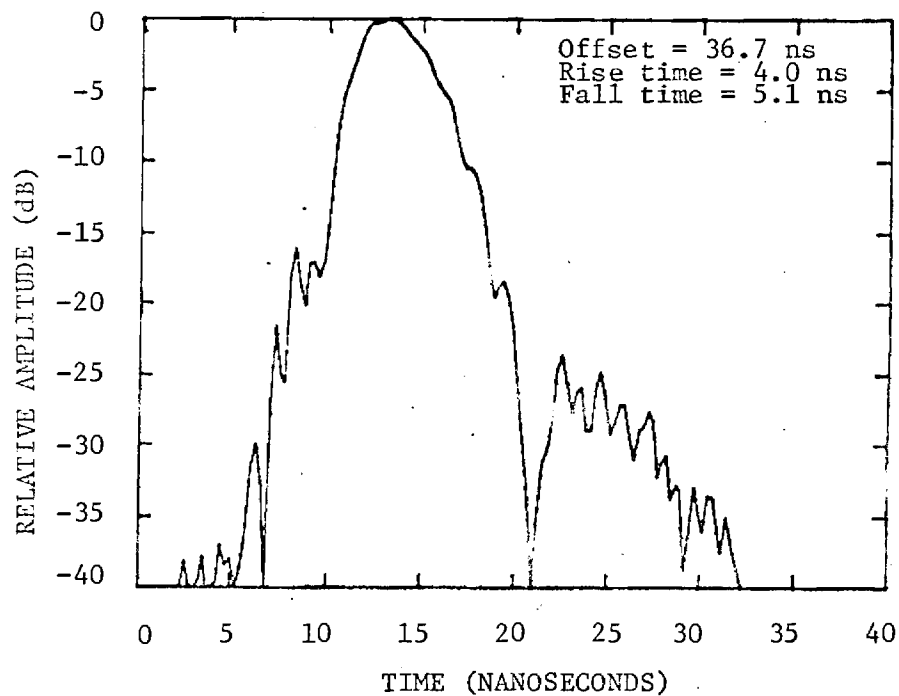


Figure 4. Degraded 1-nanosecond pulse after propagation along a 1000-cm length of X-band waveguide.



Monthly Status Report No. 8  
Contract No. F30602-75-C-0065  
16 July 1975

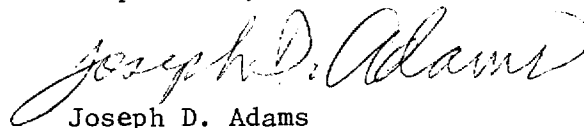
page 5

Except for the previously discussed SHA failures, the various modules of the data processor (integrator, log amp, etc.) have been constructed in breadboard form, and their proper operation has been ascertained. As mentioned in Monthly Status Reports Nos. 6 and 7, a double-ridged rectangular waveguide feed has been designed for the 2-4 GHz transmit feed. Extensive VSWR data have been taken on this feed during the past month. Acceptable performance is being obtained except for a very narrow band about 2 GHz. At 2 GHz, the VSWR is about 3.5:1. Several minor modifications to the feed are feasible, and it is expected that acceptable performance across the entire octave will be obtained.

Next month, efforts will include breadboard testing of components and further comparisons of direct phase measurement systems versus group velocity type of measurement systems. In addition, a trip is planned to RADC for project discussions and briefing of RADC personnel.

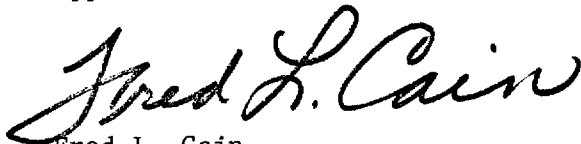
During this reporting period, it is estimated that 338 professional manhours were expended. It is estimated that the cumulative professional manhours expended since contract initiation is 2363 and that approximately 58% of the technical effort has been completed.

Respectfully submitted,



Joseph D. Adams  
Project Director

Approved:



Fred L. Cain  
Manager,  
Electromagnetic Effectiveness



ENGINEERING EXPERIMENT STATION  
GEORGIA INSTITUTE OF TECHNOLOGY • ATLANTA, GEORGIA 30332

13 August 1975

Rome Air Development Center  
Griffiss Air Force Base,  
New York 13441

Attention: Mr. Martin Jaeger, OCTS

Reference: Contract No. F30602-75-C-0065

Title: "Broadband Antenna Measurement Techniques-Phase II"

Subject: Monthly Status Report No. 9

Dear Sir:

A summary of progress on the referenced contract for the period 1 July through 31 July is contained herein. Progress this month on the Hybrid system was hindered by the previously reported unavailability of some equipment which had been returned to various manufacturers for repair. The transmit feed horn has been modified slightly and rechecked with satisfactory results being obtained. On 18 July, a trip was made to RADC to discuss project status and further work directions with the RADC Project Engineer. In regard to the phase/amplitude system studies, frequency sampling requirements and a system configuration which does not require a direct data link between the transmit and receive sites have been considered.

As previously reported in Monthly Status Report No. 8, several items of equipment which had been purchased for use in the Hybrid system was found to be defective. This defective equipment included the transmitter sweep oscillator, the receiver SPDT diode switch, and three sample-and-hold amplifiers. The sweeper RF plug-in unit was originally returned to the manufacturer on 19 June. This plug-in was repaired and returned to Georgia Tech on 10 July. However, upon checkout of the entire sweeper (RF plug-in plus mainframe), it was found that the unit still did not operate properly. Thus, the entire sweeper was returned to the manufacturer a second time on 11 July. The unit was returned to Georgia Tech again on 31 July. Checkout of the repaired unit to date indicates that it is now operating within its specified performance. With regard to the SPDT switch, it was found to be defective as described in Monthly Status Report No. 8, and it was returned to the manufacturer on 26 June. The manufacturer advised Georgia Tech that this switch had a shorted diode which they replaced. Upon return of this unit on 30 July, it was found to be operating well within specification. Insertion loss was 1.5 dB or less (specification of 1.5 dB max) while the "off" state insulation was greater than 60 dB (specification of 60 dB min) across the 2-4 GHz frequency range.

Monthly Status Report No. 9  
Contract No. F30602-75-C-0065  
13 August 1975

page 2

As discussed in Monthly Status Report No. 8, three sample-and-hold amplifiers (SHAs) were returned to the manufacturer for repair. These SHAs were received by the manufacturer on 3 July. However, the manufacturer's plant was closed for vacation the following two weeks. Return of these units is expected in early August. Upon return of these units in proper operating condition, assembly and checkout of the Hybrid system will be accelerated.

In order to protect the traveling wave tube (TWT) amplifier in the Hybrid system transmitter from excessive reflected power, some type of isolation is required at its output port. A three-port circulator with an internally terminated third port was chosen for this purpose. The terminated circulator approach was chosen over the standard ferrite isolator since it is the more economical approach at the required power level. This circulator was received during the month, tested, and found to be within specification (0.5 dB or less insertion loss and 20 dB or greater isolation). During this reporting period, the previously described double-ridged rectangular waveguide feed horn was slightly modified, and one of the ridges was removed. Test results with this single-ridged guide and horn were satisfactory, with the highest VSWR being 2.5:1. Radiation tests on this horn are planned for August.

On 18 July, Messrs. J.D. Adams and W.P. Cooke of Georgia Tech visited RADC to discuss project status and further work directions with the RADC Project Engineer. Significant items of interest requiring continued efforts include (1) more definition of the tradeoff between frequency resolution and total frequency excursion, and (2) investigation of the feasibility of implementing a swept frequency phase/amplitude system with no direct data link between the transmit and the receive sites. With regard to number (1) above, a practical limitation exists on the total number of frequency sample points which should be used at each spatial sample point when measuring and recording broadband antenna phase and amplitude data. With currently available hardware, 1000 discrete frequencies are the limitation on the number of frequency points which can be remotely programmed. However, this 1000 point capability appears to be entirely adequate. For example, considering the 2-4 GHz range, 1000 point resolution would allow frequency sampling each 2 MHz. For many tests, resolution of 2 MHz would not be justifiable and sampling could be increased to 10 or 100 MHz increments. With a broadband microwave component, its transfer characteristics should be smooth over at least a 10 MHz interval and this sampling increment would give correct results. If extremely fine frequency resolution is desired about some particular operating frequency, fine resolution can be obtained by restricting the total frequency range.

Monthly Status Report No. 9  
Contract No. F30602-75-C-0065  
13 August 1975

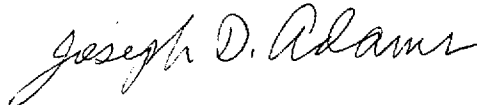
page 3

For convenience, previous phase/amplitude system configurations have assumed the availability of a telephone data link between the transmit and receive sites. However, in some antenna test situations, it may not be practical to obtain a telephone hookup between the transmit and receive sites. An approach is now under investigation in which the transmitted frequency and other transmit parameters are controlled at the transmit site. The transmit signal would be modulated or coded in such a manner to allow synchronization of data recording operations at the receiver site. This concept is similar to that currently being implemented on the Hybrid system.

Next month, assembly and checkout of Hybrid system components and phase/amplitude system tradeoff studies will continue.

During this reporting period, it is estimated that 344 professional manhours were expended. It is estimated that the cumulative professional manhours expended since contract initiation is 2707 and that approximately 63% of the technical effort has been completed.

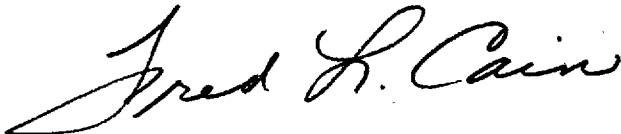
Respectfully submitted,



Joseph D. Adams  
Project Director

JDA/jm

Approved:



Fred L. Cain  
Technical Area Manager  
Electromagnetic Effectiveness



ENGINEERING EXPERIMENT STATION  
GEORGIA INSTITUTE OF TECHNOLOGY • ATLANTA, GEORGIA 30332

12 September 1975

Rome Air Development Center  
Griffiss Air Force Base  
New York 13441

Attention: Mr. Martin Jaeger, OCTS

Reference: Contract No. F30602-75-C-0065

Title: "Broadband Antenna Measurement Techniques - Phase II"

Subject: Monthly Status Report No. 10

Gentlemen:

A summary of progress on the referenced contract for the period 1 August through 31 August is contained herein. During this reporting period, phase/amplitude system tradeoff studies and hybrid system breadboard development continued.

Efforts under this contract have included the evaluation of both direct phase measurements and group delay techniques for the determination of broadband antenna phase dispersion properties. In conjunction with Scientific-Atlanta, Inc. it has been concluded that the group delay approach offers the better solution to the antenna measurement problem. The advantage of the group delay approach lies primarily in the fact that all phase information is derived from a single RF channel. Recall that the group delay technique involves the modulation of an RF carrier to produce two phase-coherent sidebands which are spaced an equal frequency increment above and below the carrier. These sidebands and the carrier are received by the test antenna, and the phase difference between the sidebands is measured as a function of carrier frequency. This measured information is the group delay which can be digitally integrated to produce phase dispersion. Since all of the RF signals are transmitted and received through common channels, there is no requirement to maintain relative electrical lengths as a function of both frequency and time of two channels with widely separated receiver mixers. It should not be assumed, however, that such a use of group delay techniques as envisioned here is a routine application. Currently, narrow band group delay measurement sets are employed to characterize communications channels over narrow bandwidths. Furthermore, the group delay characteristics of a single component within that channel (i.e., the antenna) are not derived with these sets. Thus, advances in the application of group delay techniques are required.

Hybrid system development efforts during this reporting period included transmitter tests and breadboard development of circuits for the logic

controller. The transmitter sweep oscillator/TWT amplifier combination was tested as a unit to determine the TWT output power, gain, and relative harmonic level as functions of frequency and input power level. As expected, the second harmonic level is a strong function of TWT drive level and frequency. Since the TWT is an octave bandwidth (2-4 GHz) device, when operating at the low end of the band (2 GHz), the second harmonic (4 GHz) falls within the high gain region of the TWT. When operating at a 10-watt output level and a frequency of 2 GHz, equal fundamental and second harmonic power output was obtained. As the operating frequency is increased, the harmonic content decreases; at a frequency of 3 GHz, the second harmonic power was 36 dB below the fundamental. Reducing the power level also reduces the relative second harmonic content. At an output power of 1 watt and a frequency of 2 GHz, the second harmonic was 13 dB below the fundamental. Thus, it may be seen that the TWT output will require filtering to reduce the harmonic content to an acceptable level. Two low-pass filters (high frequency cutoffs of 3 GHz and 4 GHz) have been ordered for this purpose, and they are expected by the end of September.

As discussed in Monthly Status Report No. 9, three sample-and-hold amplifiers (SHAs) had been returned to the manufacturer for repair. These SHAs were repaired and returned to Georgia Tech during August. Evaluation of these repaired units indicated that they are now operating satisfactorily. Additional circuit development during this month was primarily directed toward the logic controller subsystem. Recall that the logic controller subsystem is responsible for providing five sets of digitally compatible commands which controls the operation of various segments of the Hybrid system. These commands are the integrate and dump commands to the integrator, control commands to the three SHAs, and the command which controls the antenna selection switch.

All of the logic controller subsystem modules which generate these commands have been breadboarded and these five sets of digital commands are available for use in the Hybrid system. Proper synchronization of the digital waveforms with respect to the sweep generator timing cycle was also verified. The circuits required for presetting the system initially and resetting it after each sweep of the sweep generator remain to be completed. Also, some refinements of the logic controller will be required to obtain precise timing of the digital commands.

Next month, efforts will include additional breadboard construction of the data processor subsystem and its integration with the logic controller subsystem, breadboarding of the preset and reset circuitry in the logic controller subsystem, further design of the group delay system, and pattern tests on the transmit feed horn.

Monthly Status Report No. 10  
Contract No. F30602-75-C-0065  
12 September 1975

page 3

During this reporting period, it is estimated that 260 professional manhours were expended. It is estimated that the cumulative professional manhours expended since contract initiation is 2967 and that approximately 68% of the technical effort has been completed.

Respectfully submitted,



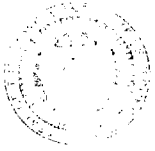
Joseph D. Adams  
Project Director

JDA/jm

Approved:



Fred L. Cain  
Chief,  
Electromagnetic Effectiveness Division



# ENGINEERING EXPERIMENT STATION

GEORGIA INSTITUTE OF TECHNOLOGY • ATLANTA, GEORGIA 30332

23 October 1975

Rome Air Development Center  
Griffiss Air Force Base  
New York 13441

Attention: Mr. Martin Jaeger, OCTS

Reference: Contract No. F30602-75-C-0065

Title: "Broadband Antenna Measurement Techniques-Phase II"

Subject: Monthly Status Report No. 11

Gentlemen:

A summary of progress on the referenced contract for the period 1 September through 30 September is contained herein. During this reporting period, phase/amplitude system design studies and hybrid system breadboard development continued.

Efforts this month on the Hybrid system development included completion of the data processor subsystem breadboard, integration of the logic controller subsystem breadboard with the data processor subsystem breadboard, and preliminary hybrid system performance evaluation. The last three stages of the data processor subsystem breadboard (two sample-and-hold amplifier stages and a difference amplifier stage) were individually constructed and tested. Recall that the differential amplifier stage subtracts the outputs from two sample-and-hold amplifier (SHA) stages, one of which holds the processed swept frequency response of the test antenna while the other holds the processed swept frequency response of the reference antenna. All of these data processor stages are of course under command of the logic controller.

The complete breadboards (data processor subsystem and the logic controller subsystem) were integrated to form the processor segment of the Hybrid system. Using representative RF signals for the test and reference antenna responses, the system performed as expected over an RF dynamic range of approximately 30 dB. A receiver dynamic range of 40 dB is the design goal. Upon evaluation, it was determined that the crystal detector was the limiting factor on system performance at low power levels. Recall that this crystal detector is specially designed for square law response over a power range of 0 dBm to -40 dBm (40 dB dynamic range). However, for RF power levels of approximately -35 dBm, the detected signal-to-noise ratio (SNR) at the input to the data processor was marginal. At an RF power level of -40 dBm, this SNR was approximately unity.



Since this SNR level is undesirable, the noise power must be reduced. The most obvious approach for reducing the total noise power is to reduce the noise bandwidth. Consequently, several modifications involving the use of narrow band filters have been considered. One approach would be to simply low-pass-filter the video output of the crystal detector. This filter would be designed to pass the frequency components of the swept frequency response and attenuate high frequency noise components. There are two sources of noise power in the crystal detector, Gaussian wide band noise and  $1/f$  noise (flicker noise). These two sources combine to create the total noise power. The low pass filter would attenuate the majority of the Gaussian noise and part of the flicker noise.

The next approach, although more sophisticated, would attenuate a larger portion of the noise from both sources. This approach would require modulating the transmitter (at perhaps 25 kHz) and band-pass-filtering (25 kHz center frequency) in the receiver. A demodulator and a low-pass-filter would also be required in the receiver. This technique would also require a demodulator in the logic controller subsystem to remove the 25 kHz modulation on the reference antenna response; however, a band-pass and low-pass filter should not be necessary because the logic controller subsystem is designed to work at a relatively high signal level and noise is not expected to be a problem.

The improvement in SNR using either technique cannot be computed exactly because the crystal detector manufacturer does not have measured noise level data as a function of video bandwidth for this detector. Based on typical noise level data provided by the manufacturer, using a low-pass-filter (5 kHz cut off frequency) should result in a SNR of about 8 dB at the -40 dBm RF signal level. Therefore, the low-pass-filter approach should provide adequate improvement in the SNR. In addition, a low-pass-filter is required with either approach. Therefore, design of a 5 kHz low pass, active filter is currently under way.

A single-ridge rectangular waveguide feed horn designed for the transmit antenna system has been described in previous status reports. During this reporting period, pattern tests were run on this feed horn. The patterns are now under study, and an appropriate reflector will be selected.

With regard to the phase-and-amplitude system design studies, efforts this month were devoted to evaluation of techniques for phase locking the modulate/demodulate signals at the transmit and receive sites, respectively, and for synchronizing of transmitter and receiver operations without a direct data link. The most attractive approach for phase locking the modulate and demodulate signals appears to be through common locking to a WWV broadcast.

Monthly Status Report No. 11  
Contract No. F30602-75-C-0065  
23 October 1975

page 3

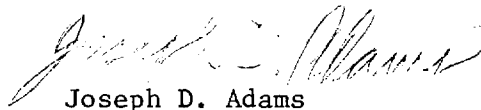
Commercially available hardware which is specifically designed for this purpose is now being evaluated to determine its suitability for the desired application. Locking to a WWV standard broadcast is a proven and common technique which is practical throughout the continental U.S. and Hawaii.

To obtain synchronization of the transmit and receive operations without a data link, an approach involving an operator at each site with voice communication is under consideration. Such transmitter parameters as frequency range (e.g., 2-4 GHz), frequency step (e.g., each 10 MHz), and step rate would be programmed by the transmitter site operator. All other parameters would be under computer control (through an operator) at the receiver site.

Efforts next month will include the design, construction, and implementation of a low pass active filter into the data processor subsystem. The effectiveness of this technique in improving the SNR will be evaluated. Phase-and-amplitude system design and implementation studies will continue.

During this reporting period, it is estimated that 303 professional manhours were expended. It is estimated that the cumulative professional manhours expended since contract initiation is 3270 and that approximately 71% of the technical effort has been completed.

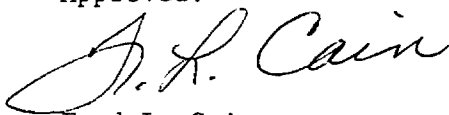
Respectfully submitted,



Joseph D. Adams  
Project Director

JDA/jm

Approved:



Fred L. Cain  
Chief,  
Electromagnetic Effectiveness Division



A-1694

# ENGINEERING EXPERIMENT STATION

GEORGIA INSTITUTE OF TECHNOLOGY • ATLANTA, GEORGIA 30332

18 November 1975

Rome Air Development Center  
Griffiss Air Force Base  
New York 13441

Attention: Mr. Martin Jaeger, OCTS

Reference: Contract No. F30602-75-C-0065

Title: "Broadband Antenna Measurement Techniques - Phase II"

Subject: Monthly Status Report No. 12

Gentlemen:

A summary of progress on the referenced contract for the period 1 October through 31 October is contained herein. During this reporting period, phase/amplitude system design studies and hybrid system breadboard development continued. During the month, a contract modification which extends the contract period by two months and which provides certain Government Furnished Equipment, both at no change in contract cost, was received.

The amplitude only Hybrid system breadboard development efforts continued during this reporting period. It had been previously reported (Monthly Status Report No. 10) that due to improper operation of the directional detector (which provides a dc signal proportional to power level), transmitter power variation was about 4 dB across the 2-4 GHz range. The directional detector was sent to the manufacturer for repair, and it was returned to Georgia Tech on 27 October. Tests with the directional detector in the transmitter system now show that in the sweep frequency mode of operation, power level across the entire 2-4 GHz range is constant within  $\pm 1$  dB. This variation will have no effect on the accuracy of results achieved with the Hybrid system.

In Monthly Status Report No. 11, the matter of excessive noise following the RF detector in the receiver was discussed. As indicated in that Status Report, a low pass, three pole, active filter was designed and constructed from materials on hand. This filter's passband is from approximately dc to 5 kHz. Using this filter following the detector to limit the noise bandwidth, the improvement in signal-to-noise ratio was sufficient to permit operation over a full 40 dB of dynamic range, and it appears that receiver/data processor design goals will be achieved with this technique. Final hardware requirements (cabinets, card holders, connectors, etc) are being determined and placed on order so that the "finished" breadboard can be assembled.

With regard to phase and amplitude system studies, efforts were devoted to several areas. Design analyses show that phase locking of the group delay modulate and demodulate 5 MHz sources to a WWV broadcast can be achieved with commercially available components. A preliminary design with hardware specifications and cost estimates has been performed. This common phase locking of the modulate and demodulate signal sources to WWV will eliminate the need for a 5 MHz link between the transmit and receive sites.

In view of the desired capability to measure antenna patterns with the phase and amplitude system on ranges "up to 7000 feet", the question of maximum test antenna size has been raised. The possible limitation of interest here arises from a decrease in received signal level as range is increased to satisfy the conventional far-field requirement. With a 7000 ft. range, the maximum antenna diameter ranges from approximately 59 feet at 1 GHz to 15 feet at 15 GHz. Table I summarizes the maximum test antenna diameter at various ranges and frequencies. The nominal gains at 50% efficiency and the free space power loss for each frequency and range combination are also given. Table II presents the received signal level at various ranges and frequencies, assuming (1) a transmitter power of 10 watts, (2) a transmit antenna gain of 30 dB, and (3) the maximum test antenna size in each case. Since the minimum received power for any case presented is -4 dBm and the S/A Series 1700 receiver sensitivity is specified as -90 dBm or better, there is considerable received power-level margin. Consequently, it can be concluded that system sensitivity presents no limitation on the use of extremely long ranges to test large antennas.

Preliminary definition of a "free-running" group delay measurement system which requires no data link has been completed. Under this system concept, the transmit and the receive site operations are under control of an operator at each site. Coordination is maintained by voice link. Of course, operations at each site proceed essentially in a "hands-off" manner after the test parameters (frequency, antenna pattern cut, etc.) have been established by the operator. The primary impact of the "free-running" type of system as opposed to a direct data link for synchronization appears to be a need for a reduced data rate to insure that all system components have stabilized between data points.

Efforts next month will include initiation of the construction and packaging of the Hybrid system finished breadboard, and continuation of phase/amplitude system tradeoff analysis. A trip to RADC near the end of the month is anticipated.

TABLE I

ANTENNA RANGE PARAMETERS AT VARIOUS DISTANCES

Max. Antenna Dia.(ft)	Gain @ 50% eff,dB	Free Space Loss,dB	Frequency,GHz
Range = 1 mi.			
13	53	120	15
16	51	117	10
23	48	111	5
29	46	106	3
Range = 7,000 ft. (1.33 mi)			
15	54	123	15
18.5	52	119	10
26	49	113	5
34	47	109	3
Range = 10,000 ft. (1.93 mi)			
18	56	126	15
22.5	54	122	10
32	52	116	5
40	49	112	3
Range = 26,400 ft. (5 mi)			
30	60	134	15
36	58	131	10
51	55	125	5
66	53	120	3

TABLE II

RECEIVED SIGNAL LEVEL FOR MAXIMUM TEST ANTENNA DIAMETER

Freq., GHz	Space Loss, dB	Max. Test Antenna Gain,dB	Received Power,dBm
Range = 1 mile			
15	120	53	+3
10	117	51	+4
5	111	48	+7
3	106	46	+10
Range = 7,000 ft. (1.33 mi)			
15	123	54	+1
10	119	52	+3
5	113	49	+6
3	109	47	+8
Range = 10,000 ft (1.93 mi)			
15	126	56	0
10	122	54	+2
5	116	52	+6
3	112	49	+7
Range = 26,400 ft. (5 mi)			
15	134	60	-4
10	131	58	-3
5	125	55	0
3	120	53	+3

Notes:

1. Transmitter Power = 10 watts (40 dBm).
2. Transmit Antenna Gain = 30 dB.

Monthly Status Report No. 12  
Contract No. F30602-75-C-0065  
18 November 1975

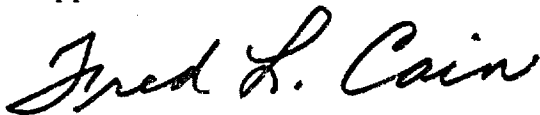
page 5

During this reporting period, it is estimated that 269 professional manhours were expended. It is estimated that the cumulative professional manhours expended since contract initiation is 3539 and that approximately 76% of the technical effort has been completed.

Respectfully submitted,

  
Joseph D. Adams  
Project Director

Approved:



Fred L. Cain  
Chief,  
Electromagnetic Effectiveness Division

JDA/jm



A-1694

# ENGINEERING EXPERIMENT STATION

GEORGIA INSTITUTE OF TECHNOLOGY • ATLANTA, GEORGIA 30332

17 December 1975

Rome Air Development Center  
Griffiss Air Force Base  
New York 13441

Attention: Mr. Martin Jaeger, OCTS

Reference: Contract No. F30602-75-C-0065

Title: "Broadband Antenna Measurement Techniques - Phase II"

Subject: Monthly Status Report No. 13

Gentlemen:

A summary of progress on the referenced contract for the period 1 November through 30 November is contained herein. During this reporting period, final breadboard construction of the amplitude-only Hybrid system and preliminary design studies of the phase and amplitude system continued. Also, on 24 November, Messrs. J. D. Adams and W. P. Cooke of Georgia Tech visited RADC for technical discussions with the RADC Project Engineer.

Phase and amplitude system design efforts included preliminary hardware definition with identification of possible candidates for each of the major system components. A group-delay type of measurement system which requires no direct link between the transmit and receive sites has been configured. The carrier frequency is stepped between each measurement point, and phase tracking between the sideband modulation and demodulation signals at the transmit and receive sites is obtained through common synchronization to a standard frequency WWV broadcast. The required frequency accuracy and stability are obtained through phase locking to a low-frequency crystal controlled synthesizer. Transmit site operations are controlled by an operator through a programmable terminal. Receive site operations and system synchronization are under control of an on-site minicomputer and operator. Available off-the-shelf hardware specifications have been reviewed to estimate a total system hardware cost and to define areas requiring hardware development and/or modification. Based on preliminary design trade-offs and hardware reviews, the estimated hardware cost of a complete computer controlled system (as described above) is a minimum of \$120K at today's prices. This estimated cost does not include either software development or any engineering services for system integration, hardware development, and etc. As expected then, the total cost of a full phase and amplitude antenna measurement system is significant. Of course, it would be possible to demonstrate the system concept through a limited set of measurements at a reduced cost.



Development of the Hybrid system breadboard continued during the month of November. The Hybrid system breadboard performance was evaluated in the laboratory, and based on this evaluation, the Hybrid system "finished" breadboard should meet all design goals. Efforts this month concentrated on identifying final hardware requirements and placing purchase orders. Determination of the final hardware and component requirements included examining both the cost and effectiveness of candidates and choosing those items which offered the better performance at comparable cost. Items placed on order during this month include a twin drawer cabinet, a reflector for use with the single-ridge rectangular waveguide feedhorn, power supplies, printed circuit boards, card racks, connectors, and assorted electronic components. One drawer of the cabinet will enclose both the data processor and logic controller subsystems while the other drawer will contain the power supplies and the RF components of the Hybrid system receiver.

Efforts this month were also devoted to final package considerations. Items that were considered important include: a self-contained unit, conveniently accessible RF and electronic hardware, modular circuit construction, and user convenience within current cost constraints. As previously mentioned, the "finished" breadboard Hybrid system receiver will be completely packaged in a two drawer cabinet. By utilizing pull-out drawers, both the RF and electronic hardware will be easily accessible for either alignment or repair. The data processor and logic controller subsystems will be built on printed circuit boards and placed in a card holder rack. Finally, the entire package will be oriented toward use at the technician level.

On 24 November, Messrs. J. D. Adams and W. P. Cooke of Georgia Tech visited the RADC Project Engineer to review project status. Possible follow-on work to the present program was also discussed during this meeting. It is anticipated that a follow-on program which involves phase and amplitude system demonstration with a minimum of hardware procurement will be initiated. This system demonstration phase will also provide a better definition of system measurement accuracy versus individual component specifications.

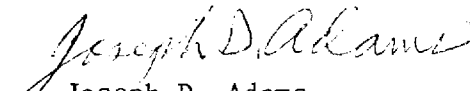
Efforts next month will be directed toward completing construction on the final circuit boards for the Hybrid system data processor and logic controller, integrating the single-ridge rectangular waveguide feedhorn with the dish reflector, assembly of the RF drawer, and assembly of various hardware items into the cabinet. Further definition of the phase and amplitude system preliminary design will continue.

Monthly Status Report No. 13  
Contract No. F30602-75-C-0065  
17 December 1975


page 3

During this reporting period, it is estimated that 308 professional manhours were expended. It is estimated that the cumulative professional manhours expended since contract initiation is 3847 and that approximately 88% of the technical effort has been completed.

Respectfully submitted,

  
Joseph D. Adams  
Project Director

Approved:

  
Fred L. Cain  
Chief,  
Electromagnetic Effectiveness Division



# ENGINEERING EXPERIMENT STATION

GEORGIA INSTITUTE OF TECHNOLOGY • ATLANTA, GEORGIA 30332

19 January 1976

Rome Air Development Center  
Griffiss Air Force Base  
New York 13441

Attention: Mr. Martin Jaeger, OCTS

Reference: Contract No. F30602-75-C-0065

Title: "Broadband Antenna Measurement Techniques - Phase II"

Subject: Monthly Status Report No. 14

Gentlemen:

A summary of progress on the referenced contract for the period 1 December through 31 December is contained herein. During this reporting period, final breadboard construction of the amplitude-only Hybrid system and preliminary design studies of the phase and amplitude system continued. Also, some effort was devoted to generating a finished version of the previously developed pulse distortion analysis computer program. Due to the closing of Georgia Tech for Christmas holidays, the work period for the month of December was considerably less than a full month.

The pulse distortion analysis program has been previously developed (see Status Report No. 8) and verified. Predicted pulse distortions using representative pulsewidths and waveguide transfer functions have been obtained with the program. Efforts during this reporting period have included generation of a punched card deck and a listing of the program. The punched card deck also has a printout on each card of that card's coding. Concurrently with the generation of this card deck and program listing, additional comments to aid in user interpretation and convenience have been added to the program. With the addition of particular I/O cards as required by the RADC Computer Center, this program is ready for sponsor use.

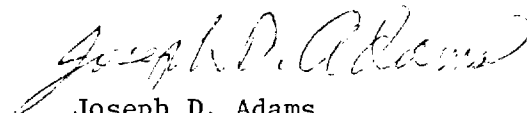
Construction of the Hybrid system final breadboard package continued during this reporting period. Timely receipt of purchased parts and equipment continues to present a schedule problem; however, at this time all major items of equipment have been received. The transmit antenna paraboloidal reflector was received after being in transit approximately two weeks, and support and feed structures are now being fabricated or adapted from existing hardware at Georgia Tech. Since the Hybrid circuits have already been breadboarded and tested in the laboratory, no major difficulties are foreseen in completion of the final breadboard assembly.

Phase and amplitude system studies during the month of December included an examination of short pulse transit time effects in aperture antennas and the applicability of CW-derived broadband patterns to short pulse antenna response. It appears that, except for possible higher-order interaction effects which may occur with short pulses, CW-derived broadband patterns correctly predict short pulse behavior unless the operating pulse width is less than the aperture excitation or "fill" time. A more detailed investigation to determine if there are any practical limitations in this area is continuing. Also this month, a microwave link alternative to WWV synchronization of the modulate/demodulate group delay signal was investigated. As expected, the microwave link approach is considerably more expensive and it is not an attractive alternative. The best synchronization approaches are a direct cable hookup for short distances and WWV synchronization for longer distances.

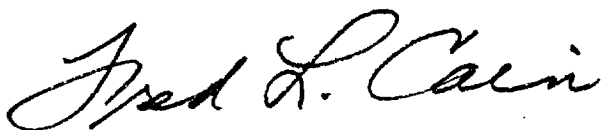
Efforts next month will be directed toward completion of the Hybrid system breadboard construction and tests and the phase/amplitude system preliminary design studies.

During this reporting period it is estimated that 276 professional manhours were expended. It is estimated that the cumulative professional manhours expended since contract initiation is 4123 and that approximately 94% of the technical effort has been completed.

Respectfully submitted,

  
Joseph D. Adams  
Project Director

Approved:



Fred L. Cain  
Chief,  
Electromagnetic Effectiveness Division

# ENGINEERING EXPERIMENT STATION

GEORGIA INSTITUTE OF TECHNOLOGY • ATLANTA, GEORGIA 30332

25 February 1976

Rome Air Development Center  
Griffiss Air Force Base  
New York 13441

Attention: Mr. Martin Jaeger, OCTS

Reference: Contract No. F30602-75-C-0065

Title: "Broadband Antenna Measurement Techniques - Phase II"

Subject: Monthly Status Report No. 15

Gentlemen:

A summary of progress on the referenced contract for the period 1 January through 31 January is contained herein. During this reporting period, final breadboard construction of the amplitude-only Hybrid system data processor and logic controller was completed and the construction and testing of the transmit antenna was completed.

As indicated in Monthly Status Report No. 13, the final breadboard version of the Hybrid system receiver unit is being packaged in a self-contained cabinet. This cabinet contains the receiver RF hardware, the data processor, and the logic controller. For convenience in alignment, the RF hardware is contained in a separate drawer. The data processor and the logic controller are contained in another separate drawer. The data processor occupies five printed circuit cards, and the logic controller occupies an additional four printed circuit cards. In both cases, wire-wrap construction techniques are used (as opposed to soldering). Next month, this final breadboard will be checked out in the laboratory before the entire hybrid system is moved to the antenna range for testing.

With receipt of the transmit antenna paraboloidal reflector late in December, efforts were renewed this month to complete construction of the transmit antenna system. The previously completed single-ridged feed horn was measured on a phase-center range to determine its phase-center location as a function of frequency.

The E-plane phase center varies from nearly the horn aperture at 2 GHz to approximately 2 cm inside the aperture at 4 GHz. The H-plane phase center varies from about 1 cm outside the aperture plane at 2 GHz to about 1.5 cm inside the aperture plane at 4.0 GHz. Consequently, use of this horn as primary illuminator over the 2-4 GHz range will require some de-focusing of the feed over part of the frequency band. A feed support structure which allows both translational and rotational adjustment of the horn was designed and constructed. Through antenna range pattern tests

Monthly Status Report No. 15  
Contract No. F30602-75-C-0065  
25 February 1976

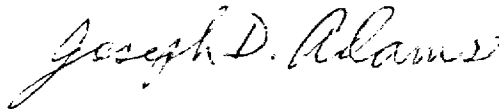
page 2

on the completed system, it was found that the best compromise in feed location was to place the feed aperture at the focal point of the reflector.

Efforts next month will include laboratory and antenna range tests on the Hybrid system, and initiation of production of the final technical report.

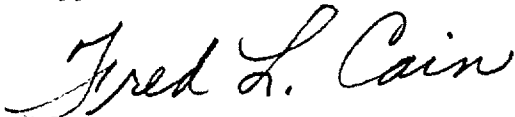
During this reporting period, it is estimated that 302 professional manhours were expended. It is estimated that the cumulative professional manhours expended since contract initiation is 4425 and that approximately 97% of the technical effort has been completed.

Respectfully submitted,



Joseph D. Adams  
Project Director

Approved:



Fred L. Cain  
Chief,  
Electromagnetic Effectiveness Division

H-1684



# ENGINEERING EXPERIMENT STATION

GEORGIA INSTITUTE OF TECHNOLOGY • ATLANTA, GEORGIA 30332

23 March 1976

Rome Air Development Center  
Griffiss Air Force Base  
New York 13441

Attention: Mr. Martin Jaeger, OCTS

Reference: Contract No. F30602-75-C-0065

Title: "Broadband Antenna Measurement Techniques - Phase II"

Subject: Monthly Status Report No. 16

Gentlemen:

A summary of progress on the referenced contract for the period 1 February through 29 February is contained herein. During this reporting period, laboratory and antenna range tests of the Hybrid system were conducted, and preparation of the final technical report was begun. In addition, the RADC Project Engineer visited Georgia Tech on 17 and 18 February for project status briefings and to observe antenna range tests of the Hybrid system.

As indicated in Monthly Status Report No. 15, construction of the Hybrid system data processor and logic controller on printed circuit cards has been completed. The data processor and logic controller were integrated and assembled with the receiver into a self-contained cabinet which contains all the necessary power supplies, connectors, and cables and equipment for the receive-site portion of the Hybrid system. The transmit site equipment consists of two standard instruments (the sweep oscillator and travelling wave tube amplifier) plus the necessary interconnecting cables and the level sensor for maintaining constant power versus frequency.

Laboratory tests showed that all circuits of the Hybrid system were performing properly. The various receive site operations of detection, integration, sample-and-hold, LOG, and subtraction were performed in synchronization with transmitter sweep cycles for bandwidths from 1 GHz to a few MHz. These are the functions required to obtain integrated (average) antenna response referenced to response of a standard antenna. After these laboratory tests, the Hybrid system was moved to the antenna range for field testing.

For field tests, the broadband 2-4 GHz antenna which has been previously described (see Status Report No. 15) was used for the transmit antenna. An existing Georgia Tech antenna consisting of a paraboloidal reflector and a dielectrically loaded C-band feed horn was used as the test antenna. A standard gain horn was used as the reference antenna. Except for a limitation in the instantaneous dynamic range of the logic controller and data processor,

Monthly Status Report No. 16.  
Contract No. F30602-75-C-0065  
23 March 1976

page 2

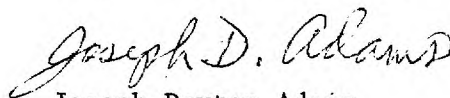
the Hybrid system field performance was as expected. Apparently due to in-band stray radiation interference, instantaneous dynamic range in the field was limited generally to about 30 dB. However, at certain times (beginning about midnight) when extraneous interference would be expected to be minimal, a dynamic range of 37-38 dB could be obtained. It should be noted that since this problem was caused by in band interference, RF filtering offers no solution to this problem. Because of the 30 dB dynamic range, further field tests were terminated and the system was returned to the laboratory.

During discussions with the RADC Project Engineer on 18 February, Georgia Tech agreed to devote additional effort to improve the dynamic range of the system. However, no contract funds are available for this work, and the contract technical work period had expired. Therefore, this additional technical work will be at Georgia Tech expense, and an additional one month no-cost time extension was requested.

Efforts next month will be devoted to evaluation of methods which might be used to improve the dynamic range of the Hybrid system in the field, and to appropriate modification of the system. In addition, preparation of the final technical report will proceed.

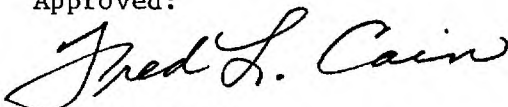
During this reporting period, it is estimated that 192 professional manhours were expended. It is estimated that the cumulative professional manhours expended since contract initiation is 4617 and that 100% of the technical effort has been completed.

Respectfully submitted,



Joseph Dayton Adams  
Project Director

Approved:



Fred L. Cain  
Chief,  
Electromagnetic Effectiveness Division





# ENGINEERING EXPERIMENT STATION

GEORGIA INSTITUTE OF TECHNOLOGY • ATLANTA, GEORGIA 30332

26 April 1976

Air Force Systems Command  
Rome Air Development Center  
Griffiss Air Force Base  
New York 13441

Attention: Mr. Martin Jaeger, OCTS

Reference: Contract No. F30602-75-C-0065

Title: "Broadband Antenna Measurement Techniques - Phase II"

Subject: Monthly Status Report No. 17 (Final Status Report)

Dear Sir:

Progress on the referenced contract for the period 1 March through 15 April is described herein. During this reporting period, the Hybrid system modifications were completed, and the system was tested on the antenna range. All the system design goals were met, including a dynamic range of greater than 40 dB. A Final Technical Report describing all work done under this contract has been prepared for RADC review.

Subject to RADC approval of the Final Technical Report, all contract requirements have been fully met. No professional man hours were charged to the contract during this reporting period. A total of approximately 4617 professional manhours have been expended on this contract. Attachment I to this status report is the contractually required certificate of manhours expended on the contract.

Respectfully submitted,

Joseph D. Adams  
Project Director

Attachment

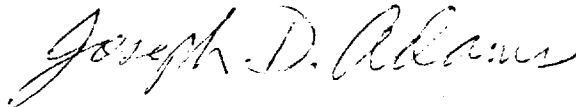
Approved:

Fred L. Cain  
Chief,  
Electromagnetic Effectiveness Division

ATTACHMENT I

Monthly Status Report No. 17  
Contact No. F30602-75-C-0065  
26 April 1976

CERTIFICATE OF TOTAL MAN-HOURS EXPENDED. This is to certify that based on monthly estimates of man-hours expended, the cumulative total of professional man-hours expended from contract outset to date as set forth in this report is correct. This certificate covers only the professional man-hours expended in support of work for which a level of effort is specified in the contract schedule.

A handwritten signature in cursive script, reading "Joseph D. Adams".

Joseph D. Adams  
Project Director

Date: 26 April 1976

A-1694

RADC-TR-76-190  
Final Technical Report  
June 1976



## BROADBAND ANTENNA MEASUREMENT TECHNIQUES - PHASE II

Georgia Institute of Technology

Approved for public release;  
distribution unlimited.

**ROME AIR DEVELOPMENT CENTER  
AIR FORCE SYSTEMS COMMAND  
GRIFFISS AIR FORCE BASE, NEW YORK 13441**

This report has been reviewed by the RADC Information Office (OI) and is releasable to the National Technical Information Service (NTIS). At NTIS it will be releasable to the general public including foreign nations.

This report has been reviewed and is approved for publication.

APPROVED:

*Martin Jaeger*  
MARTIN JAEGER  
Project Engineer

APPROVED:

*Moses A. Diab*  
MOSES A. DIAB  
Acting Technical Director

FOR THE COMMANDER:

*John P. Huss*  
JOHN P. HUSS  
Acting Chief, Plans Office

Do not return this copy. Retain or destroy.

UNCLASSIFIED

SECURITY CLASSIFICATION OF THIS PAGE (When Data Entered)

REPORT DOCUMENTATION PAGE		READ INSTRUCTIONS BEFORE COMPLETING FORM
1. REPORT NUMBER <b>RADC-TR-76-190</b>	2. GOVT ACCESSION NO.	3. RECIPIENT'S CATALOG NUMBER
4. TITLE (and Subtitle) <b>BROADBAND ANTENNA MEASUREMENT TECHNIQUES - PHASE II</b>		5. TYPE OF REPORT & PERIOD COVERED <b>Final Technical Report 15 Nov 74 - 15 Mar 76</b>
7. AUTHOR(s) <b>Joseph D. Adams William P. Cooke Barry J. Cown</b>		6. PERFORMING ORG. REPORT NUMBER <b>N/A</b>
9. PERFORMING ORGANIZATION NAME AND ADDRESS <b>Georgia Institute of Technology Engineering Experiment Station Atlanta GA 30332</b>		8. CONTRACT OR GRANT NUMBER(s) <b>F30602-75-C-0065</b>
11. CONTROLLING OFFICE NAME AND ADDRESS <b>Rome Air Development Center (OCTS) Griffiss AFB NY 13441</b>		10. PROGRAM ELEMENT, PROJECT, TASK AREA & WORK UNIT NUMBERS <b>62702F 45060480</b>
14. MONITORING AGENCY NAME & ADDRESS (if different from Controlling Office) <b>Same</b>		12. REPORT DATE <b>June 1976</b>
		13. NUMBER OF PAGES <b>161</b>
		15. SECURITY CLASS. (of this report) <b>UNCLASSIFIED</b>
		15a. DECLASSIFICATION/DOWNGRADING SCHEDULE <b>N/A</b>
16. DISTRIBUTION STATEMENT (of this Report)  <b>Approved for public release; distribution unlimited.</b>		
17. DISTRIBUTION STATEMENT (of the abstract entered in Block 20, if different from Report)  <b>Same</b>		
18. SUPPLEMENTARY NOTES <b>RADC Project Engineer: Martin Jaeger/OCTS</b>		
19. KEY WORDS (Continue on reverse side if necessary and identify by block number) <b>Antenna Measurements                      Pulse Distortion Broadband Antenna Patterns              Phase/Amplitude System Spatial Pattern                              Group Delay System</b>		
20. ABSTRACT (Continue on reverse side if necessary and identify by block number) <b>This report presents the results of a program to study advanced antenna measurement concepts and to breadboard certain promising instrumentation approaches. The applications of most interest are relatively high gain antennas in the 1-15 GHz region. A typical instantaneous bandwidth of 1 GHz is required. On the current phase of this program, an octave bandwidth 2-4 GHz amplitude - only system was designed, breadboarded, and tested. This system will provide average pattern information over any portion of the 2-4 GHz</b>		

DD FORM 1 JAN 73 1473 EDITION OF 1 NOV 65 IS OBSOLETE

UNCLASSIFIED

SECURITY CLASSIFICATION OF THIS PAGE (When Data Entered)

UNCLASSIFIED

SECURITY CLASSIFICATION OF THIS PAGE(When Data Entered)

GHz octave. This amplitude - only system is described, and measured data are presented. Tradeoff studies of a direct phase measurement system versus a group delay type of measurement system for broadband antenna measurements were completed. It was concluded that a group delay type of system represented the better approach toward realization of a broadband phase and amplitude antenna measurement system. Preliminary studies and design definition of a group delay type of system were completed, and the results are presented. In addition, a computer program which predicts antenna pulse distortion effects from measured phase and amplitude data, with arbitrary input pulse shapes, was developed. Recommendations for demonstration of the broadband phase-and-amplitude system are presented.

UNCLASSIFIED

SECURITY CLASSIFICATION OF THIS PAGE(When Data Entered)

## PREFACE

This final technical report describes the work performed under Contract F30602-75-C-0065, Project No. 4506, during the period from 15 November 1974 to 15 March 1976.

The work on this contract was performed by the Electromagnetic Effectiveness Division, Applied Engineering Laboratory of the Engineering Experiment Station, Georgia Institute of Technology, with the support of Scientific-Atlanta, Inc., under subcontract. The work was designated at Georgia Tech as Project A-1694, and the RADC Project Engineer was Mr. Martin Jaeger.

## EVALUATION

This study performed an analysis and investigation of broadband antenna measurement techniques and instrumentation applicable to a new generation of microwave high resolution AF radars being developed for ECCM tactical applications and for use in target identification. The program objective is to provide advanced techniques for determining the phase and amplitude properties, radiation pattern response and pulse distortion characteristics of high-gain broad signal bandwidth antenna systems. Emphasis was placed on antennas operating in the 1 to 15 GHz frequency region over instantaneous signal bandwidths up to 1 GHz.

The effort is a direct continuation of basic studies accomplished on prior Contract F30602-73-C-0194. It experimentally established the feasibility of a 2 to 4 GHz swept frequency electronically integrating system for measuring broadband antenna pattern amplitude response. The breadboard system met, and in some respects exceeded specified design goals, and has provided a significant advancement in broadband measurement technology.

Expanded analysis conducted on the second, more flexible, system concept resulted in incorporation of a group delay type of phase measurement approach into the design of the computer controlled phase and amplitude measurement system. In this system concept measured phase and amplitude data can be digitally processed to determine any antenna property including its broadband spatial pattern response and the antenna's effect on pulse distortion. The system represents a new dimension in antenna testing and can be used in determining dispersion characteristics of a variety of transmission components employed by broadband microwave radar systems.

This antenna measurement techniques study provided a diagnostic and research tool having direct application to the Digital Coded Radar Program. The effort supports TPO-5 in the RADC Technology Plan.

*Martin Jaeger*  
MARTIN JAEGER  
Project Engineer



## TABLE OF CONTENTS

<u>Section</u>	<u>Page</u>
I. INTRODUCTION . . . . .	1
A. GENERAL . . . . .	1
B. CONTRACT OBJECTIVES. . . . .	2
C. SUMMARY OF WORK PERFORMED. . . . .	3
1. Amplitude-Only System. . . . .	3
2. Phase-and-Amplitude System . . . . .	5
3. Pulse Distortion . . . . .	10
II. AMPLITUDE-ONLY SYSTEM BREADBOARD DEVELOPMENT . . . . .	13
A. INTRODUCTION . . . . .	13
B. BREADBOARD SYSTEM. . . . .	16
1. Transmitter. . . . .	16
2. Transmit Antenna . . . . .	23
3. Receiver . . . . .	43
4. Hybrid System Data Processor . . . . .	52
a. Description. . . . .	52
b. Component Selection. . . . .	58
5. Logic Controller . . . . .	63
a. Description. . . . .	63
b. Component Selection. . . . .	68
6. Packaging. . . . .	69
C. TEST RESULTS . . . . .	72
III. PHASE-AND-AMPLITUDE SYSTEM STUDIES . . . . .	91
A. INTRODUCTION . . . . .	91
B. TRADEOFF STUDIES . . . . .	92
1. Concept Review . . . . .	92
2. Evaluation . . . . .	96

## TABLE OF CONTENTS (contd)

<u>Section</u>	<u>Page</u>
C. DESCRIPTION OF THE GROUP DELAY SYSTEM . . . . .	97
1. Concept . . . . .	97
2. Equipment Description . . . . .	100
D. DATA RATES AND DATA RECORDING CONSIDERATIONS. . . . .	116
E. TEST ANTENNA SIZE CONSIDERATIONS. . . . .	123
IV. PULSE DISTORTION ANALYSIS . . . . .	127
A. INTRODUCTION . . . . .	127
B. THEORETICAL CONSIDERATIONS . . . . .	128
1. Fourier Transform Techniques . . . . .	128
2. Typical Distortion Effects . . . . .	131
C. COMPUTER CALCULATIONS. . . . .	137
1. The Fast Fourier Transform . . . . .	137
2. Description of Computer Program. . . . .	140
3. Computed Pulses. . . . .	143
V. CONCLUSIONS AND RECOMMENDATIONS. . . . .	155
A. CONCLUSIONS . . . . .	155
B. RECOMMENDATIONS. . . . .	157
VI. REFERENCES . . . . .	161

## LIST OF FIGURES

<u>Figure</u>	<u>Page</u>
1. Simplified block diagram of amplitude-only Hybrid system . . . . .	4
2. CW pattern of four-foot paraboloidal reflector at a frequency of 3.5 GHz . . . . .	6
3. Broadband pattern of four-foot paraboloidal reflector for a bandwidth of $\pm$ 500 MHz centered at 3.5 GHz . . . . .	7
4. Simplified block diagram illustrating direct measurement of antenna phase response . . . . .	9
5. Block diagram of Hybrid system breadboard transmitter . . . . .	17
6. TWT gain and required input power for 1 watt output . . . . .	21
7. TWT gain and required input power for 10 watt output. . . . .	22
8. Photograph of assembled S-band Hybrid system breadboard transmitter . . . . .	24
9. Variation of transmitter power level versus frequency for 2-4 GHz sweep and 10 watts average power output . . . . .	25
10. Variation of transmitter power level versus frequency for 2-4 GHz sweep and 1 watt average power output . . . . .	25
11. Cross-section of (a) single and (b) double ridge rectangular waveguide . . . . .	30
12. Sketch of original double ridge feed horn . . . . .	31
13. Sketch of final single ridge feed horn used in the broadband transmit antenna . . . . .	35
14. Photograph of broadband transmit antenna system with level sensor mounted at the feed input . . . . .	38
15. H-plane transmit antenna pattern at a frequency of 2 GHz . . . . .	39
16. H-plane transmit antenna pattern at a frequency of 4 GHz . . . . .	40

## List of Figures continued

<u>Figure</u>	<u>Page</u>
17. E-plane transmit antenna pattern at a frequency of 2 GHz . . . . .	41
18. E-plane transmit antenna pattern at a frequency of 4 GHz . . . . .	42
19. Hybrid system receiver block diagram . . . . .	45
20. Voltage response of Hybrid system crystal detector versus input power for various video load values. . . . .	51
21. Hybrid system data processor simplified block diagram . . . . .	53
22. Hybrid system logic controller simplified block diagram. . . . .	64
23. Photograph of the analog integrator/sample-and-hold board, showing the analog integrator (AD 43K Op Amp plus components), the integrate/dump switch (RCA type CD 4066 CMOS-FET switch), and the SHA #1 (AD SHA-4). . . . .	70
24. Photograph of the digital logic board which generates digital commands to control the data processor board of Figure 23 . . . . .	71
25. Photograph of receiver, data processor, and logic controller drawer with RF shield in place . . . . .	73
26. Photograph of receiver, data processor, and logic controller drawer with RF shield removed . . . . .	74
27. Photograph showing closeup view of the five data processor subsystem cards and the four logic controller cards . . . . .	75
28. Photograph of Hybrid system cabinet which contains the receiver, data processor, and logic controller subsystems and dc power supplies . . . . .	76
29. Photograph of paraboloidal reflector test antenna mounted on antenna positioner . . . . .	77

List of Figures continued

<u>Figure</u>	<u>Page</u>
30. View of Georgia Tech antenna range receive site, as seen from transmit facility, showing test antenna mounted in place . . . . .	78
31. Broadband pattern of test antenna for a bandwidth of 5 MHz centered at 3.5 GHz . . . . .	80
32. Broadband pattern of test antenna for a bandwidth of 10 MHz centered at 3.5 GHz . . . . .	81
33. Broadband pattern of test antenna for a bandwidth of 20 MHz centered at 3.5 GHz . . . . .	82
34. Broadband pattern of test antenna for a bandwidth of 50 MHz centered at 3.5 GHz . . . . .	83
35. Broadband pattern of test antenna for a bandwidth of 100 MHz centered at 3.5 GHz . . . . .	84
36. Broadband pattern of test antenna for a bandwidth of 200 MHz centered at 3.5 GHz . . . . .	85
37. Broadband pattern of test antenna for a bandwidth of 500 MHz centered at 3.5 GHz . . . . .	86
38. Broadband pattern of test antenna for a bandwidth of 1000 MHz centered at 3.5 GHz . . . . .	87
39. CW pattern using Scientific Atlanta Receiver at a frequency of 3.5 GHz . . . . .	88
40. Illustration of the incremental phase measurement concept in the laboratory . . . . .	93
41. Extension of the direct incremental phase measurement concept to the far-field antenna range . . . . .	93
42. Block diagram of possible direct measurement phase and amplitude system . . . . .	94
43. Block diagram of group delay sideband processor . . . . .	98
44. Block diagram showing the frequency conversions which occur in a group delay measurement system . . . . .	99

## List of Figures continued

<u>Figure</u>	<u>Page</u>
45. Stabilized programmable WWV-locked transmitter system for group delay measurements . . . . .	102
46. Measured field intensity contours for WWV/Boulder standards broadcast . . . . .	104
47. Block diagram of a system for phase locking to a WWV standards broadcast . . . . .	105
48. Block diagram of group delay receive site subsystem . . . . .	108
49. Tracking phase-locked receiver block diagram . . . . .	110
50. Simplified block diagram of Scientific Atlanta Series 1700 Receiver in the two-channel configuration . . . . .	111
51. Time and frequency domain correspondence for rectangular pulse train . . . . .	132
52. Sketch depicting the phase response as a function of frequency for a hypothetical system and the relevant statistical parameters utilized in statistical analysis of pulse distortion effects. $f_0$ is the fundamental frequency of the incident pulse spectrum, and $f_1$ and $f_2$ , respectively, are the lower and upper limits of the pulse spectrum . . . . .	134
53. Number of operations required for computing a discrete Fourier Transform by the conventional DFT and the FFT . . . . .	139
54. Simplified flow diagram of pulse distortion computer program FTRANS . . . . .	141
55. Sketch of the amplitude envelope of a stretched cosine-squared pulse of total pulse width $T$ , 3-dB pulse width $\Delta t_3$ and rise time $\Delta t_r$ . $\zeta$ denotes the half-period of the cosine portion of the pulse, and $\Delta t_1$ is the half-width of the rectangular portion of the pulse . . . . .	144
56. Frequency spectrum for a 3-nanosecond stretched cosine-squared pulse . . . . .	146
57. Incident 5-nanosecond pulse . . . . .	147

## List of Figures continued

<u>Figure</u>	<u>Page</u>
58. Degraded 5-nanosecond pulse after propagation along a 100-cm length of X-band waveguide . . . . .	147
59. Degraded 5-nanosecond pulse after propagation along a 300-cm length of X-band waveguide . . . . .	148
60. Degraded 5-nanosecond pulse after propagation along a 1000-cm length of X-band waveguide . . . . .	148
61. Incident 3-nanosecond pulse . . . . .	149
62. Degraded 3-nanosecond pulse after propagation along a 100-cm length of X-band waveguide . . . . .	149
63. Degraded 3-nanosecond pulse after propagation along a 300-cm length X-band waveguide . . . . .	150
64. Degraded 3-nanosecond pulse after propagation along a 1000-cm length of X-band waveguide . . . . .	150
65. Incident 1-nanosecond pulse . . . . .	151
66. Degraded 1-nanosecond pulse after propagation along a 100-cm length of X-band waveguide . . . . .	151
67. Degraded 1-nanosecond pulse after propagation along a 300-cm length of X-band waveguide . . . . .	152
68. Degraded 1-nanosecond pulse after propagation along a 1000-cm length of X-band waveguide . . . . .	152

## LIST OF TABLES

<u>Table</u>	<u>Page</u>
1. Summary of Design Goals for the Hybrid System . . . . .	14
2. Component Summary for S-Band Hybrid System Breadboard Transmitter . . . . .	19
3. Hughes 1177H01 TWT Performance Characteristics. . . . .	20
4. Average VSWR Data for Double Ridge Waveguide Feed Horn. . .	32
5. Average VSWR Data for Single Ridge Waveguide Feed Horn. . .	34
6. Amplitude Taper with Reflector of Various f/D Ratios and the Single Ridge Feed Horn of Figure 13 . . . . .	36
7. Measured Gain of Transmit Antenna . . . . .	44
8. Component Summary for S-Band Hybrid System Breadboard Receiver. . . . .	46/47
9. Typical Series 1700 Receiver Sensitivity. . . . .	112
10. Antenna Range Parameters at Various Distances . . . . .	124
11. Received Signal Level for Maximum Test Antenna Diameter. . . . .	125



## SECTION I

### INTRODUCTION

#### A. GENERAL

Modern day radar systems for many applications require broad instantaneous RF bandwidths. Current or planned broadband radar systems require bandwidths on the order of 1 GHz. Of course, a 1 GHz bandwidth translates to a pulsewidth on the order of 1 nanosecond. For certain other systems, generation of RF pulsewidths into the picoseconds regions is of interest. To realize the intended benefit of these very narrow pulses, a fast rise time and a well-defined leading edge must be maintained. This requirement means that all transmission and radiation components must have a broad 3-dB bandwidth and well-behaved phase characteristics over this bandwidth. One deterrent to the development of broadband radar components with the desired phase and amplitude properties has been the lack of practical techniques for their measurement. This deficiency has been particularly notable with respect to evaluation of high gain microwave antennas.

To alleviate this problem, the Rome Air Development Center is sponsoring a research program at Georgia Tech to develop innovative techniques for evaluation and analysis of high gain microwave antennas over octave instantaneous signal bandwidths. This report describes the work accomplished on the second phase of this program. On the first phase of this program, under Contract F30602-73-C-0194, various broadband measurement techniques were synthesized and evaluated. The approaches which were evaluated included systems based on both broadband noise sources and swept frequency sources. It was

concluded that the use of swept frequency techniques offered the most convenient and cost effective approach toward the realization of practical broadband measurement systems. Preliminary design of a broadband swept frequency amplitude-only system was completed, and two different approaches toward realization of a phase-and-amplitude measurement system were identified on Phase I.

On the present program, an S-band (2-4 GHz) swept frequency amplitude-only system design has been completed, the system has been breadboarded and tested on the antenna range. In addition, further tradeoff studies of the two phase-and-amplitude measurement approaches have been completed, a measurement approach has been selected, and preliminary design of the phase-and-amplitude system has been completed.

#### B. CONTRACT OBJECTIVES

As previously indicated, work on this contract extends basic studies initiated on Contract F30602-73-C-0194 for RADC. The overall objectives of this contract were to study and investigate advanced techniques to measure, analyze, and record the amplitude, phase, and radiation patterns of broad signal bandwidth antenna systems. The frequency range of interest is from 0.2 to 15.0 GHz, with emphasis on the region from 1 to 15 GHz.

Specifically, the objectives of this contract may be stated in terms of three tasks, (1) to complete the design, breadboarding, and laboratory testing of a 2-4 GHz swept frequency amplitude-only system, (2) expand the phase-and-amplitude system analyses initiated under previous contract to include trade-off evaluation of system concepts, selection of a measurement approach, and preliminary design of a computer controlled phase-and-amplitude measurement system based on the selected approach, and (3) development of computer

software which will process measured broadband phase-and-amplitude antenna data to predict the antenna effects (distortion) on a given original pulse. In addition to these efforts, a significant amount of antenna range testing of the amplitude-only system has been accomplished.

### C. SUMMARY OF WORK PERFORMED

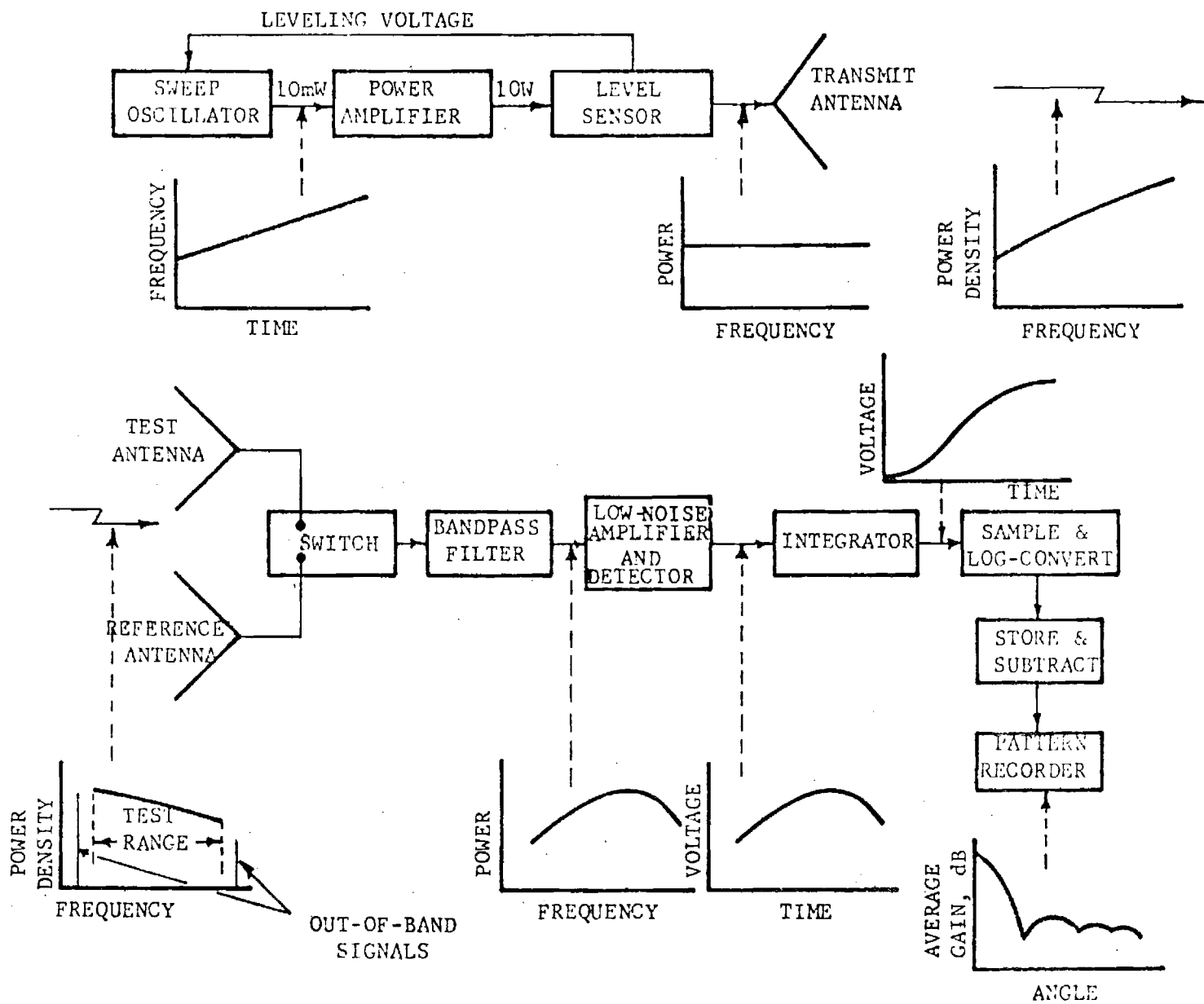
#### 1. Amplitude-Only System

Two new antenna measurement concepts have been investigated and evaluated. The first concept may be described as an amplitude-only swept frequency electronically integrating system. Based on preliminary system design performed under Contract F30602-73-C-0194, final design of a 2-4 GHz system was completed. For analysis and development purposes, this system was divided into four subsystems: the transmitter, receiver, data processor, and logic controller subsystems.

The amplitude-only system concept may be understood with reference to the simplified block diagram shown in Figure 1. This system produces results which are equivalent to those which would be obtained with a broadband noise source but it is based on a swept signal. Hence, this system was originally identified as the Hybrid system. This system produces average antenna gain by electronically integrating the test antenna response to a signal which is swept across the desired test frequency range. That is, in this system time domain integration of a swept frequency signal is used instead of frequency domain integration of broadband noise.

Important waveform considerations at various circuit points in the system are depicted by the sketches with dotted lines indicating the appropriate circuit point on the block diagram in Figure 1. An important feature of this Hybrid system is that amplitude variations (such as those due to variations in transmit antenna gain and space loss) are compensated

Figure 1. Simplified block diagram of amplitude-only Hybrid system.



automatically in the receiver. This compensation is equivalent to obtaining constant power density at the test antenna aperture. Thus, tailoring of the transmit antenna gain versus frequency is not needed. Basically, compensation is based on electronically determining the ratio of test antenna response to the response of a reference antenna whose gain versus frequency characteristics are known. This system can provide average antenna responses over any bandwidth up to the transmitter sweep range.

A 2-4 GHz version of this amplitude only system has been breadboarded and tested, both in the laboratory and on the antenna range. Details of this design and test results are presented in Section II. The effect of a broadband signal on antenna response is illustrated by the patterns presented in Figures 2 and 3. Figure 2 shows the CW pattern of a four-foot diameter paraboloidal reflector at 3.5 GHz. Figure 3 shows the pattern obtained for a bandwidth of  $\pm 500$  MHz, centered at 3.5 GHz. Note the smearing-out of the sidelobes and the filling-in of the nulls. These are typically effects which are obtained when the signal bandwidth is increased. This type of average spatial pattern information may be important, for example, in the analysis of radar response in a sidelobe noise jamming environment.

## 2. Phase-And-Amplitude System

The second new concept which was investigated is a computer controlled swept frequency phase-plus-amplitude broadband diagnostic tool. In certain important applications, an amplitude only system may not provide all of the information which is necessary in determining the performance of broadband radar systems. For example, both phase and amplitude information is necessary in determining the antenna effect upon pulse shape and in defining pulse compression performance limitations. Measured phase and amplitude data

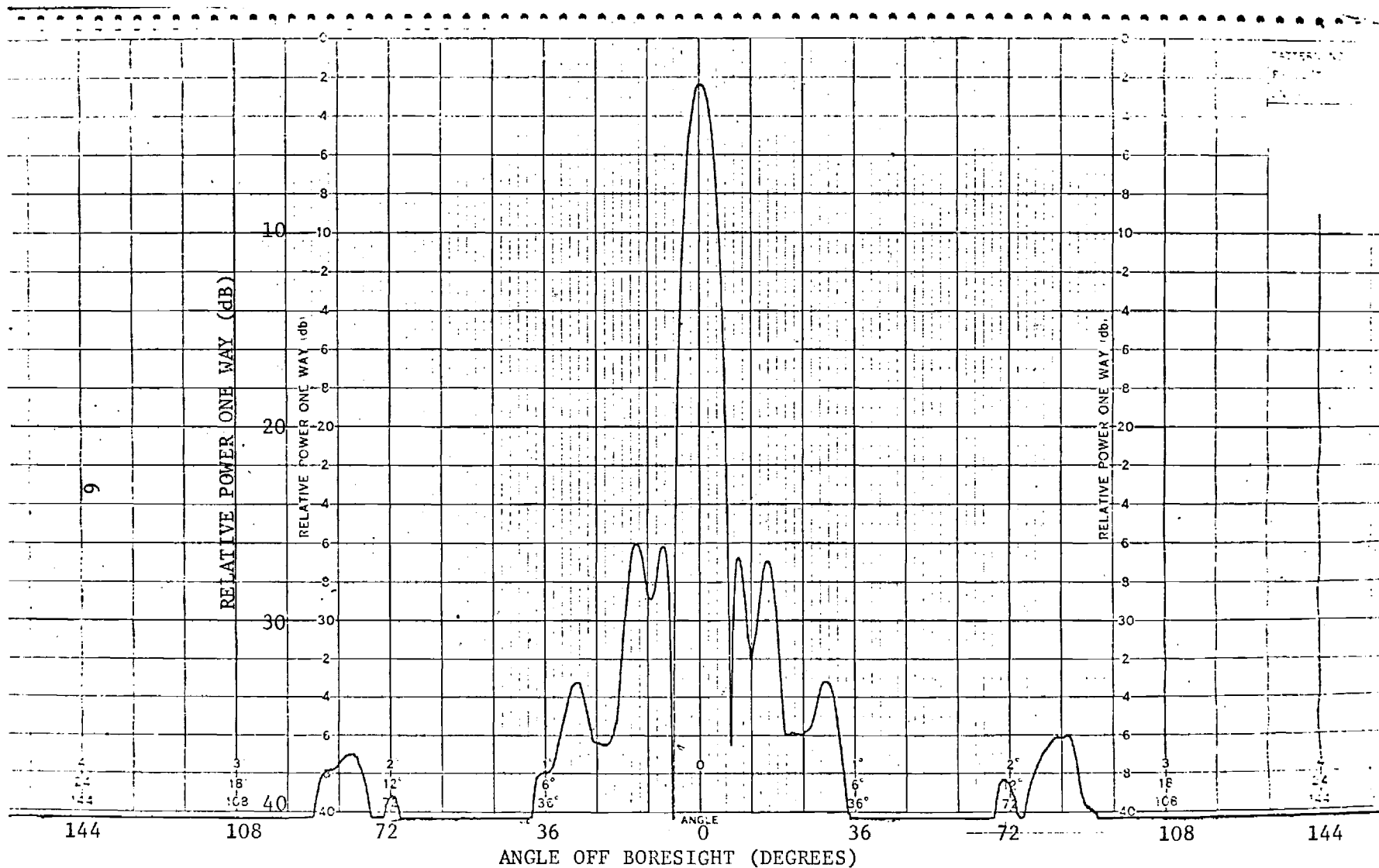


Figure 2. CW pattern of four-foot paraboloidal reflector at a frequency of 3.5 GHz.

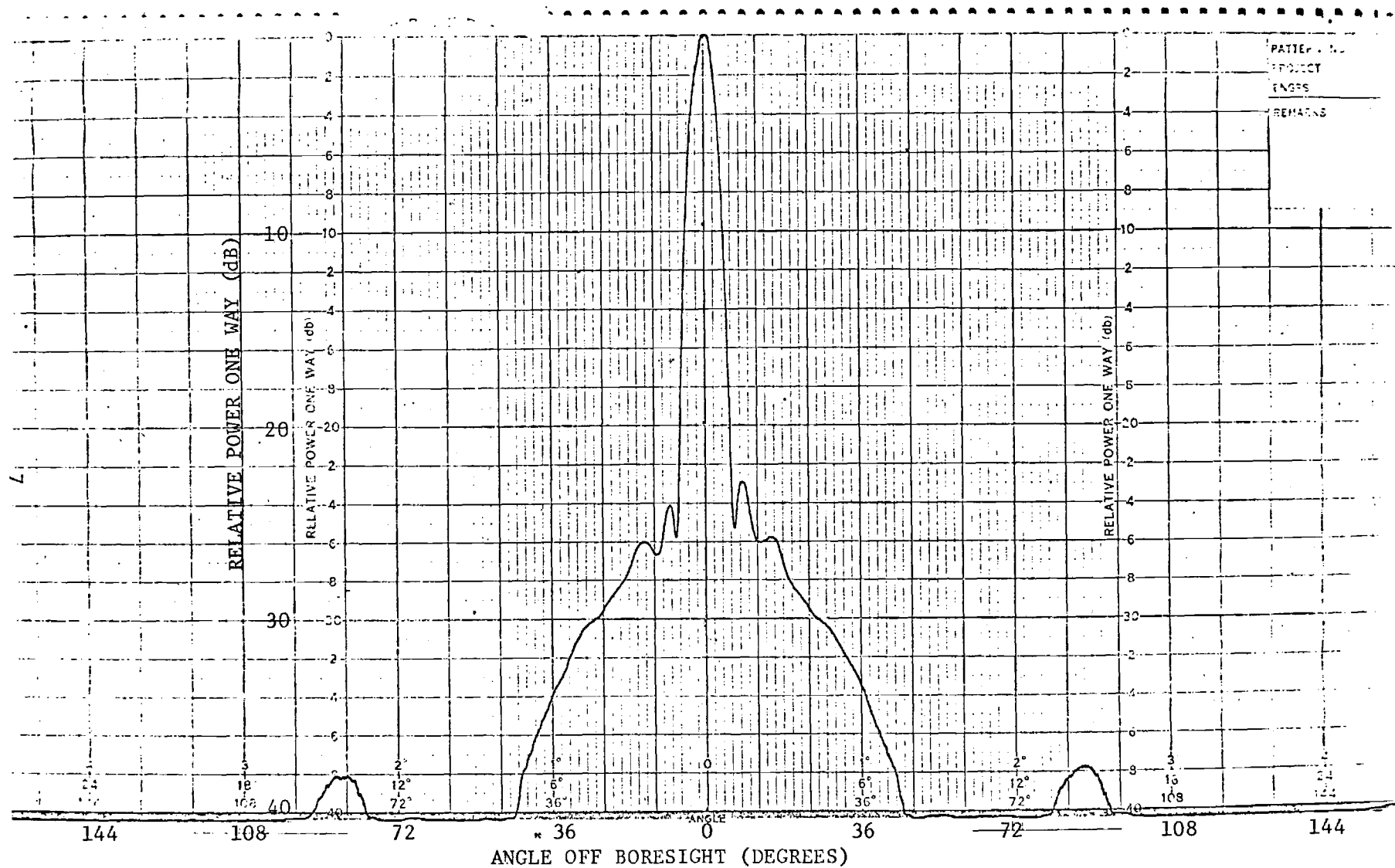


Figure 3. Broadband pattern of four-foot paraboloidal reflector for a bandwidth of  $\pm 500$  MHz centered at 3.5 GHz.

can be digitally processed to determine any antenna property which is desired, such as broadband average gain, broadband average spatial patterns, CW patterns or gain at any selected discrete frequency within the frequency sweep range, and pulse distortion effects. It should be emphasized that such a measurement and use of antenna phase information represents a new dimension in microwave antenna testing. These new measurement systems will materially aid in the development of new antennas which are capable of satisfying the requirements of a new generation of highly sophisticated and accurate radar systems.

Two measurement approaches for implementation of a phase-plus-amplitude system were investigated and evaluated. The first approach is based on a direct measurement of test antenna phase response by determining the relative phase between a CW signal received through the test antenna and that same CW signal but received through a reference antenna. This CW signal may be frequency stepped across the measurement range to obtain broadband phase information. A block diagram of this type of system is shown in Figure 4.

The second phase measurement approach is based on a measurement of the relative phase between two coherent sidebands of a modulated CW carrier. If this carrier and sidebands are swept across the desired measurement range, the relative sideband phase data for a given sideband frequency separation represents the group delay, which may be integrated to obtain the phase response. With this group delay type of system, all the phase information is received through a single channel, i.e., the test antenna channel. With the direct phase measurement system, the relative phase must be maintained between two channels (test and reference) which may have widely separated mixers and different electrical lengths. The group delay approach thus



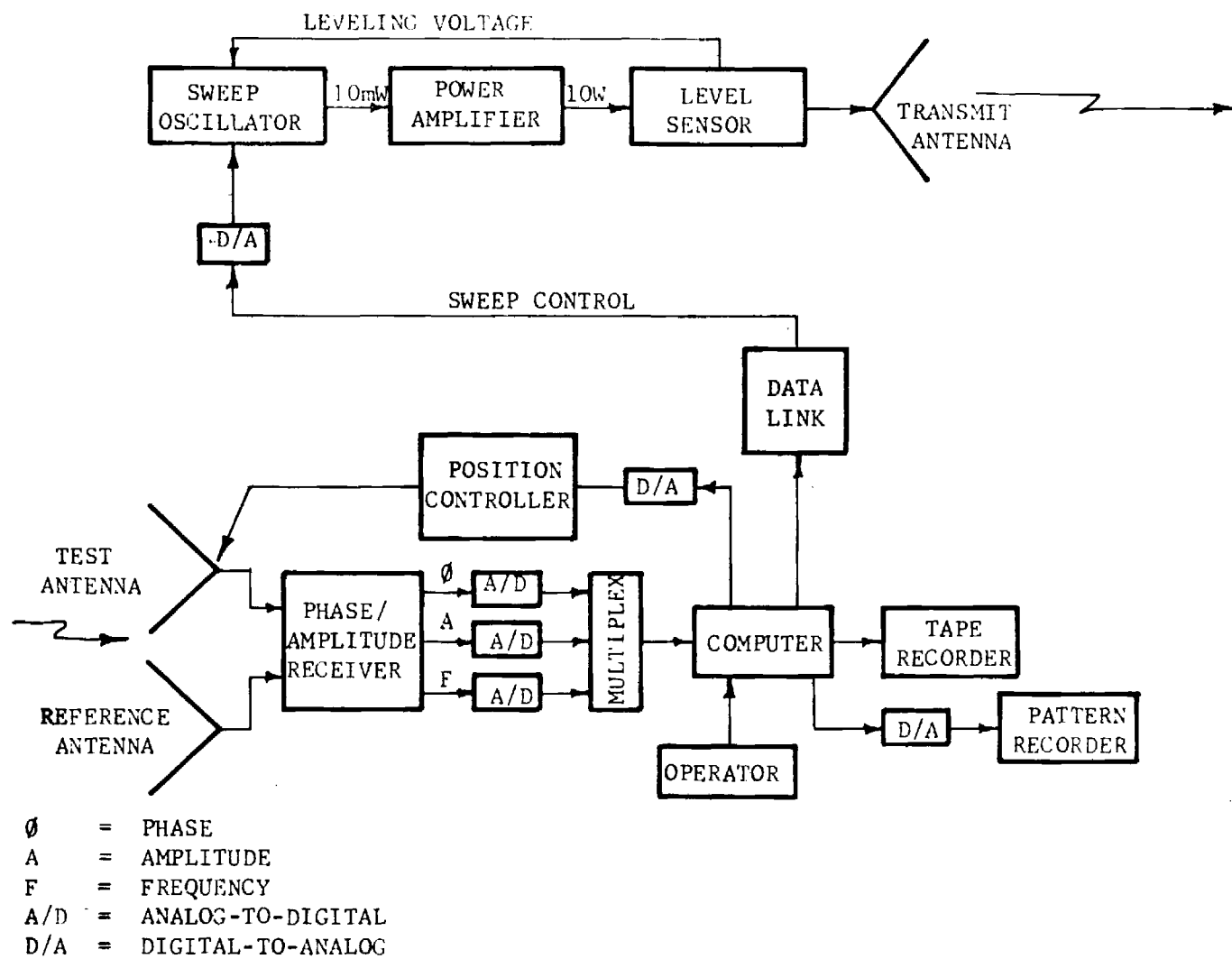


Figure 4. Simplified block diagram illustrating direct measurement of antenna phase response.

appears to offer a better solution to the problem of obtaining a stable, accurate, broadband, phase-and-amplitude antenna range system. Therefore, this approach was selected for further design and evaluation. Preliminary design study of a broadband group delay type of phase-and-amplitude measurement system has been completed. Diagrams of this system are presented in Section III . This system employs a programmable octave bandwidth microwave signal source which is stabilized to a crystal controlled synthesizer. The sideband modulator at the transmit site and the demodulator at the receive site are both phase locked to a common highly stable signal in order to obtain phase coherency. This system generates a highly stabilized carrier and two phase coherent sidebands which may be automatically stepped across the measurement range of interest. At the receive site, the test signal (carrier plus sidebands) are received through the test antenna, and the relative phase between the sidebands is measured as a function of carrier frequency. This relative sideband phase and carrier amplitude information is digitally recorded for later processing to obtain any desired antenna property such as pulse distortion effects, selected CW or broadband spatial patterns, or phase errors. Detailed preliminary design studies on this system are presented in Section III.

### 3. Pulse Distortion Analysis

One application of the system just summarized is the measurement of phase and amplitude data for the calculation of pulse distortion effects. The severity of the pulse distortion effects depends on both the original pulse and the bandpass characteristics of the antenna. Therefore, analytical techniques are needed which can utilize measured antenna phase and amplitude data to predict pulse distortion effects for arbitrary

original pulses. This analytical technique thus eliminates the need to actually measure antenna response with every specific pulse of interest. A computer program for calculating such pulse distortion was developed and exercised for three representative pulses and selected amplitude and phase transfer characteristics.

This type of analysis is based on a specialized discrete Fourier Transform, and it is practical because of the Fast Fourier Transform (FFT) which allows efficient digital computer calculation. In particular, the amplitude of the distorted pulse as a function of time is given by the Fourier Transform of the original pulse spectrum and the complex transfer function of the antenna. A computer program was developed which performs this pulse distortion calculation for either analytical pulse shapes and transfer functions or for discrete measured pulse shapes and antenna transfer functions. For illustration, this computer program was used to calculate the distorted pulse envelope of three different original pulses which have undergone various phase and amplitude distortions.

The family of distorted pulses bear out certain expected trends. For a given incident pulse, the magnitude of distortion, as manifested in the increased rise and fall times, degradation of the overall pulse shape, and the appearance of time sidelobes, increases for greater amplitude and phase errors. Furthermore, for given phase and amplitude errors, the magnitude of these same distortion effects is generally greater for narrower incident pulses. These effects, and others, along with a complete discussion of the analytical and computer techniques are presented in Section IV.

## SECTION II

### AMPLITUDE-ONLY SYSTEM BREADBOARD DEVELOPMENT

#### A. INTRODUCTION

A detailed description and analysis of the swept frequency amplitude-only system concept has been given in the Final Technical Report on Contract F30602-73-C-0194 [1]. A major effort on the current contract has been the breadboarding and testing of an S-band (2-4 GHz) system. This section will review the system design concept, discuss the 2-4 GHz implementation, and present test data.

The Hybrid amplitude-only system is based on a design concept which meets the measurement goals identified in the contract statement-of-work and which will provide growth capability by incorporation of a major portion of the transmitter into the expected phase-and-amplitude system. Since the receiver and data processor portions of the amplitude-only system would not be incorporated into the phase-and-amplitude system, these portions in particular were designed to minimize cost. At the same time it must be recognized that this Hybrid system provides a significant new measurement capability. Meeting the system design goals has required the use of state-of-the-art components and techniques, and maintaining state-of-the-art performance over an extremely large bandwidth · dynamic range product. Table 1 summarizes the design goals for the Hybrid system. It should be noted that these are design goals to be simultaneously met. The parameters of Table 1 will be discussed in detail in connection with the hardware implementation of the Hybrid system, and they will be related to test data.

TABLE 1  
SUMMARY OF DESIGN GOALS FOR HYBRID SYSTEM

---

Frequency Range:	2-4 GHz
Instantaneous Bandwidth:	1 GHz anywhere in 2-4 GHz range
Transmitter Power Output:	$\leq 10$ watts
Max. Transmitter Power Variations:	$\pm 1$ dB
Spurious Radiation:	Harmonic 20 dB below carrier, non-harmonics 60 dB below carrier
Receiver Sensitivity:	-80 dBm
Dynamic Range:	Sufficient to observe -40 dB sidelobes
Amplitude Error:	$\pm 0.25$ dB
Out-of-Band Rejection:	20 dB

---

The most straightforward receiver design for obtaining broad instantaneous bandwidth (no tuning or LO tracking) with good sensitivity is the wideband RF receiver with a low-noise RF amplifier. The design guideline, from Table 1, for receiver sensitivity is -80 dBm. For any receiver, the sensitivity is limited by thermal noise. Thermal noise power  $N$  is given by

$$N = kT_0 B, \quad (1)$$

where  $k$  = Boltzman's constant,

$T_0$  = reference noise temperature = 290°k, and

$B$  = noise bandwidth.

Taking  $B$  as 2 GHz, the thermal noise is found to be

$$\begin{aligned} N &= (4 \times 10^{-21} \text{ joules})(2 \times 10^9 / \text{sec}) \\ &= 8 \times 10^{-12} \text{ watts} = 8 \times 10^{-9} \text{ mW, or} \\ N &= -81 \text{ dBm.} \end{aligned}$$

Thus, a perfect receiver with 2 GHz bandwidth would have a noise floor level of -81 dBm. Of course, it is not possible to obtain perfect noise-free components (0 dB noise figure), and a real 2 GHz bandwidth receiver will have a noise floor greater than -81 dBm. However, the receiver/data processor combination integrates over one transmitter sweep for each data point, and an improvement in signal-to-noise ratio is thereby obtained. This improvement in signal-to-noise ratio translates directly into increased sensitivity. Furthermore, as discussed later in this Section (subsection B-4), the video bandwidth in the data processor is limited to 5 kHz. Thus, a significant improvement in sensitivity is obtained through integration and noise limiting.

The hardware impact of each of the factors introduced above will be fully considered in the following sub-section.

## B. BREADBOARD SYSTEM

### 1. Transmitter

A block diagram of the amplitude-only system transmitter is given in Figure 5. This transmitter consists of a sweep oscillator, travelling wave tube (TWT) power amplifier, isolator, low pass filter, and a directional detector to provide a leveling voltage to the sweep oscillator. The transmit antenna indicated schematically in Figure 5 is discussed in the following sub-section. Of course, the basic signal is provided by the sweep oscillator. The TWT provides the gain required to increase the power to the 10 watt level. Since octave bandwidth TWTs may have significant second harmonic output (depending on frequency and drive power), a low pass filter is used to reduce these harmonics to an acceptable level. The isolator absorbs the reflected harmonics and prevents their being returned to the output of the TWT. The directional detector consists of a crystal detector matched to a directional coupler. Thus, this device provides a voltage which is directly proportional to the forward power at the filter output. This voltage is fed into the sweep oscillator, which responds in such a manner to maintain constant power at the directional detector input. Thus, variations of TWT gain and other component responses versus frequency are compensated. The specific implementation of Figure 5 for the breadboard system is discussed in the following paragraphs.

The TWT amplifier used in the breadboard system is a Hughes Aircraft Co. Model 1177H01. This tube uses periodic permanent magnet (PPM) focusing and forced air cooling. A summary of amplifier specifications is contained in

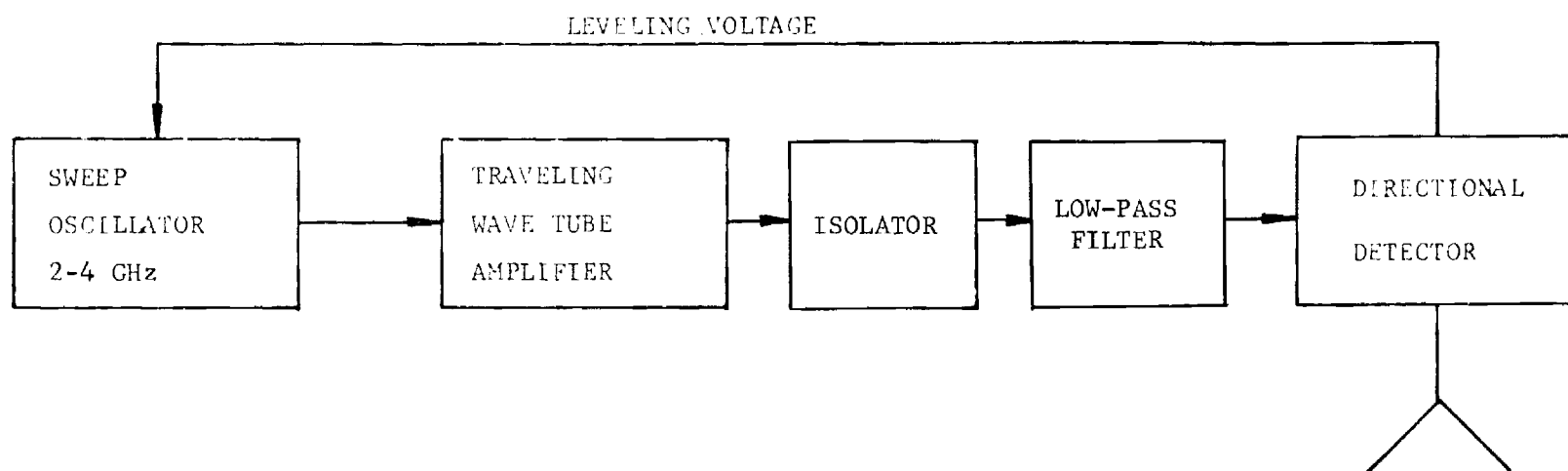


Figure 5. Block diagram of Hybrid system breadboard transmitter.



Table 2 . Table 3 presents a summary of measured TWT performance parameters. The required power input, measured gain, and second harmonic level are shown for output powers of 1 watt, 10 watts, and saturated power. Note that at 2 GHz with either 10 watts or saturated output, the second harmonic power is equal to the fundamental power. At 2 GHz, the second harmonic (4.0 GHz) is within the TWT passband so that it is amplified also. As the fundamental frequency increases above 2.0 GHz, the second harmonic becomes further removed from the TWT passband and its relative level decreases. To remove these second harmonics, either one of two low pass filters may be used. The two filters which are used in the breadboard are Engleman Microwave Models F130N and F140N. These two filters have upper cut-off frequencies ( $f_c$ ) of 3.0 GHz and 4.0 GHz, respectively. The proper filter is selected for the particular frequency range over which measurements are to be made. These two filters have the following rejection characteristics: 25 dB @  $1.25 f_c$ , 50 dB @  $1.5 f_c$ , and 60 dB @  $1.6 f_c$ . Thus, when operating from 2 GHz to 3 GHz, the 3.0 GHz low pass filter is used, and by interpolation it may be shown that at 2.0 GHz, the second harmonic is rejected by about 35 dB. As the fundamental increases from 2.0 GHz to 3.0 GHz, greater second harmonic rejection is obtained.

Note also from Table 3 that to obtain a constant power output, the input power must be varied. Figures 6 and 7 show the required input power to obtain 1 watt and 10 watts constant outputs, respectively. Thus, the power leveling loop must cause the sweeper power output to vary in this manner.

The sweep oscillator which was selected for the breadboard transmitter is the Weinschell Model 430A Mainframe with Model 432A 2-4 GHz RF plug-in.

TABLE 2

## COMPONENT SUMMARY FOR S-BAND HYBRID SYSTEM BREADBOARD TRANSMITTER

<u>Sweep Oscillator</u>	<u>TWT Amplifier</u>	<u>Level Sensor (Directional Detector)</u>
Nominal Power output: 15 mW	Power Output Capability: 10 watts CW	Frequency Range: 2-4GHz
Frequency Range: 2-4 GHz	Nominal Gain: 30 dB	Output Voltage Flatness $\pm 0.2$ dB
Sweep Modes:	Frequency Range: 2-4 GHz	Max. Input Power: 10 W
Repetitive Sweep between Any Present Limits within 2-4 GHz,	Beam Supply Regulation: $\pm 0.1\%$	Directivity: 26 dB
Fixed Bandwidth Sweeps about Selectable Center Frequency	Helix Voltage Regulation: $\pm 0.1\%$	Max. Insertion Loss: 0.5 dB
Non-Sweep CW Mode	Line Voltage Variation: $\pm 10\%$	
Remote On/Off Control	Interlocks/Interrupts:	
Remote CW Frequency Selection	Time Delay	
Leveled Power Control Range: 15 dB	Beam/Helix Overcurrent	
Sweep Linearity: $\pm 0.5\%$	Thermal Cutout	
Sweep Time: Adjustable from 10 msec to 100 sec per sweep	Power Line Interrupt	
Non-Harmonic Spurious: >60 dB below carrier	Load VSWR: 2.5:1	
External Level Accuracy: $\pm 0.1$ dB plus level signal error	Noise Figure: $\leq 35$ dB	
	Filament: Regulated DC	
	Collector Mode: Depressed	

TABLE 3

## HUGHES 1177H01 TWT PERFORMANCE CHARACTERISTICS

Frequency, GHz	Power Input, mw	Power Output, Watts	Gain, dB	Relative 2nd Harmonic, dB
10 Watts Output				
2.0	4.0	10	34.0	0
2.5	1.14	10	39.4	-26
3.0	0.8	10	41.0	-36
3.5	1.8	10	37.4	-44
4.0	4.1	10	33.9	-32
Saturated Output				
2.0	21.9	22	30.0	0
2.5	12.0	31	34.1	-19
3.0	13.2	38	34.6	-38
3.5	21.9	41	32.7	-42
4.0	36.3	35*	---*	-32
1 Watt Output				
2.0	0.8	1	31	-13
2.5	0.1	1	40	-32
3.0	0.07	1	41.5	-43
3.5	0.21	1	36.8	-47
4.0	0.48	1	33.2	-42
*Not Saturated Due to Insufficient Drive Power				

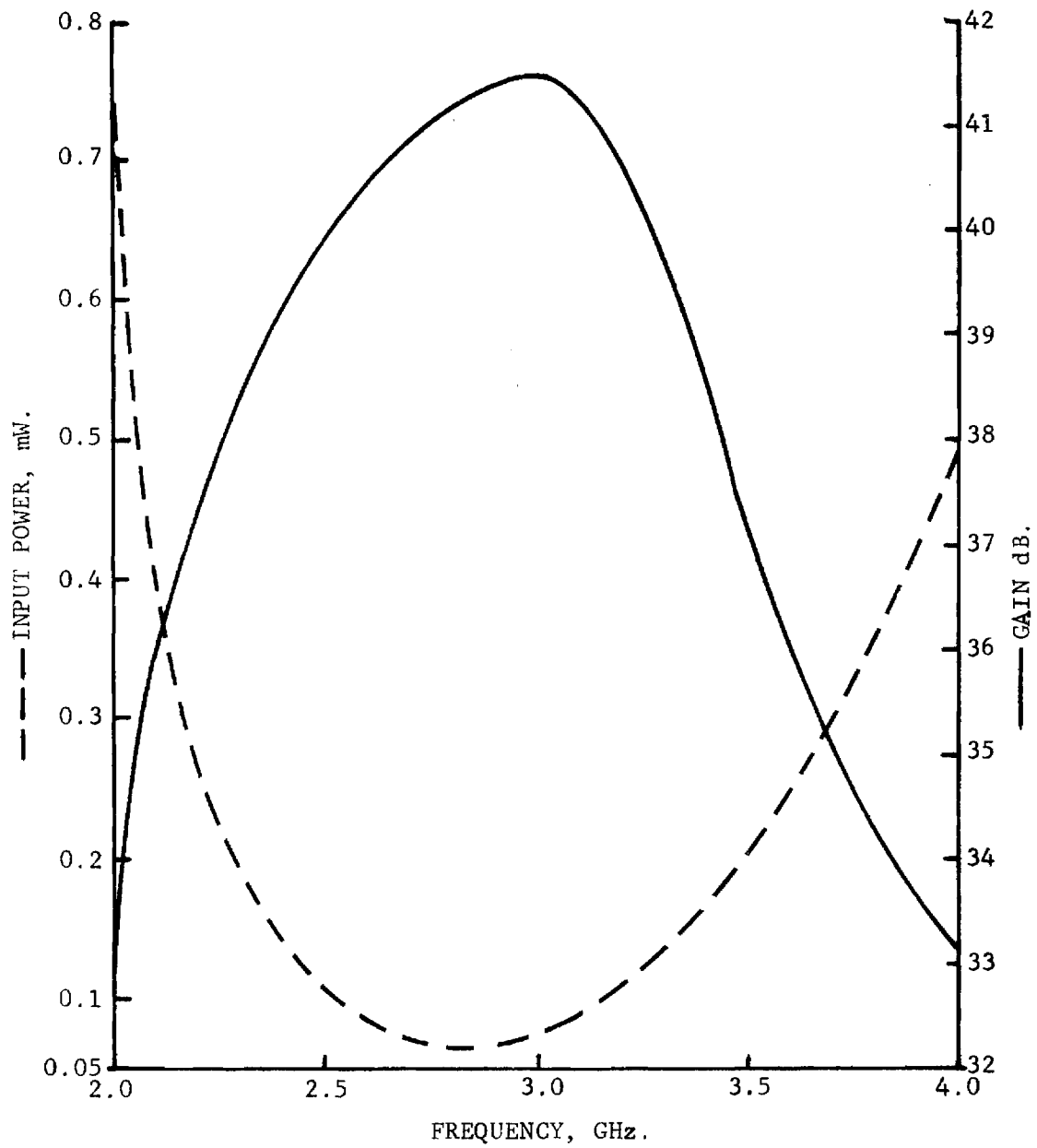


Figure 6. TWT gain and required input power for 1 watt output.

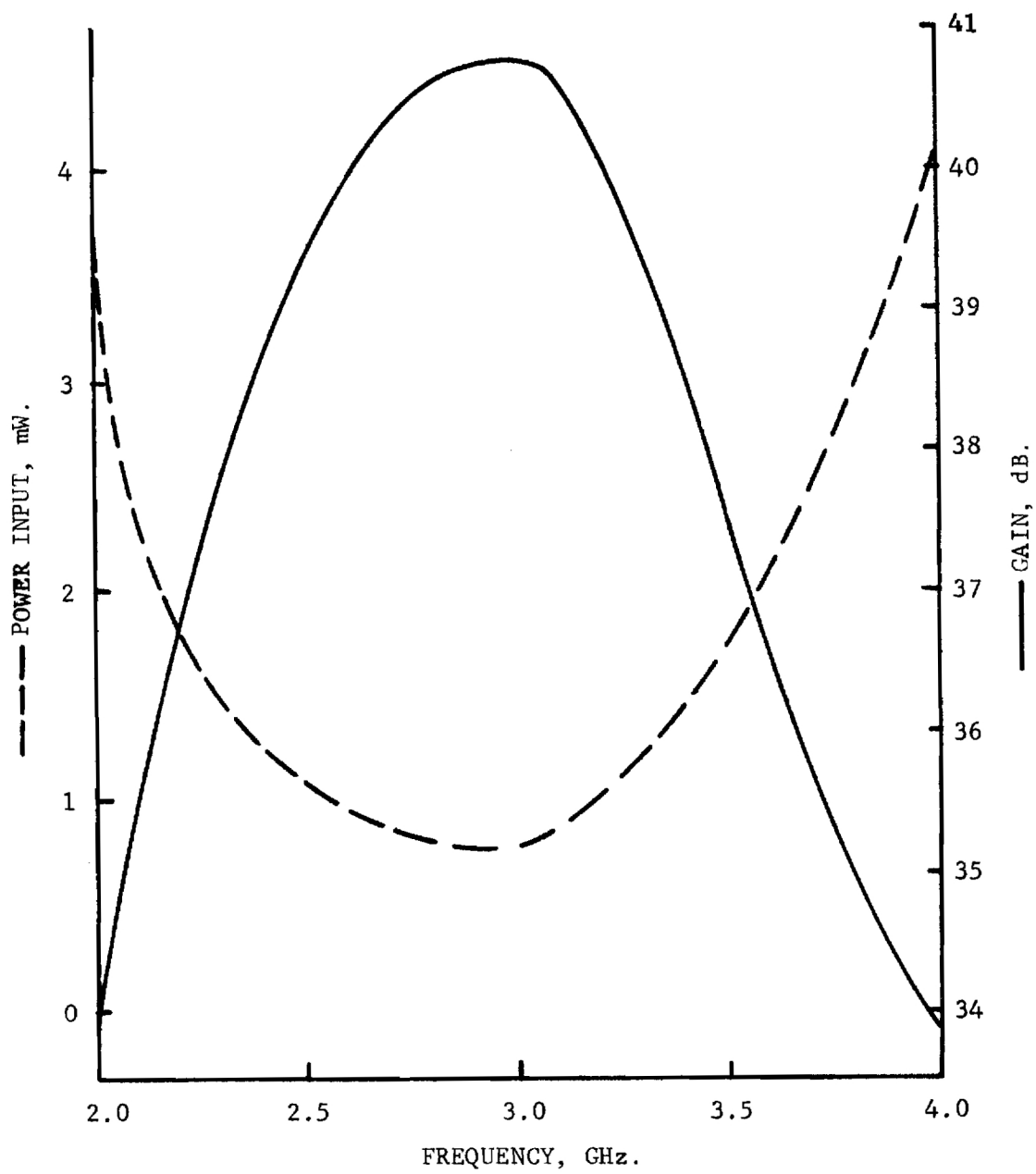


Figure 7. TWT gain and required input power for 10 watts output.

These RF units employ solid state sources for long term reliability. A summary of the major parameters of this sweep oscillator is contained in Table 2. For growth to a computer controlled system, this sweep oscillator may also be remotely controlled through a 12-line BCD input. Up to 1000 discrete frequencies may be selected, and RF power may be remotely controlled. In addition, for precise control of frequency, phase locking to a highly stabilized reference is a standard capability.

The directional detector which is used in the breadboard unit is the Hewlett Packard Model 787D. Major parameters are summarized in Table 2. The isolator device which is used is an Addington Labs Model 10110293 internally terminated three-port circulator. Measured data on this unit show a minimum isolation of 22 dB.

A photograph of the assembled transmitter is shown in Figure 8. Figures 9 and 10 show the relative output power versus frequency for average outputs of 10 watts and 1 watt, respectively. Note that the total variation in each case is within the  $\pm 1$  dB design goal.

## 2. Transmit Antenna

Since the Hybrid breadboard system may be required to operate over any 1 GHz interval within the 2-4 GHz frequency octave, it is required to have a single transmitting antenna which will cover this entire octave. Previous system sensitivity analysis indicated that a gain of at least 30 dB is required at 4 GHz [1]. With a typical illumination function and 50 percent efficiency, achieving this gain requires an aperture of about 4 feet. A 4-foot reflector with a broadband feed is the most cost effective means for achieving the required gain and bandwidth. For concept demonstration, the breadboard system is only required to

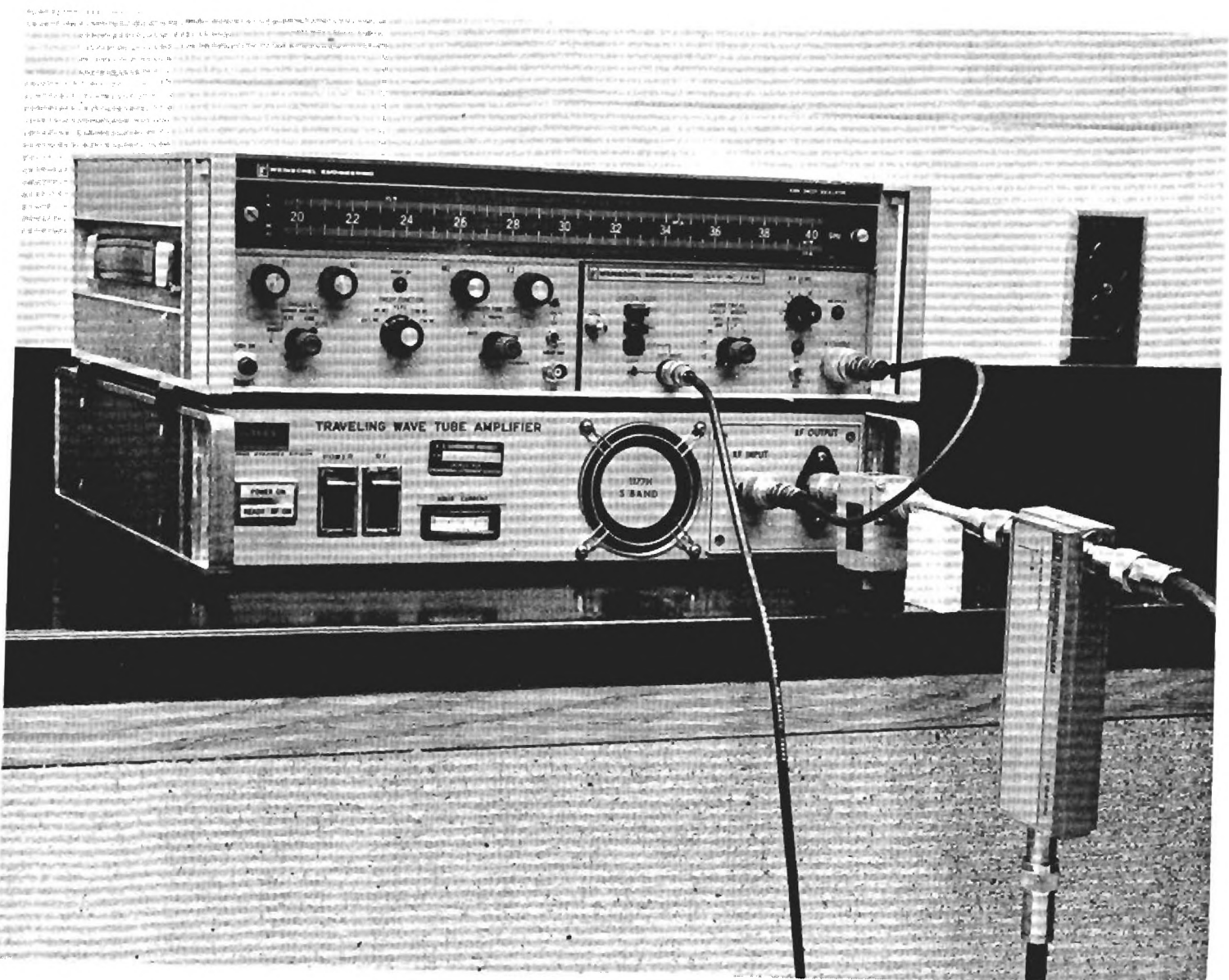


Figure 8. Photograph of assembled S-band Hybrid system breadboard transmitter

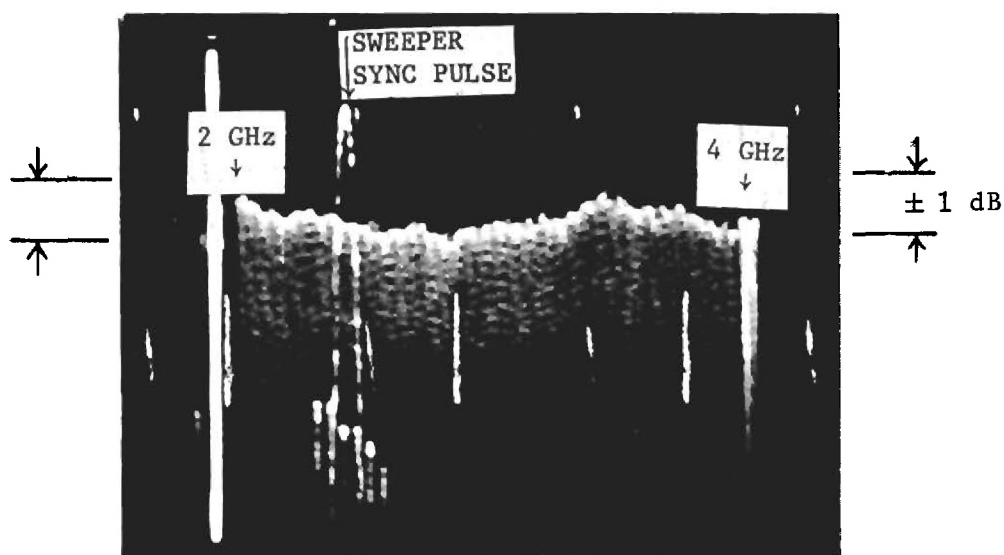


Figure 9. Variation of transmitter power level versus frequency for 2-4 GHz sweep and 10 watts average power output.

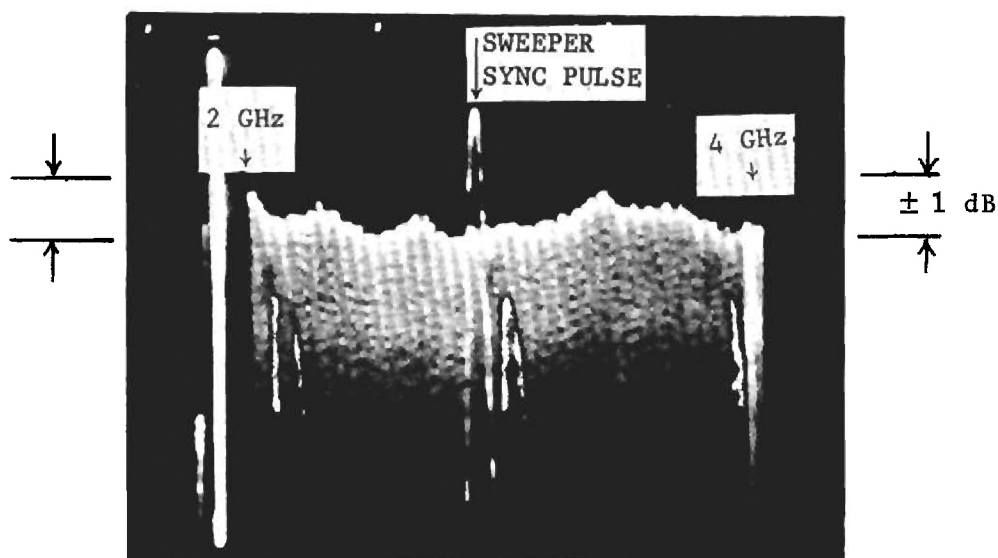


Figure 10. Variation of transmitter power level versus frequency for 2-4 GHz sweep and 1 watt average power output.



operate with linear polarization. Of course, the breadboard Hybrid system could be upgraded to test antennas of any polarization by suitable modifications to the transmitting and reference antennas.

Several alternatives were considered for achieving the broadband linearly polarized feed. A survey of the market was made to determine the cost and performance of both broadband feed horns and other forms such as log periodics. First, purchase of a quad-ridged dual-polarized horn was considered. This type of horn in commercial versions typically covers octave or waveguide bands (1-2 GHz, 2-4 GHz, 4-8 GHz, 8-12 GHz, or 12-18 GHz) from 1 GHz to 18 GHz. VSWR is typically up to 3.0:1, and the 3-dB beamwidth varies from about 60 degrees at the low end of each frequency band to about 35 degrees at the high end. Cost of these units is about \$2500. Because of this high cost, alternative approaches were considered.

A log-periodic feed was next considered for the breadboard system. The log periodic may be very broadband, covering several octaves of frequency. This antenna type is generally considered to be frequency independent since its beamwidth is essentially constant over its entire operating frequency. However, the phase center of the log periodic moves along the antenna as the frequency varies. This phase center movement causes considerable axial defocusing of the system with attendant loss in gain. Furthermore, this phase center movement corresponds to a phase dispersion error for broadband signals. For future work in which this breadboard antenna might be used for phase and amplitude measurements, a large phase dispersion is undesirable. Accordingly, it was concluded that the most cost-effective approach would be for Georgia Tech to design and construct a simple feed horn which would meet the breadboard testing requirements of an amplitude-only system. A basic

consideration in designing a 2-4 GHz octave feed horn is that the ordinary waveguide frequency range must be extended. The normal operating range for S-band (WR-284) waveguide is 2.60-3.95 GHz. The dominant mode ( $TE_{10}$ ) cutoff is 2.078 GHz; below the normal operating frequency of 2.60 GHz, phase dispersion increases rapidly until cutoff at 2.078 GHz.

The low frequency range can be extended by either dielectrically loading the waveguide or by introduction of metal ridges. Dielectric loading decreases the wavelength for a given frequency. The required dielectric loading to achieve a desired reduced cutoff frequency may be calculated as follows. Waveguide systems are normally operated so that only the dominant  $TE_{10}$  mode can propagate at a given time. However, a number of both transverse electric (TE) and transverse magnetic (TM) modes may propagate. As implied by these designations, the TE modes have no electric field parallel to the direction of propagation, and the TM modes have no magnetic field parallel to the direction of propagation. Depending on the waveguide dimensions and the frequency, various wave configurations are possible for both TE and TM modes. A particular wave configuration is indicated by a double subscript mn, that is  $TE_{mn}$  or  $TM_{mn}$ . The value of m refers to the number of half-cycle E-field variations along the broader guide dimension, and n refers to the number of half-cycle E-field variations along the narrow guide dimensions.

The cutoff frequency for  $TE_{mn}$  modes is given by [2]

$$f_c = \frac{1}{2\sqrt{\mu\epsilon}} \sqrt{\left(\frac{m}{a}\right)^2 + \left(\frac{n}{b}\right)^2} \quad (1)$$

where  $\mu$  = permeability of the waveguide medium,

$\epsilon$  = permittivity of the waveguide medium,

a = waveguide broad wall dimension,

b = waveguide narrow wall dimension, and

m and n are as defined above. For the  $TE_{10}$  mode and S-band waveguide (a = 2.840 inches, b = 1.340 inches), Equation (1) reduces to

$$f_c = \frac{1}{14.4 \times 10^{-2} \sqrt{\mu \epsilon}} .$$

So that the feed would not be operating too near cutoff, assume an  $f_c = 1.8$  GHz. Substituting this value for  $f_c$  and the value of  $\mu$  for free space ( $1.257 \times 10^{-6}$  volt sec/amp m), the required value of  $\epsilon$  is found to be

$$\epsilon = 1.18 \times 10^{-11} \text{ amp sec/volt m.}$$

Now, since the permittivity of free space is  $8.85 \times 10^{-12}$  amp sec/volt m, the required dielectric loading is found to be

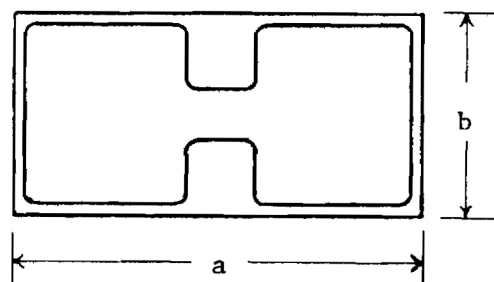
$$\epsilon_r = 1.18 \times 10^{-11} / 8.85 \times 10^{-12} = 1.33.$$

Of course, dielectric loading would not only lower the cutoff frequency for the  $TE_{10}$  mode but the cutoff frequency for higher order modes would be lowered also. For the  $TE_{20}$  mode, evaluation of Equation (1) for a relative dielectric constant of 1.33 leads to a  $TE_{20}$  mode cutoff of 3.62 GHz. Thus, for that portion of the desired operating frequency from 3.62 GHz to 4.0 GHz, multi-moding would be possible. Higher order modes can be generated by discontinuities or irregularities in the waveguide, and if they do exist the feed aperture distribution will be altered. This could severely distort the secondary beam and reduce the antenna gain. Thus, dielectric loading does not appear attractive for an octave or greater bandwidth.

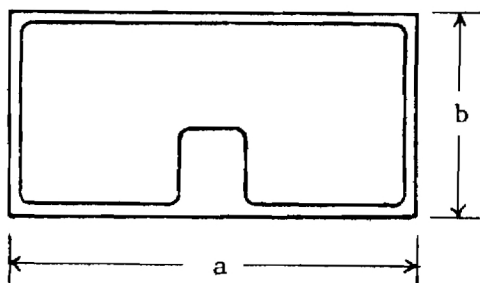
Ridged waveguides have been in use in very broadband systems since World War II. Both single ridge and double ridge configurations are used,

as shown in Figure 11. Standardization of ridged waveguides has resulted in the definition of two classes with bandwidth ratios of 2.4:1 and 3.6:1. In the 2.4:1 bandwidth class, one standard frequency band covers the 2.0-4.8 GHz range. For both the single and double ridge configurations of this waveguide, the  $TE_{10}$  cutoff frequency is 1.695. For the single ridge configuration, the  $TE_{20}$  cutoff frequency is 4.933 GHz, and for the double ridge configuration the  $TE_{20}$  mode cutoff frequency is 4.984 GHz. Thus, either of the ridged waveguide configurations will allow propagation of the 2-4 GHz range without higher order modes. It was therefore decided to construct a ridged horn illuminator for the breadboard transmit antenna system.

The basic configuration which was selected for initial evaluation is shown in Figure 12. The UG-53/U flange mates with standard rectangular S-band waveguide. Thus, a standard commercially available coax-to-waveguide adapter can be used to excite the feed horn. The dimensions of those portions of the ridges which extend beyond the flange into the waveguide area are designed so that a Scientific/Atlanta Model 11A-2.6 coax-to-waveguide adapter will bolt directly to the flange. However, this adapter must be modified by removing the lower portion of the dielectric barrel which surrounds the probe into the waveguide. This modification allows the longer ridge to extend to the shorting plate. The E-plane dimension of the horn is tapered to 2 inches at the aperture. The ridges are simply cut to a logarithmic taper from the 2 inch dimension at the aperture to a one-half inch spacing at the flange. (The double ridge configuration of Figure 12 would have a  $TE_{10}$  to  $TE_{20}$  mode wavelength cutoff ratio of about 4:1.) Measured VSWR data for the double ridge horn with a modified S/A Model 11A-2.6 coax-to-waveguide adapter attached are shown in Table 4.



11 (b)



11 (a)

Figure 11. Cross-section of (a) single and (b) double ridge rectangular waveguide.

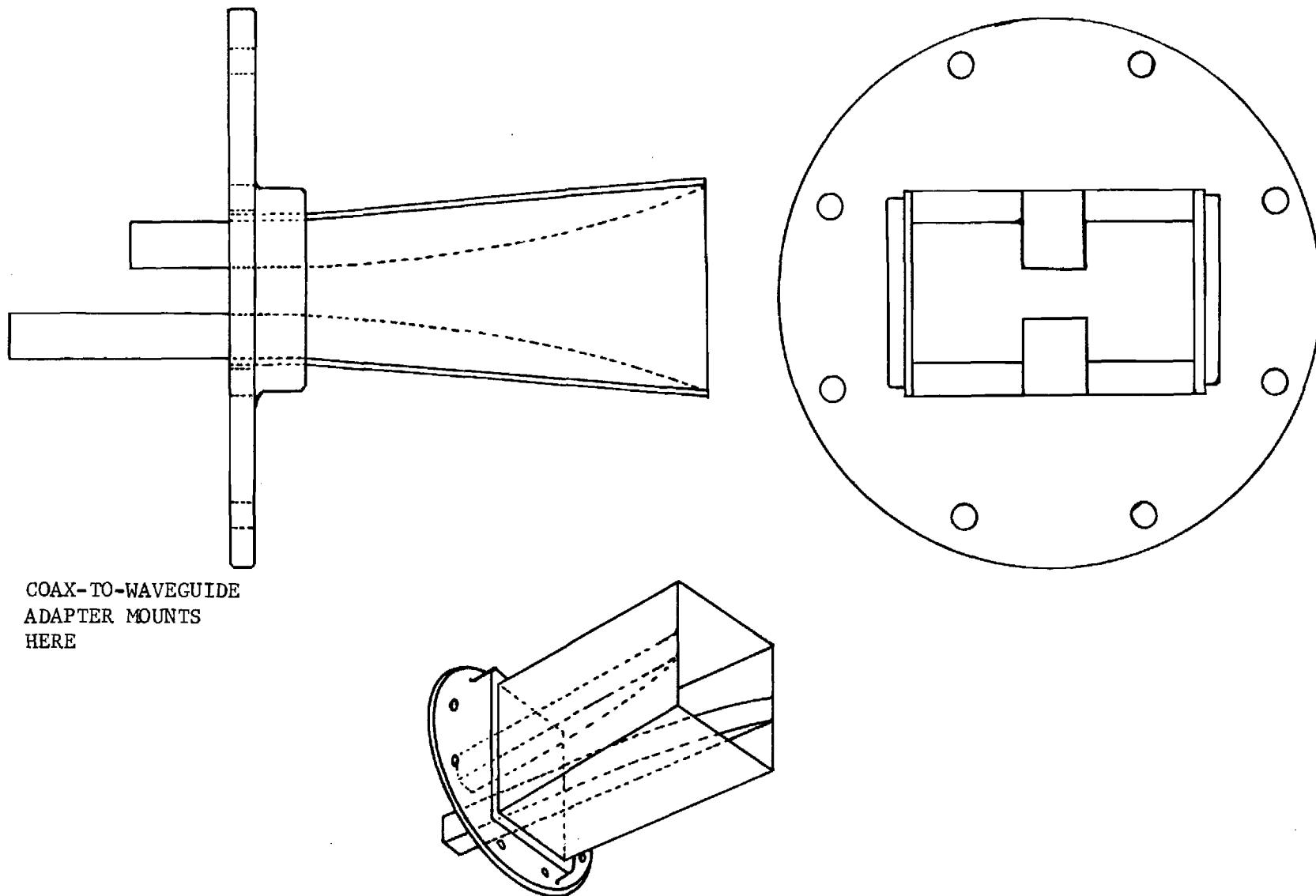


Figure 12. Sketch of original double ridge feed horn.

TABLE 4  
AVERAGE VSWR\* DATA FOR DOUBLE RIDGE  
WAVEGUIDE FEED HORN

Frequency, GHz	Average VSWR*
2.0	3.60
2.2	2.60
2.4	3.20
2.6	2.77
2.8	2.67
3.0	2.40
3.2	2.77
3.4	2.87
3.6	2.02
3.8	1.92
4.0	2.40
* Average of three data sets	

The VSWR shown in Table 4 for the lower end of the frequency band is higher than desired. It is believed that these high VSWRs arise from reflections at the coax-to-waveguide transition. In particular, the upper ridge of Figure 12 presents an abrupt discontinuity at the probe into the waveguide. Accordingly, the upper ridge was removed and the horn plus adapter was retested. Average VSWR data for the single ridge horn are shown in Table 5. As can be seen from Tables 4 and 5, the single ridge horn has the better VSWR performance. The data of Table 5 are acceptable for a broadband feed, and it was decided to use the single ridge configuration.

The single ridge horn which was used in the breadboard system is shown in Figure 13. To determine the reflector aperture illumination which would be achieved with this single ridge horn, both E-plane and H-plane pattern data were recorded each 0.2 GHz from 2.0 GHz to 4.0 GHz. The amplitude taper which would be achieved with this single ridge horn and reflectors of various  $f/D$  ratios (focal length to diameter) is shown in Table 6. The values shown in Table 6 do not include any space attenuation factor to account for additional space loss to the periphery of the reflector vis-a-vis the loss to the center of the reflector. This extra amplitude taper due to the space attenuation effect depends on the particular  $f/D$  ratios. From Table 6, the case of an  $f/D$  ratio of 0.30 is most desirable since the larger  $f/D$  ratios do not result in enough amplitude taper to obtain suitable sidelobes in the far field. For the  $f/D$  ratio of 0.30, space loss provides about 4 dB of additional taper over that shown in Table 6 [3]. Thus, with the single ridge feed and a paraboloidal reflector of 0.30  $f/D$ , the H-plane aperture illumination taper would vary from about -14 dB at 2.0 GHz to about -19 dB at 4.0 GHz. The corresponding E-plane tapers would be -10 dB and -20 dB.



TABLE 5  
AVERAGE VSWR\* DATA FOR SINGLE RIDGE  
WAVEGUIDE FEED HORN

Frequency, GHz	Average VSWR*
2.0	2.40
2.2	1.48
2.4	1.60
2.6	2.40
2.8	1.88
3.0	1.93
3.2	2.30
3.4	2.10
3.6	2.05
3.8	2.10
4.0	2.40
* Average of two data sets	

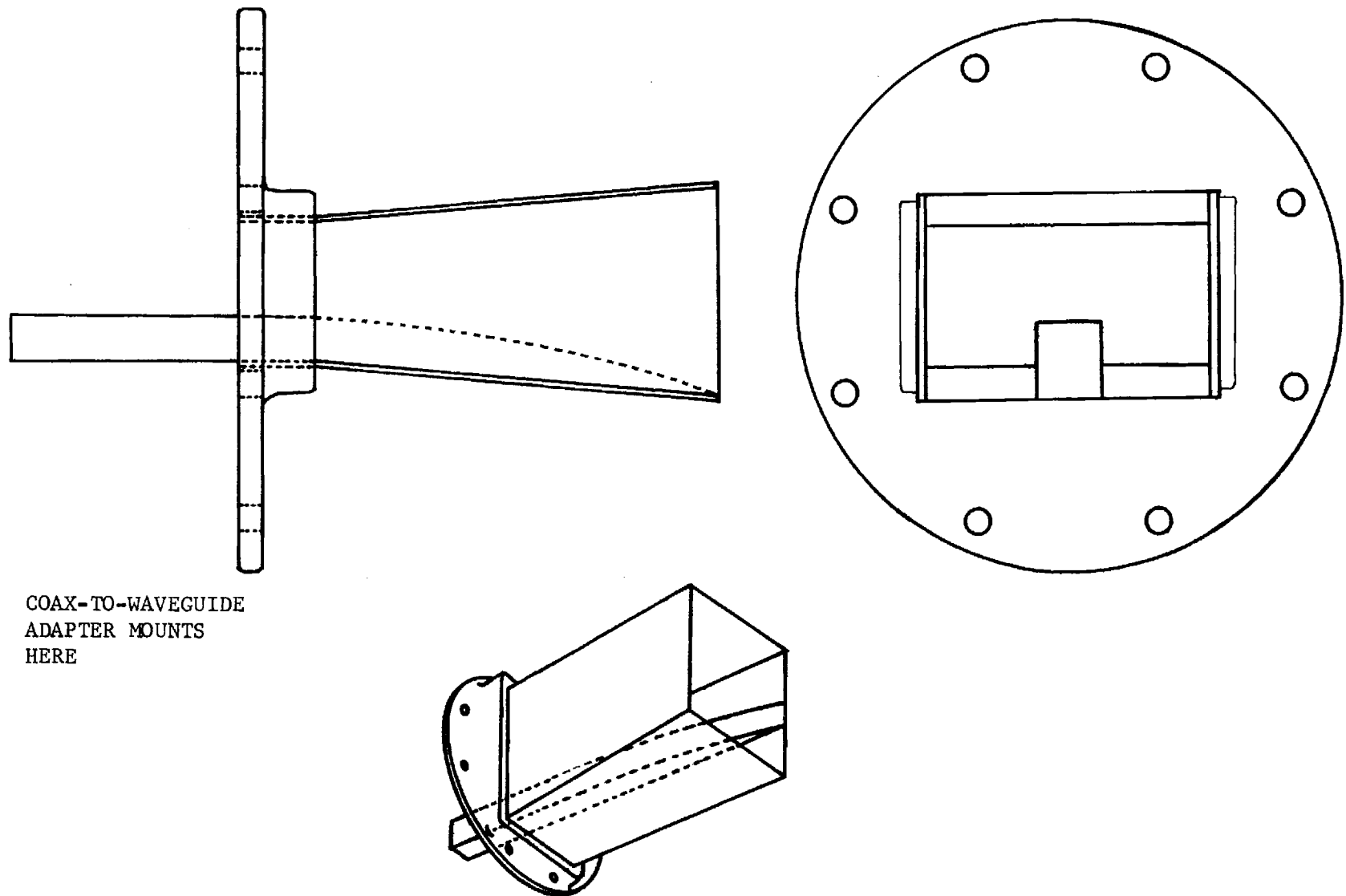


Figure 13. Sketch of final single ridge feed horn used in the broadband transmit antenna.

TABLE 6

AMPLITUDE TAPER\* WITH REFLECTORS OF VARIOUS  $f/D$  RATIOS  
AND THE SINGLE RIDGE FEED HORN OF FIGURE 13

Frequency, GHz	H-Plane Taper, dB	E-Plane Taper, dB
$f/D = 0.30$		
2.0	-10.5	- 6.0
2.4	-14.5	- 9.0
3.0	-15.0	- 5.0
3.6	-16.5	-13.0
4.0	-15.0	-16.0
$f/D = 0.33$		
2.0	- 6.5	- 4.0
2.4	-11.5	- 7.0
3.0	-12.0	- 5.0
3.6	-14.5	-12.0
4.0	-13.5	-15.0
$f/D = 0.375$		
2.0	- 6.5	- 2.0
2.4	-10.5	- 6.0
3.0	-10.0	- 5.0
3.6	-11.0	-10.0
4.0	-12.0	-11.0
* These values do not include space loss effects		

As a rule of thumb, these illumination tapers would lead to a maximum first sidelobe level of about -20 dB [3].

For feed/reflector systems, not only the aperture illumination taper (amplitude), but also the phase distribution across the aperture must be considered. If the feed has a phase center, and if the feed is placed so that its phase center and the focal point of a paraboloidal reflector coincide, the phase across the aperture will be uniform. Thus, it was desirable to determine the phase properties of the single ridge feed. In the E-plane, the phase center varied from about the horn face at 2.0 GHz to about 1.7 cm inside the horn at 4.0 GHz. In the H-plane, the phase center varied from about 1 cm outside the horn face at 2.0 GHz to about 1.3 cm inside the horn at 4.0 GHz. Since the minimum operating wavelength is 7.5 cm (at 4.0 GHz) and the total variation in phase center is less than 2 cm, it is possible to place the feed so that the phase deviation across the aperture is less than 90 degrees. Actual placement of the feed was by trial-and-error to obtain the best compromise in far-field patterns across the frequency range.

A simple feed support system was designed and constructed so that the feed could be moved along the axis of the paraboloidal reflector to obtain the best overall far-field patterns across the 2-4 GHz frequency range. The feed support structure and the feed are shown mounted on the reflector in Figure 14. Final H-plane patterns at 2 and 4 GHz are shown in Figures 15 and 16, respectively. Corresponding E-plane patterns are shown in Figures 17 and 18. For any given frequency, lower sidelobes, and perhaps a more symmetrical pattern could be obtained by optimum positioning of the feed. However, the patterns of Figures 15 through 18 represent the best compromise in feed location.

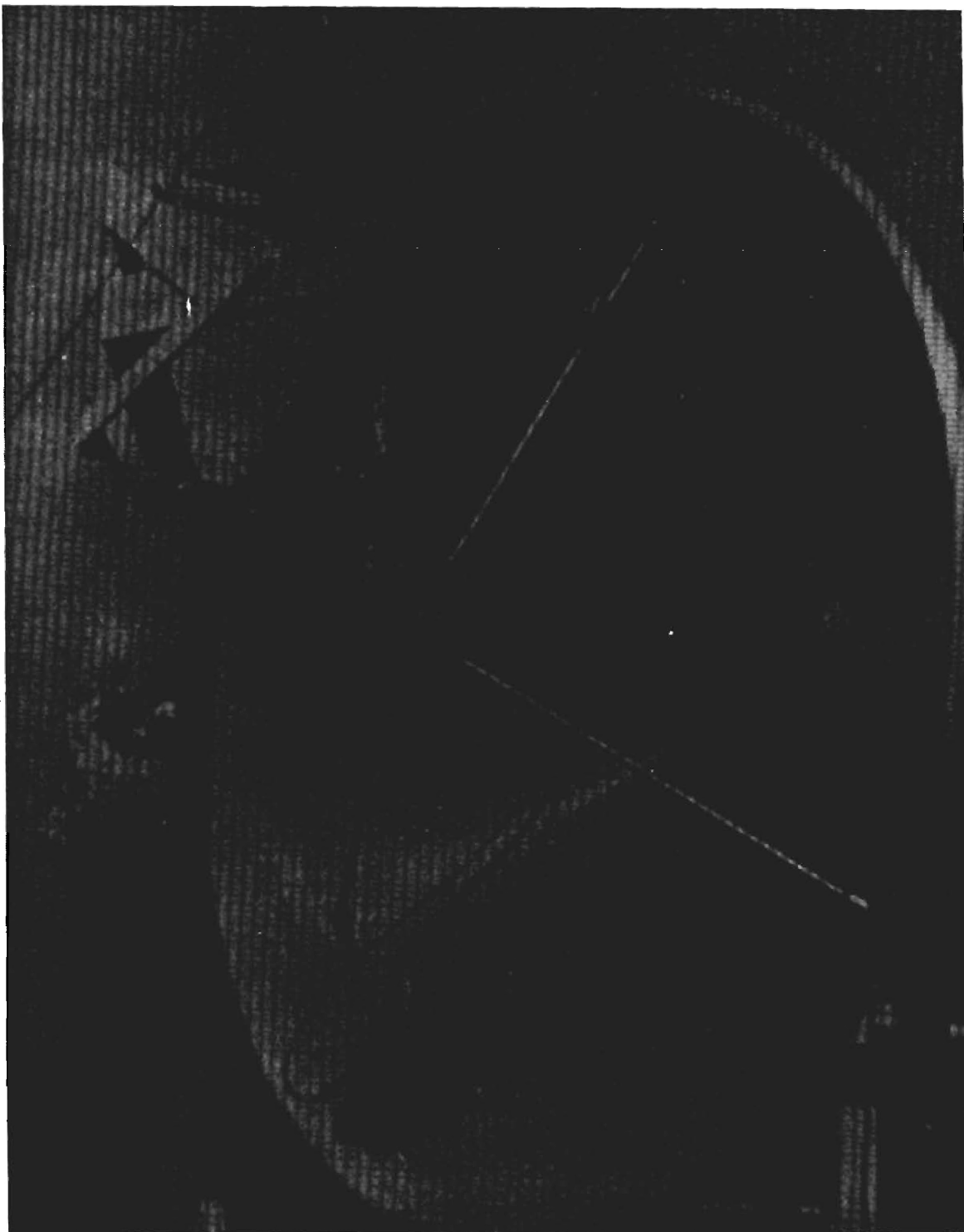


Figure 14. Photograph of broadband transmit antenna system with level sensor mounted at the feed input.

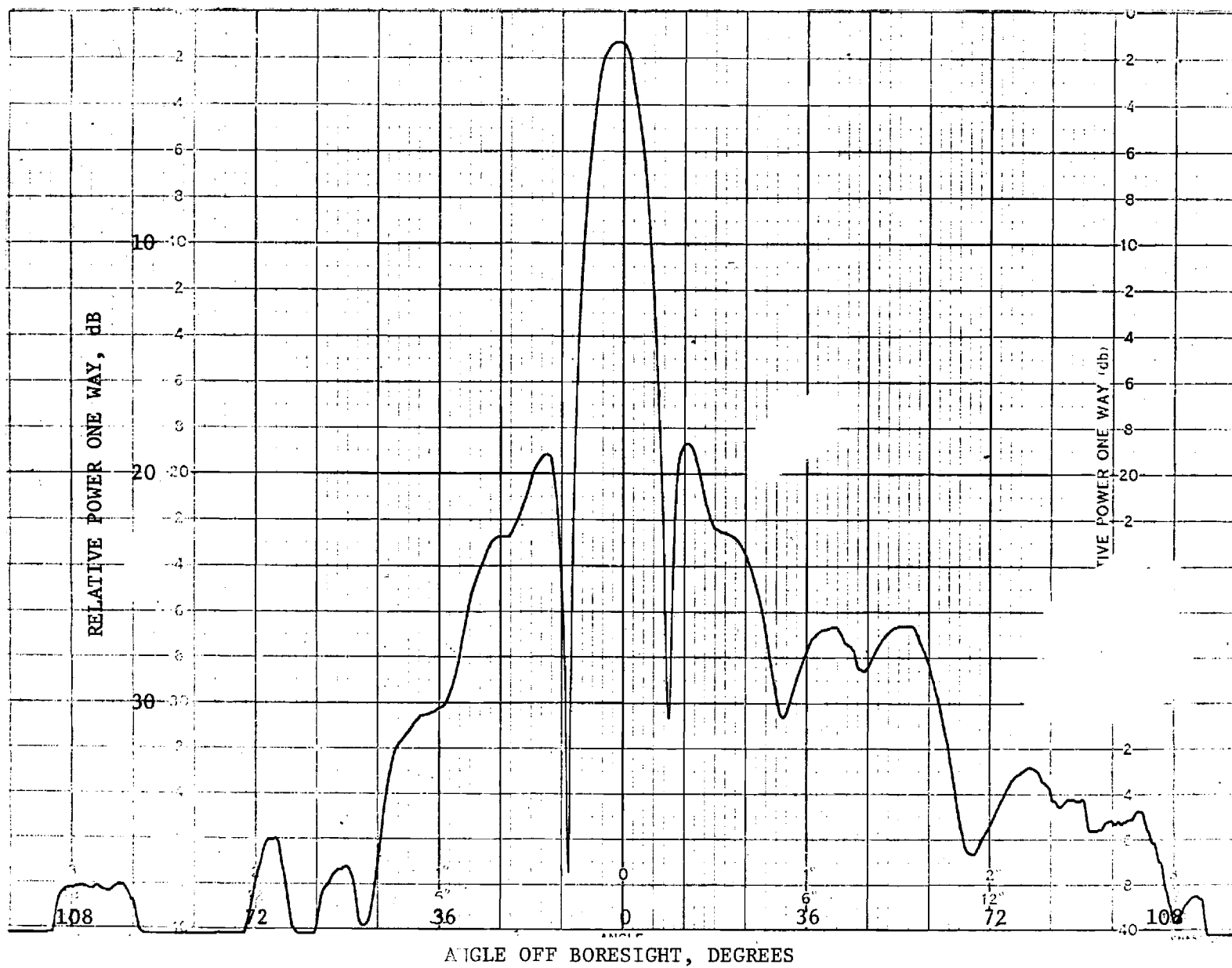


Figure 15. H-plane transmit antenna pattern at a frequency of 2 GHz.

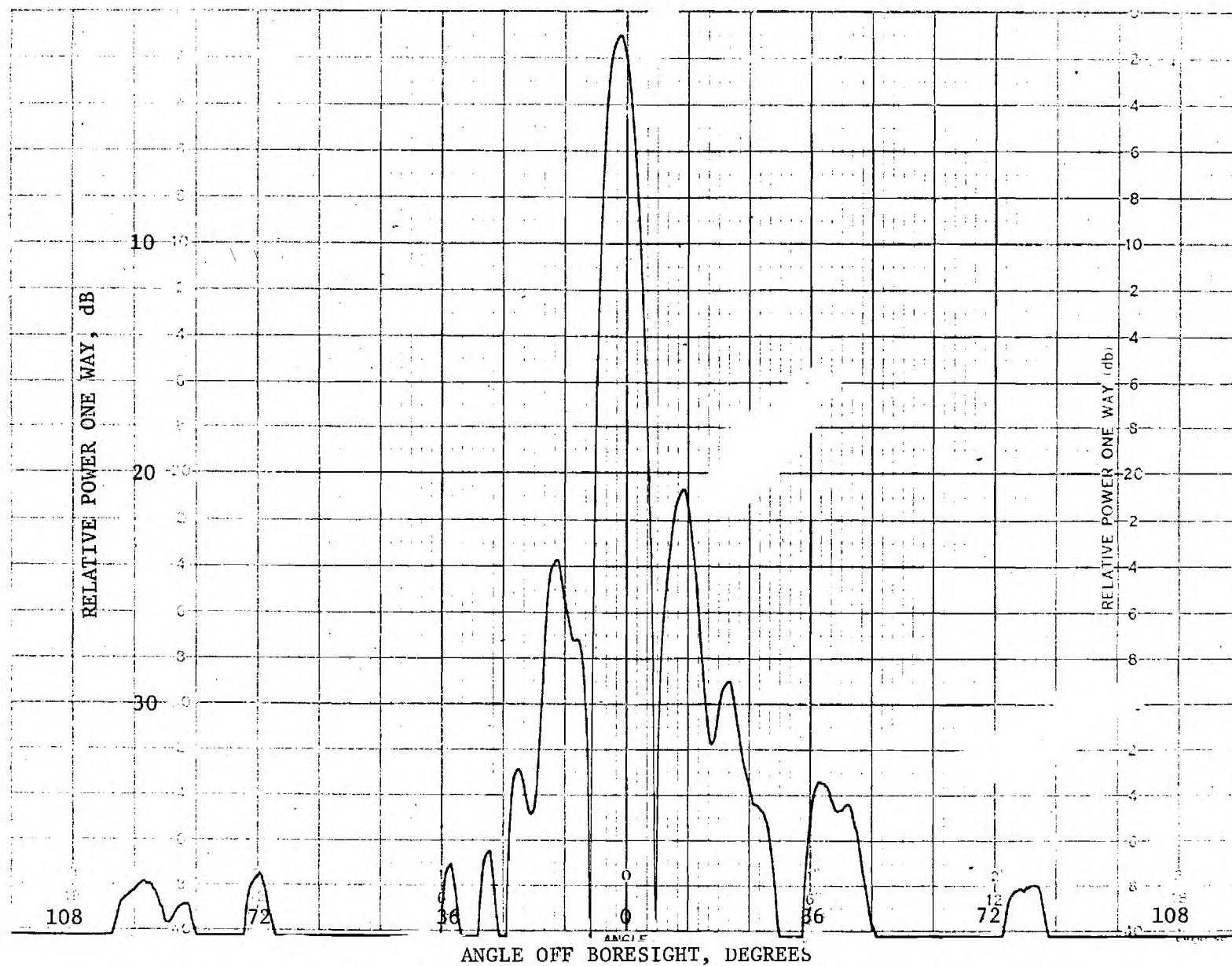


Figure 16. H-plane transmit antenna pattern at a frequency of 4 GHz.

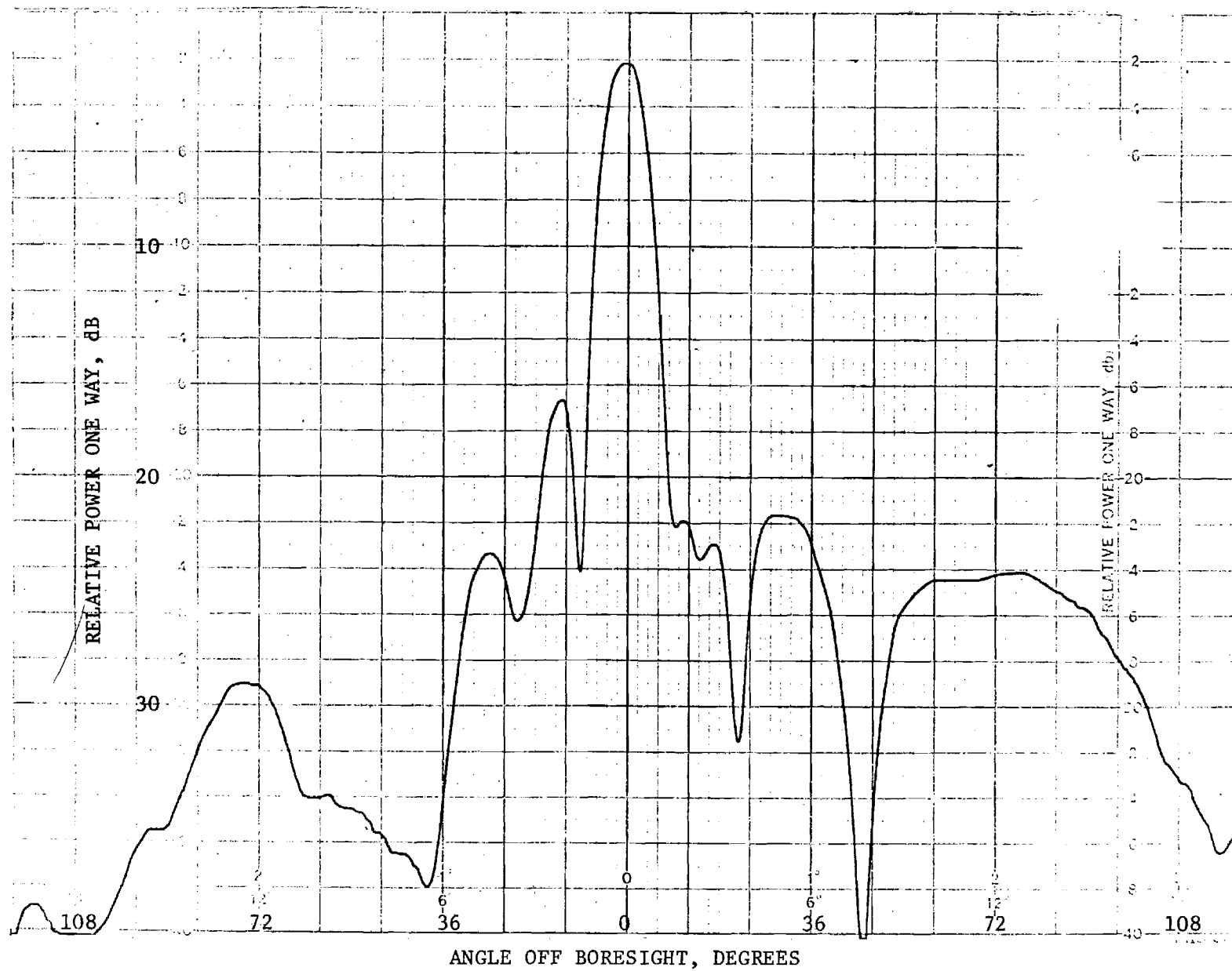


Figure 17. E-plane transmit antenna pattern at a frequency of 2 GHz.



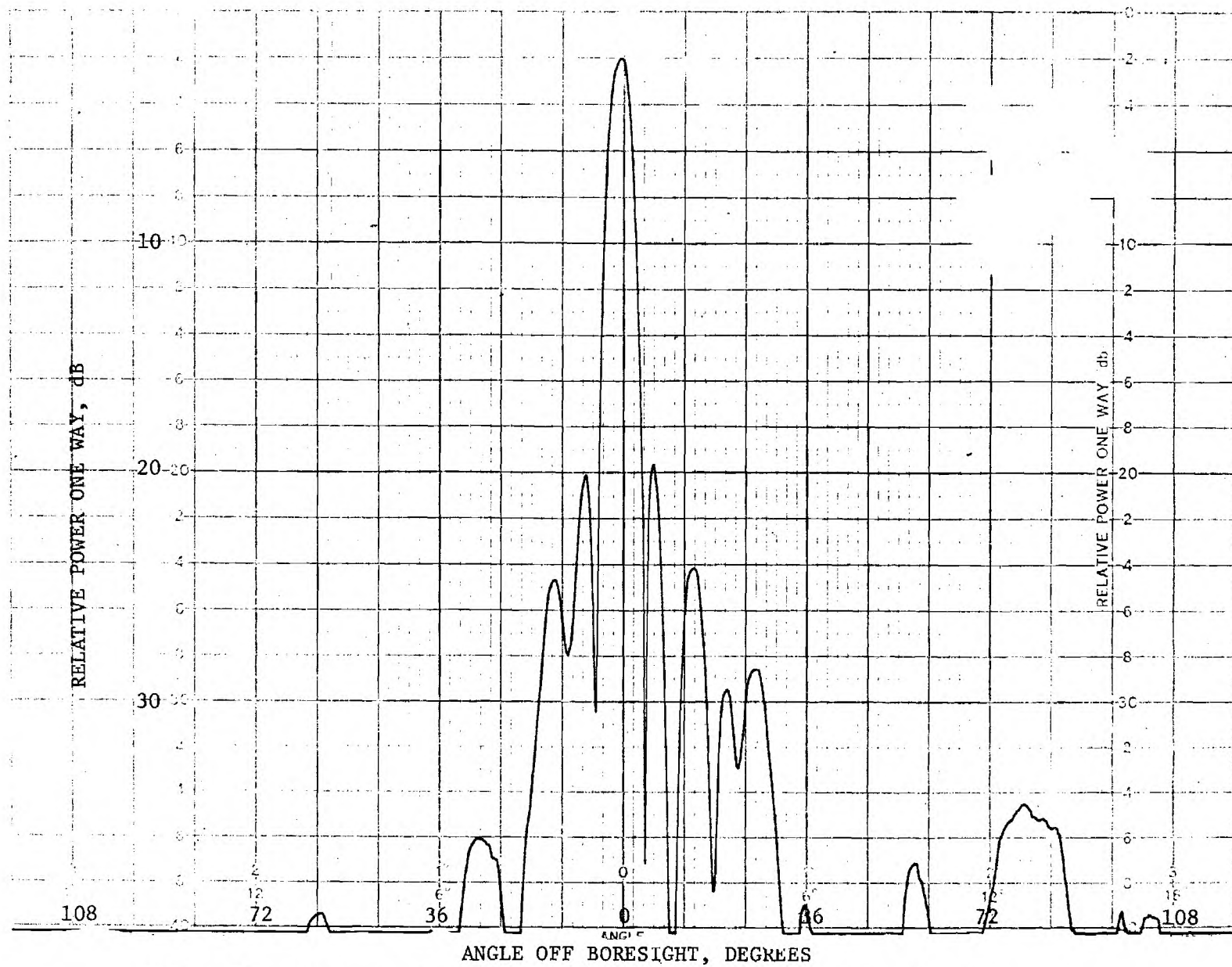


Figure 18. E-plane transmit antenna pattern at a frequency of 4 GHz.

The gain of the transmit antenna system was measured by the substitution method with a standard gain horn used as the reference. Measured gains are shown in Table 7. These gains correspond to an efficiency of about 50 to 60 percent.

### 3. Receiver

A block diagram of the breadboard Hybrid system receiver is shown in Figure 19. Both the test and reference antenna inputs are applied to a PIN diode switch. The PIN diode switch used in the Hybrid system is General Microwave Model ADM 870. A summary of its performance characteristics as well as that of other devices used in the Hybrid system receiver are shown in Table 8. A portion of the reference antenna RF signal is obtained using a 10 dB coaxial coupler to drive a tunnel diode detector. The coupler used is Americon Model 2020-6609 and Aertech Industries built the tunnel diode detector (Model DOM 204BRS-1). The output from the tunnel diode detector is used by the logic controller subsystem to control signal processing in the Hybrid system data processor.

The power level of the selected RF output from the PIN diode switch is controlled by an ARRA Model 4674-30AA precision variable attenuator. This attenuator is adjustable from 0 dB to 30 dB, and according to Georgia Tech measurements, it is flat at any attenuation setting within approximately  $\pm 1$  dB across the 2 to 4 GHz range. The purpose of the variable attenuator is to control the level of the RF signals applied to the crystal detector. The crystal detector selected for use in the Hybrid system is the Alfred Model 1002, and it has a guaranteed square-law voltage response (within  $\pm 0.5$  dB) for RF power levels of 0 dBm to -40 dBm. Thus, the attenuator is set so that the maximum RF signal power does not exceed 0 dBm at the input to

TABLE 7

## MEASURED GAIN OF TRANSMIT ANTENNA

Frequency, GHz	Gain, dB above isotropic
2.5	28*
3.0	29
3.5	31
3.9	32
* Standard-gain-horn value extrapolated at this frequency	

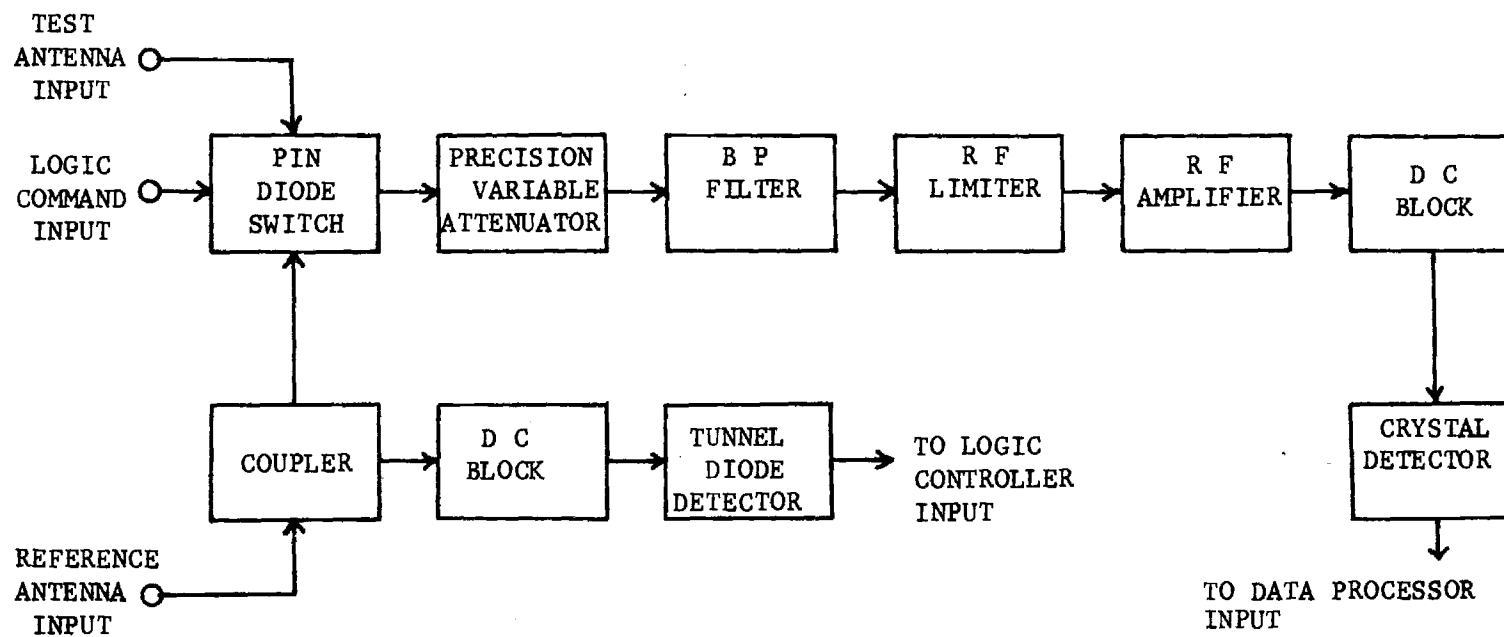


Figure 19. Hybrid system receiver block diagram.

TABLE 8  
COMPONENT SUMMARY FOR S-BAND HYBRID SYSTEM BREADBOARD RECEIVER

<u>PIN Diode Switch</u>	<u>BP Filter</u>	<u>Low-Noise Amplifier</u>
Frequency: 2 - 4 GHz	Passband: 2 - 4 GHz	Type: Transistor
Maximum Insertion Loss: 1 dB	Rejection: 40 dB below 1.4 GHz and above 5.2 GHz	Frequency: 2 - 4 GHz
Switching Time: $\leq 0.5 \mu\text{sec}$	Passband Maximum VSWR: 2:1	Noise Figure: 5 dB
Isolation: 60 dB	Insertion Loss: 1 dB max	Gain: 32.5 dB
Type: SPDT with integral driver		Gain Flatness: $\pm 1/2$ dB
		Power out at 1 dB Gain Compression: +10 dBm
<u>Limiter</u>	<u>Coupler</u>	<u>Crystal Detector</u>
Frequency: 2 - 4 GHz	Frequency: 2 - 4 GHz	Frequency Range: 2 - 4 GHz
Power Handling: 1 W	Insertion Loss: 0.2 dB	Square Law Response: $\pm 0.5$ dB from 0 dBm to -40 dBm
CW Leakage: 65 mW	Coupling: 10 dB	Minimum Useful Input: -50 dBm
Insertion Loss @ 0 dBm or less: $\leq 1.0$ dB	Directivity: $\geq 20$ dB	Voltage Sensitivity: 250 mV/mW
		Maximum Input: 100 mW

(continued)

TABLE 8 (cont)  
 COMPONENT SUMMARY FOR S-BAND HYBRID SYSTEM BREADBOARD RECEIVER

<u>Precision Variable Attenuator</u>	<u>Tunnel Diode Detector</u>
Frequency range: 2 - 4 GHz	Frequency Range: 2 - 4 GHz
Attenuator Range: 0 - 30 dB	Minimum Useful Input:
Maximum Variation: $\pm 2$ dB	-51 dBm
Insertion Loss: 0.5 dB	Voltage Sensitivity: 1V/mW
	Maximum Input: 50 mW

the crystal detector. It should be noted that the flatness of the attenuator across the 2 to 4 GHz range is important to insure that "spikes" much greater than 0 dBm do not occur; however, any deviation from a completely flat attenuator response does not influence the Hybrid system accuracy. One of the features of the Hybrid system is amplitude compensation. This capability is discussed further in sub-Section B-4, but basically amplitude compensation normalizes the test antenna response to that of the reference antenna. This feature cannot only provide absolute average gain information of the test antenna with respect to established average gain characteristics of the reference antenna, but it also can cancel any attenuator (or other) non-uniformities with frequency.

The variable attenuator is followed by a 2-4 GHz bandpass filter, Sage Laboratories Model 20C40CA379. This filter allows the receiver to reject RF signals outside the desired test frequency range. The filter output is fed to a RF limiter, Alpha Industries Model MT-3260A4. The limiter provides protection for the low-noise RF amplifier since its limiting threshold begins at approximately +7 dBm and the maximum signal input to the amplifier may be as high as +10 dBm.

A low-noise RF amplifier is utilized to increase the sensitivity and hence the RF dynamic range of the Hybrid system. The amplifier, Avantek Model AM-4062M, has a gain of  $32\text{--}1/2\text{ dB} \pm 1/2\text{ dB}$  over the 2-4 GHz range with a noise figure of 5 dB. As previously discussed with regard to the variable attenuator, any deviation from a flat response by the amplifier also will not affect the Hybrid system accuracy. The combined effect of the RF amplifier and the variable attenuator, allows the Hybrid system to accept RF power levels in either test or reference channel from 0 dBm to -30 dBm when both

THIS PAGE INTENTIONALLY LEFT BLANK.



the reference and test antennas are positioned at boresight. The Hybrid system is designed to process signals from the test antenna which are 40 dB below those achieved at antenna boresight. As a result, depending on the attenuator setting, the upper level of the 40 dB RF dynamic range window can be set at RF levels from the test antenna from 0 dBm (30 dB attenuator setting) to -30 dBm (0 dB attenuator setting). Therefore, the Hybrid system is designed to process RF signals as low as -70 dBm without considering integration. As will be shown later, processing gains lower the minimum level to -80 dBm or less.

The RF amplifier output is fed through a dc block to the crystal detector. The dc blocks (both inner and outer conductor) were utilized in the RF transmission line prior to both the tunnel diode detector and crystal detector. These devices alleviated ground loop problems between the receiver and the Hybrid system data processor. The crystal detector provides a dc output to the data processor which is proportional to the power level of the RF signal. As previously mentioned, the detector has a square-law voltage response range of 40 dB for RF power levels of 0 dBm to -40 dBm (see Figure 20). The corresponding dc voltages range from 100 mV to 10  $\mu$ V, respectively. The RF amplifier has a 1 dB gain compression at an output power of +10 dBm, and it is completely saturated at +13 dBm. Thus, the RF amplifier output will saturate before damaging the crystal detector because the maximum RF signals to the detector can be 20 dBm. Obviously, for proper operation, the RF power level to the detector should not exceed approximately 0 dBm during operations. The following calibration is performed under swept conditions:

For optimum performance, the RF power level from both the test and reference antennas, positioned at boresight, should be equal and adjusted to

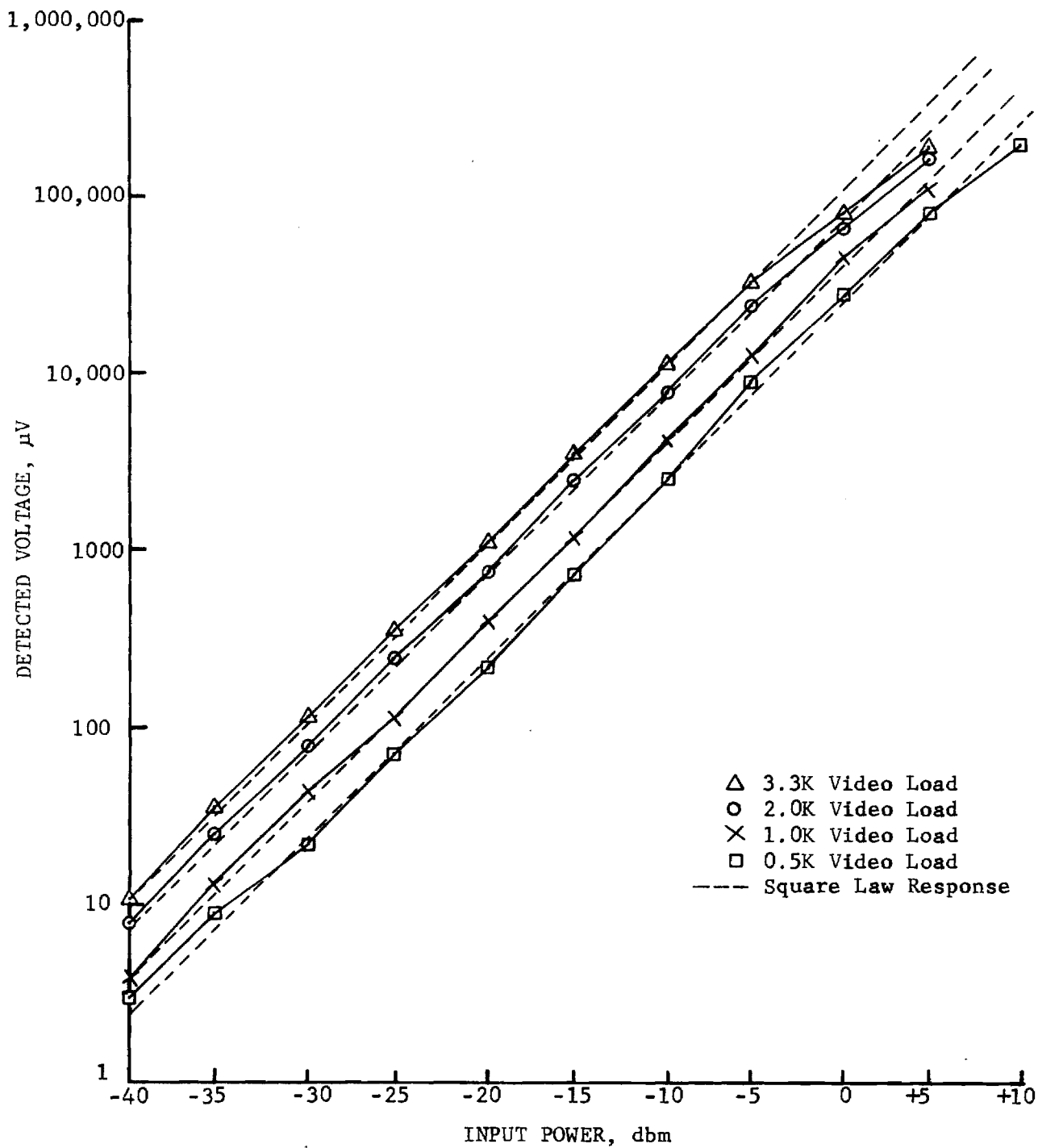


Figure 20. Voltage response of Hybrid system crystal detector versus input power for various video load values.

approximately 0 dBm at the crystal detector input. Unless both antennas have identical broadband gain characteristics, the signals are unequal. In order to achieve the goal of equal RF power level from the test and the reference antennas, a set of precision broadband attenuators are used. The approach used is to set the variable attenuator to provide approximately 0 dBm power level to the detector from the antenna with the smaller RF power level, then the appropriate precision attenuators are utilized to lower the higher RF power level from the higher gain antenna to that same level. The attenuators are conveniently placed as needed at the input to the Hybrid system.

#### 4. Hybrid System Data Processor

##### a. Description

The Hybrid system data processor interfaces with two subsystems. The data processor subsystem uses the crystal detector output in the receiver, from both the reference antenna and the test antenna, to produce an "average" antenna response over the desired frequency range. Recall that the Hybrid system "times shares" inputs from the test antenna and the reference antenna. The logic controller subsystem is responsible for controlling the time sharing of the receiver and the data processor subsystems, and for synchronization of the receiver and data processor subsystems with the sweep generator. The following paragraphs will discuss the data processor subsystem in detail.

A block diagram of the data processor subsystem is given in Figure 21. As previously discussed, the data processor subsystem is that part of the system which acts on the crystal detector output voltage to provide compensated average antenna gain data. The time-varying signal from the detector represents the frequency dependent response of the antenna under test, plus

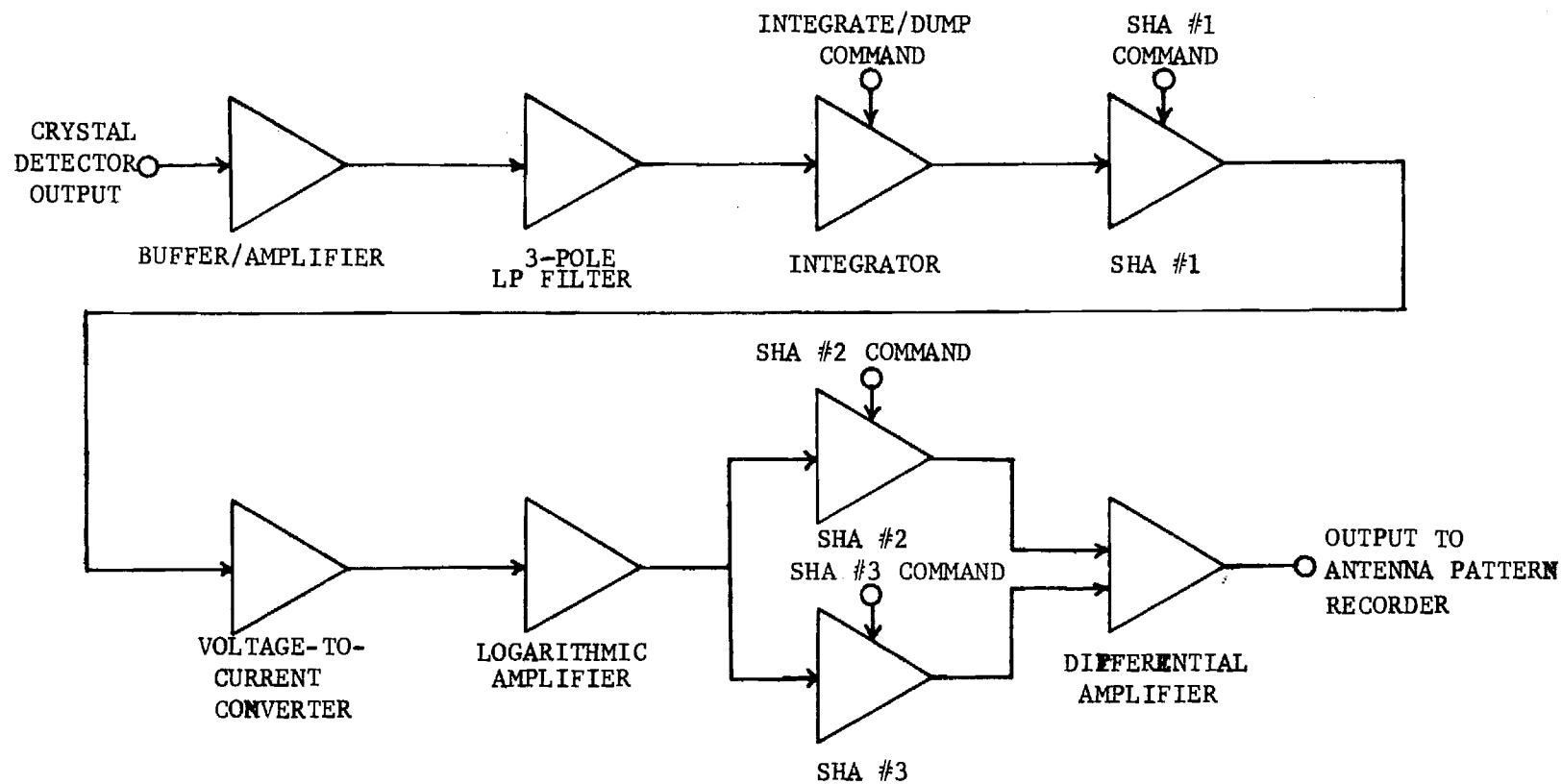


Figure 21. Hybrid system data processor simplified block diagram.

variations due to any other frequency dependent elements (such as the variable attenuator, RF amplifier, etc.) in the entire measurement network from the transmitter through the detector. As previously mentioned, the effect of all of these other variations is removed by amplitude compensation in the data processor subsystem, and the compensation feature will be further discussed later in this section. The data processor consists essentially of circuits which buffer and amplify the crystal detector output, filters the amplified signal, integrates the filtered output over one sweep period, and a sample-and-hold amplifier which samples the integrator output at the end of each sweep period and holds this value until the logarithm can be performed by the log amplifier. This logarithm signal is fed to a sample-and-hold amplifier network combined with a differential amplifier. One of the sample-and-hold amplifiers in this network always contains the most recent value of the logarithm of the test antenna's average response over the desired frequency range, while the other sample-and-hold amplifier contains the most recent value of the logarithm of the reference antenna's average response over this sweep range. The differential amplifier output is the difference of these two log signals which were stored in the sample-and-hold amplifier circuits. This log difference (which corresponds to power ratio) is the integrated (average) response of the test antenna, which is expressed in dB form and is referred to the average response of the reference antenna.

The first stage of the data processor subsystem features a buffer/amplifier circuit. The output from the crystal detector is amplified using a low noise operational amplifier in the non-inverting mode. This stage also provides buffering between the relatively high impedance of the crystal detector and the low impedance of the remaining processor circuitry.

The buffer/amplifier output is low pass filtered by a three pole active filter. This filter has a 3 dB bandwidth of 5 KHz and 60 dB/decade roll off transfer function. The purpose of this filter is to reduce the effects of noise power output from the video detector. The active filter has a voltage gain of 2. This gain combined with the gain of the buffer/amplifier provides an overall voltage gain of approximately 82. The voltage gain of the buffer/amplifier is set so that the active filter, as well as the following circuitry, is not in saturation for maximum crystal detector output.

The next stage in the processor is the analog integrator. The output voltage  $e_o$  of the integrator is given by

$$e_o = \frac{1}{RC} \int_0^{t_i} e_i(t) dt, \quad (2)$$

where for this application R is a 20 k $\Omega$  low noise thin film carbon resistor, C is a high quality 0.1 $\mu$ f polystyrene capacitor,  $t_i$  is the integration time (typically 10 msec), and  $e_i(t)$  is the input voltage to the integrator. The operational amplifier used in the analog integrator is an FET type featuring both low noise and low voltage drift. It should be noted that low noise thin film carbon resistors were used throughout both the data processor and logic controller subsystems. A 50 k $\Omega$  cermet trimpot controls the input voltage level to the integrator from the active filter. For purposes of system calibration, this trimpot provides the capability for setting the integrator output to a specified voltage level based on RF input power.

The sample-and-hold amplifier #1 (SHA #1) must sample the integrator output at the end of each integration period and hold that value during the transmitter recycle period plus the time required for either SHA #2 or SHA

#3 combination to obtain the logarithm of this value. The integrator output voltage covers four decades (40 dB) from 1 mV to 10 V. Therefore, to reduce the magnitude of error at the low voltage range, the SHA voltage droop rate must be minimized. To insure the error due to droop rate does not exceed 1 percent under worse case conditions (hold 1 mV for 2.5 msec) the SHA droop rate can not exceed 4  $\mu\text{V}/\text{msec}$ . Other parameters which measure SHA performance are settling time and acquisition time. The definitions of these measures of performance as well as the devices selected for use in the Hybrid system will be discussed later in this section under Component Selection. The commands which control the SHA mode (either sample or hold) are digital commands. These commands and how they are formulated are discussed in the logic controller sub-section.

The accuracy and dynamic range of standard logarithmic amplifiers (Log Amp) can be considerably improved by operating them in a current input mode rather than in a voltage input mode. Consequently, a voltage-to-current converter (VCC) is utilized as the input element to the logarithmic amplifier, as shown in Figure 21. Four decades of input current (corresponding to the four decades of signal voltages of 1 mV to 10 V from the SHA #1) to the Log Amp are required. Based on this input voltage range to the VCC, biasing resistors were chosen to provide a current range of  $-10^{-4}$  amperes (at a 10V input) to  $-10^{-8}$  amperes (at a 1mV input), since this is the midrange of a typical Log Amp's input capability. Negative output current flow for positive input voltages is inherent in the VCC design utilized, but this is compatible with selected Log Amp devices. The Log Amp output voltage range is from -1V to +3V for the  $-10^{-4}$  amperes to  $-10^{-8}$  amperes input current, respectively.

Sample-and-hold amplifiers #2 and #3 are identical to the SHA #1. At the end of the test and reference antenna integration intervals, SHA #2 and SHA #3, respectively, sample the Log Amp output and hold the values until each respective output is updated on alternate transmitter sweeps. Like the SHA #1, the SHA #2 and SHA #3 receive their sample and hold commands from the logic controller subsystem.

The final stage in the data processor subsystem is a differential amplifier which subtracts the output of the SHA #3 from the output of SHA #2. Recall that subtracting the logarithm of two values is equivalent to taking the logarithm of their ratio. Therefore, subtracting the reference antenna logarithmic results (stored in the SHA #3) from the test antenna logarithmic results (stored in the SHA #2) provides the average test antenna gain with respect to the reference antenna. Hence, the output from the differential amplifier provides both the test antenna average pattern and its average absolute gain when using a reference antenna with established gain characteristics. As pointed out earlier, this log subtraction or normalization technique cancels any non-linear effects with respect to frequency response in the Hybrid system beginning with the PIN diode switch and continuing through to the crystal detector [1]. Another attractive feature is the ability of the amplitude compensation scheme to negate the effects of any momentary drop in transmitter output power. The output voltage range from this stage is typically 0V to 4V; however, the output voltage swing is adjustable up to 10V.

The transmitter sweep time is normally set at 10 msec plus 2 msec recycle. Therefore, the SHA #1, which contains the integrator output, is updated every 12 msec. It should be noted that the transmitter sweep and



recycle times can be varied without loss of synchronization, making the Hybrid system compatible with other sweep periods. Since the test and the reference antennas are selected on alternate transmitter sweeps, SHA #2 and SHA #3, which contain the test and reference antenna responses, respectively, are updated every 24 msec. Since the reference antenna will be stationary, the output of SHA #3 will remain essentially constant for a given frequency sweep range.

Very large antenna positioners have maximum scan rates on the order of 0.5 rpm. Even at this maximum scan rate, in 24 msec the test antenna would rotate through only 0.072 degree. Broadband average antenna response will not change dramatically over this angular increment. Therefore, even for the maximum angular rotational speed of the antenna positioner, there is no appreciable change in successive values of either SHA #2 or SHA #3 output, and as a result, the differential amplifier output is a smooth function of time (or test antenna spatial coordinate).

For use with the Hybrid system, the Scientific-Atlanta 1520 Rectangular Pattern Recorder is equipped with the Series 1556 dc-chopper preamplifier. When so equipped, dc input voltages of up to 100 volts are permitted. Full scale sensitivity is 0.01 volt and the noise level is 10  $\mu$ V rms. Thus, the 0-4 V input signal range interfaces directly with this recorder.

#### b. Component Selection

The component requirements for this subsystem includes five Op Amps, three SHAs, and a Log Amp. These devices and their respective manufacturers, which include Analog Devices (AD), Datel, Optical Electronics, Inc. (OEI), and Teledyne Philbrick, were reviewed. Performances and cost data were obtained, and each device was cataloged according to its

function (Op Amp, SHA, etc) to facilitate comparison of their specifications. Each function in the data processor subsystem (integration, voltage-to-current conversion, etc.) was carefully reviewed to specify performance requirements and acceptable error tolerances needed to meet overall system demands. Using this information and the data provided by the manufacturers, each device was examined to determine what tradeoffs existed considering both subsystem requirements and cost. This approach was utilized to reduce the overall construction cost while meeting system performance requirements.

(1) Operational Amplifiers--One of the objectives for this data processor subsystem design was utilization of only one type of Op Amp. This objective has several advantages from both a cost and construction point of view. If just one type of Op Amp is sufficiently versatile to be used throughout the circuit where Op Amps are required, it has the potential to reduce circuit construction costs. Factors which influence this decision are the circuit demands and the cost of purchasing and designing around a variety of Op Amps which tend to be tailored for a specific application versus one which would have universal applications. Additional factors are the price breaks available by purchasing several Op Amps of the same type and the added ease of maintaining spares. From the construction point of view, using a universal Op Amp allows the use of one type of mating socket and trimpot as well as simplifying power supply requirements.

Several field effect transistor (FET) Op Amps had suitable specifications for meeting the "universal requirements". FET type Op Amps were chosen over other types because of their high input impedance and low bias currents. These features were considered necessary to improve particularly the performance and accuracy of the integrator and the differential

amplifier in the circuit. Other important features include both low noise and low voltage drifts in an Op Amp, especially since the input voltage range to the data processor from the crystal video detector is a relatively low 10  $\mu$ V to 100 mV. As a result of these requirements (low noise, low voltage drifts, broad range of applications, etc.), as well as cost, the Analog Devices 43K was selected.

(2) Sample and Hold Amplifiers--Typical processor operating conditions require the SHA #1 to hold voltages between 1 mV and 10 V for a period of approximately 2.5 msec while the SHA #2 and SHA #3 combination are required to hold voltages between -1 V and 3 V for a period of approximately 22.5 msec. Therefore, to insure that error due to voltage droop by the SHA #1 does not exceed 1 percent under worse case conditions (hold 1 mV for 2.5 msec) the SHA droop rate can not exceed 4  $\mu$ V/msec. The droop rate is the measure of the amount of voltage lost during the "hold" interval by the SHA. Although low droop rate performance is necessary for the SHA #2 and the SHA #3, it is more critical at the SHA #1 stage of the processor. Errors of millivolts in the SHA #1 circuitry impact more heavily on the system performance than at the SHA #2/SHA #3 stage.

Other parameters besides droop rate that measure SHA performance include settling time and acquisition time. Settling time is the measure of the amount of time required by the SHA to acquire the input signal, within a specified accuracy, when switched from sample to hold. Conversely, acquisition time is the measure of the amount of time required by the SHA to acquire the input signal, within a specified accuracy, when switched from hold to sample.

Based on an analysis of system demands, the droop rate, which is considered the most critical parameter for this application, should not exceed 8  $\mu\text{V}/\text{msec}$  and a more acceptable value would be 4  $\mu\text{V}/\text{msec}$ . The next parameter considered most critical is the settling time of the SHA. The maximum allowed value for this specification is 300  $\mu\text{sec}$ , and once again half this value, 150  $\mu\text{sec}$ , is more desirable. The least critical parameter for this application is acquisition time; approximately 500  $\mu\text{sec}$  is a tolerable value while 300  $\mu\text{sec}$  is considered desirable.

Although either of these requirements (droop rate, settling or acquisition time) are not difficult to meet with most SHAs, all of these requirements together dictate high quality SHAs. From the rather large variety of SHAs commercially available, only three were chosen which had the potential of meeting the design specifications at modest price. After reviewing the capabilities and cost of each device, it was decided to obtain all three SHAs on a no cost loan for evaluation at Georgia Tech.

Several problems contributed to the need for this evaluation. Definitions for performance of SHAs typically are not standardized between manufacturers and published specifications may be listed either as "typical" or "maximum" values. After reviewing test specifications and talking to manufacturers, it is not uncommon to find variations by an order of magnitude between a "typical" and a "maximum" specification. As a result, the comparison of SHA performance between manufacturers is difficult if not possibly misleading.

The objective of the SHA evaluation was to measure three parameters, droop rate, settling time, and acquisition time, in a breadboard circuit that would simulate the SHAs intended use. Other parameters like output

noise level and signal feedthrough in the hold mode were also measured for purposes of comparison. Although the amount of signal feedthrough in the hold mode is normally very small, in particular situations it can cause noticeable distortion of the output waveform, which is another source of error.

Based on the test results, the Analog Devices AD SHA-3 was considered the best SHA of those tested for use in the data processor subsystem. Measured values for droop rate, settling time, and acquisition time were typically 3  $\mu\text{V}/\text{msec}$ , 3  $\mu\text{sec}$  (to 0.01 percent of the final value), and 170  $\mu\text{sec}$ , respectively. After examining the output responses from this SHA (as well as the others) when it was switched from hold to sample, the magnitude of the switching transients was observed to be several volts depending on the type of input applied. Specifications on this parameter were not available from information received initially, and therefore, it was not considered to be a problem. Preliminary analysis had shown that switching transients of this magnitude posed a potential problem in the Hybrid system. The performance of the AD SHA-3 and the AD SHA-4 only differ in one area. Fortunately, one of the parameters in this area is switching transients. According to detailed specification information, the maximum switching transient for the SHA-3 is 7 V while for the SHA-4, it is only 200mV. As a result, the SHA-4 was purchased instead of the SHA-3.

(3) Logarithmic Amplifiers--Several logarithmic amplifiers from commercial sources were available which met design requirements. Performance parameters of interest included dynamic range, input bias current, and log conformity. After reviewing the specifications of each device including errors due to non-conformity and other sources, the AD 755 had

comparable or better performance while costing approximately half the price of the other two Log Amps. Hence, the AD 755 was purchased for use in the data processor subsystem.

## 5. Logic Controller

### a. Description

The logic controller subsystem is responsible for providing five sets of TTL (Transistor-Transistor Logic) and CMOS (complementary metal oxide silicon) compatible digital commands to selected segments of the Hybrid system. These commands are an integrate or dump command to the integrator, commands to three sample-and-hold amplifiers (SHA #1, SHA #2, and SHA #3), and a command to control the antenna selection switch. This switch allows the Hybrid system to process data from either the reference antenna or the test antenna. The logic controller subsystem monitors the response of the sweep generator through the reference antenna and uses this information to coordinate its operations with the sweep generator. The subsystem features include synchronization of all digital commands with the sweep generator and automatic preset. A design goal of both the logic controller and data processor subsystems was flexibility. Based on this objective, the logic controller functions are keyed strictly on the sweep generator. As a result, this feature allows the sweep period to be adjusted without loss of synchronization and makes the Hybrid system compatible with the majority of sweep generators. The remainder of this section discusses the circuit design for each of the five segments of the logic controller.

(1) Synchronization and Preset--The logic controller subsystem circuit diagram is shown in Figure 22. The synchronization segment of this subsystem is composed of a buffer/amplifier (B/A), a low pass active

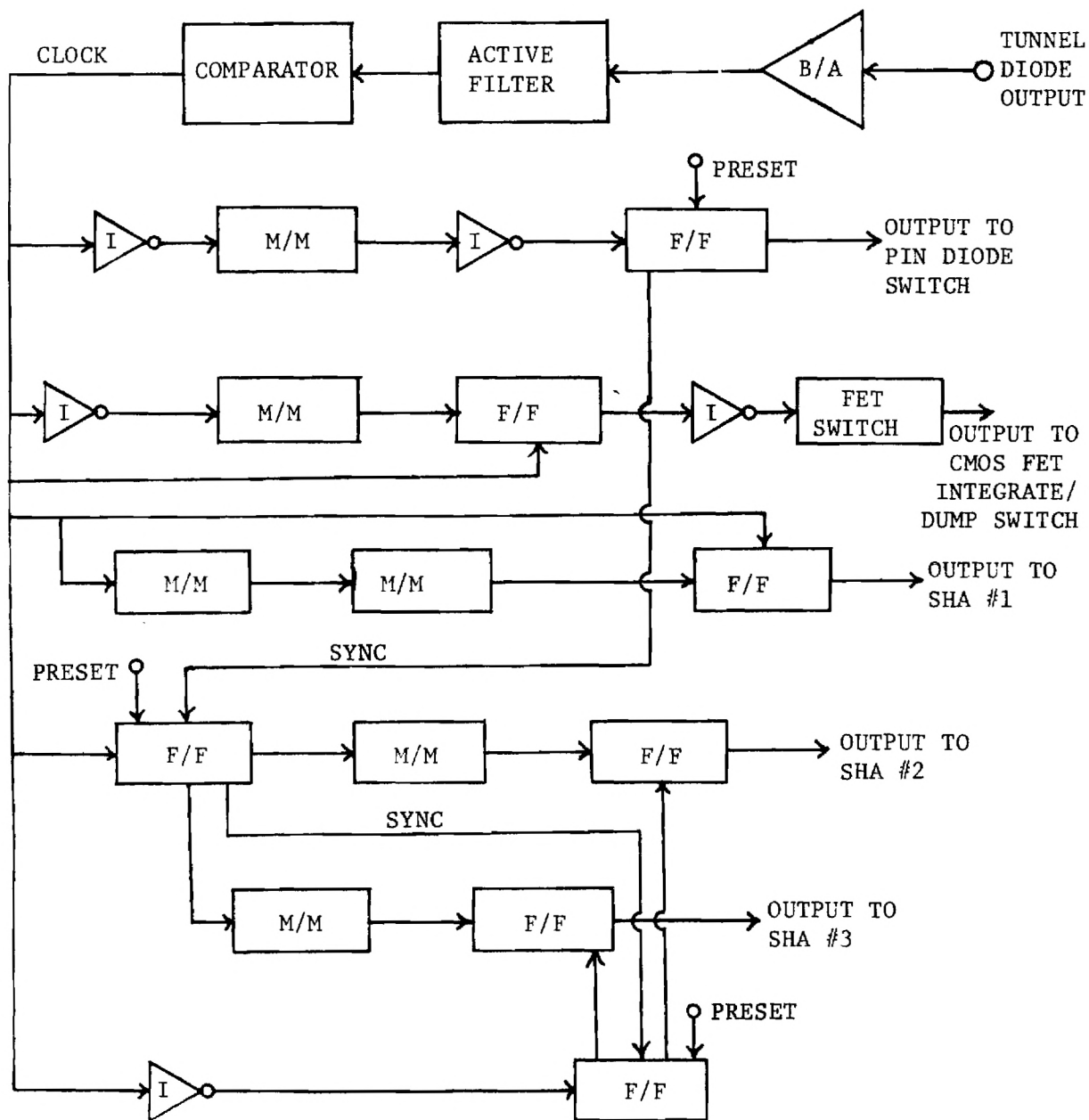


Figure 22. Hybrid system logic controller simplified block diagram.

filter, and a voltage comparator. The output from the tunnel diode video detector is amplified using an operational amplifier configured in the non-inverting mode with a voltage gain of approximately 100. The amplifier also buffers the video detector from the other circuitry. The buffer/amplifier output is low pass filtered by a three pole active filter. The filter has the same performance characteristics as the low pass active filter used in the data processor subsystem, specifically a 3-dB bandwidth of 5kHz and a 60-dB/decade roll off rate. The purpose of this filter is to reduce the noise power in the video detector output. Combining the active filter voltage gain of 2 with the gain of the buffer/amplifier provides a two stage voltage gain of approximately 200. The amplified and filtered video detector response is fed to the voltage comparator. This device is designed with hysteresis to prevent noise from causing false triggering. The output from the voltage comparator is the CLOCK which synchronizes and triggers the other digital circuits. The comparator output is TTL compatible, and it goes high (logic 1) when the sweep generator is in the sweep mode and it goes low (logic 0) when the sweep generator is recycling.

The preset circuitry generates a pulse when the Hybrid system is turned on. This pulse is applied to the appropriate flip-flop preset terminals, and it sets all digital logic to the proper initial state. This insures that all digital commands are synchronized with respect to each other when the sweep generator begins transmission.

(2) Antenna Selection Command--The antenna selection switch is a PIN diode device controlled by a self-contained driver unit making it TTL compatible. This switch allows the data processor subsystem to receive swept RF data from either the reference antenna or the test antenna. The



operation of the RF switch is synchronized with the control commands to the SHA #2 and SHA #3. The synchronization of the digital commands to these three devices insures that the SHA #2 always holds the processed results from the test antenna and that the SHA #3 holds the processed results from the reference antenna.

Formulation of the PIN diode switch digital control waveform requires a monostable multivibrator, a D-type edge-triggered flip-flop, and two inverters. The monostable multivibrator provides adjustable time delayed switching with respect to the CLOCK. This feature prevents the switch from being triggered at the same time the generator ends its sweep and the antenna switching from interfering with other operations. The final waveform is TTL level logic at half the CLOCK frequency with both leading and trailing edge delay.

(3) Integrate/Dump Command--The analog integrator in the data processor subsystem integrates the swept RF response of either the test or reference antenna. During the sweep generator recycle interval, the result is transferred from the integrator before it is cleared (dumped) in preparation for the next transmitter sweep. The integrate or dump command requires several stages to formulate. The first stage utilizes a D-type edge-triggered flip-flop, a monostable multivibrator (one shot) and an inverter. These devices, when clocked, generate a waveform similar to the CLOCK except that the leading edge is delayed. The amount of the delay is adjustable and this capability allows flexibility in initiation of the integration dump command.

A CMOS-FET switch was selected to perform the actual integration dump function. This dump function is accomplished upon command using the switch output terminal to change from high impedance (off) to low impedance (on). This action discharges the stored voltage across the capacitor in the analog

integrator circuit. Because the voltage range across the capacitor is negative (-12V to 0V), the CMOS-FET switch requires a control waveform with logic levels of 0V and -15V. Formulation of this waveform is accomplished beginning with the TTL level waveform described in the preceding paragraph. This waveform is in the desired format except its logic levels are 0V and 5V. The TTL waveform is therefore converted from 0V and 5V levels to 0V and 15V levels and shifted to provide the needed voltage levels of 0V and -15V.

Although TTL compatible FET switches are available, the CMOS-FET switch was utilized because its feedthrough performance is smaller than any of the TTL compatible FET switches examined. Poor feedthrough performance from the TTL compatible FET switches would distort the integrator output at low voltages and affect overall system performance. The remaining circuitry (an FET switch and inverter) is used to convert from TTL level logic to CMOS level logic and shift the voltage swing. The final integrate or dump command, when compared to the CLOCK, is CMOS compatible, inverted, shifted, and leading edge delayed.

(4) SHA Command--As previously discussed, three sample-and-hold amplifiers are used in the data processor subsystem. Recall that the first SHA (SHA #1) samples the integrator output at the end of each integration period and holds that sampled value until slightly after the beginning of the following integration period. At the end of the test and reference antenna intervals, the SHA #2 and SHA #3, respectively, sample the log output and hold the values until the respective output is updated on alternate transmitting sweeps.

Referring to Figure 22, separate circuitry is required to command SHA #1 and the SHA #2/SHA #3 combination. The SHA #1 is in the sample mode

during the majority of the generator sweep period. When the sweep generator is recycling, the logic controller places the SHA #1 into the hold mode and it remains in this state briefly after the generator begins the next sweep. This is done to insure that the SHA #2 or SHA #3 have adequate time to acquire the appropriate processed signals. These commands to the SHA #1 are accomplished digitally by clocking the combination of a D-type edge-triggered flip-flop and two monostable multivibrators. The final waveform is TTL compatible, and when compared to the CLOCK, it is inverted and trailing edge delayed.

The remaining SHA digital circuitry controls the SHA #2 and SHA #3. The data processor design requires that the SHA #2 and SHA #3 alternately hold data for a complete clock period before being updated. Therefore, the SHA #2 and SHA #3 command waveforms are at half the CLOCK frequency, one clock pulse out of phase with respect to each other, and the waveforms are leading edge delayed. Again, the adjustable leading edge with respect to the CLOCK allows flexibility for timing of mode switching.

#### b. Component Selection

Component selection for the logic controller did not require as extensive in-depth analysis as was required to select components for the data processor subsystem. Following the circuit design phase, choosing components to perform specific tasks (inverter, monostable multivibrator, etc) was straightforward. The components selected include SN7406 (inverter), SN74121 (monostable multivibrator), SN7474 (D-type edge-triggered flip-flop), 1H5021 (FET switch), and CD4066 (CMOS-FET switch). Typically, performance of the 7400 series TTL compatible devices is standard between

manufacturers. As a result, these components could be purchased from a variety of manufacturers with assurance of comparable performance characteristics.

Although the purchase of these devices (both the 7400 Series and FET type switches) represent a minor cost when compared to other components in the Hybrid system, attempts were made to minimize the cost of their purchase. Likewise, component selection for the remaining stages of the logic controller subsystem (both amplifiers, active filter, and comparator) was straightforward. Unlike in the data processor subsystem, component performance characteristics such as noise level, voltage drift, etc., are not as critical for the operational amplifiers used in the buffer/amplifier and active filter of the logic controller. Therefore, the remaining components selected includes high quality Analog Devices 741 operational amplifiers and a type LM311 voltage comparator.

#### 6. Packaging and Construction

The breadboard Hybrid system transmitter was assembled from standard commercially available components. A photograph of this transmitter has been shown in Figure 8. The Hybrid system receiver, data processor, and logic controller were constructed and packaged into a self-contained two-drawer cabinet. The data processor and the logic controller was constructed on printed circuit cards using wire-wrap electrical bonds. Figures 23 and 24 show two of the finished circuit cards. Five such cards were used for the data processor, and four cards were used for the logic controller.

Initially the RF components and dc power supplies were packaged in one drawer and the logic controller and the data processor were packaged in the second drawer. Both drawers were left open except for the cabinet

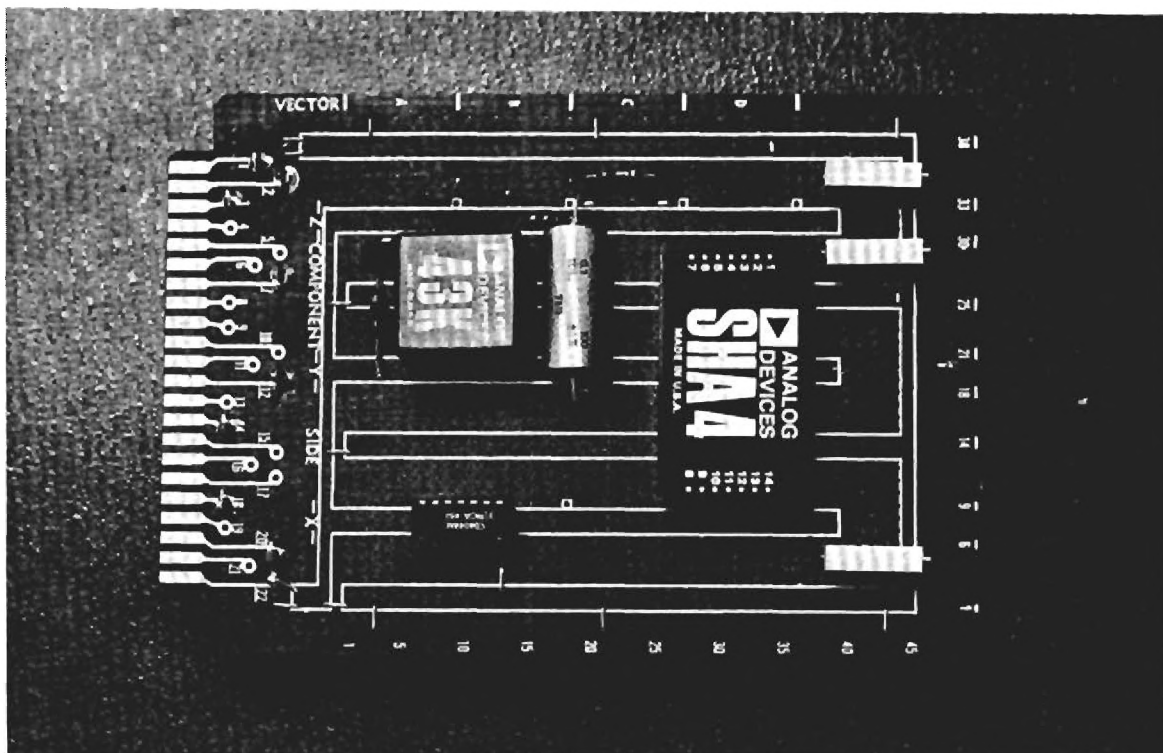


Figure 23. Photograph of the analog integrator/sample-and-hold board, showing the analog integrator (AD 43K Op Amp plus components), the integrate/dump switch (RCA type CD4066 CMOS-FET switch), and the SHA #1 (AD SHA-4).

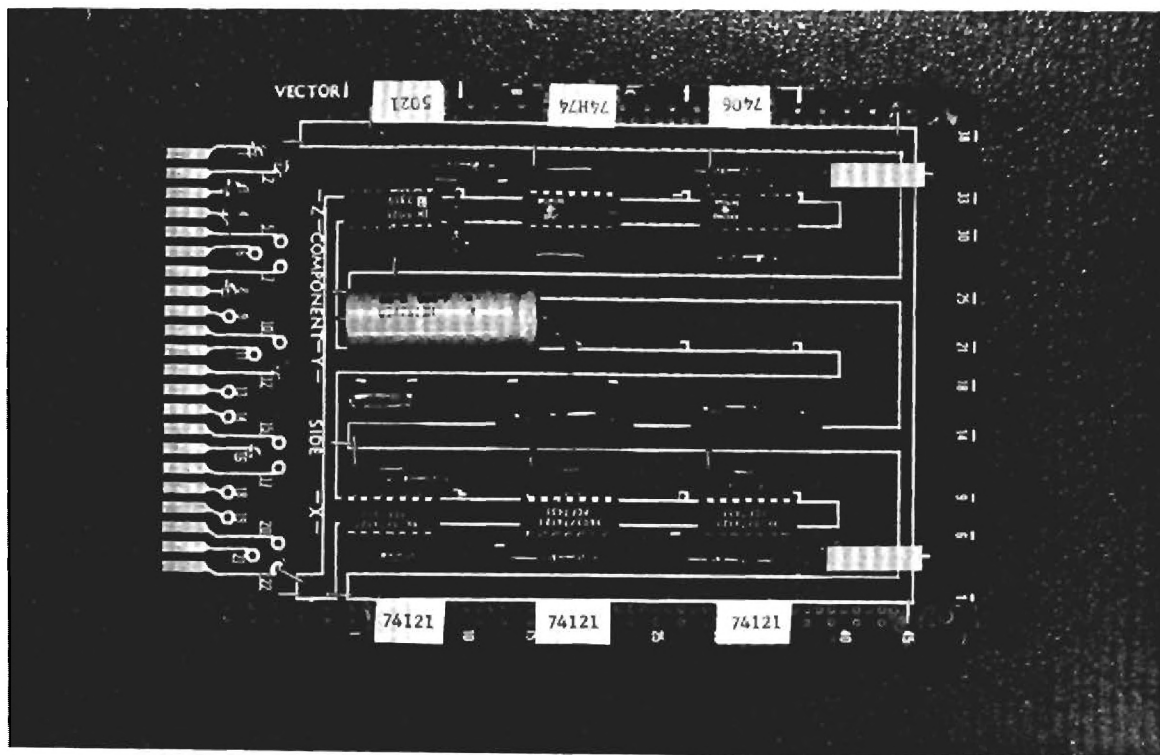


Figure 24. Photograph of the digital logic board which generates digital commands to control the data processor board of Figure 23.

itself. With this arrangement, good performance was obtained in the laboratory. However, upon tests on the antenna range, it was found that the ambient RF level caused sufficient interference to limit low-level performance so that only about a 30-dB dynamic range could be obtained.

Accordingly, the system was reconfigured so that all the RF components, the data processor, and the logic controller were packaged in the same drawer. The dc power supplies were in a separate drawer. A metal partition separated the RF components from all other hardware, and an additional metal cover was placed over the entire drawer. An RF shield was used between the cover and the drawer to limit RF leakage into the drawer. Figure 25 shows a photograph of this drawer with the cover in place. The interior of the drawer is shown in Figure 26. This figure shows the RF components and the pc cards on opposite sides of the metal partitions. The entire complement of data processor and logic controller cards is shown in Figure 27, and a view of the cabinet is shown in Figure 28. The ARRA level set attenuator is mounted on the front panel. This final construction was much improved over the original version and RF interference was reduced sufficiently to obtain greater than 40 dB of dynamic range.

### C. TEST RESULTS

To demonstrate operation of the Hybrid system, pattern measurements were made on a test antenna which consisted of a 48-inch diameter paraboloidal reflector with a dielectrically loaded C-band feed horn. The reference antenna was a standard gain S-band horn. Measurements were made at various bandwidths from 2.5 GHz to 4.0 GHz. Figure 29 shows a photograph of the test antenna mounted on the positioner turntable. Tests were run on the Georgia Tech 1000 ft. range. Figure 30 shows a view looking from



Figure 25. Photograph of receiver, data processor, and logic controller drawer with RF shield in place.



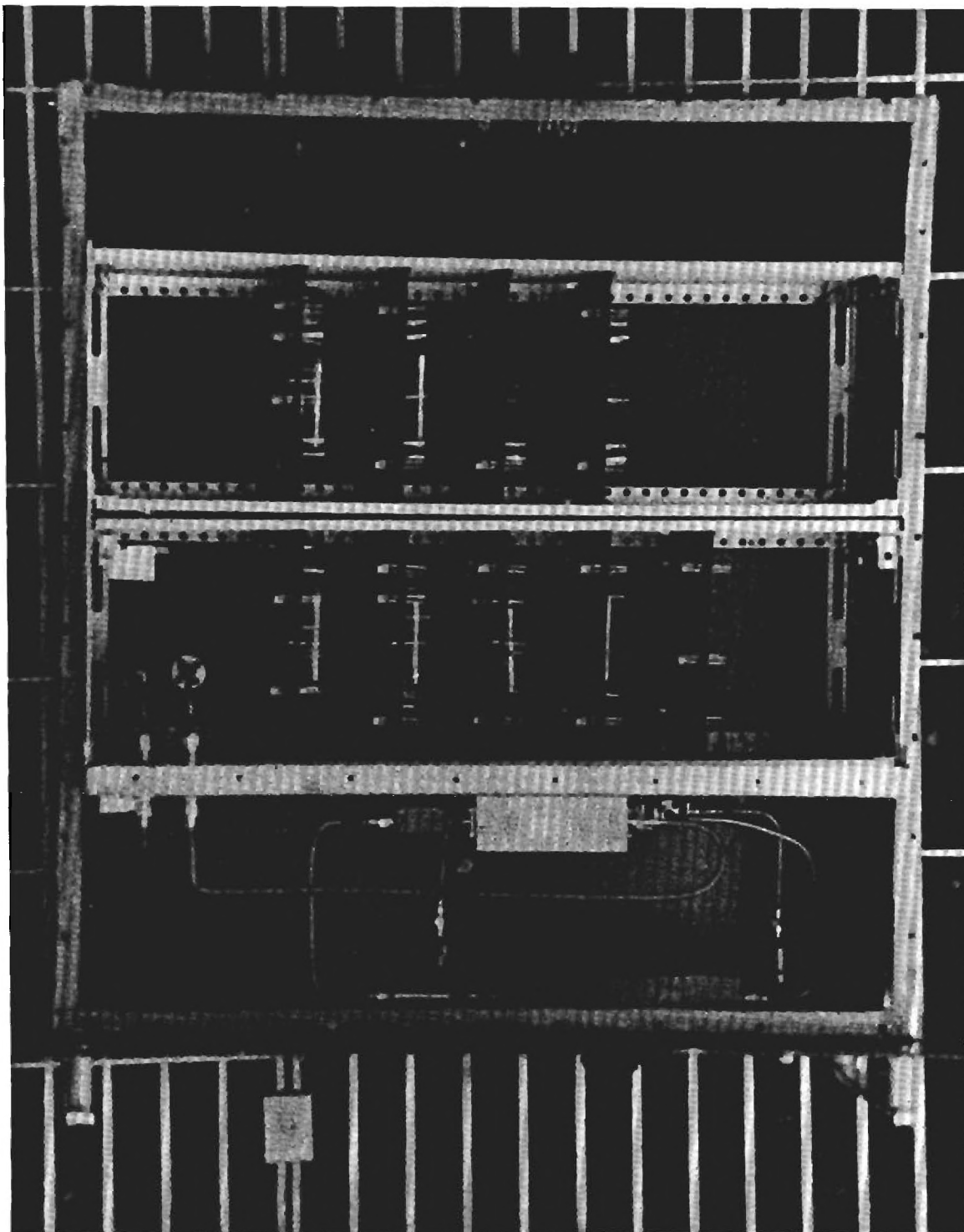


Figure 26. Photograph of receiver, data processor, and logic controller drawer with RF shield removed.

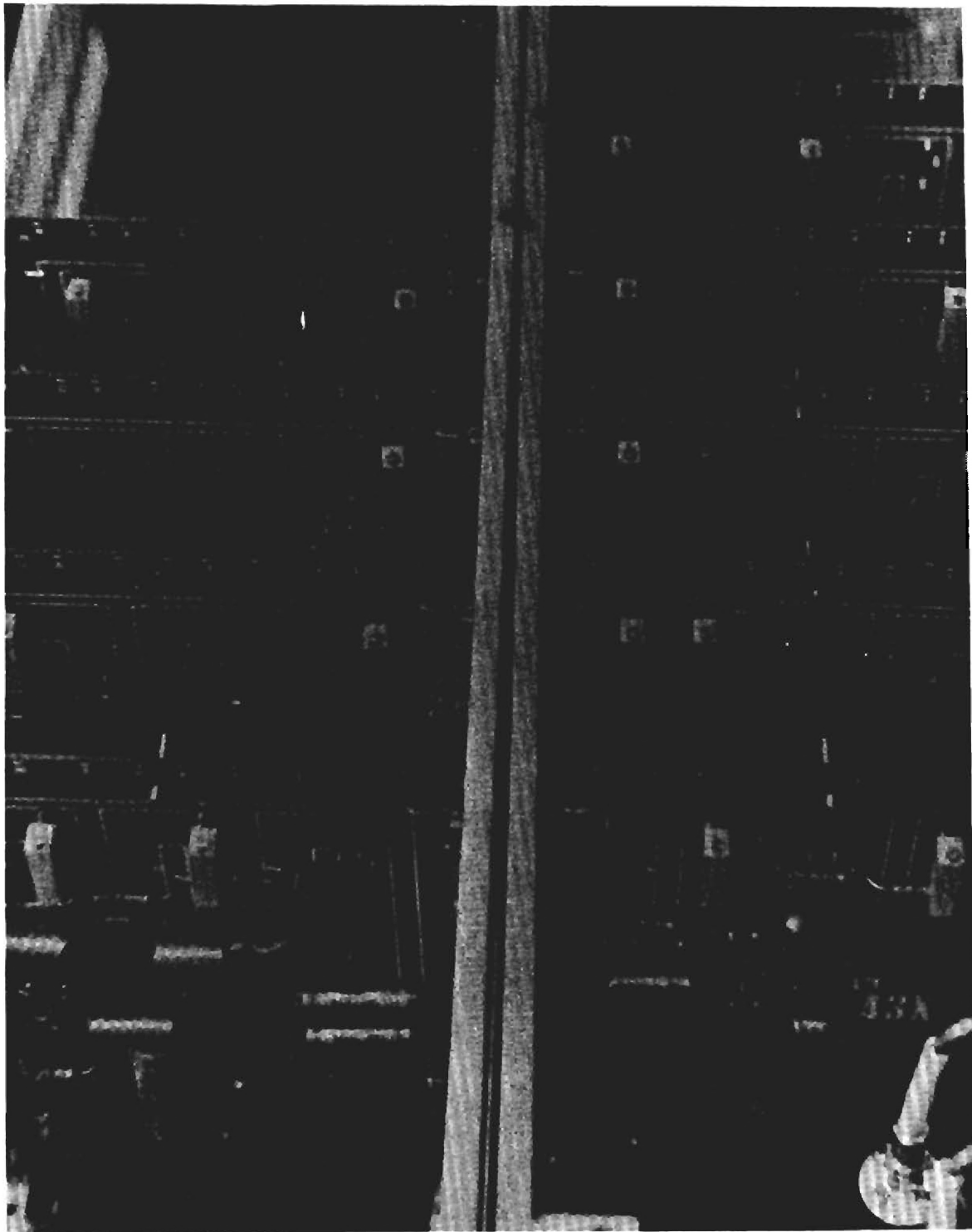


Figure 27. Photograph showing closeup view of the five data processor subsystem cards and the four logic controller cards.

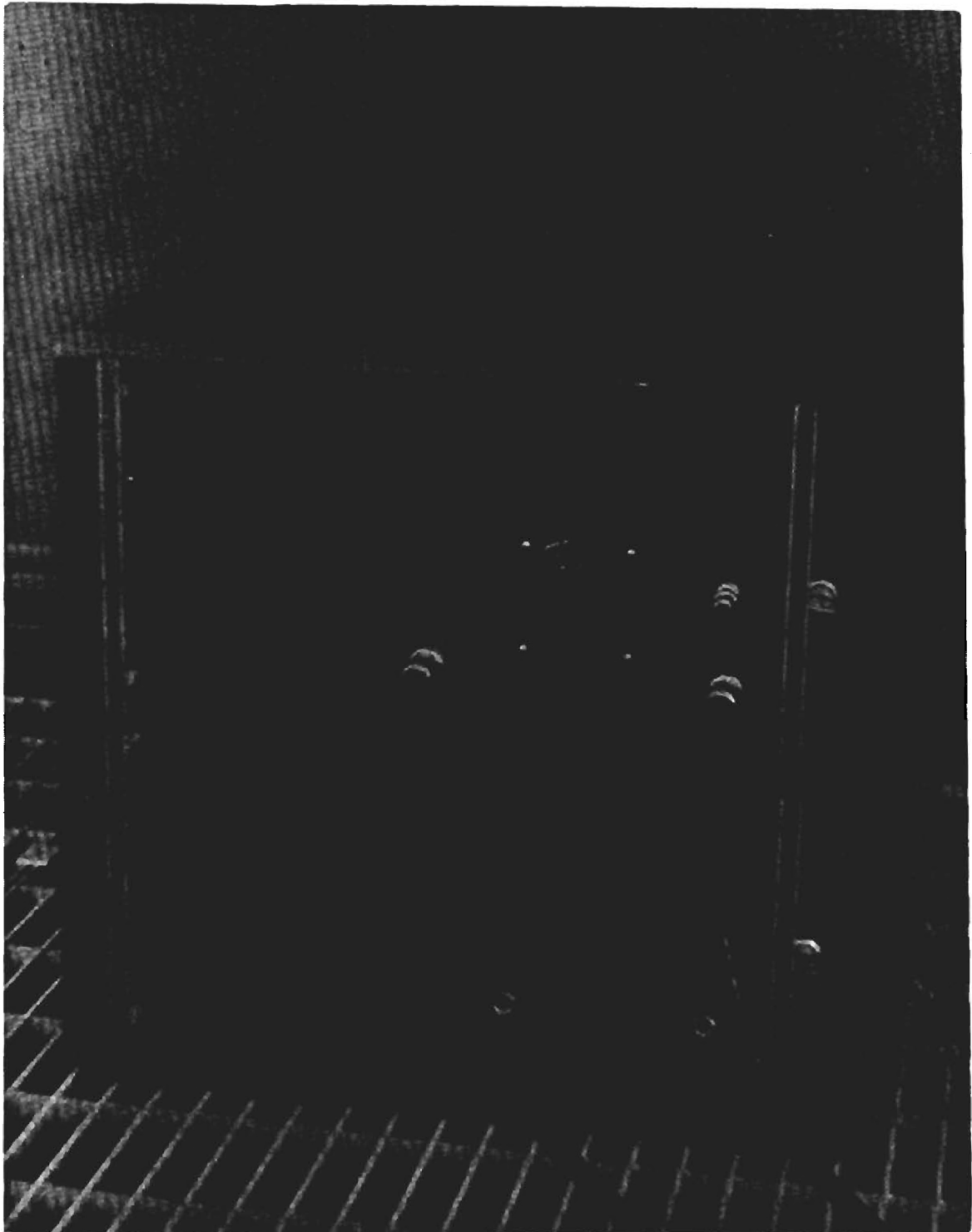


Figure 28. Photograph of Hybrid system cabinet which contains the receiver, data processor, and logic controller subsystems and dc power supplies.

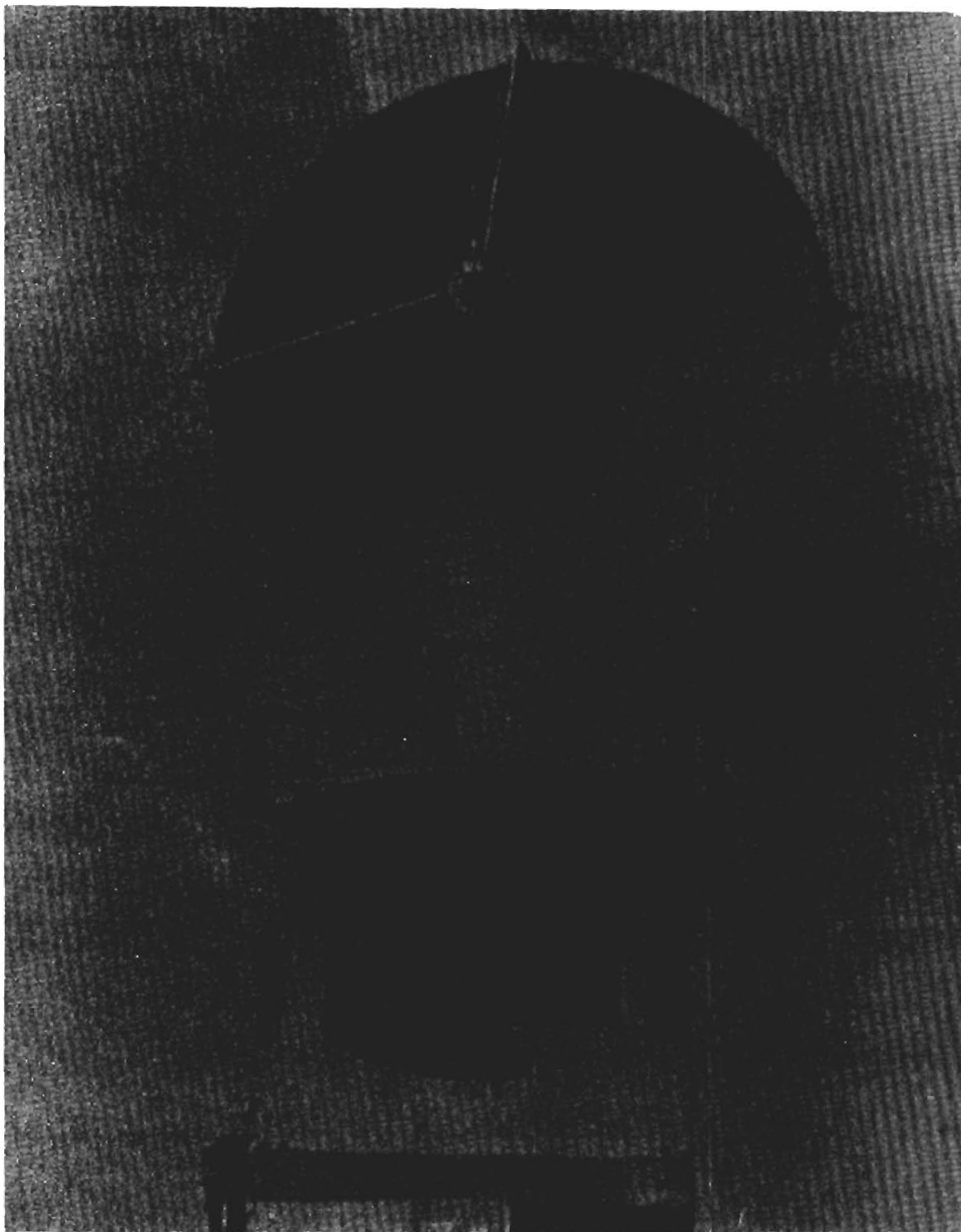


Figure 29. Photograph of paraboloidal reflector test antenna mounted on antenna positioner.

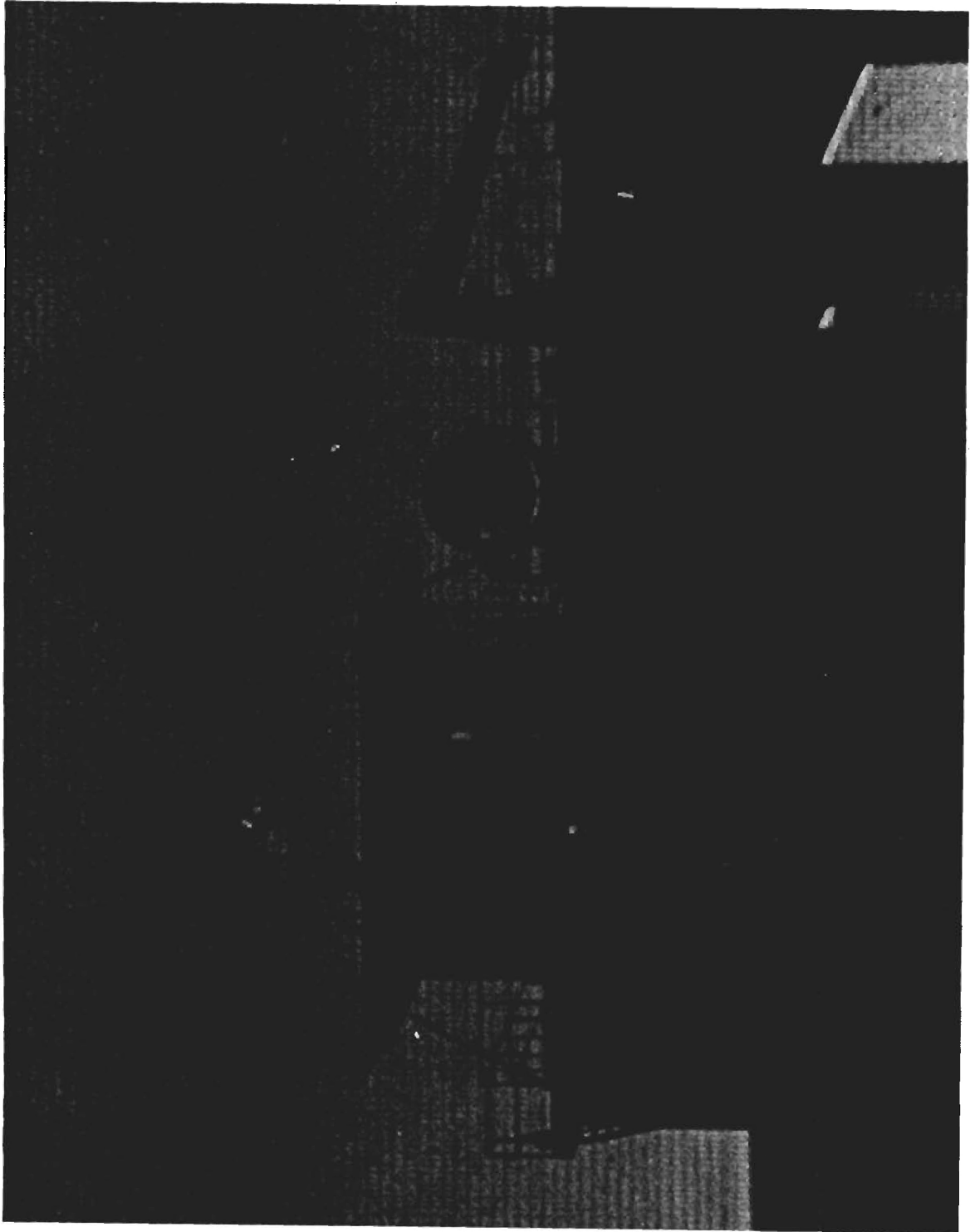


Figure 30. View of Georgia Tech antenna range receive site, as seen from transmit facility, showing test antenna mounted in place.

the transmit to the receive site on this range. For these tests, an average radiated power of about 10 watts was maintained, and the level sensor was mounted directly at the transmit antenna feed horn so that any transmitter cable effects would be compensated.

Figures 31 through 38 show a series of patterns for increasing bandwidth with the center frequency held constant at 3.5 GHz. Bandwidth varies from 5 MHz to 1 GHz. Throughout the recording of this set of data, calibration of the system was checked by inserting precision broadband attenuators in the test antenna line and marking the appropriate response on the pattern. Figures 31 and 38 show calibration points at 10, 20, 30, and 40 dB. Based on measured Hybrid system voltage output during this calibration, it was observed that accuracy was limited by the pattern recorder response. It should be noted that these patterns were recorded for a full  $\pm 180$  degrees. Reduction of the patterns to report size resulted in clipping the patterns beyond about  $\pm 150$  degrees.

As expected from analyses [1], the effect of increasing bandwidth is to fill in the nulls until at a sufficiently broad bandwidth no sidelobe structure remains. For this test antenna, this effect is nearly complete in the vicinity of  $\pm 500$  MHz bandwidth (Figure 38). All of the patterns in Figures 31 through 38 were recorded with 40 dB of instantaneous dynamic range. Somewhat more dynamic range was achieved with the Hybrid system as may be seen by the straight line (not noise limited) at the -40 dB level of the patterns. For comparison, a CW 3.5 GHz pattern using the S/A receiver is shown in Figure 39. The CW pattern was run with paper fed into the recorder so that this pattern is flipped 180 degrees with respect to the broadband patterns.

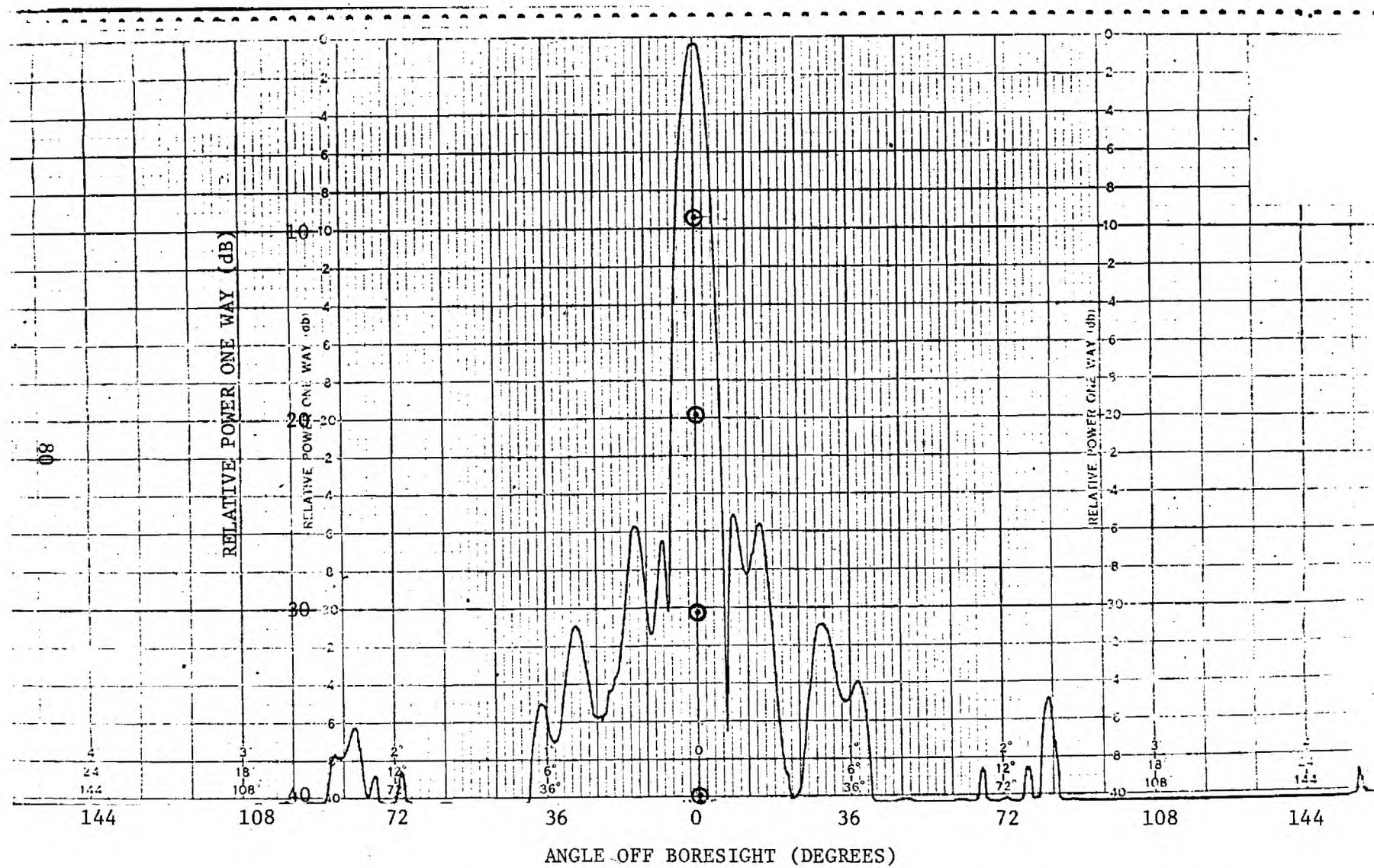


Figure 31. Broadband pattern of test antenna for a bandwidth of 5 MHz centered at 3.5 GHz.

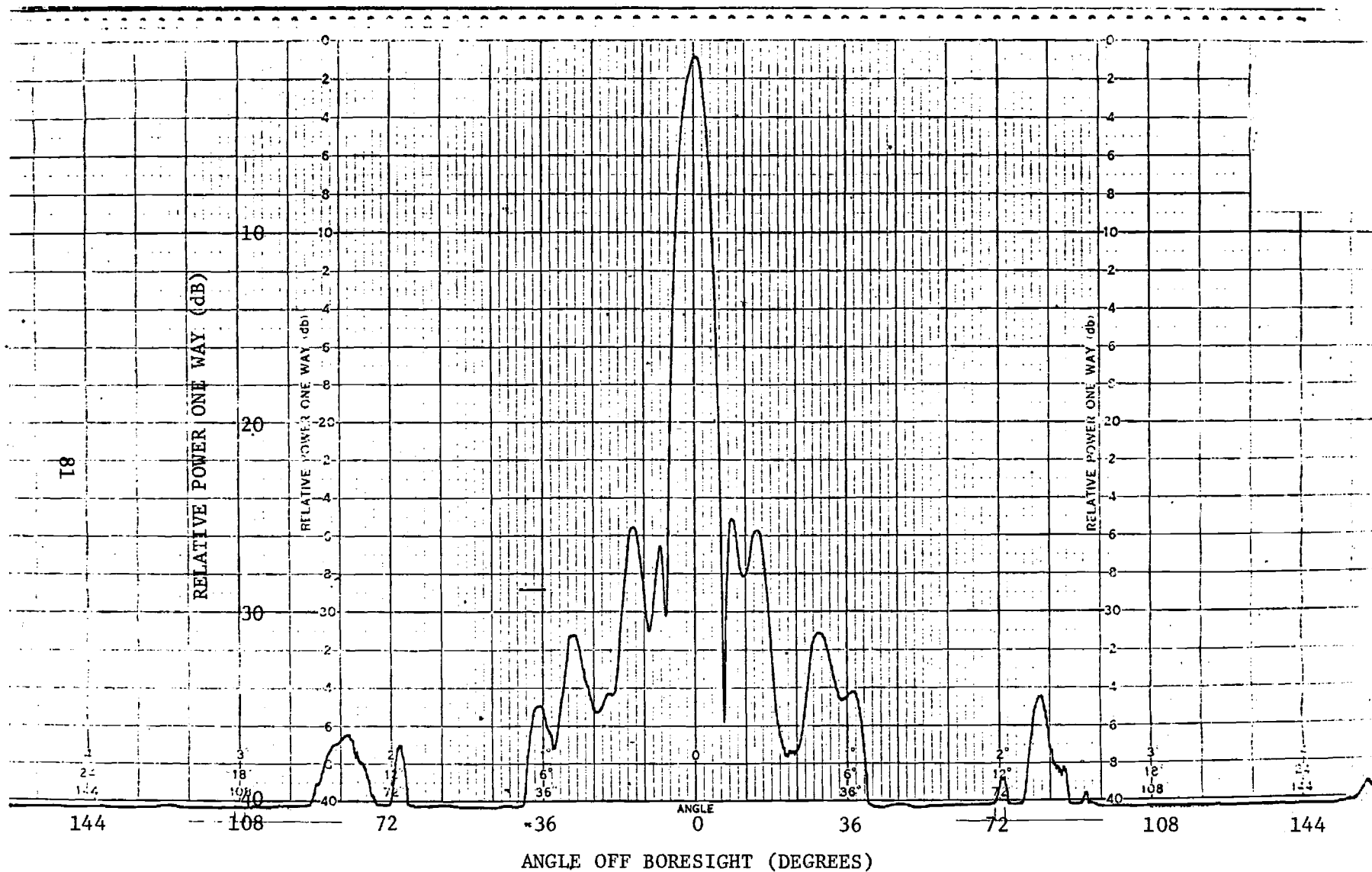


Figure 32. Broadband pattern of test antenna for a bandwidth of 10 MHz centered at 3.5 GHz.



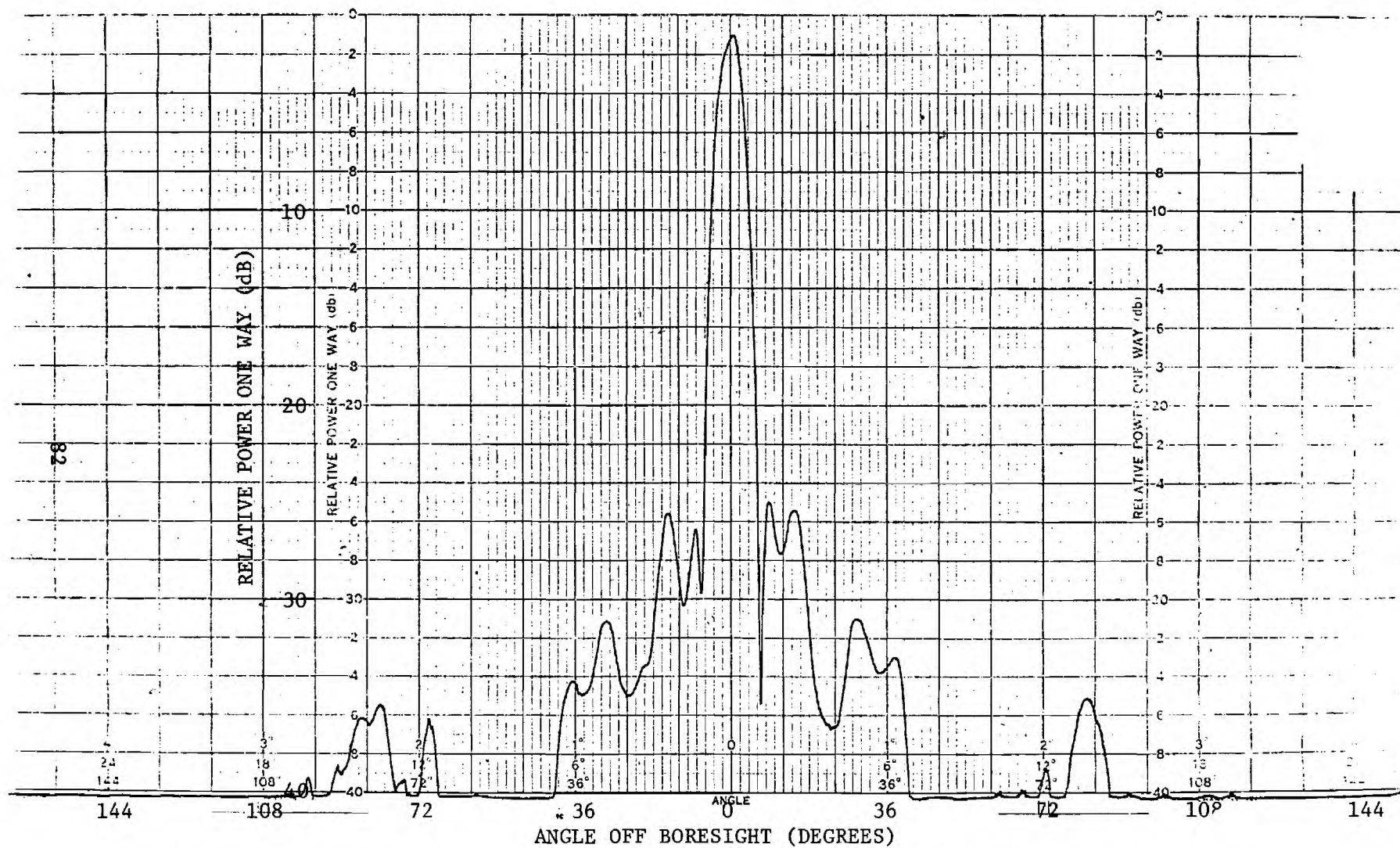


Figure 33. Broadband pattern of test antenna for a bandwidth of 20 MHz centered at 3.5 GHz.

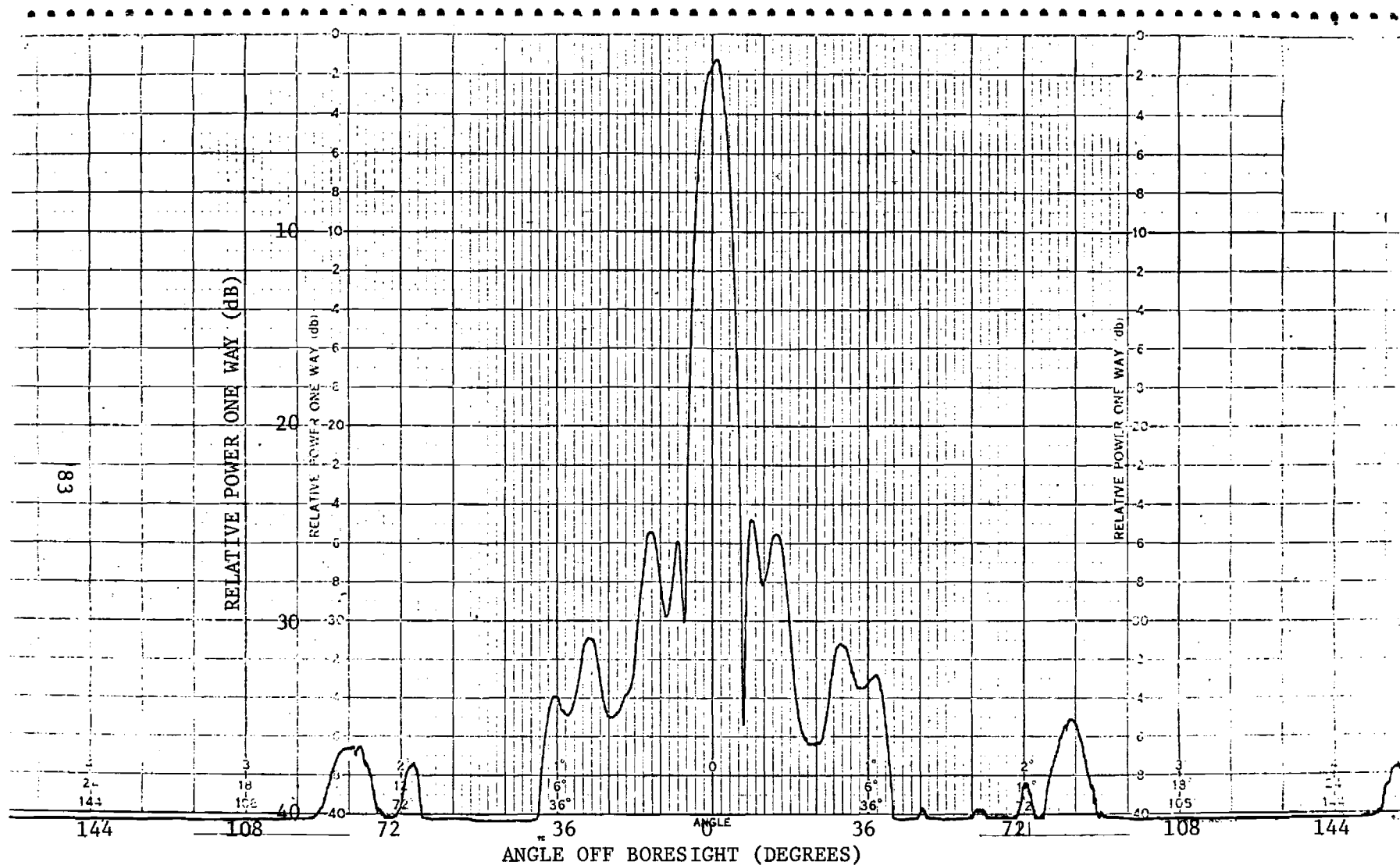


Figure 34. Broadband pattern of test antenna for a bandwidth of 50 MHz centered at 3.5 GHz.

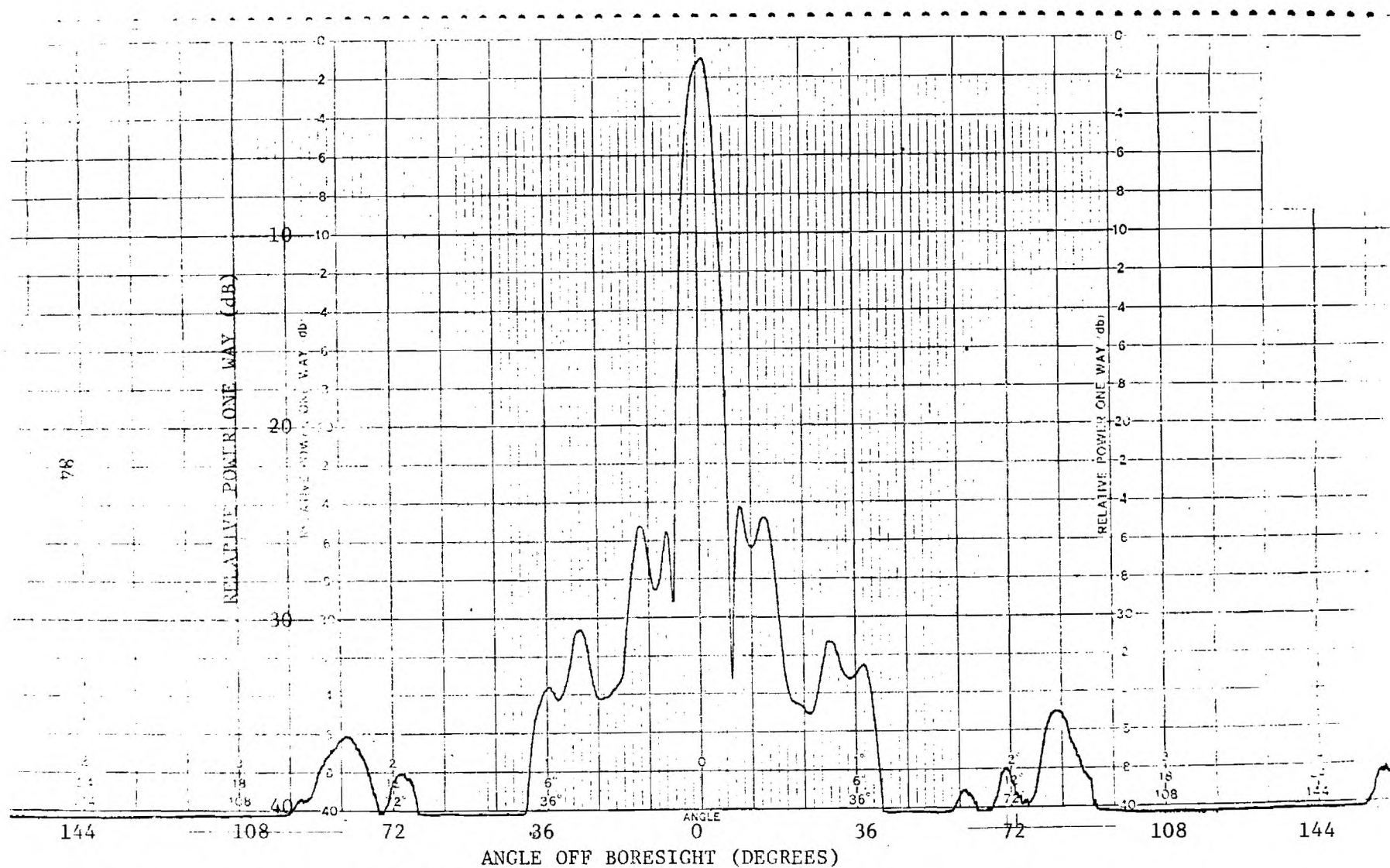


Figure 35. Broadband pattern of test antenna for a bandwidth of 100 MHz centered at 3.5 GHz.

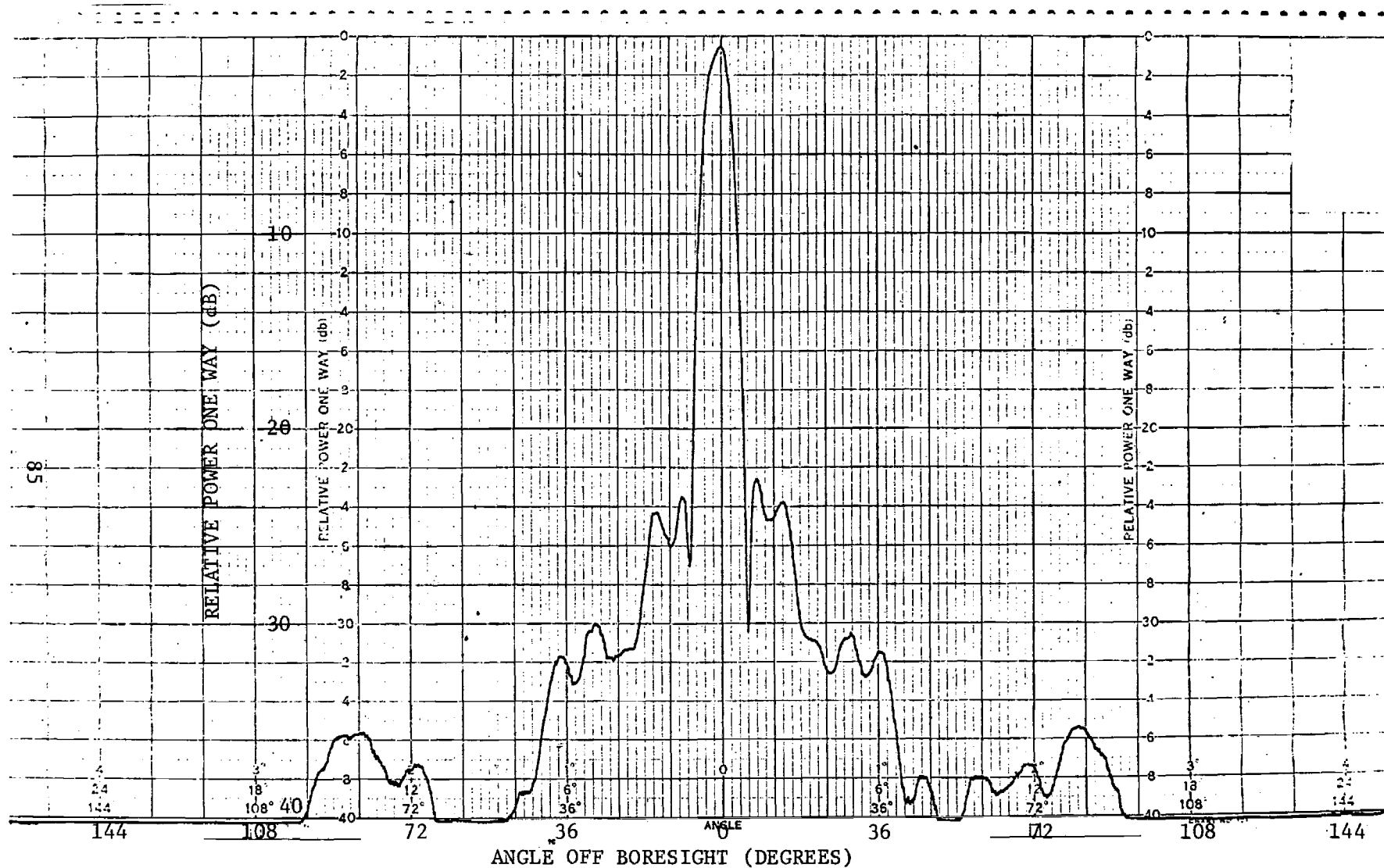


Figure 36. Broadband pattern of test antenna for a bandwidth of 200 MHz centered at 3.5 GHz.

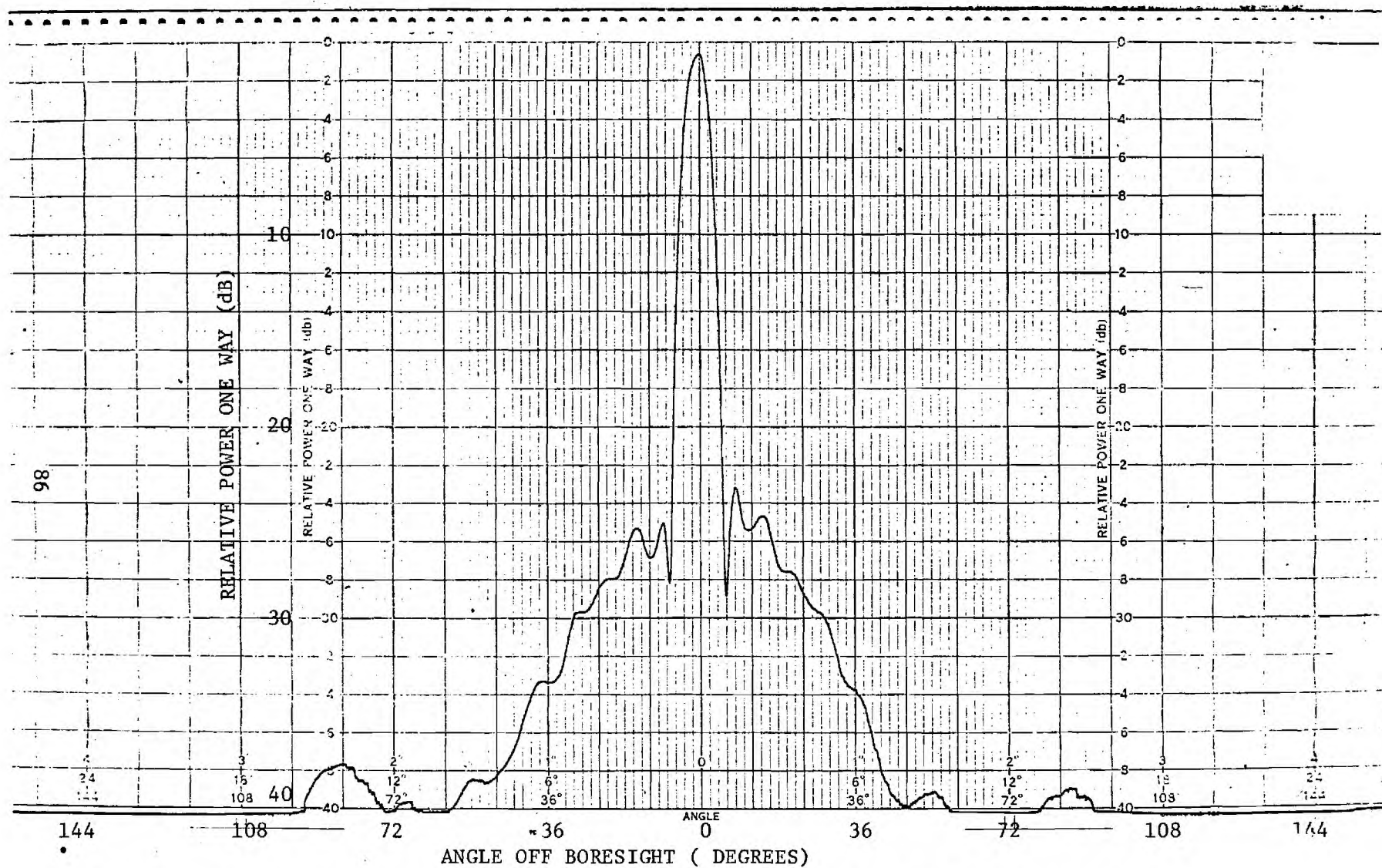


Figure 37. Broadband pattern of test antenna for a bandwidth of 500 MHz centered at 3.5 GHz.

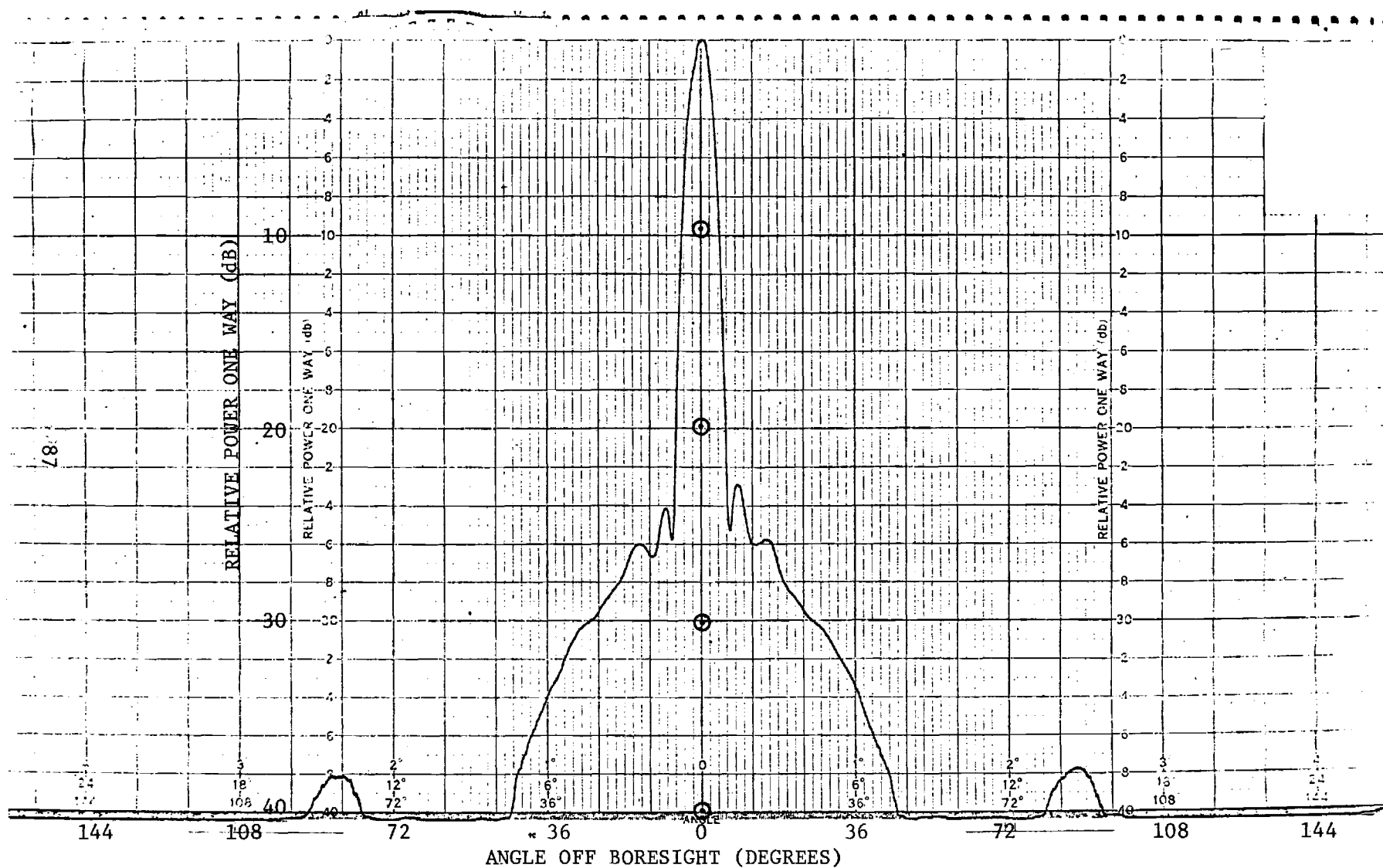


Figure 38. Broadband pattern of test antenna for a bandwidth of 1000 MHz centered at 3.5 GHz.

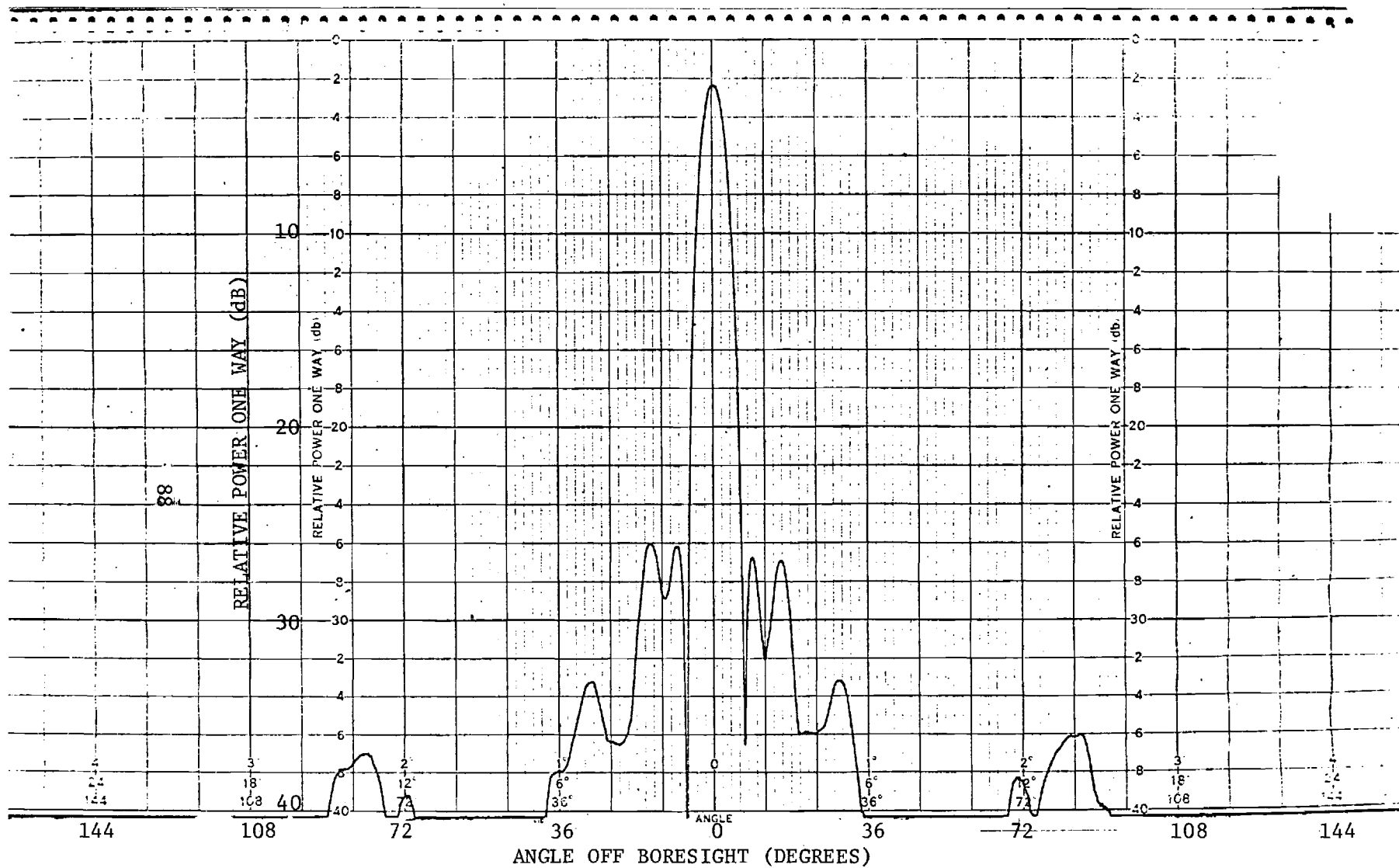


Figure 39. CW pattern using Scientific Atlanta Receiver at a frequency of 3.5 GHz.

Insight into the sensitivity of the Hybrid system may be gained as follows. On boresight, the RF level at the input to the low-noise amplifier was set at -30 dBm during recording of the data described above. To determine if processing down to -80 dBm was feasible, the S/A pattern recorder was re-calibrated for a 50 dB dynamic range. This re-calibration amounts to a scale compression. Patterns run under these conditions show structure down to the -50 dB level without noise limiting. Thus, sensitivity of -80 dBm is illustrated.



## SECTION III

### PHASE-AND-AMPLITUDE SYSTEM STUDIES

#### A. INTRODUCTION

Preliminary investigations to determine the feasibility of performing broadband phase-and-amplitude measurements in the far-field of short pulse radar antennas were conducted under Contract F30602-73-C-0194, and the results were presented in the Final Technical Report on that contract [1]. It was concluded that a computer-controlled sweep-frequency phase-plus-amplitude system for broadband antenna measurements could be practically realized. Such a system would provide the information for determining both time domain pulse information and arbitrary bandwidth (up to one octave) pattern data. Two possible implementations of such a system were identified, typical operating parameters were selected, and calibration requirements were investigated. On the present study, further system tradeoff studies between a group delay type of phase measurement system versus a direct phase measurement system were conducted. It was concluded that use of group-delay techniques represent the better approach toward realization of an accurate, usable, broadband antenna measurement system. In this section, the system tradeoff studies will be reviewed, a preliminary group-delay system design will be presented, and typical operating parameters and system applications will be discussed.

## B. TRADEOFF STUDIES

### 1. Concept Reviews

Efforts on this program have included the study and evaluation of two distinctly different approaches for measurement of broadband antenna phase response data. One approach is based on a direct measurement of the relative phase between swept frequency test and reference signals, and the second approach is based on a measurement of the phase differential between two sidebands which are separated from a swept carrier by a fixed amount. These two concepts were described in detail in the final technical report on Contract F30602-73-C-0194. These two concepts and typical associated hardware will be briefly reviewed, and then tradeoff comparisons will be presented.

It is required to determine that quantity commonly termed incremental phase delay, i.e., the change in phase delay with change in some parameter such as frequency. Incremental phase delay is generally measured in the laboratory by a phase comparison between a reference signal and a signal which passes through the device under test. This measurement concept is illustrated by Figure 40. By extension, direct far-field incremental phase delay measurements may be postulated. A simple illustration of this concept is shown in Figure 41.

A more detailed block diagram of a possible direct measurement phase-and-amplitude swept frequency system is shown in Figure 42. The transmitter of this postulated system would consist of a sweep oscillator, a power amplifier, and a level sensor which provides a feedback loop for maintaining constant transmitter power output. A broadband transmitting antenna with well behaved phase properties is also required.

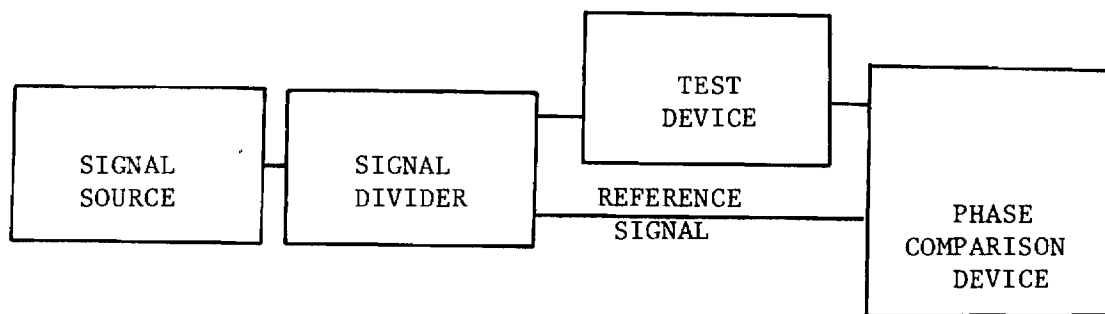


Figure 40. Illustration of the incremental phase measurement concept in the laboratory

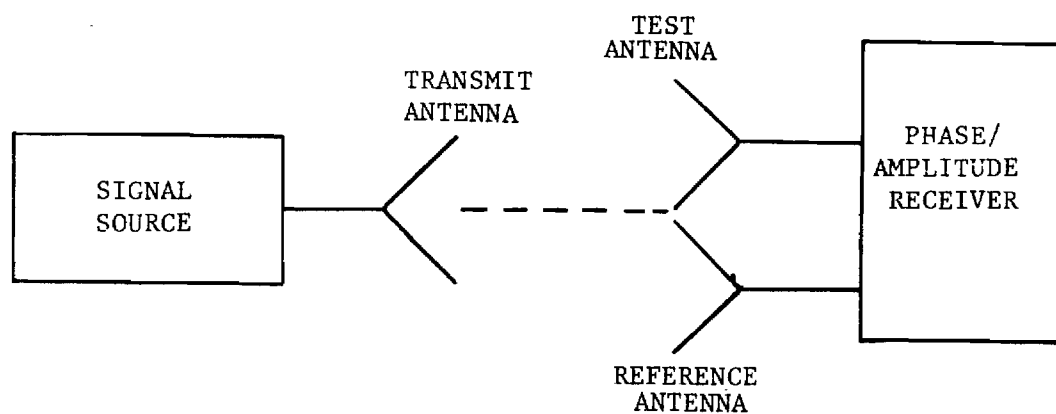


Figure 41. Extension of the direct incremental phase measurement concept to the far-field antenna range

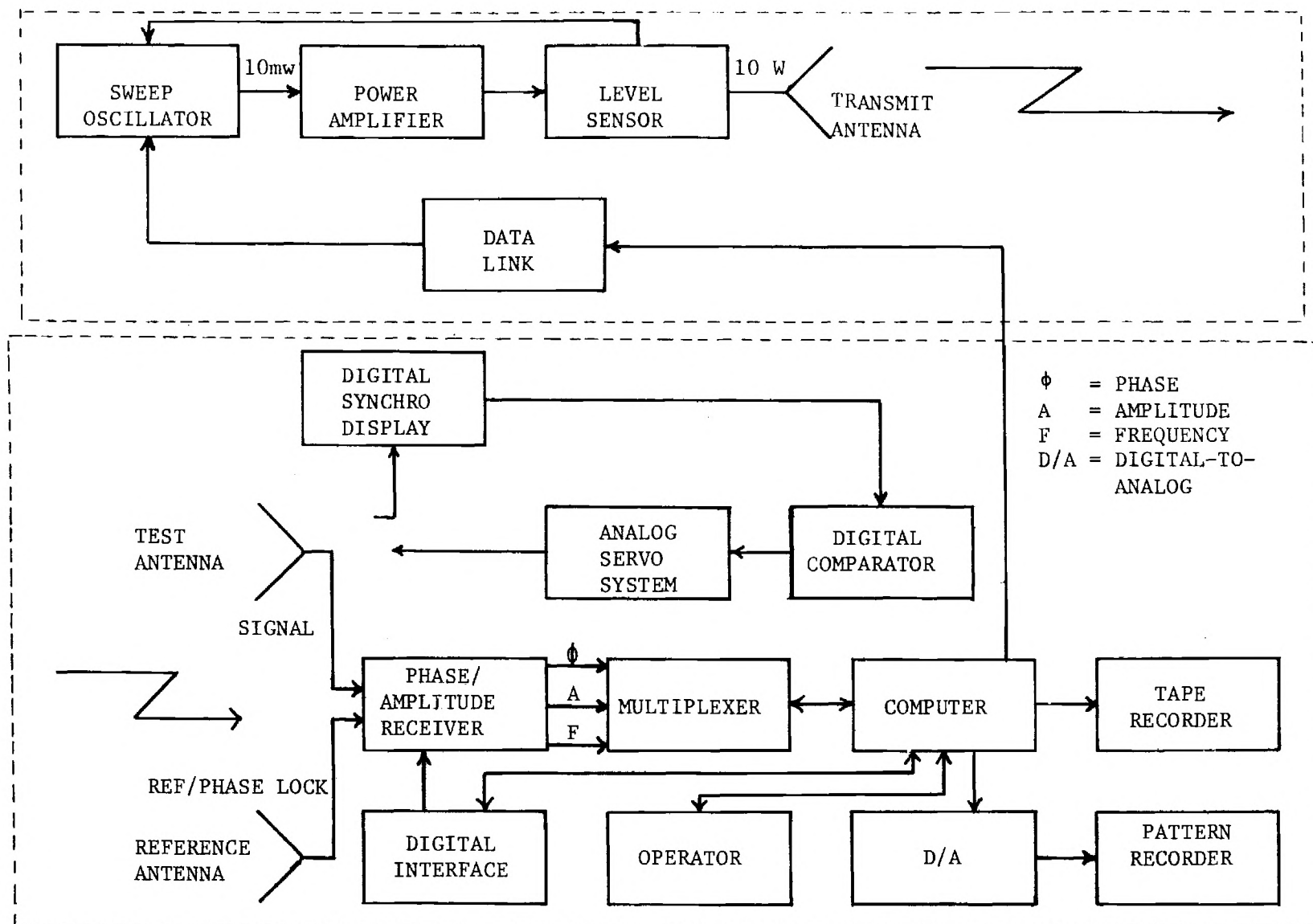


Figure 42. Block diagram of possible direct measurement phase and amplitude system

The configuration of the receiving site subsystem and that subsystem's overall hardware requirements are strongly influenced by the receiver which would be used. At the present time, the most appropriate receiver appears to be a new Scientific-Atlanta, Inc. (S/A), product. This new product is called a Series 1700 Programmable Receiver. In certain respects, this series of receivers is similar to the established Series 1750 Phase/Amplitude Receivers. There are, however, these two important differences: (1) the Series 1700 Receivers incorporate a fast tuning local oscillator which can be coupled to a signal source for automatic tracking at rates up to 10 GHz/sec and (2) with appropriate accessories, the Series 1700 Receiver will be fully computer compatible.

The second type of phase measurement system which was considered is based on a measurement of group delay. Consider the modulation of an RF carrier to produce two phase-coherent sidebands spaced an equal frequency increment above and below the carrier. When the resultant waveform (carrier-plus-sidebands) is passed through the component (e.g., an antenna) under test, each constituent part of the waveform will undergo a phase delay which is a characteristic of that frequency for that component under test. After propagating through the antenna under test, the sidebands may be "stripped off" of the carrier and the relative phase between them may be determined. From a series of measurements as the carrier is stepped across the frequency range of interest, a curve of measured phase delay versus frequency may be derived. In general, to obtain the phase delay of a single component, the phase characteristics of other components in the RF path must be known. Basically, implementation of a group delay measurement system requires the addition of synchronized modulate and demodulate

signal sources at the respective transmit and receive sites of Figure 42, and the addition of sideband processing circuits to the receiver.

## 2. Evaluation

As indicated earlier, it has been concluded that the group delay technique offers the better approach toward antenna far-field phase measurements over wide bandwidths. The advantages of the group delay technique arise from the fact that all the phase information is derived from a single RF channel. That is, there is no requirement to transmit a phase reference signal through a separate channel. Since a reference channel is not required, there is no need to maintain relative electrical lengths, as a function of frequency, between two channels (test and reference) with widely separated receiver mixers. Furthermore, even if all the required phase correction information for the direct phase measurement approach could be determined and maintained as a function of the desired test variables (frequency and antenna position), the direct phase measurement approach would likely lead to rapid excursion in the measured (uncorrected) relative phase data. Such rapid phase excursion would limit measurement speed and accuracy. With the group delay technique, any one measurement will determine the relative phase, in a single channel, between two sidebands which are spaced on the order of 10 MHz apart. Currently, narrow band group delay sets are employed to characterize communication channels. Thus, there is some experience with equipment somewhat similar to that recommended here. The basic receiver employed in the recommended system would be the new S/A Series 1700 Programmable Receiver; thus, measurement accuracies similar to the Series 1750 accuracies are expected. This topic is discussed in more detail in the following sub-section.

## C. DESCRIPTION OF THE GROUP DELAY SYSTEM

### 1. Concept

As indicated above, the group delay system requires modulation of the carrier to produce two equally spaced sidebands, which are coherent. Modulation of the carrier with either single tone AM or FM is convenient and produces two sidebands equally spaced on opposite sides of the carrier. Thus, one can measure relative phase delay between the sidebands and the carrier as the carrier frequency is tuned across the measurement band. Ideally, one would measure the phase difference  $d\phi$  between two sidebands separated by a frequency difference  $d\omega$  at a carrier frequency  $\omega_c$  and then integrate to obtain the phase function  $\phi$ . However, in a real measurement system the sideband separation would be non-zero so that  $d\phi/d\omega$  would be approximated by  $\Delta\phi/\Delta\omega$  in which  $\Delta\omega$  is the sideband separation.

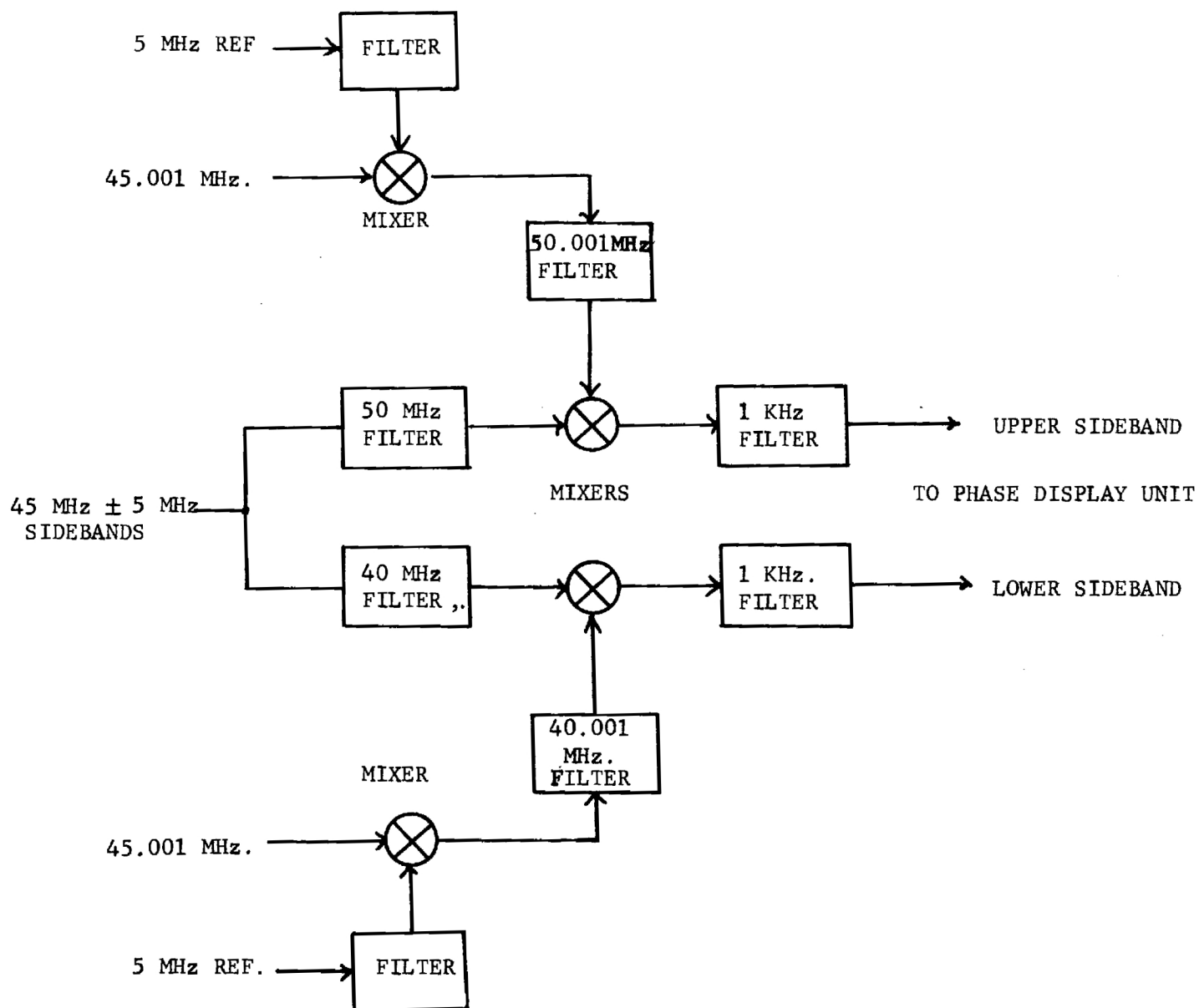
Consider the sideband processor shown in Figure 43. This processor is capable of acting on the S/A series 1700 Receiver IF signal (45 MHz center frequency plus sidebands) to obtain the phase difference  $\phi'$  which is defined by

$$\phi' = \Delta\phi/\Delta\omega \quad . \quad (3)$$

Figure 44 symbolizes the various frequency conversions which take place in the sideband processor of Figure 43. The symbols which are used in Figure 44 are defined as follows:

- $\omega_c$  = Microwave carrier frequency,
- $\phi_c$  = Phase delay at carrier frequency,
- $\omega_r$  = Modulation frequency,
- $\phi_1$  = Phase delay at the upper sideband,
- $\phi_2$  = Phase delay at the lower sideband,
- $\omega_1$  = First IF frequency (45 MHz),

Figure 43. Block diagram of group delay sideband processor.





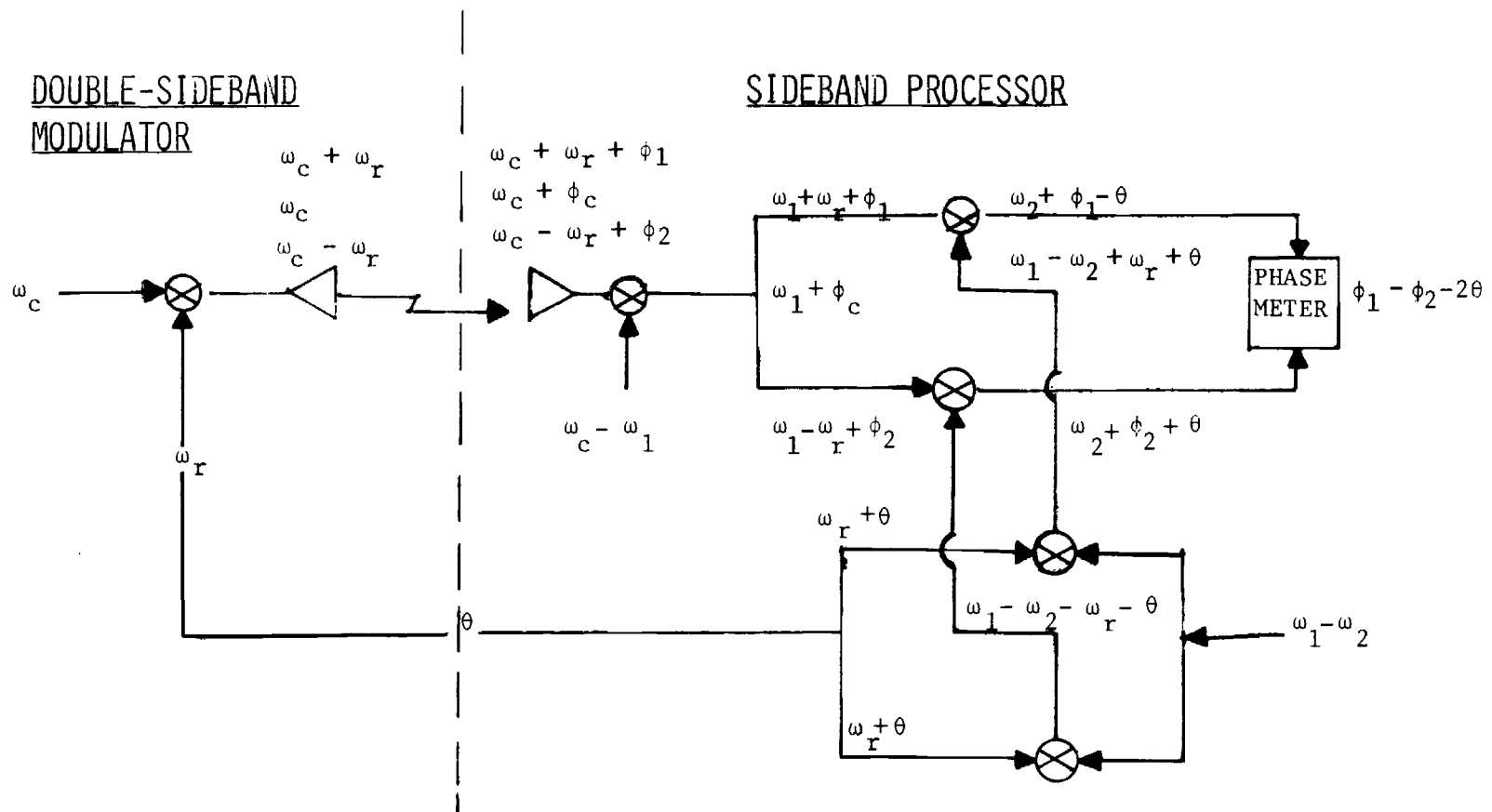


Figure 44. Block diagram showing the frequency conversions which occur in a group delay measurement system.

$\omega_2$  = Second IF frequency (1 kHz), and

$\theta$  = Phase delay of modulation reference link.

The modulation frequency  $\omega_r$  is herein tentatively chosen to be 5 MHz. The result of the sideband processing is thus seen to be a set of measurements  $(\phi_1 - \phi_2 - 2\theta)|_{\omega_i}$  where  $\omega_i$  represents the set of frequencies to which the carrier is tuned. The two 1 kHz signals represented on Figure 44 by  $\omega_2 + \phi_1 - \theta$  and  $\omega_2 + \phi_2 + \theta$  are the second IF signals which contain the upper and lower sideband phase information, respectively, and which may be input directly to a phase measurement and display unit to determine the relative sideband phase delay.

With a stable modulation reference path and phase-locked modulate and demodulate signals, the measured differential phase is directly proportional to the sideband frequency difference and the dispersion in the network. This indicates that there are two ways to use sideband differential phase measurements to measure phase characteristics of an antenna. These two ways are (1) keep the modulating frequency,  $\omega_r$ , constant and sweep the carrier, or (2) keep the carrier constant and vary  $\omega_r$ . For GHz bandwidths, method (1) is more practical since method (2) would require instantaneous bandwidths of up to 1 GHz for various mixers, amplifiers, etc. With method (1), any departure from constant  $\Delta\phi/\Delta\omega$  as the carrier is swept would be due to total dispersion in the measurement channel (including test antenna). To determine dispersion due to the test antenna, the measurement channel must be calibrated; that is, its phase characteristics without the test antenna must be known. From this calibration data and the measured  $\Delta\phi/\Delta\omega$ , the test antenna phase response can be found.

## 2. Equipment Description

A stabilized programmable WWV-locked transmit system for group

delay measurements is shown in block diagram form in Figure 45. As indicated earlier, the relative phase between the modulator (at the transmit site) and the demodulator (at the receive site) must be constant during a set of measurements. These two signal sources could be phase locked (to maintain constant relative phase) by several means, including (1) a direct coaxial cable hookup between the two sites, (2) a microwave link, and (3) phase locking of both sources to a common highly stable reference. For short distances over even terrain, the most economical approach in many cases would be a direct coaxial cable hookup. However, for very long distances and/or very rough terrain, running a coaxial cable may not be practical. Thus, it is desirable that the system design provide for phase locking with no direct hookup.

Cost estimates indicate that a microwave link would be about five times more costly than common modulate and demodulate synchronization to WWV. In addition, microwave links at more than one carrier frequency might be required in order to prevent interference with the test signal. Phase locking to the National Bureau of Standards (NBS) radio station WWV is the preferred approach and it is discussed in detail in the following paragraphs.

The National Bureau of Standards radio station WWV broadcast standard radio frequencies of 2.5, 5, 10, 20 and 25 MHz on a continuous basis day and night. All carrier and modulation frequencies at WWV are derived from cesium-controlled oscillators and they are accurate to within  $\pm 1$  part in  $10^{11}$ . Day-to-day deviations are normally less than 1 part in  $10^{12}$ . The effective radiated power is 13 kW; continuous coverage of the continental U.S. and nearby regions of Mexico and Canada is provided. Similar service is provided in the Pacific by an NBS station in Hawaii. In Europe, a

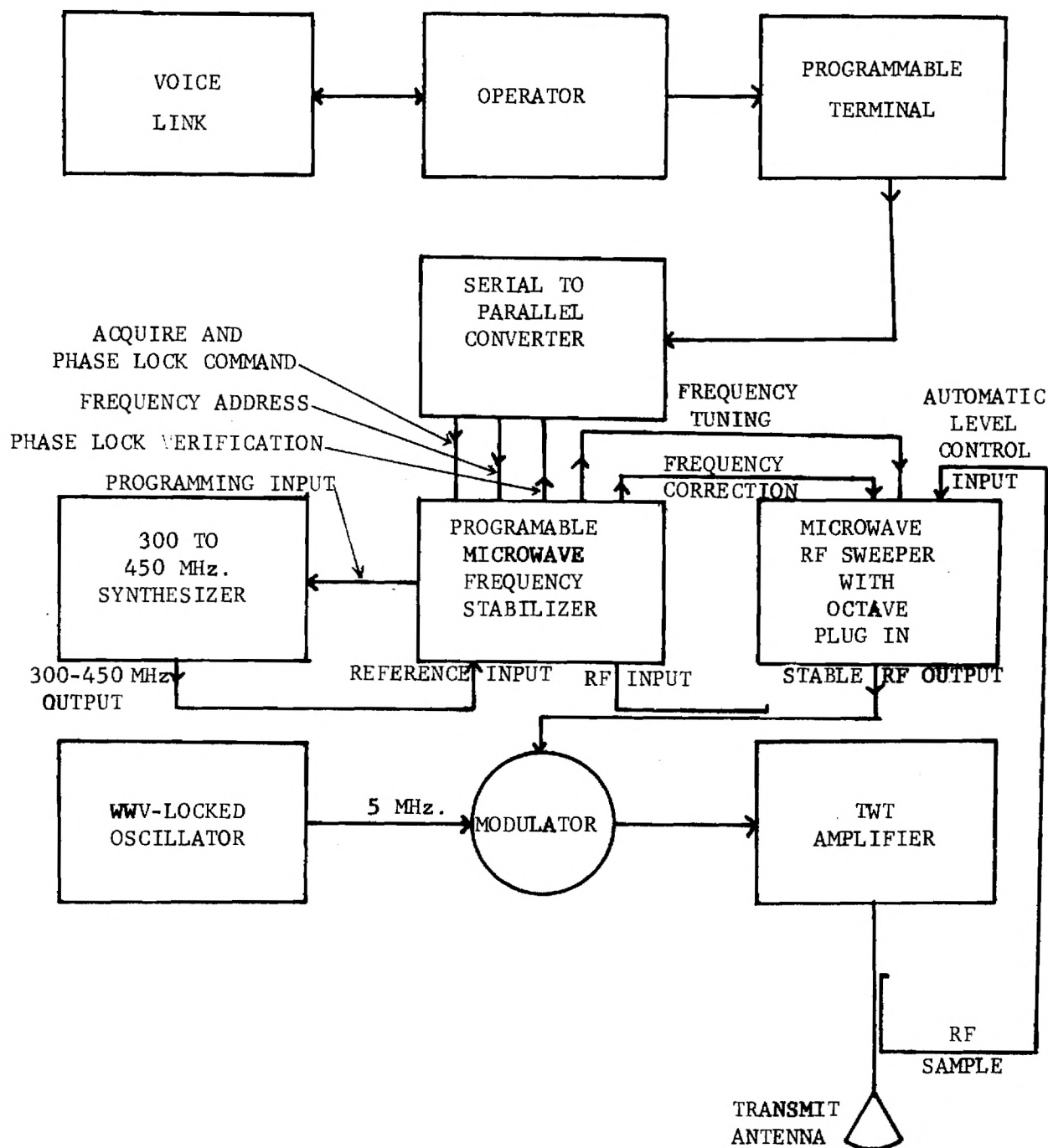


Figure 45. Stabilized programmable WWV-locked transmitter system for group delay measurements.

60 kHz broadcast from MSF in the U.K. provides a link to the National Physical Laboratory Standards, and 75 kHz standards are broadcast by HBG in Prangins, Switzerland. Thus, locking to a standards broadcast is a widely applicable technique.

Measured field intensity contours from WWV/Boulder are shown in Figure 46. A system for reception and locking to WWV should be designed to operate at the lowest field intensity levels and provide several dB of margin for adverse propagation conditions.

A block diagram of a system for locking a 5 MHz modulate or demodulate source to WWV is shown in Figure 47. A frequency synthesizer is required for the signal source in order to obtain high frequency stability and accuracy. Suitable frequency synthesizers are commercially available. For example, one model has an output frequency range of 1 kHz to 13 MHz and it can be phase locked to any external signal which is a sub-harmonic of 20 MHz and which has an amplitude of 200 mV to 2 V rms. Locking at the WWV 10 MHz signal is assumed here.

If we assume that the receiving antenna has an effective height of 1 meter at 10 MHz (approximately 1/2 wavelength dipole), the signal at the antenna terminals would be a minimum of about 50  $\mu$ V anywhere within the continental U.S. The WWV receiving antenna is followed by a very narrow band filter (say, 100 kHz bandwidth) to reject any interference and reduce the noise power level. The thermal noise at room temperature in a 100 kHz band is approximately -124 dBm. In a 50 ohm system, this corresponds to a noise voltage level of  $1.41 \times 10^{-7}$  volts. Thus, the ideal signal-to-noise voltage ratio would be  $\frac{50 \times 10^{-6}}{1.41 \times 10^{-7}}$ , or a factor of about 51 dB. Now, since the locking signal to the frequency synthesizer must be a minimum of

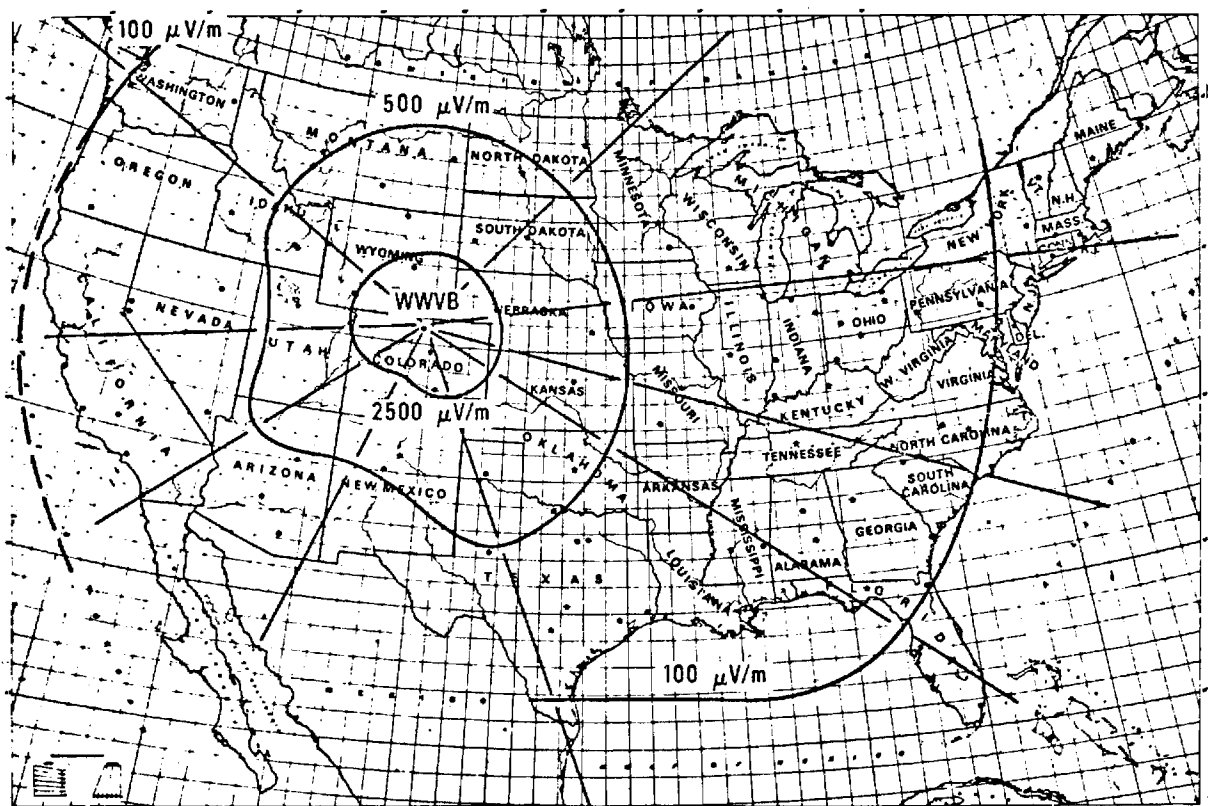


Figure 46. Measured field intensity contours for WWVB/Boulder standards broadcast.

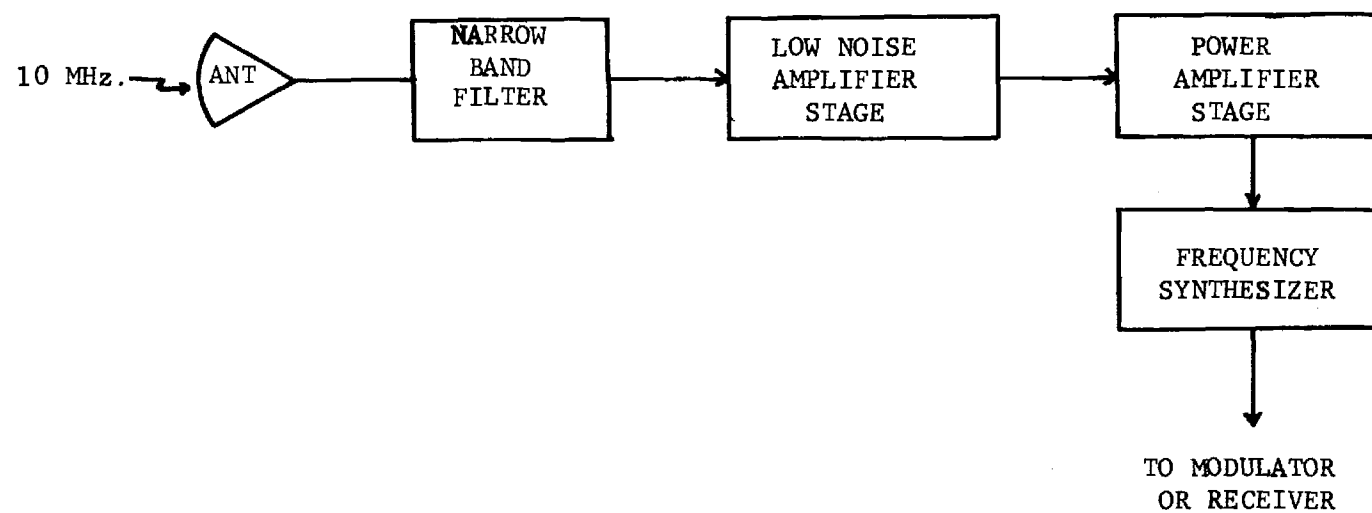


Figure 47. Block diagram of a system for phase locking to a WWV standards broadcast.

200 mV rms , amplification of the signal is required. Amplification from 50  $\mu$ V to 200 mV requires a power gain of 72 dB, and the power amplifier stage must provide an output of 200 mV, or approximately 0 dBm in a 50 ohm system. Available low noise amplifier stages can provide about 45 dB of gain with a noise figure of 2.0 dB. Medium power amplifiers of 40 dB gain with a +20 dBm gain compression of 1 dB and a noise figure of 4.5 dB are available. These two amplification stages would provide a margin of 13 dB above the minimum signal required for locking.

Returning to a discussion of the transmit site block diagram, the Programmable Microwave Frequency Stabilizer operates under remote control inputs from a terminal which is commanded by an on-site operator. The Programmable Microwave Frequency Stabilizer in turn controls the frequency of the Microwave RF Sweeper, and stabilizes its output to an accuracy equivalent to that of the UHF Synthesizer. The RF Sweeper and the TWT Amplifier are the units currently used in the Hybrid system transmitter. Since no direct cable or telephone hookups are allowed between the transmit and receive sites, the transmit site sub-system and the receive site sub-system must be "free-running", except for the common phase-locking to WWV described above. This free-running feature of the system will be discussed in detail in a following sub-section.

A block diagram of the receive site sub-system is shown in Figure 48. The Series 1700 S/A receiver is a phase-locked super heterodyne type which employs harmonic mixing. It is generally similar in operation to the well-known S/A 1750 receivers except that it employs a frequency-agile YIG tuned local oscillator and it is fully computer compatible. With the appropriate plug-ins and accessories, all readouts are in a digital format. A block



THIS PAGE INTENTIONALLY LEFT BLANK.

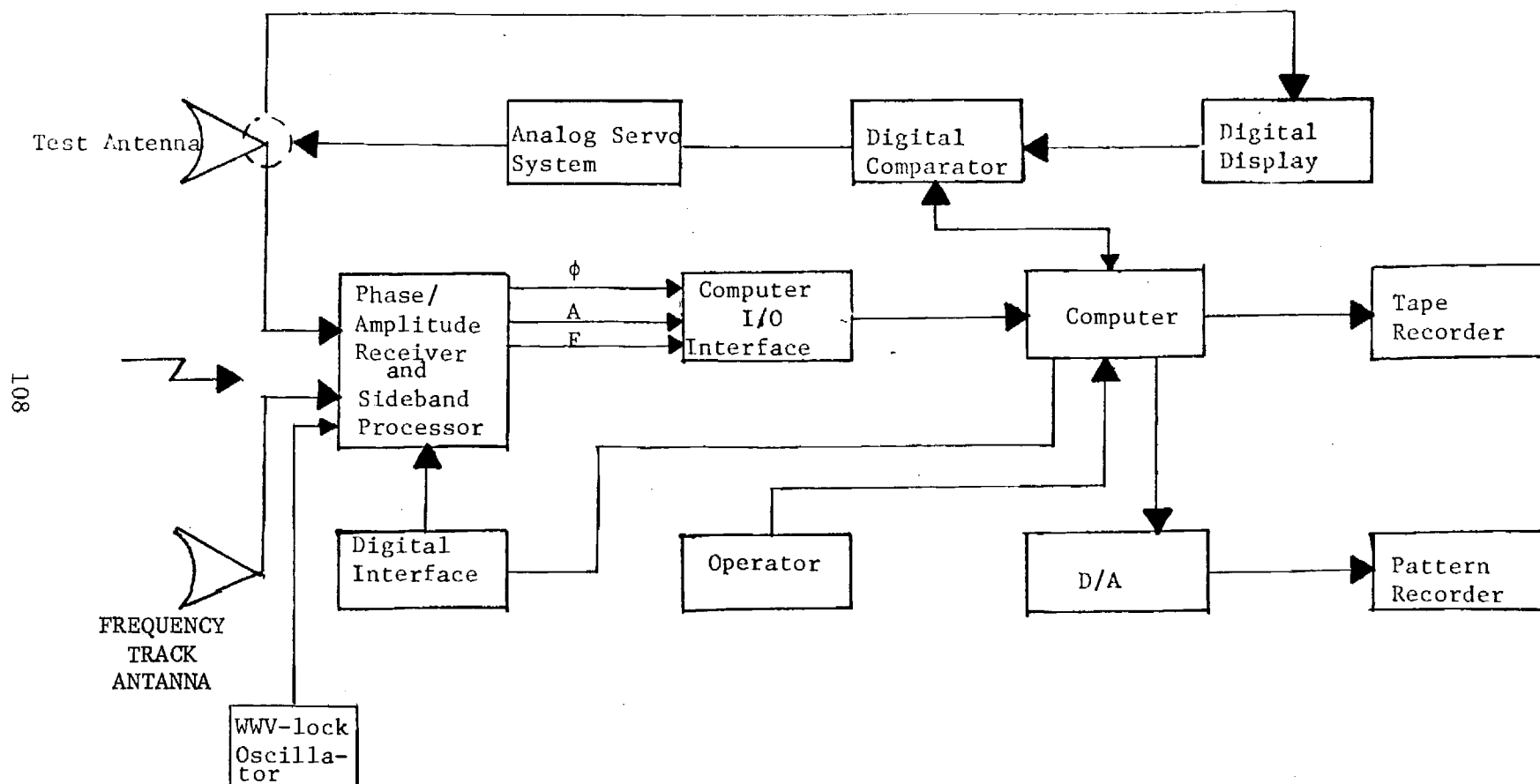


Figure 48. Block diagram of group delay receive site subsystem.

diagram of this receiver is shown in Figure 49. As shown in the figure, the receiver 1 kHz output signals are fed to either the sideband processing circuits or to digital phase and amplitude display units.

A block diagram of the swept-frequency receiver configured for two channel operation is shown in Figure 50. In this configuration, the tracking signal is derived by sampling the reference channel. (An alternate three-channel input has a dedicated tracking input.) With the two channel configuration, the minimum signal level input is that required for Automatic Phase Control (APC). Typical sensitivities are given in Table 9. It may be seen that, sensitivity of the APC channel is from 35 to 40 dB less than the sensitivity of the signal channel. In the present application, the reference antenna would be boresighted to the transmit site and remain fixed while the test antenna scans. Since test antenna sidelobes down to at least -40 dB must be observable, boresight signal level requirements at the mixer inputs of the two channels are within about 5 dB. The signal channel will require about 5 dB more total gain; thus, the reference antenna can be somewhat smaller than the test antenna. The maximum mixer input in either channel is -25 dBm; thus, instantaneous dynamic range is approximately 65 dB, minimum. Amplitude accuracy (including S/A series 1830 Digital Amplitude Display Plug-in) is approximately 0.05 dB/10 dB below -25 dBm mixer input. Phase accuracy (including S/A Series 1820 Phase Display Plug-in) is approximately 0.35 degree/10 dB below -25 dBm input. Thus maximum amplitude and phase errors would be approximately 0.4 dB and 1.4 degrees, respectively. For minimum error under dynamic conditions, in which phase and/or amplitude may change rapidly, data rates should be limited to a new phase and amplitude sample each 50 milliseconds, or approximately a 20 Hz data rate.

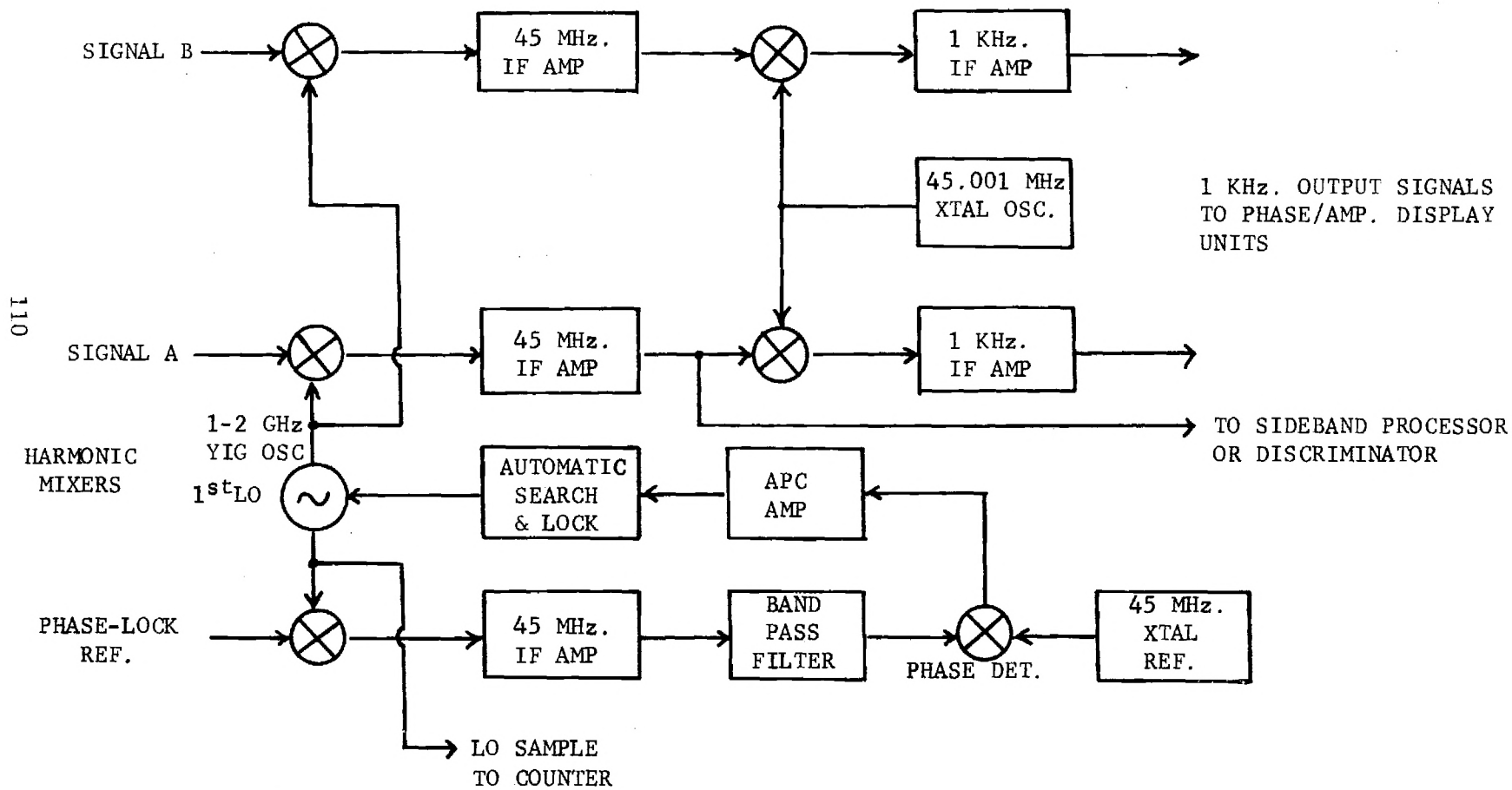


Figure 49. Tracking phase-locked receiver block diagram.

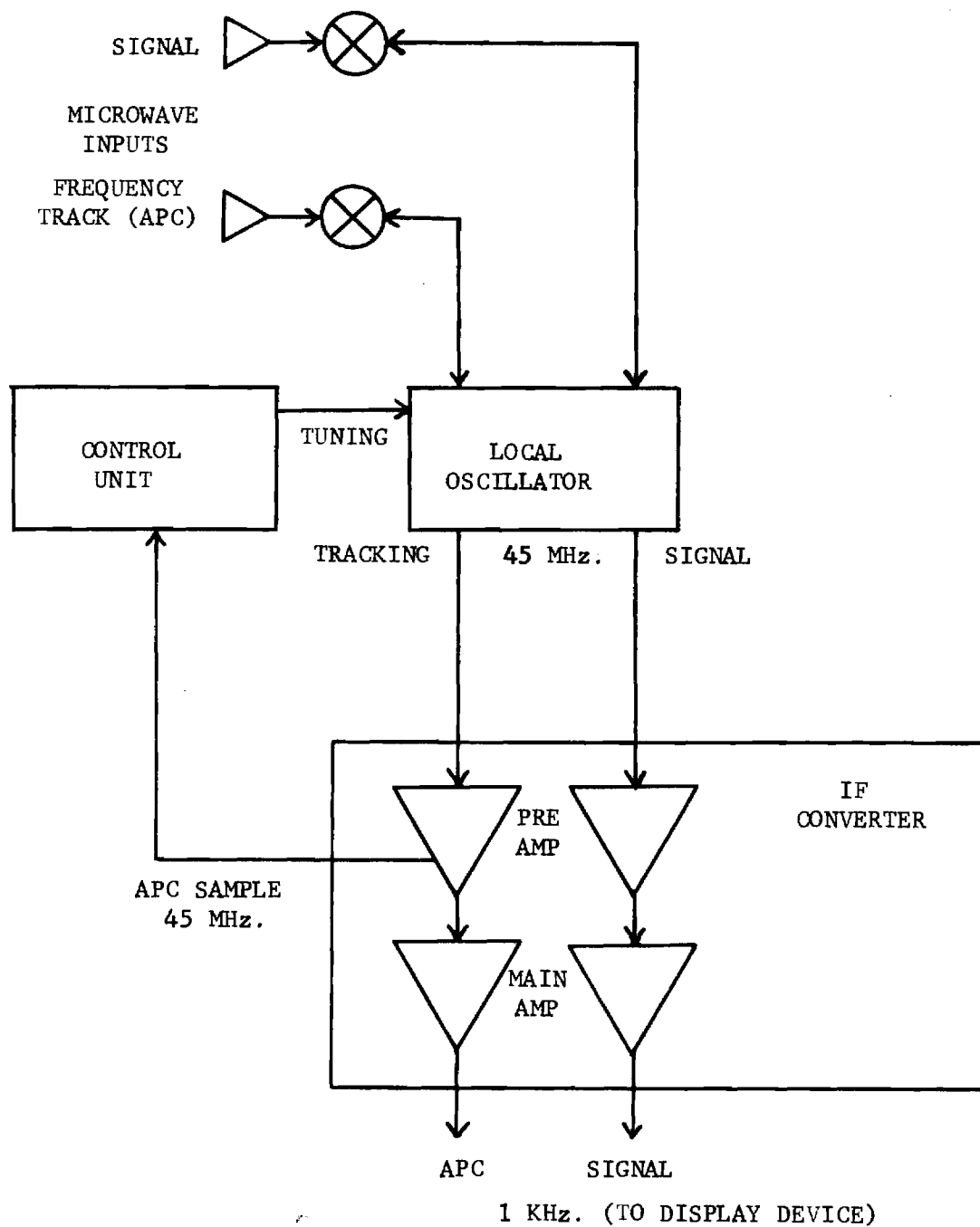


Figure 50. Simplified block diagram of Scientific Atlanta Series 1700 Receiver in the two-channel configuration.

TABLE 9  
TYPICAL SERIES 1700 RECEIVER SENSITIVITY

Frequency (GHz)	Signal Channel (dBm)	APC Channel (dBm)
1 to 2	-110	-75
2 to 4	-104	-70
4 to 8	- 98	-65
8 to 12.4	- 94	-60
12.4 to 18	- 90	-55
0.1 to 1	-100	-70

Initially it was assumed that the phase measurement system would employ a direct data link between the receiving and transmitting sites. The purpose of the data link would be to transmit off/on and frequency selection commands from the master system control facility at the receiving site to the transmit site. The commands would, of course, have to be correlated with test antenna position for data recording at the desired spatial positions. Under operator and software control, the receiving site minicomputer would generate these commands for transmission over a standard telephone line. This telephone line could be either a direct hookup or a dialed connection through telephone company switching equipment. Since a telephone line data link may be expensive or unpractical at certain remote locations, the group delay measurement system which is proposed does not require a data link.

The signal source shown in Figure 45 has the capability of being commanded to any one of 1000 discrete frequencies with a 12-line BCD input from the programmable frequency stabilizer. This 1000 different frequencies capability is more than adequate for any bandwidths under consideration on this program. For example, in a 2-4 GHz system, frequency steps each 2 MHz across the entire range is possible with 1000 selection. If finer resolution than 2 MHz is required for special applications, the total frequency coverage can be reduced accordingly so that the total number of discrete frequency samples is limited to 1000. For example, at a frequency step of 1 MHz, the total frequency range would be limited to 1000 MHz (1 MHz/step x 1000 steps).

The programmable terminal generates a pre-selected series of BCD words which correspond to the desired test frequencies. Flexibility in

setting the step rate (speed) is desirable, and implementation of this feature should be investigated during hardware design. The operator enters data for control of the frequency step size and rate. Parameters which are under operator control include time between successive cycles of the word sequences, dwell time at each digital word, and range of the digital words. In terms of the microwave source output, these parameters would correspond to frequency rep rate, time at each frequency sample point, total frequency sample points, and total frequency range. Ideally, these parameters would be settable by the operator via a keyboard, or some other equally convenient means.

In addition to the above considerations relative to a "free-running" system, RF transmission must be coded to indicate the beginning of each new frequency-step cycle so that data recording at the receive site can be timed to occur at the proper intervals. This timing can perhaps be accomplished by sensing at the receive site the beginning of each RF cycle, in a manner similar to that used on the Hybrid system.

Operation of the system might proceed as follows. Test frequencies are selected by an operator and entered at the keyboard of the programmable terminal. These stored frequency words are then passed sequentially, with appropriate time delays between words, to the microwave frequency stabilizer. The stabilizer calculates the required reference frequency and programs the synthesizer to that frequency. The stabilizer also programs the microwave sweep generator to the approximate microwave frequency. This approximate frequency is then further tuned and phase locked to the exact microwave frequency by mixing with a harmonic of the synthesizer frequency. Phase lock verification is provided to the terminal. After a suitable



time delay (10-50 msec) for phase measurement at the receive site, a new frequency word is entered into the stabilizer and the above described process repeats. Meanwhile, the stabilized RF output from the sweeper is modulated with a 5 MHz signal which is phase locked to WWV. This modulation produces an RF carrier and two phase coherent sidebands at the RF  $\pm$  5 MHz. A final TWT amplifier raises the signal to the desired power level before radiation.

Receive site operations are under control of the on-site minicomputer. The minicomputer controls the operation of the receive site so that phase and amplitude measurements are made at the desired frequencies and test antenna spatial positions. The receive site operator enters the measurement frequencies and the test antenna spatial positions into the computer; thereafter, operation of the receive site sub-system is automatic until the set of measurements is completed and/or the operator enters new test data. With regard to spatial position, the digital comparator provides a means of closing the analog servo system with a digital command. The digital comparator thus allows the test antenna positioner to be controlled by the computer. The comparator provides a dc output (for positioner control) which is proportional to the difference between the computer command and the actual antenna position as provided from the digital display unit. When the correct test antenna position is reached, the computer is given a ready command so that measurements may begin. Meanwhile, the transmitter is cycling through the range of test frequencies. The computer monitors the frequency data from the receiver, and the first time the minimum test frequency is reached, the sideband differential phase and the amplitude data are measured and read into memory along with the test antenna position

and frequency. The transmitter steps to the next test frequency, until the whole frequency range (say 2.0 GHz to 3.0 GHz) has been covered. The computer then provides a new position command, and the above described process repeats until data at all the desired spatial positions have been recorded. Data from computer memory is dumped on magnetic tape at appropriate intervals. Amplitude data at any one of the test frequencies can be selected for processing and display on the pattern recorder.

It appears that with frequency data available to the computer in real time, implementation of independent free-running transmit and receive sites may not present any unusually difficult technical problems. However, it will be necessary to use a sufficiently low data rate to insure that frequencies are stabilized and the phase data has reached its final value before reading data into the computer. The maximum data rate will be on the order of one test frequency each 100 msec.

#### D. DATA RATES AND DATA RECORDING CONSIDERATIONS

As indicated above, the data measurement rate for the proposed group delay system is limited by both the required receiver measurement and the time required for the transmitter to stabilize after each frequency step. This sub-section will address the effect of the receiver and other band-limiting components on system data recording rates, and typical operational system parameters and data recording considerations will be discussed.

A typical test scenario would be for the test antenna to slowly rotate over the desired angular increment while the test frequency is repetitively stepped through the measurement range. To initiate a data recording sequence, the receive site operator enters into the computer such parameters

as: (1) spatial antenna pattern cut, (2) data to be recorded (phase and/or amplitude), (3) antenna rotation rate or step increment, (4) spatial sample increments, (5) frequency step rate, (6) frequency increments, and (7) frequency component (if any) to be plotted in real time on the pattern recorder. The computer generates initial antenna position data which are fed through the digital comparator to initiate the antenna movement. As the antenna rotates, position data are continuously received by the comparator from the encoders on the positioner. As each of the pre-set angular increments is reached, the comparator notifies the computer which generates the appropriate commands so that a set of phase, frequency, and amplitude data is recorded at prescribed angular increments over the full scan sector.

It may be seen that for broadband antenna measurements, there are two sample variables to be considered. These variables are spatial coordinates and frequency. Basically, there are two sampling approaches which should be considered. With the first approach, the antenna under test would be slowly and continuously rotated. At specified angular positions, the test signal would be rapidly stepped through the frequency range of interest. The frequency step rate should be such that the antenna could be considered essentially stationary over the frequency range. With the second approach, the test antenna would be incrementally stepped to a new position and remain stationary while the test signal is stepped over the desired frequency range. The relative desirability of the two approaches depends on the test antenna size and the required accuracy of the data. Since test signal sampling is required for either of these approaches, this sampling requirement will be discussed first.

The upper limit of the frequency track rate for the Series 1700 receiver is specified at 10 MHz/msec. The frequency scan rate of the sweep oscillator is specified in terms of the minimum time required to sweep over the full band. Thus, scan rate depends on bandwidth. For the 1-2 GHz octave, the maximum scan rate is 100 MHz/msec. For the 12.4-18 GHz interval, maximum scan rate is 560 MHz/msec. For other frequency ranges, the maximum scan rates are intermediate between these limits. Thus, the 10 MHz/msec receiver limit must be maintained for the receiver to track. After the transmitter is commanded to step to each new frequency, approximately 50 msec are required to insure phase lock of the test frequency.

Since many microwave components, including antennas, have bandwidths of at least 100 MHz, consider frequency sampling at 100 MHz intervals for illustration. At a frequency step rate of 10 MHz/msec, a 100 MHz frequency sampling interval implies a minimum 10 msec between the individual samples. However, about 50 msec intervals are required for transmitter phase locking and about 50 msec are required for phase measurement. Thus, 100 msec is required for each test frequency. This implies a basic data rate of 10 Hz. Measuring and recording frequency, phase, and amplitude at each sample point increases the total data rate to 30 Hz, and requires recording a data word each 33 msec. This data rate is easily accommodated by most minicomputers on the market today. Alternately, at this data rate, the data could be recorded directly on magnetic tape affording increased data storage capacity. Sampling every 100 MHz over a 1 GHz range results in 10 frequency sample points. Recording frequency, phase, and amplitude at each sample point would require storing 30 data words for each spatial point. (With proper software "bookkeeping," spatial angle need be recorded

only at the beginning of each frequency sweep.)

The most appropriate spatial sampling interval will depend on the test antenna size and the desired accuracy. For illustration, consider an antenna having a 3 dB beamwidth of one degree for which measurements are to be made over a 1 GHz range. (A 1 degree 3 dB beamwidth requires approximately a 25 foot diameter aperture at the S-band frequency of 3 GHz.) A capability to record pattern cuts over  $\pm 180$  degrees is required. The optimum positioner scan rate is primarily dependent on two competing factors. These are the desirability of minimizing the total pattern recording time (fast scan) and of minimizing movement of the test antenna during a measurement interval (slow scan). Examination of these factors leads to selection of a relatively slow antenna scan rate on the order of 0.10 deg/sec. Thus, 60 minutes are required to record an entire  $\pm 180$  degree pattern. With the previously considered frequency sampling interval of 100 MHz and with 100 msec between samples, one second is required to cover a 1 GHz frequency range. During this time at an antenna sweep rate of 0.10 deg/sec, the antenna would sweep through 0.10 degree. This much movement would amount to one-tenth of the beamwidth, and the resulting data uncertainty would be tolerable in most regions of the pattern. To achieve greater accuracy, it would be required to reduce antenna scan rate. For regions in which high accuracy is desired, the scan rate for this example could be reduced to about 0.010 deg/sec. The resulting uncertainty would be 0.010 deg which is comparable to the readout accuracy of typical positioners so that a slower antenna scan rate would not be beneficial in improving data accuracy.

For a 1 degree total half-power beamwidth, the first nulls would

occur near approximately  $\pm 1.3$  degree off beam center, and successive nulls would occur at further 1 degree increments. If 10 sample points per side-lobe provides sufficient resolution, a spatial sample is required each 0.1 degree; because the null-to-null width of the main beam is about 2 degrees, 20 sample points to define the main beam are necessary. At the previously assumed positioner rotation rate (0.10 deg/sec), 0.1 degree spatial increments occur every second. Since one second is required to cover the frequency measurement range, the frequency sweep rate, spatial sample rate, and positioner scan rate are all compatible. The above discussion illustrates the type of tradeoff analysis which is required for a given antenna and measurement frequency range.

For small antennas which can be conveniently step scanned and stopped for data recording, the recording time per pattern may perhaps be reduced to less than 60 minutes. A programmable positioner controller is available which can provide scan increments as small as 0.1 degree (S/A Model 2004 Plus Model 4561 Servo Repeater-Converter). Based on antenna size (and beamwidths) and type of positioner available, the stepped-scan approach should be examined for specific applications. In addition, it may be necessary to use a stepped scan if phase and/or amplitude are rapidly changing as spatial position or frequency is changed.

The above discussions have addressed both the spatial and frequency domain sampling requirements of the phase and amplitude measurement system. The following paragraphs will address data handling and analysis. This discussion will include such ideas as amount of data to be handled, how the data is conditioned before recording, the mechanics of data recording, and the analysis of data for such purposes as pulse distortion prediction.

As discussed above, a typical data set would consist of frequency, amplitude, and phase data points at each of 10 frequencies for each spatial sample point of an antenna pattern cut. Thus, each spatial point contributes 30 data words. Spatial sampling each 0.1 degree for a full 360 degree pattern cut requires 3,600 spatial samples, or 108,000 data words per 360 pattern. Since minicomputers do not have this much available storage, some accommodations must be made. The problem is further compounded by the requirement for approximately 4k of storage for control software. As a minimum, consider about 20k of computer memory plus some auxiliary magnetic tape storage. Now, since each spatial point provides 30 data words, each 4k computer memory block could store data for over 100 spatial positions before dumping onto auxiliary storage. With Direct Memory Access, present minicomputers can dump 3000 data words in about 10 msec. Thus, computer storage can be easily cleared between adjacent spatial samples (one second apart). Tape storage media of practically any desired capacity are available. For example, a cassette recorder is currently used on the automated Georgia Tech near field range to provide over 130,000 words of auxiliary storage. Thus, this type of cassette can store complete phase, amplitude, and frequency data each 0.1 degree over a full 360 degree pattern cut, if desired. Of course, a reel-to-reel magnetic tape recorder (such as the RADC-owned HP 2020E) can provide even greater storage; 75-100 full pattern cuts on one reel of high-quality magnetic tape.

Antenna diagnostics which require handling a large amount of data must be performed by a large general purpose off-site digital computer. Tapes recorded on site by such recorders as the HP 2020E digital tape

recorder can be read directly by most computers, including the Honeywell 600-line, which would be suitable for off-site diagnostics. However, since all of the data which could possibly be recorded for a single antenna will not be needed for any one given diagnostic, some on-site analysis is possible with certain minicomputer configurations. For time domain pulse distortion analysis (see Section IV), approximately 32k words of storage are required for the program. Pulse distortion analysis would likely require only main beam phase and amplitude data at the various frequency sample intervals (for example, each 100 MHz over a 1 GHz bandwidth). Thus, if the on-site computer storage is at least 43k, on-site pulse diagnostics is practical. Core storage of most minicomputers can be varied between 16k and 64k since core storage options in 8k or 4k blocks are offered. The pulse distortion program can be recorded on tape and read into the computer and executed after the required data have been recorded.

Average pattern information over less than a full 360 degree sector will frequently be of interest. Furthermore, only the amplitude data are required to obtain average pattern information. Thus, if average pattern information over a 90 degree sector, and a 1 GHz bandwidth, is desired at spatial sampling increment of 0.1 degree and at a frequency sampling increment of 100 MHz, 9k data points must be processed. Program storage for average pattern calculation should require less than 32k words of storage so that if 42k words of core storage are available, both main beam pulse distortion and limited average pattern analysis can be accomplished on site.



## E. TEST ANTENNA SIZE CONSIDERATIONS

At various times on both this and the preceding study, a desired capability to measure antenna patterns on ranges "up to 7000 feet" has been discussed. Since a 7000-foot range limits the maximum test antenna diameter at 15 GHz, for example, to about 15 feet, the question of test antenna size limitations has arisen. This sub-section addresses this question and presents tabulated data which show that for all practical purposes, the proposed measurement system in itself imposes no limitations on test antenna size.

Table 10 shows the maximum antenna diameter which can be tested, within the far field restriction, at various test ranges, as a function of frequency. Here the far field is taken as  $2D^2/\lambda$  where D is the maximum aperture diameter and  $\lambda$  is the wavelength at the test frequency. At 15 GHz, for example, the maximum test antenna diameter varies from 13 feet on a 5000 feet test range to 30 feet on a 5 mile test range. The table also presents two other parameters of interest. First, the expected antenna gain for that antenna diameter and frequency, assuming a 50% efficiency, is given. Next, the free space attenuation  $(4\pi r/\lambda)^2$  at a given range r and frequency is presented.

From Table 10 and two basic assumptions concerning the transmitter power level and the transmit antenna gain, the data of Table 11 can be derived. The two assumptions are a transmitter power level of 10 watts and a transmit antenna gain of 30 dB. As will be shown, these are not critical assumptions; they represent typical values applicable to the system under study. For convenience in calculating the received power level, free space loss as a function of range and frequency is also

TABLE 10  
ANTENNA RANGE PARAMETERS AT VARIOUS DISTANCES

Maximum Antenna Dia. (ft)	Gain @ 50% Eff, dB	Free Space Loss, dB	Frequency, GHz
Range = 1 mi.			
13	53	120	15
16	51	117	10
23	48	111	5
29	46	106	3
Range = 7,000 ft. (1.33 mi)			
15	54	123	15
18.5	52	119	10
26	49	113	5
34	47	109	3
Range = 10,000 ft. (1.93 mi)			
18	56	126	15
22.5	54	122	10
32	52	116	5
40	49	112	3
Range = 26,400 ft. (5 mi)			
30	60	134	15
36	58	131	10
51	55	125	5
66	53	120	3

TABLE 11

## RECEIVED SIGNAL LEVEL FOR MAXIMUM TEST ANTENNA DIAMETER

Freq., GHz	Space Loss, dB	Max. Test Antenna Gain, dB	Received Power, dBm
Range = 1 mile			
15	120	53	+3
10	117	51	+4
5	111	48	+7
3	106	46	+10
Range = 7,000 ft. (1.33 mi)			
15	123	54	+1
10	119	52	+3
5	113	49	+6
3	109	47	+8
Range = 10,000 ft (1.93 mi)			
15	126	56	0
10	122	54	+2
5	116	52	+6
3	112	49	+7
Range = 26,400 ft. (5 mi)			
15	134	60	-4
10	131	58	-3
5	125	55	0
3	120	53	+3

## Notes:

1. Transmitter Power = 10 watts (40 dBm).
2. Transmit Antenna Gain = 30 dB.

repeated in Table 11. The last column of Table 11 gives the received signal level on the main beam of the test antenna as a function of frequency and range. Since the sensitivity of the S/A Series 1700 receiver is at least -90 dBm, it may be seen that there is a considerable power margin, even under the worst conditions (15 GHz and 5 mile range). Allowing for pattern recording down to a level 40 dB below the peak of the main beam, the transmitter power/transmit antenna gain combination has a safety margin of at least 46 dB under the assumed conditions. Thus transmitter power could be reduced and test range could be increased if desired.

It may be concluded then that with 1-10 watts of transmitter power, a transmit antenna gain of 30 dB, and a receiver sensitivity of at least -90 dBm, the proposed measurement system introduces no limitations on the maximum size of antenna which can be tested.

## SECTION IV

### PULSE DISTORTION ANALYSES

#### A. INTRODUCTION

The ability to reliably and efficiently predict the performance of high resolution, broadband pulsed radar systems which employ very narrow pulses is mandatory if the many potential benefits of broadband radars are to be fully realized. In particular, the degradations in range resolution and range accuracy caused by the non-ideal frequency response of antennas must be known so that realistic performance predictions can be made and operational criteria can be established. Degradations in rise time and pulse width, as well as the possible appearance of time sidelobes, result from pulse distortion. The severity of the distortion depends on both the frequency spectrum of the incident pulse and the complex voltage transfer function of the antenna system (and/or other transmission line components). Therefore, analytical techniques are needed which accurately predict the distortion effects for arbitrary time pulses and transfer functions. Such analyses are possible, and when based on a specialized discrete Fast Fourier Transform, rapid computation of pulse distortion effects via a digital computer is a practical technique. In this section, theoretical aspects of the Fourier Transform computational method are briefly discussed, a computer program for calculating pulse distortion is described, and computations of the pulse distortion of three selected narrow pulses are presented and discussed. The analyses and results presented in the section are presented from the viewpoint of pulse transmission. Descriptive terms such as generated pulse and radiated pulse are therefore used. However, the method also applies to pulse reception.

## B. THEORETICAL CONSIDERATIONS

### 1. Fourier Transform Techniques

The distorted pulse waveforms can be computed from the measured complex voltage transfer functions and the frequency spectrum of the original pulses via Fourier Transform techniques [4]. The specific application of interest here is the calculation of antenna-caused pulse distortion in broadband radar systems. Since the antenna voltage function is measured as a function of a spatial angle, the pulse distortion effects can be computed as a function of spatial angle. In particular, the relation between the amplitude of the radiated pulse (in the time domain), the pulse's frequency spectrum, and the complex voltage transfer function of the antenna may be expressed analytically as

$$A(\theta, t) = \frac{1}{2\pi} \int_{-\infty}^{\infty} g(\theta, \omega) h(\omega) e^{j\omega t} d\omega, \quad (3)$$

where

$A(\theta, t)$  = radiated pulse at spatial angle  $\theta$ , as a function of time,

$g(\theta, \omega)$  = complex antenna voltage transfer function at spatial angle  $\theta$ , as a function of frequency,

$h(\omega) = \int_{-\infty}^{\infty} H(t) e^{-j\omega t} dt$  = the frequency spectrum of the generated pulse, and

$H(t)$  = generated pulse in the time domain.

Consider the direct evaluation of the integral of Equation (3). As indicated earlier, this is the Fourier inversion integral. Note that the antenna gain function must be specified for both negative and positive angular frequencies  $\omega$ . This is no problem for realizable antennas. In particular, consider the antenna gain to be specified by the equation

$$g(\theta, \omega) = |g(\theta, \omega)| e^{j\phi(\omega)}. \quad (4)$$

THIS PAGE INTENTIONALLY LEFT BLANK.

The Fourier integral then becomes

$$A(\theta, t) = \frac{1}{2\pi} \int_{-\infty}^{\infty} h(\omega) |g(\theta, \omega)| e^{j\phi(\omega)} e^{j\omega t} d\omega . \quad (5)$$

The above integral can be evaluated if the pulse spectrum and complex gain function are specified. However, because of the rapid variation of the  $\exp(j\omega t)$  term and the necessity for integrating over a large range in  $\omega$ , the numerical evaluation of the integral is very tedious if a direct integration procedure is employed. Use of the Fast Fourier Transform (FFT) on a digital computer allows for efficient evaluation of the  $\exp(j\omega t)$  term. The problem of evaluating the integral over a wide frequency range can be reduced by making a transformation in frequency. This frequency transformation amounts to a conversion of the carrier frequency  $\omega_0$  to a frequency specified by

$$\omega^- = \omega - \omega_0 \text{ for } 0 < \omega < \infty \quad (6)$$

and

$$\omega^+ = \omega + \omega_0 \text{ for } -\infty < \omega < 0 . \quad (7)$$

The transform may then be written as the sum of two integrals with limits of  $-\infty$  to  $\omega_0$  and of  $-\omega_0$  to  $+\infty$ . In the usual case, the total bandwidth  $\Delta\omega$  of the signal spectrum will be much less than the carrier frequency  $\omega_0$ , and a reduction in integration limits can be realized. Since the integrals yield no contribution for frequencies  $\omega$  outside the band specified by  $-\frac{\Delta\omega}{2} \leq \omega \leq \frac{\Delta\omega}{2}$ , this leads to a savings in computational time.

Consider an idealized rectangular period pulse train of pulse width  $\tau$  and pulse reception time  $T$  which amplitude modulates an RF carrier of frequency  $\omega$ . The envelope of the spectral (frequency) content of this

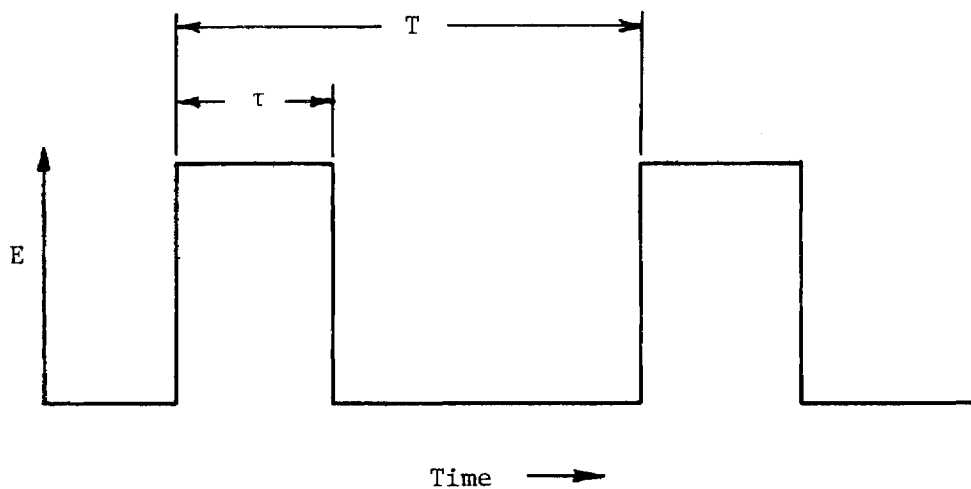


waveform is the well known  $\frac{\sin(\omega\tau)}{\omega\tau}$  represented in Figure 51. If the pulse width is one nanosecond, the total width of the main lobe is 2 GHz. Each spectral line is separated by the pulse repetition frequency and the main lobe is centered about the carrier frequency. Now, when this waveform passes through a non-ideal bandlimited device, such as an antenna, the relative amplitudes and phases of the spectral components will be modified. If the complex gain of the antenna is known, the resulting relative amplitudes and phases can be found by multiplying the original spectral content by the complex gain (transfer) function. The resulting modified spectral content is then transformed back to the time domain and envelope detected to obtain the distorted pulse shape. Care must be taken to insure that the complete time domain information is obtained in order to examine the time sidelobes which may result from the antenna bandpass characteristics.

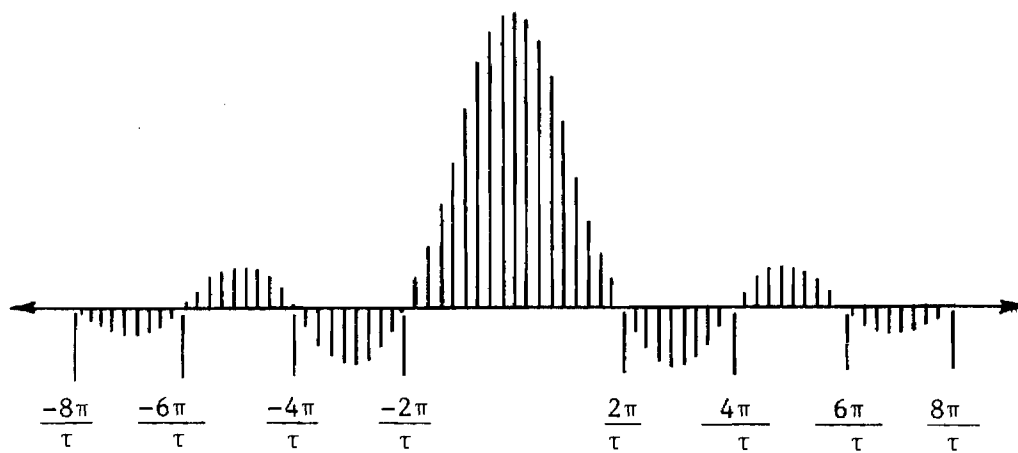
## 2. Typical Distortion Effects

The distortions which occur in the radiated pulse can arise from two mechanisms, which are (1) a non-linear phase shift as a function of frequency, and (2) a non-consistent amplitude transfer function. In the general case, both mechanisms may be present and, hence, contribute to distortion. The distortion effects which occur typically cause increased rise and fall times, a reduction in peak amplitude, and the appearance of time sidelobes. Additionally, the distorted pulse may also exhibit noticeable asymmetry. Moreover, the antenna introduces a time delay which depends solely on the linear component of the phase shift.

Consider first a complex transfer function which has a non-linear phase shift response and an amplitude function which is constant and equal to 1 over a wide frequency band. The resulting distorted pulse envelope as given



(a) Periodic Rectangular Pulse Train



(b) Resultant Spectrum of a Carrier Amplitude Modulated with a Rectangular Pulse.

Figure 51. Time and frequency domain correspondence for rectangular pulse train.

by Equation (5) becomes

$$A(t) = \frac{1}{2\pi} \int_{-\frac{\Delta\omega}{2}}^{+\frac{\Delta\omega}{2}} h(\omega) e^{j\phi(\omega)} e^{j\omega t} d\omega . \quad (8)$$

Before describing a computer program using the Fast Fourier Transform to calculate pulse distortion effects, i.e.,  $A(t)$ , exactly, the characteristics of  $A(t)$  will be examined qualitatively via elementary statistical techniques [5]. This statistical examination is presented solely to gain insight into the relative causes of pulse distortions. Conceptually, the phase-response curve is regarded as one particular member of an ensemble of random phase response curves. The ensemble of random curves to which the actual curve belongs is defined by two statistical parameters, namely, the slope of the least squares line through the actual phase response curve and the standard deviation about the least squares line. A hypothetical phase response curve and its associated statistical parameters are shown in Figure 52. These two statistical parameters define a Gaussian probability density function which is used to compute the statistical average value and standard deviation of  $A(t)$  via approximate integrations extending over the randomized variable  $\phi(\omega)$ . The statistical average value,  $\overline{A(t)}$ , and standard deviation,  $\Delta A$ , of  $A(t)$  are related to the slope of the least-squares straight line through the phase response data and the standard deviation of the data about the least squares line. These relations are expressed by Equations (9) and (10),

$$\overline{A(t)} \approx e^{-\frac{1}{2}\sigma^2} \left[ \frac{1}{2\pi} \int_{-\frac{\Delta\omega}{2}}^{+\frac{\Delta\omega}{2}} h(\omega) e^{j\omega t(t+b)} d\omega \right], \quad \text{and} \quad (9)$$

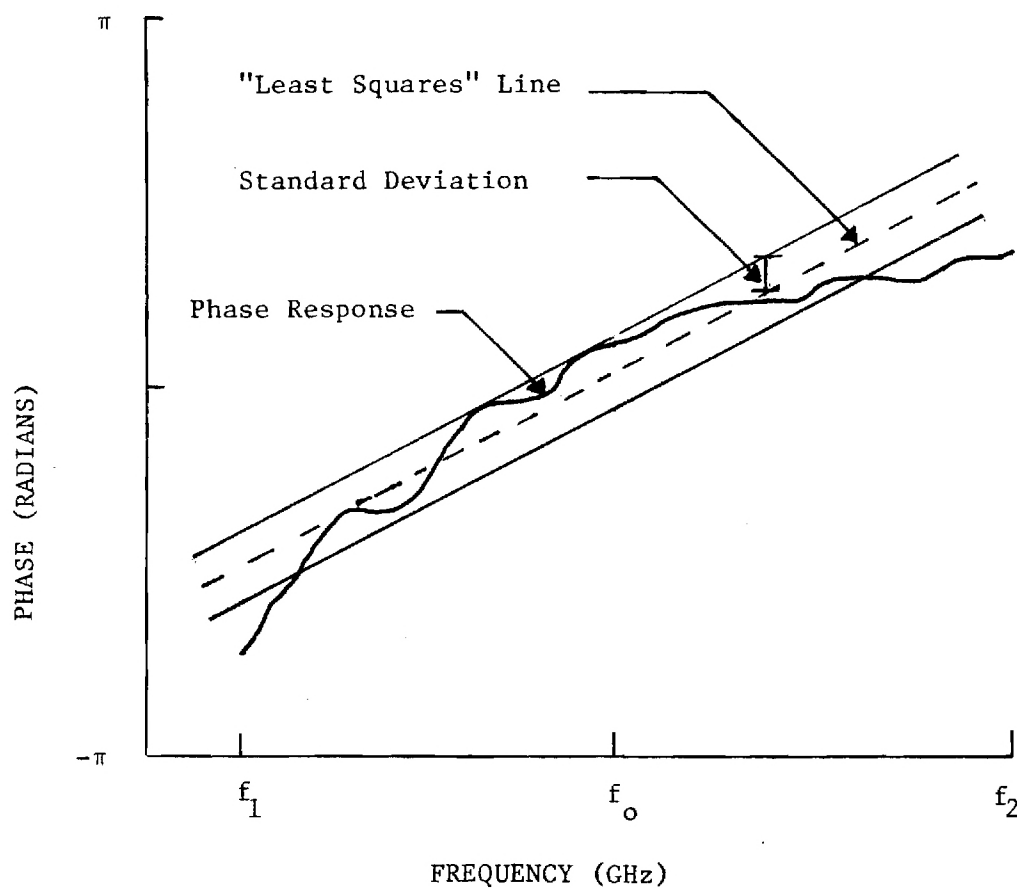


Figure 52. Sketch depicting the phase response as a function of frequency for a hypothetical system and the relevant statistical parameters utilized in statistical analysis of pulse distortion effects.  $f_0$  is the fundamental frequency of the incident pulse spectrum, and  $f_1$  and  $f_2$ , respectively are the lower and upper limits of the pulse spectrum.

$$\Delta A \approx (1 - e^{-\sigma^2})^{1/2} \left[ \frac{1}{2\pi} \int_{-\frac{\Delta\omega}{2}}^{+\frac{\Delta\omega}{2}} |h(\omega)|^2 d\omega \right]^{1/2}, \quad (10)$$

where

$b$  = slope of least-squares straight line,  $\frac{d\phi}{d\omega}$ , in nanoseconds, and

$\sigma$  = standard deviation of phase data about the least-squares lines, in radians.

The statistical average pulse envelope  $\overline{A(t)}$  is the weighted average of all of the possible individual distorted pulse envelopes produced by each of the individual phase response curves which constitute the ensemble. The standard deviation  $\Delta A$  defines the limits above and below the average pulse envelope within which 68 percent of all individual distorted pulse envelopes would lie. In the context of the present application,  $\overline{A(t)}$  can provide information concerning the amplitude and time shift of the received pulse. Similarly,  $\Delta A$  can provide information concerning changes in the shape of the pulse envelope. Consequently, the distortion effects caused by a non-linear phase response may be discerned, at least qualitatively, from Equations (9) and (10). Specifically, the presence of the multiplicative exponential factor,  $e^{-1/2\sigma^2}$ , in Equation (9) implies that the received pulse is reduced in amplitude, and the integral implies that the pulse is delayed in time by an amount  $(b)$  nanoseconds. Equation (10) implies that energy can be present at times both preceding and following the shifted incident pulse, i.e., time sidelobes can occur. Since total energy must be conserved, the reduction in amplitude must be accompanied by spreading, or broadening of the pulse envelope. This fact, along with the amplitude deviations,  $\Delta A$ , implies that the rise and fall times are increased.

The magnitude of the distortions (amplitude reduction, time sidelobes, and increased rise and fall time) depend on the magnitude of the phase shift standard deviation,  $\sigma$ . The magnitude of the phase shift standard deviation depends on the non-linearity of the phase shift. If the phase shift were exactly linear,  $\sigma$  would be zero and Equation (9) reduces to the expression for an undistorted shifted pulse while Equation (10) becomes zero. Thus, there would be no distortion, in agreement with both theory and observation.

The asymmetry which frequently occurs in the resulting pulse can be primarily attributed to the unequal average delay times at the frequencies above and below the fundamental frequency. For the present example, it may be seen that the average delay times for the frequency components above and below the fundamental frequency in Figure 52 are different because of the slope of a least-squares line through the lower frequencies is greater than the slope of a least-squares line through the upper frequencies. Additionally, the standard deviation at the lower frequencies is greater than the standard deviation at the upper frequencies. Since the upper frequencies have a smaller average delay time than the lower frequencies and also have the smaller standard deviation, the leading edge of the radiated pulse would be expected to have less distortion than the trailing edge. Consequently, in this case the radiated pulse would exhibit asymmetry.

As mentioned previously, a non-constant amplitude response can also induce distortions similar to those produced by non-linear phase shift. (However amplitude variations produce no time shift.) Amplitude effects are always present in varying degrees due to the limited bandpass of real radar systems. Variations in the amplitude response within the frequency band of the system induce distortion. A 10-dB "hole" in the amplitude response can have

dramatic effects if the hole occurs near the fundamental frequency of the pulse spectrum. On the other hand, the effects may not be noticeable if "holes" occur at frequencies corresponding to null locations in the spectrum or at far-removed spectral lines.

### C. COMPUTER CALCULATIONS

Efficient computation of pulse distortion is possible through the use of the Fast Fourier Transform. A computer program has been developed to compute the distorted pulses for arbitrary pulse shapes and complex transfer functions. The program was used to calculate the distorted pulses for three pulses of 5, 3, and 1 nanosecond 3-dB pulse width for a specific kind of complex transfer function. Computer graphics were used to display the pulses. The Fast Fourier Transform technique is briefly discussed below, followed by a description of the computer program. Finally, the computed pulse distortions are presented and discussed.

#### 1. The Fast Fourier Transform

When the waveform is sampled at discrete frequencies, or the system is to be analyzed on a digital computer, the discrete Fast Fourier Transform must be used in lieu of the continuous Fourier Transform. The Fast Fourier Transform (FFT) is simply an efficient method for computing the discrete Fourier Transform. The discrete Fourier Transform pair that applies to sampled versions of the continuous transform sampled at N discrete points can be written in the forms

$$A(t_k) = \frac{1}{N} \sum_{\ell=0}^{N-1} D(f_{\ell}) (W_N)^{\ell k} \quad , \quad (11)$$

and

$$D(f_\ell) = \sum_{k=0}^{N-1} A(t_k) (W_N)^{-\ell k} \quad (12)$$

for  $\ell = 0, 1, \dots, N-1$ , and  $k = 0, 1, \dots, N-1$ ,

where

$A(t_k)$  = amplitude of the envelope of the pulse at time  $t_k = k \left(\frac{T}{N-1}\right)$ ,  
where  $T$  is the time window,

$D(f_\ell)$  = complex frequency spectral component of  $A(t)$  for frequency  
 $f_\ell = \ell \left(\frac{f_s}{N-1}\right)$ , where  $f_s = \left(\frac{1}{T}\right)$ , and

$W_N = \exp [j(2\pi/N)]$ .

Since the time pulse represented by Equation (11) is real, the real part of the frequency spectrum,  $D(f_\ell)$ , is symmetric about the "folding" frequency,  $(f_s/2)$ , and the imaginary part is antisymmetric. Consequently, the Fourier coefficients which lie between  $N/2$  and  $N-1$  correspond to negative frequency components, while the first  $N/2$  terms correspond to positive frequency components, in analogy to the continuous case previously discussed.

Whereas a direct evaluation of either Equation (11) or Equation (12) would require nearly  $N^2$  complex multiply and add operations, FFT algorithms have been previously derived which reduce the number of computations to  $(N/2)\log_2(N)$  complex multiplications, additions, and subtractions, where  $N = 2^M$ . Figure 53 shows a comparison of the number of operations required for computing Fourier Transform directly and by using the FFT. As seen in the figure, a savings in operations of more than 200 to 1 is achieved for  $N = 1024$  sample points. The dramatic reductions in computational operations provided by the FFT are achieved by exploiting the rapid variations of the exponential function and a judicious ordering of the arithmetic operations. The derivation of the FFT equations is straightforward but tedious and



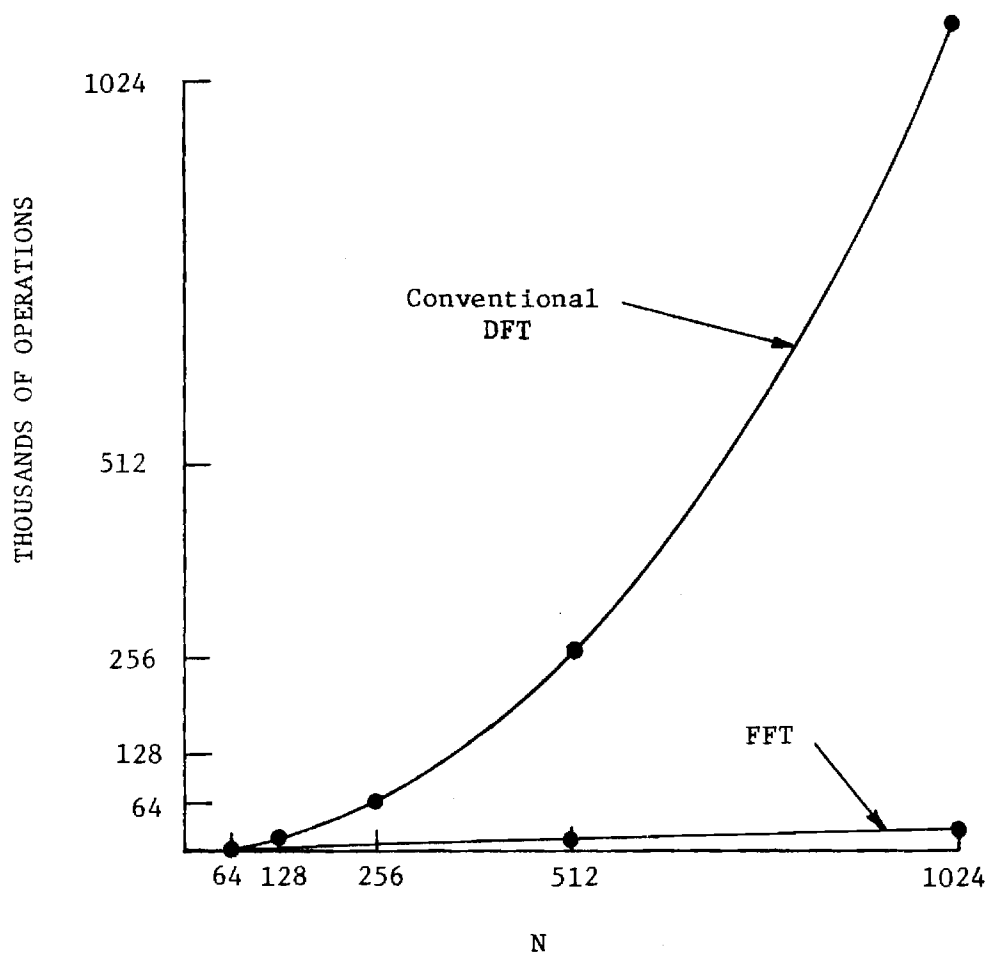


Figure 53. Number of operations required for computing a discrete Fourier Transform by the conventional DFT and the FFT.

will not be reproduced here since rigorous presentations exist in the literature [6].

The accuracy of the FFT is affected by the sampling rate and the type of data "window" employed in the computations. The sampling rate should meet or exceed the Nyquist criteria. That is, the signal to be transformed should be sampled at a rate at least twice as high as the highest significant frequency component present. A weighting function should be applied to the data near the ends of the data supply in order to minimize extraneous side-lobe energy. Consequently, cosine-squared leading and trailing edges were incorporated into the data window of the FFT algorithm.

## 2. Description of Computer Program

A flow diagram of the computer program FTRANS is depicted in Figure

54. The various symbols shown in the figure are defined as follows:

IGAM = the integer exponent of 2,

NMAX = number of discrete data points of the complex transfer function,

NFLG = an integer code associated with pulse data,

FUND = fundamental frequency of the incident pulse spectrum, in GHz,

BW = 3-dB bandwidth of incident pulse spectrum, in GHz,

SW = total sample width to be used in frequency domain, GHz,

TPW = total pulse width of incident pulse, in nanoseconds,

SCODE = an integer code associated with time offset,

MAX = number of discrete data points of the incident pulse data,

$\{t, H(t)\}$  = the set of incident time data and pulse data,

$\{f, |g(f)|, \phi(f)\}$  = the set of data for the complex transfer functions,

$h(f)$  = (discrete) frequency spectrum of the incident pulse, and

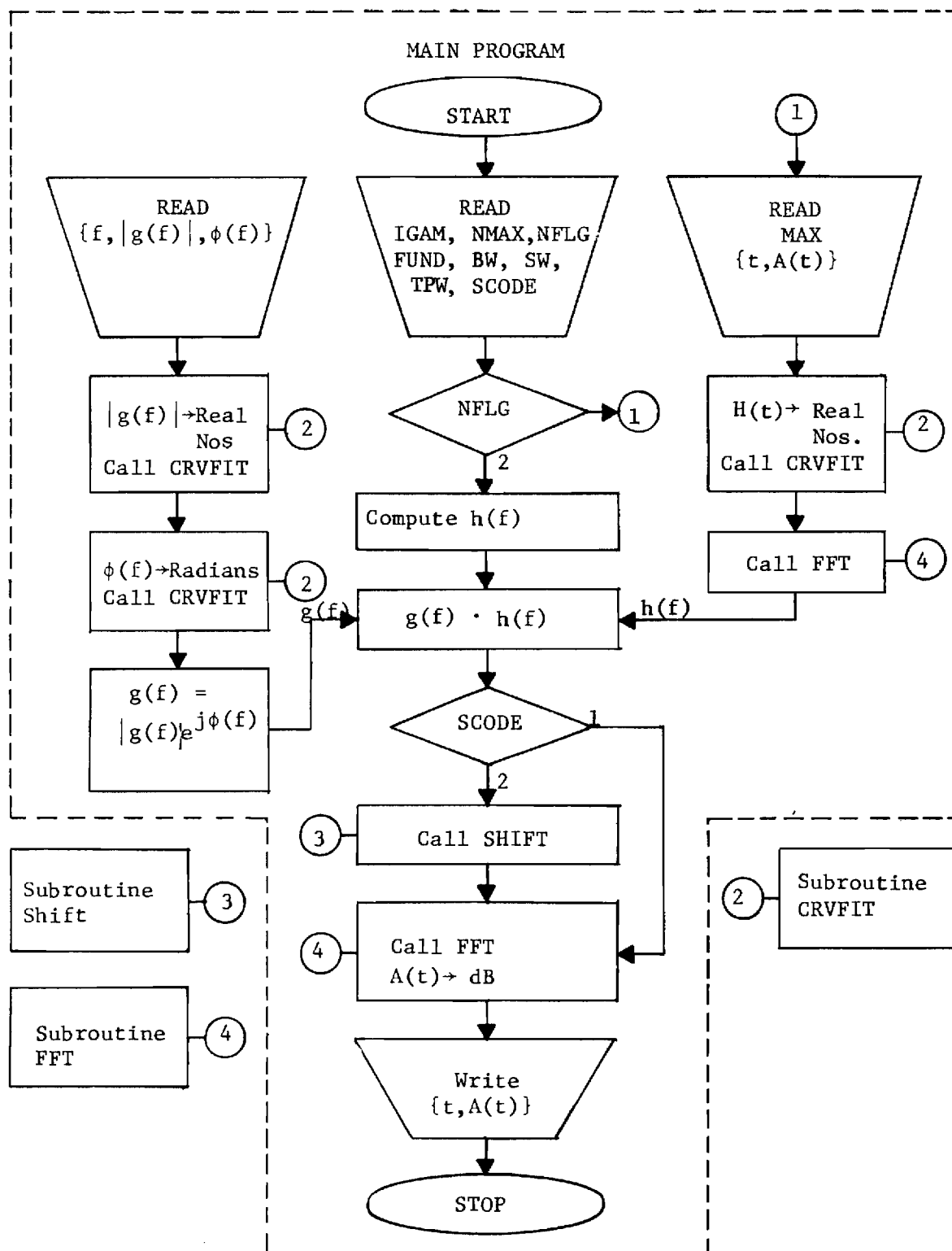


Figure 54. Simplified flow diagram of pulse distortion computer program FTRANS.

$\{t, A(t)\}$  = the set of time data and distorted pulse data.

All of the inputs indicated in the center input block as well as MAX in the right-hand input block are read locally from a teletype terminal or from the card deck. The discrete data sets for the complex transfer function and the incident pulse are read from either FASTRAND files or from card decks. The frequency inputs are in GHz and the time inputs and outputs are in nanoseconds. The amplitude part of the transfer function incident pulse data and the output pulse data are in decibels. The input phase data are in degrees.

As can be seen from the flow diagram, program FTRANS consists of a "main" program and three subroutines designed as CRVFIT, FFT, and SHIFT. The main program accommodates all inputs and outputs, performs necessary decision making processes, converts the input and output frequency and pulse amplitude data to real (linear) numbers, converts the input phase data to radians, and performs the multiplication of the incident pulse frequency spectrum with the complex transfer function. Additionally, if the integer code NFLG equals 2, the main program internally computes the frequency spectrum of an incident "stretched cosine-squared pulse" from analytical equations. (The parameters of the analytical pulse are determined by the input 3-dB bandwidth.) Subroutine CRVFIT performs a linear interpolation of the input data set to derive values of pulse amplitude, frequency amplitude, or phase shift at the discrete times or frequencies, as the case may be, required by the choice of input sample width, SW and IGAM. This is necessary because the input data will not generally be specified at the particular times or frequencies needed by the FFT algorithm. Subroutine FFT, of course, performs an efficient discrete Fourier Transform. Subroutine SHIFT provides a time offset to

counteract the sometimes large time delays which can occur for severely distorted pulses. In particular, SHIFT computes the average time delay induced by the phase data and then shifts the approximate center of these distorted pulses to 15 nanoseconds behind the leading edge of the incident undistorted pulse.

### 3. Computed Pulses

Computer program FTRANS, just previously described, was used to compute the distorted pulse envelope of three different original pulses which have propagated along three different lengths of X-band waveguide. The three different original pulses have initial 3-dB pulse-widths of 5, 3, and 1 nanoseconds, respectively; the rise and fall times (10% to 90% points) of both the 5 nanosecond and the 3 nanosecond pulses are 1 nanosecond, whereas the 1 nanosecond pulse has rise and fall times of 0.5 nanosecond. The family of radiated pulses obtained from these computations provides a useful insight into pulse distortion effects.

The envelopes of the incident pulses have a stretched cosine-squared shape, i.e., a rectangular pulse with cosine-squared leading and trailing edges. Figure 55 is a sketch of the envelope depicting pertinent parameters of the pulse. The frequency spectrum of this pulse can be obtained analytically from the continuous Fourier Transform, and is given as

$$h(\omega) = \left[ \frac{1}{\omega_T^2 - \omega^2} \right] \left[ \frac{\omega_T^2 (T/2) \sin[\omega(T/2)]}{[\omega(T/2)]} - \frac{\omega_T^2 \Delta t_1 \sin(\omega \Delta t_1)}{\omega \Delta t_1} \right. \\ \left. + 2\omega \sin(\omega \Delta t_1) \right] + \frac{2\omega \Delta t_1 \sin(\omega \Delta t_1)}{\omega \Delta t_1}, \quad (13)$$

where  $\omega_T^2 = \left( \frac{2\pi}{T} \right)^2$ , and T is the total pulse width,

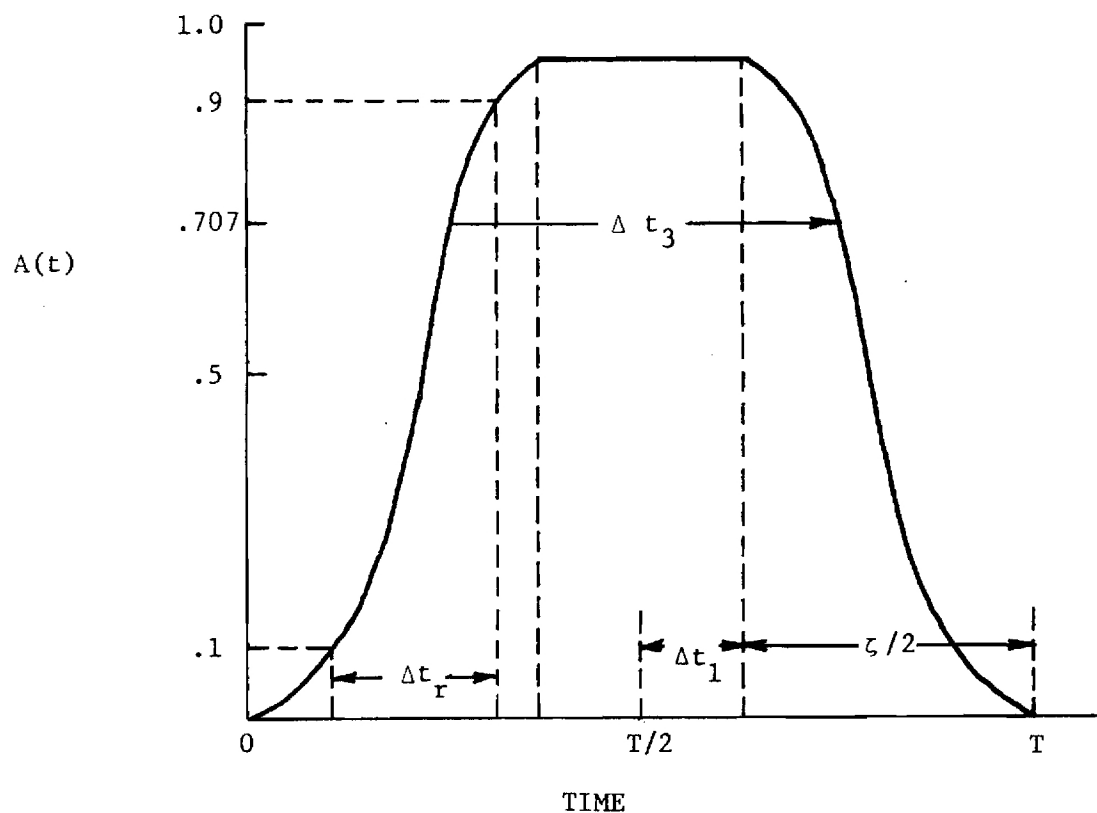


Figure 55. Sketch of the amplitude envelope of a stretched cosine-squared pulse of total pulse width  $T$ , 3-dB pulse width  $\Delta t_3$  and rise time  $\Delta t_r$ .  $\zeta$  denotes the half-period of the cosine portion of the pulse, and  $\Delta t_1$  is the half-width of the rectangular portion of the pulse.

$\Delta t_1$  = half-width of the rectangular portion of the pulse, and all other symbols are as previously defined. A plot of the frequency spectrum of a 3-nanosecond pulse is presented in Figure 56. Note that the first sidelobe is down about 17 dB and that the higher-order sidelobes rapidly diminish in strength. This is in sharp contrast to the spectrum of a pure rectangular pulse, whose first sidelobe is down only 13 dB and whose far-out sidelobes fall off much more slowly than do the sidelobes for the stretched cosine-squared pulse.

The undistorted pulses were assumed to be input to an open-ended X-band waveguide transmission line. The amplitude of the complex transfer function of the waveguide was equal to the frequency-dependent transmission coefficients at the interface between free space and the waveguide. (The transmission coefficient is independent of length.) The phase of the complex transfer coefficient was calculated from standard waveguide equations for the phase shift as a function of frequency. Since the phase shift varies as the square root of the frequency, and directly as a function of length along the waveguide, the resultant phase shift versus frequency is different for different lengths of waveguide. Thus, the complex transfer function is different for each different length of waveguide.

The calculated pulses are displayed in Figures 57 through 68. Each figure is a plot of the relative amplitude envelope as a function of time. Figures 57 through 60 involve 5-nanosecond incident pulses, Figures 61 through 64 involve 3-nanosecond incident pulses, and Figures 65 through 68 involve 1-nanosecond incident pulses. The undistorted 5, 3, and 1 nanosecond pulses are presented in Figures 57, 61, and 65, respectively. The three figures immediately following each incident pulses are distorted views of

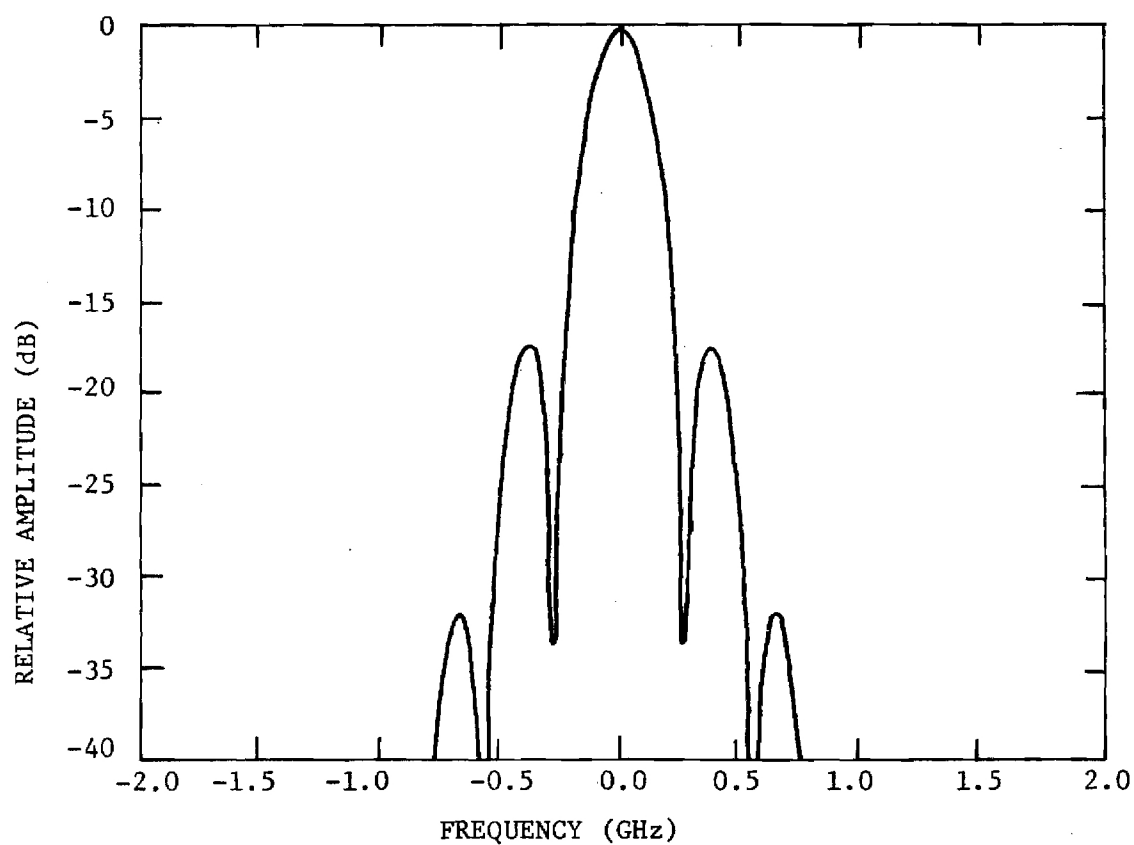


Figure 56. Frequency spectrum for a 3-nanosecond stretched cosine-squared pulse.



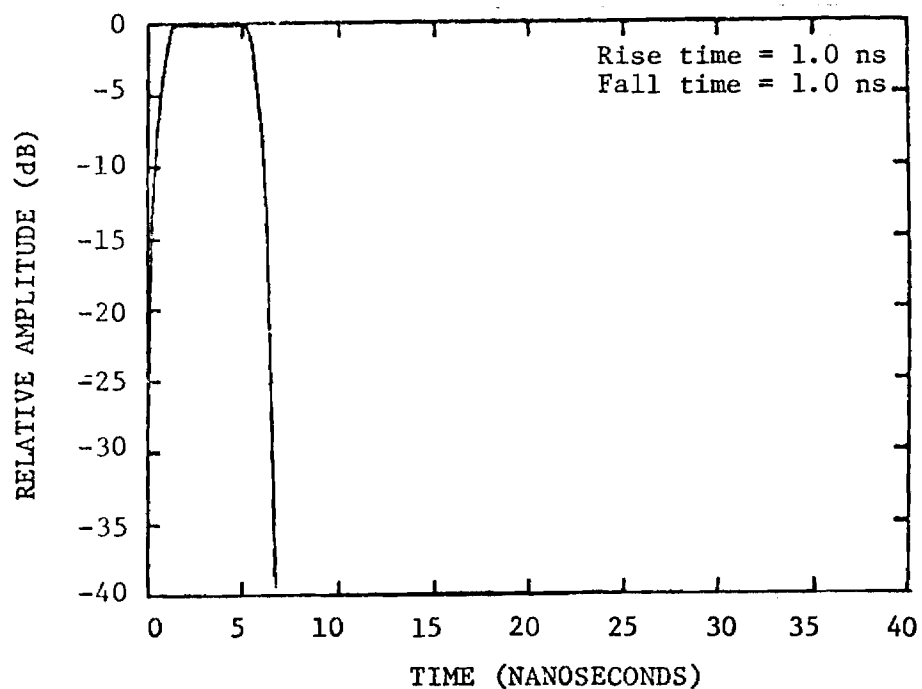


Figure 57. Incident 5-nanoseconds pulse.

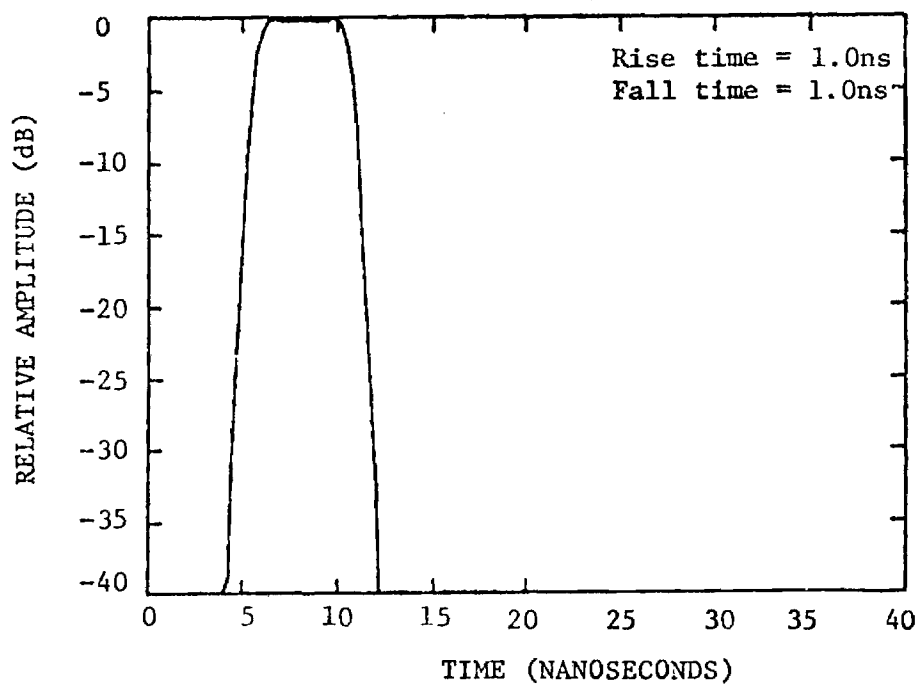


Figure 58. Degraded 5-nanosecond pulse after propagation along a 100-cm length of X-band waveguide.

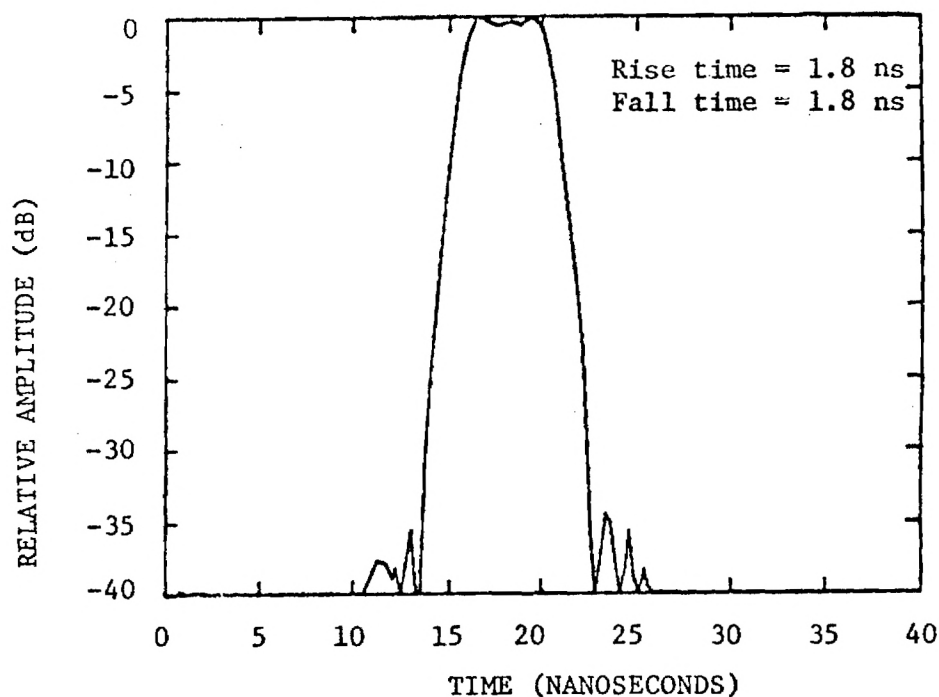


Figure 59. Degraded 5-nanosecond pulse after propagation along a 300-cm length of X-band waveguide.

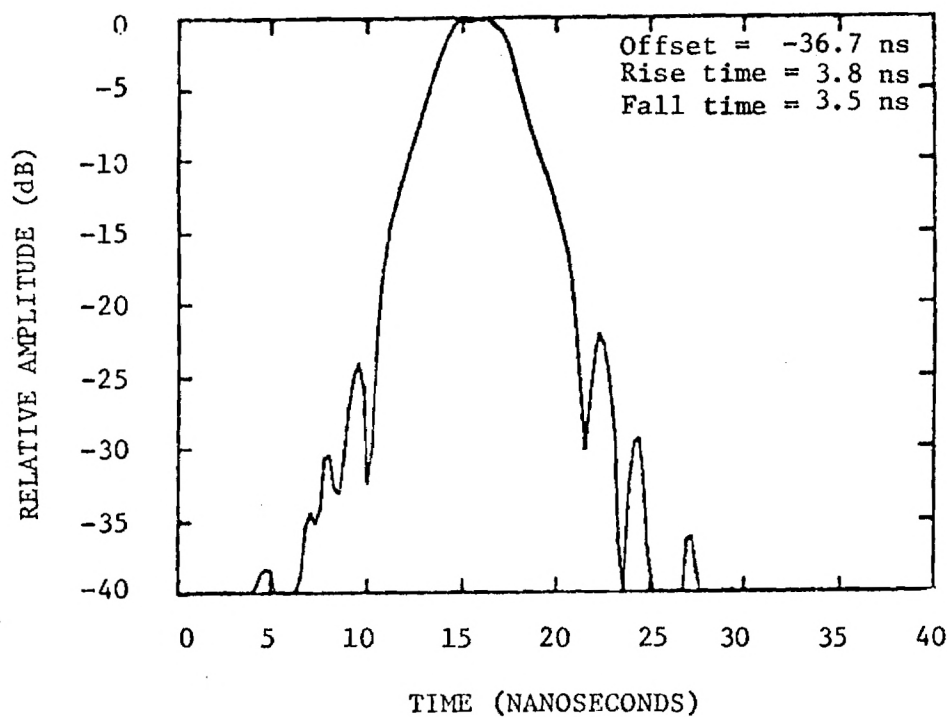


Figure 60. Degraded 5-nanosecond pulse after propagation along a 1000-cm length of X-band waveguide.

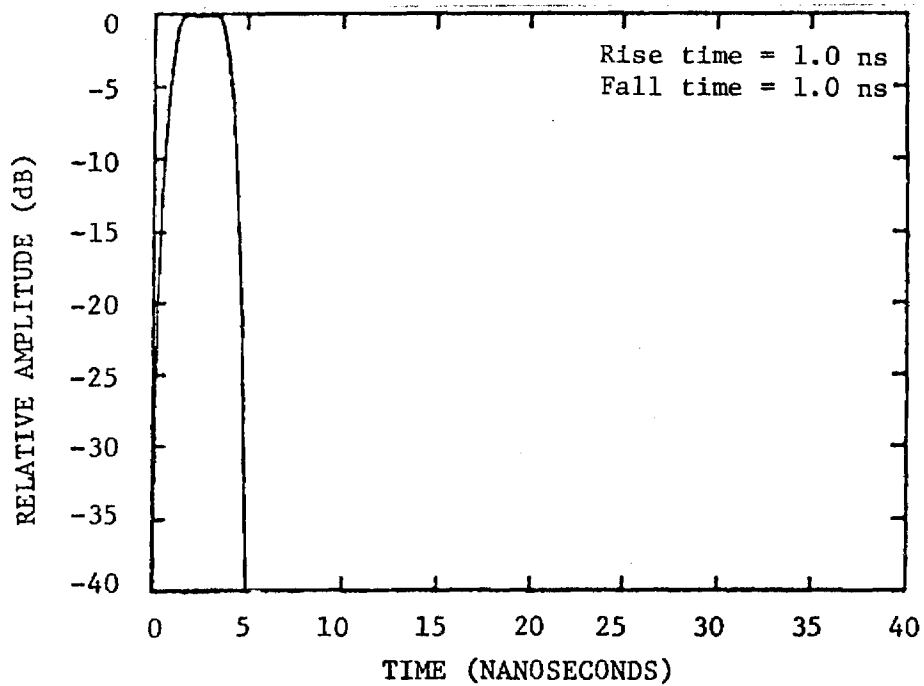


Figure 61. Incident 3-nanosecond pulse.

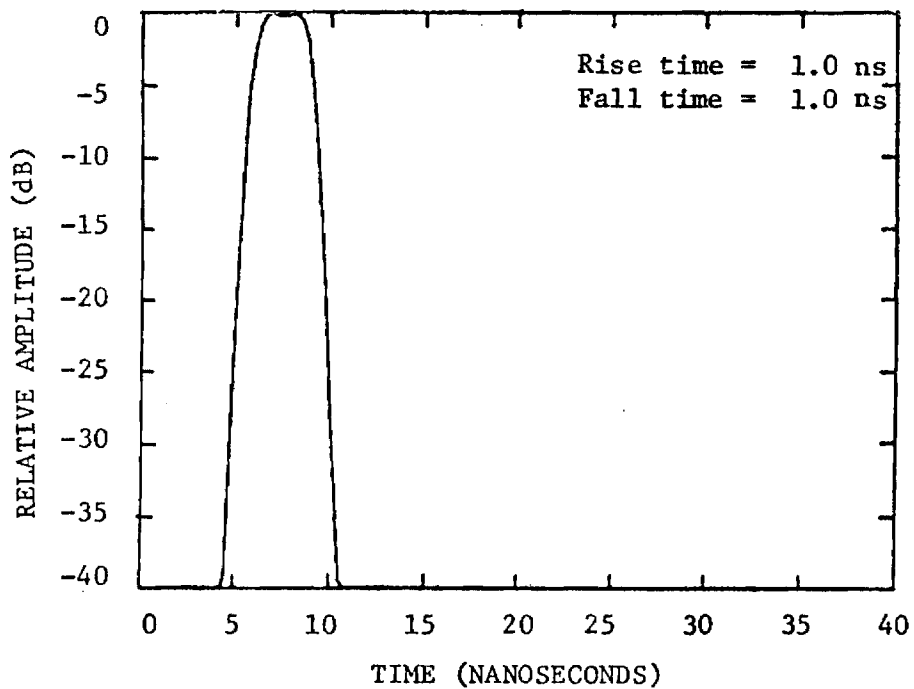


Figure 62. Degraded 3-nanosecond pulse after propagation along a 100-cm length of X-band waveguide.

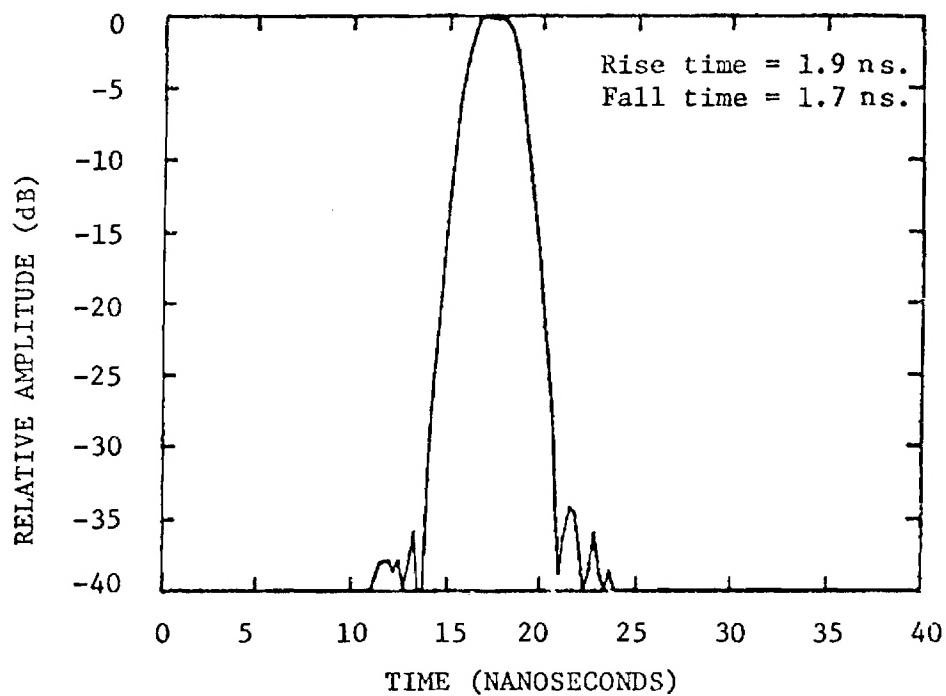


Figure 63. Degraded 3-nanosecond pulse after propagation along a 300-cm length X-band waveguide.

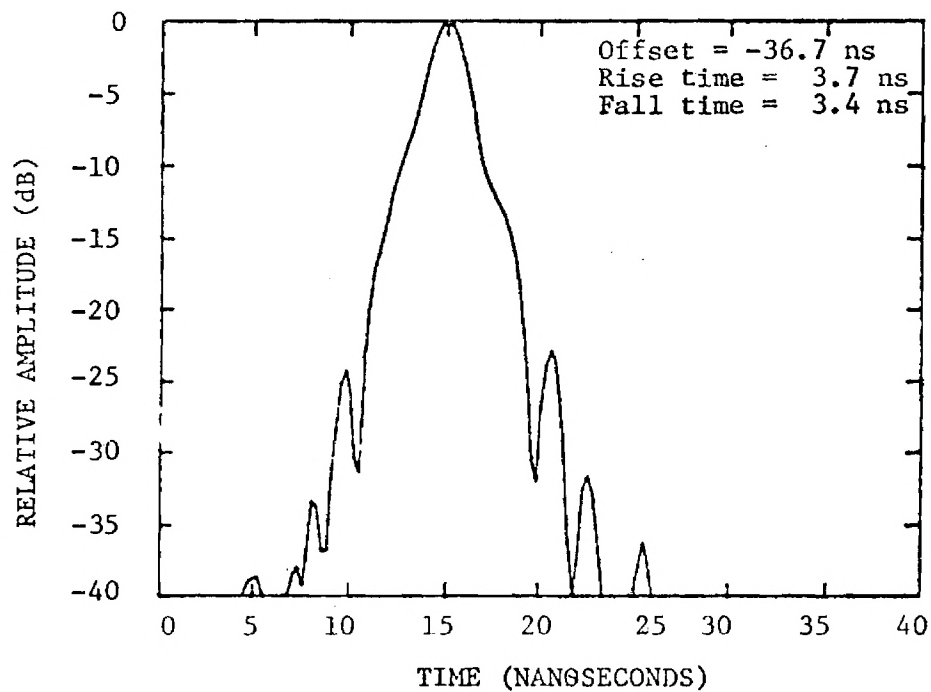


Figure 64. Degraded 3-nanosecond pulse after propagation along a 1000-cm length of X-band waveguide

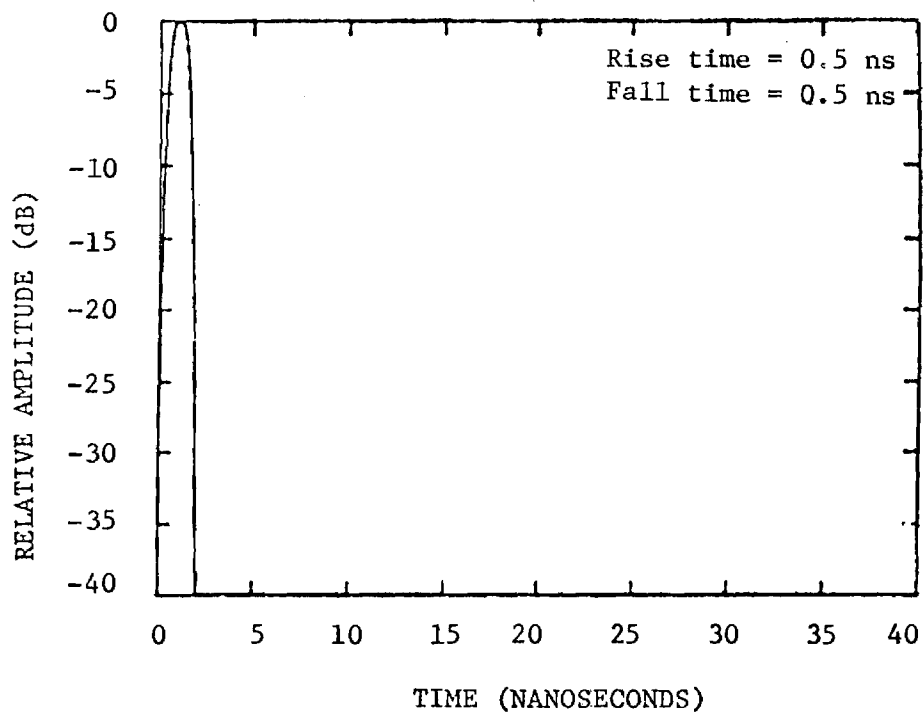


Figure 65. Incident 1-nanosecond pulse

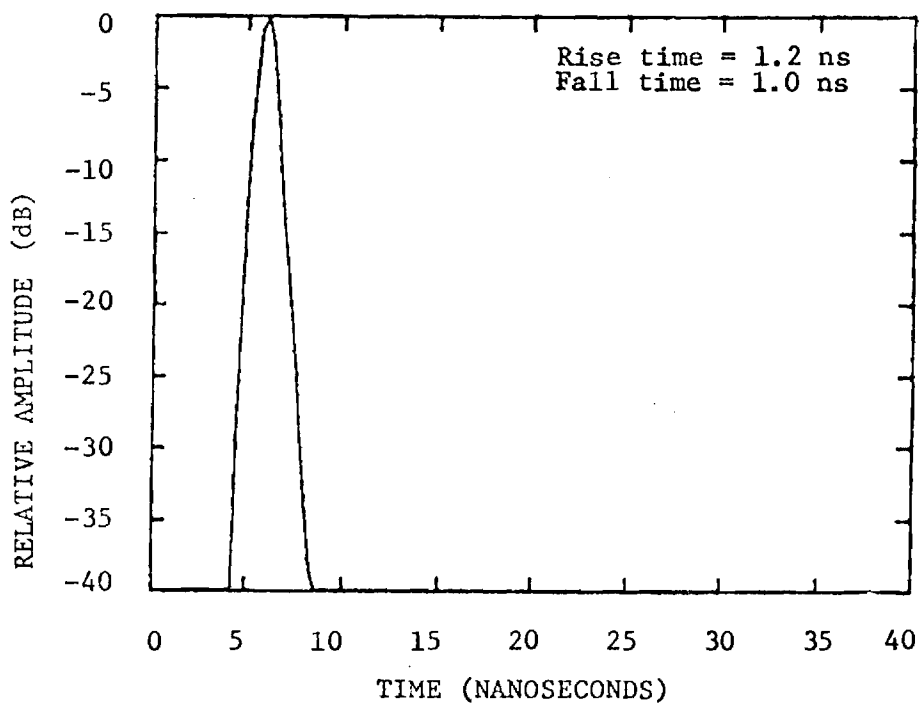


Figure 66. Degraded 1-nanosecond pulse after propagation along a 100-cm length of X-band waveguide.

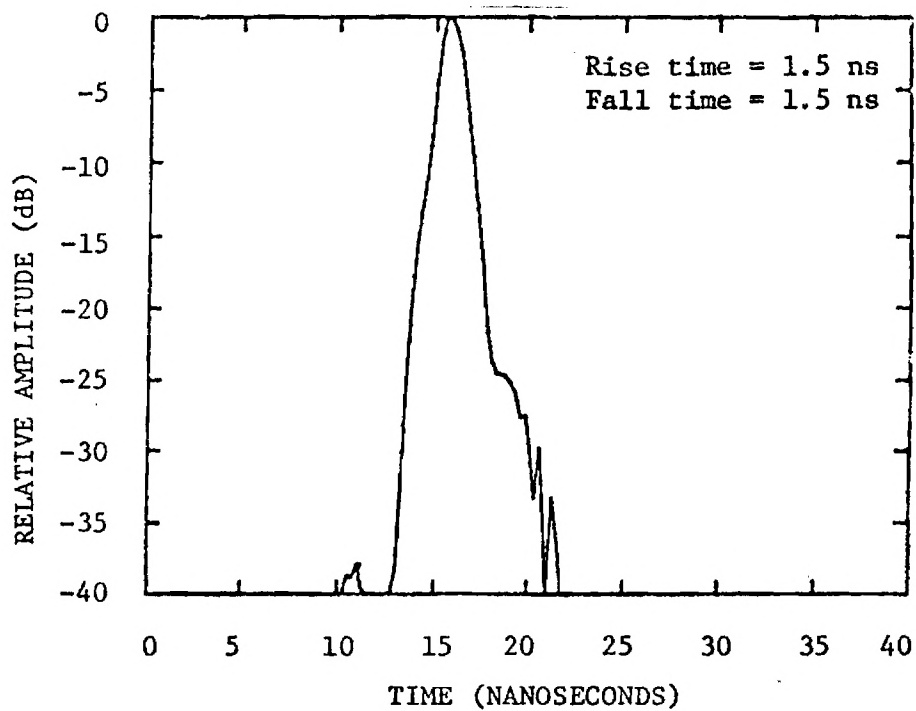


Figure 67. Degraded 1-nanosecond pulse after propagation along a 300-cm length of X-band waveguide.

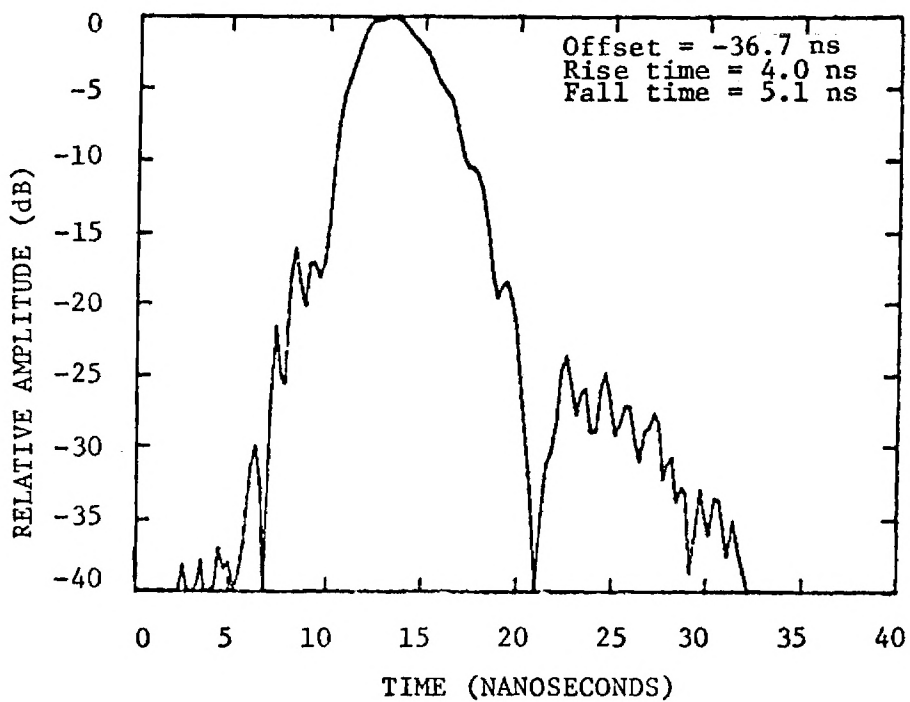


Figure 68. Degraded 1-nanosecond pulse after propagation along a 1000-cm length of X-band waveguide.

the pulse after propagation of each particular incident pulse along 100, 300, and 1000 centimeters of X-band waveguide. The pulses for the 1000 centimeter waveguide lengths have been offset 36.7 nanoseconds as noted in the corresponding figures. The rise and fall times of each received pulse are also noted in the figure.

Certain well-defined trends in the distortion effects are apparent from inspection of the various pulses. For a given incident pulse, the magnitude of the distortion, as manifested in the increased rise and fall times, degradation of the overall pulse shape, and the appearance of time sidelobes, increase for larger propagation lengths. For a given propagation length, the magnitude of these same distortion effects is generally greater for narrower incident pulses. A third trend implicitly contained in the various plots is the reduction in peak amplitude for both longer propagation lengths and narrower incident pulses. This trend may be discerned by noting that for a given incident pulse, the energy contained in each distorted pulse is constant. Since the distorted pulses are progressively spread over a larger time base for longer lengths and for narrower pulses, the peak amplitude is reduced. For plotting, each figure has been normalized to 0dB.

All of the above trends are reasonable, and agree with theoretical expectations for pulses subjected to the waveguide complex transfer function. In particular, the phase shift portion of the waveguide complex transfer function becomes progressively more non-linear as a function of frequency for longer propagation lengths. Additionally, for a given propagation length, the non-linearity of the phase shift is greater for larger bandwidths (i.e., narrower pulses). Consequently, the observed trends of the received pulses are generally consistent with the behavior implied by the

approximate analyses presented in subsection B-2. However, the detailed structure of the received pulses calculated via the FFT depends on subtle relationships between the phase and amplitudes of all the frequency components within the bandpass of the system. Consequently, the actual relative distortion effects due to a given complex transfer function on nearly identical incident pulses may differ slightly from predictions based on the approximate analyses. For example, the rise and fall times of the distorted 5 nanosecond pulse after propagation along 1000 cm are slightly greater than the rise and fall times for the narrower 3-nanosecond after the same propagation. However, the general trend toward greater rise and fall times for narrower incident pulses after modification by the waveguide transfer function is observed for more dissimilar incident pulses, as shown by comparison of either the 5-nanosecond or 3-nanosecond pulse with the 1-nanosecond pulse after propagation down a given length of waveguide. The approximate statistical analysis of subsection B-2 was presented to obtain qualitative insight into the causes of pulse distortion effects. Exact analysis for a particular case is performed with the computer prediction program.



## SECTION V

### CONCLUSIONS AND RECOMMENDATIONS

#### A. CONCLUSIONS

The work accomplished on this contract involved efforts on three tasks. These three tasks may be stated as follows: (1) design, develop, and demonstrate an S-band amplitude-only broadband antenna measurement system, (2) complete broadband phase-and-amplitude system tradeoff studies, select a broadband phase-and-amplitude measurement system approach, and perform preliminary design studies of the selected approach, and (3) develop, debug, and demonstrate a computer program for predicting pulse distortion effects from measured phase-and-amplitude data and for arbitrary original pulse shapes. These three tasks have been successfully and fully completed, resulting in a significant advancement in broadband measurement instrumentation, in the definition of a system which can completely characterize microwave antennas on a far-field antenna range, and in the development of a computer tool for performing pulse distortion diagnostics from measured phase and amplitude data.

Based on all test results collected on the Hybrid system, both the concept and its hardware implementation have been proven. These test data show that the Hybrid system is able to meet or surpass all its design goals. The Hybrid system dynamic range was of particular interest. The Hybrid system was easily able to meet the 40 dB dynamic range specifications. In fact, the system demonstrated the potential for performance up to a 50 dB dynamic range. It should be pointed out that the implementation of the Hybrid system

required the utilization of many state-of-the-art components to simultaneously meet all design goals for the system.

The Hybrid system (both concept and hardware) is an effective approach to an amplitude-only measurement system. It represents a new advancement in antenna measurement capabilities, techniques, and potential understanding of instantaneous antenna performance over a broad spectrum of frequencies. Amplitude-only spatial antenna patterns impact on a number of radar performance parameters and the ability to quickly measure these patterns over a broadband will lead to better understanding in several areas. Some of the radar performance parameters which may be affected by broadband operation include detection range, angular resolution, susceptibility to ECM techniques (such as barrage jamming), EMC/EMI, and tracking accuracy.

The Hybrid system breadboard was designed and constructed with the view of making it "user oriented" within contract cost constraints. Every effort was made, within cost constraints, to orient the entire Hybrid system toward the use at the technician level. However, several areas of the Hybrid system hardware need refinement to make it truly an "off the shelf" instrument. These areas include further improvement in component shielding and improvement in the logic controller synchronization circuitry. It was stated earlier in this section that the current breadboard Hybrid system demonstrated the potential for dynamic range performance up to 50 dB. Further improvements in shielding techniques could allow the Hybrid system to make broadband measurements accurately over 50 dB of dynamic range. Currently the circuitry in the logic controller responsible for synchronization requires a large amount of video amplification (approximately 46 dB) so that it can function over a wide range of RF input powers. Utilizing an RF amplifier in the reference antenna

sample line would considerably reduce the amount of required video gain. The reduction in video gain would reduce the system's susceptibility to interference, and thus, improve overall performance of the Hybrid system.

A computer-controlled broadband phase-and-amplitude system is required to completely characterize an antenna in terms of both its broadband spatial patterns and its pulse responses. Such a system can provide all the necessary data to perform off-line diagnostics which define that antenna's frequency and time domain performance over a variety of operating parameters. An attractive feature of the broadband phase-and-amplitude system is that once the phase and amplitude data have been recorded, subsequent pulse distortion and average pattern calculations can be performed for arbitrary pulse widths and bandwidths. Thus, unlike a time domain system, there is no requirement to repeat measurements for each pulsewidth of interest.

With the group delay type of phase measurement approach, a stable and accurate system can be achieved. With the system design which has been investigated, no phase reference or data links are required between the transmit and receive sites of the antenna test range. With locking of the group delay modulate and demodulate sources to a standard frequency broadcast (such as WWV), the need for special phase reference or data channels is avoided, thus making the system more flexible.

#### B. RECOMMENDATIONS

Realization of the desired computer-controlled phase-and-amplitude system will require system integration of a number of state-of-the-art components. In addition, the sideband processor and broadband phase-matched mixers must be developed. In addition to these hardware development and system

integration efforts, software for computer control must be developed. It is specifically recommended that an immediate program be initiated to perform the needed system design, hardware development, software development, and system integration to demonstrate the feasibility of the group delay type of phase-and-amplitude measurement system. For concept and hardware demonstration, a semi-automated approach can be utilized in which an operator controls certain parameters such as antenna scan. This approach will allow verification of the group delay technique while reducing the cost below that required for a fully automated system.

Based on the measured Hybrid system performance, a new capability has been provided. To continue further advancement in the area of amplitude-only broadband antenna measurements, the following specific actions are recommended: (1) Expand the utilization of the amplitude-only system. This Hybrid system is a definite advance in antenna measurement technology and represents a much needed capability. Even though the phase-and-amplitude system could provide the same capability, many potential users do not need the additional phase measurements. For those who require amplitude-only measurement, the Hybrid system can be implemented at a significant savings in cost and hardware. Also, the Hybrid system is now available, and a lead time of at least two years would be required, under the current program plans, before a phase-and-amplitude system will be available. (2) Hybrid system development should continue to make the device completely usable at the technician level. (3) Studies should be initiated to define how broadband performance relates to the radar performance parameters previously discussed. Broader bandwidth radar systems for several reasons are being

proposed. The impact of broadband performance on radar parameters should be determined for use during broadband radar system design.

The pulse distortion prediction computer program is an important part of a complete antenna analysis capability. Demonstration of the validity of this program through laboratory measurements is recommended. Measured pulse distortion would be compared to computed distorted pulses, such as those shown in Section IV.

The measurement and analysis techniques which have been described in this report should be viewed as complementing each other and as providing new tools to antenna designers and users. However, even though these studies were directed toward broadband antenna measurements, the use of these tools is not limited to antenna measurements and analysis. Phase and amplitude response of various transmission line components can also be measured and their broadband responses can be evaluated. Accordingly, it is recommended that new applications of these measurements and analysis tools be explored and evaluated.

## SECTION VI

### REFERENCES

1. "Broadband Antenna Measurement Techniques," J. D. Adams, F. L. Cain, and C. E. Ryan, Jr., Georgia Institute of Technology, Final Technical Report, RADC-TR-74-222, September 1974. (AD787 867)
2. WAVEGUIDE HANDBOOK, N. Marcuvitz, ed., Dover Publications, 1965.
3. ANTENNA ENGINEERING HANDBOOK, Henry Jasik, ed., McGraw-Hill, 1961.
4. SPECTRUM ANALYSIS, Application Note 63, Hewlett-Packard Company, Palo Alto, California, May 1965, pp 1-6 and 33-39.
5. PROBABILITY, RANDOM VARIABLES, AND STOCHASTIC PROCESSES, Chapters 7 and 8 A. Papoulis, McGraw Hill Book Company, 1965.
6. "A Guided Tour of the Fast Fourier Transform," G. D. Bergland, IEEE Spectrum, July 1969.

*MISSION  
of  
Rome Air Development Center*

*RADC plans and conducts research, exploratory and advanced development programs in command, control, and communications (C<sup>3</sup>) activities, and in the C<sup>3</sup> areas of information sciences and intelligence. The principal technical mission areas are communications, electromagnetic guidance and control, surveillance of ground and aerospace objects, intelligence data collection and handling, information system technology, ionospheric propagation, solid state sciences, microwave physics and electronic reliability, maintainability and compatibility.*

